

**SCREENING FOR AEROBIC ENDOSPORE-FORMING BACTERIA AS BIOCONTROL AGENTS FOR
POWDERY MILDEW DISEASE OF CUCURBITS**

By

HEATHER RAYNE TREDGOLD

Submitted in fulfilment of the academic requirements for the degree of
Master of Science in Microbiology

Discipline of Microbiology
School of Life Sciences
College of Agriculture, Engineering and Science
University of KwaZulu-Natal
Pietermaritzburg
South Africa

July 2015

ABSTRACT

Powdery mildew of cucurbits costs the South African cucurbit-growing industry millions of Rands per year in reduced yields and compromised fruit quality. Amongst the many bacterial and fungal antagonists of cucurbit powdery mildew, certain aerobic endospore-forming bacteria (AEFB) species show promise as biocontrol agents of this disease. When embarking upon biocontrol agent selection, multifaceted screening strategies are crucial. A study was undertaken with the aim of isolating AEFB from the cucurbit phylloplane for evaluation as potential antagonists of cucurbit powdery mildew using various screening approaches. Three hundred and nine AEFB isolates were isolated from cucurbit leaf material sourced from eight locations in the greater Msunduzi, KZN region. Dual-culture antifungal bioassays were performed using surrogate phytopathogenic fungi *Botrytis cinerea* and *Rhizoctonia solani* in place of the obligately biotrophic *Podosphaera* spp.. Two PCR-based genotyping methods were used to differentiate and group 55 antifungal AEFB isolates: internal-transcribed spacer region (ITS) PCR and randomly amplified polymorphic DNA (RAPD) PCR. The RAPD-PCR distinguished greater levels of genetic polymorphisms amongst isolates than did the ITS-PCR, revealing 14 different profiles as opposed to the three obtained from ITS-PCR; with 42% of isolates associated with a single RAPD-PCR banding profile. Phylogenetic relationships between representatives of each of the RAPD-PCR fingerprint groupings were determined by sequence analysis of 16S rRNA and gyrase subunit A (*gyrA*) gene fragments. In each instance, several distinct clusters were discernable, though *gyrA* sequences displayed higher levels of strain-level sequence heterogeneity. Comparisons of both gene sequence types with reference strains from the GenBank database revealed similarities to several known plant-associated strains of AEFB, including *B. amyloliquefaciens* subsp. *plantarum* and *B. subtilis*. Matrix-assisted laser deionisation-desorption time-of-flight mass spectrometry (MALDI-TOF-MS) based identification of selected AEFB was evaluated by comparing spectral data from AEFB isolates with reference strains in a Bruker BDAL Biotyper database. Only three out of the 14 isolates evaluated were identified to species level with acceptable confidence levels. This poor taxonomic resolution was ascribed to a paucity of applicable reference strains in the BDAL library. Nevertheless, mass spectra profiles of each isolate allowed for the clustering of related isolates to be achieved when dendograms were created. Antifungal compounds were extracted from 14 isolates using an acid-precipitation and methanol extraction protocol. Detection and identification of lipopeptide compounds in these extracts was assessed using thin-layer chromatography (TLC) and MALDI-TOF-MS. PCR-based screening for lipopeptide production potential using selected lipopeptide gene markers (*viz.* surfactin, iturin, bacillomycin, and

fengycin) was also evaluated for the selected 14 isolates. These isolates were found to produce multiple lipopeptide compounds; including homologues of surfactin, iturin, and fengycin. However, disparities that emerged between PCR, TLC, and MALDI-TOF-MS data suggest that some PCR primers, the *ituD* marker in particular, showed limited specificity amongst the AEFB strains screened. Based on the overall findings, nine isolates proceeded to *in vivo* screening against *Podosphaera* spp. using an agarised detached cotyledon assay and a biocontrol pot trial. Isolates achieving the most effective antagonism of *Podosphaera* spp. differed in each respective assay. Isolate cce175 provided the highest antagonism in the biocontrol pot trial, and isolate sqo279 provided the best results in the detached cotyledon assay. The impacts of inoculum preparation were assessed using isolate cce175 in a biocontrol pot trial. Treatments varied in cell growth phase and assessed cell-free supernatant, whole broth, and cell-only fractions on biocontrol efficacy compared to a Tebuconazole (430 g/l) fungicide control. None of the treatments were found to impact disease at a statistically significant level. The merits and limitations of the various screening approaches used, and issues surrounding the isolation and assessment of biocontrol efficacy in plant-associated AEFB, are discussed.

DECLARATION

I, Heather Rayne Tredgold, declare that

- (i) The research reported in this thesis, except where otherwise indicated, is my original work.
- (ii) This thesis has not been submitted for any degree or examination at any other university.
- (iii) This thesis does not contain other persons' data, pictures, graphs or other information, unless specifically acknowledged as being sourced from other persons.
- (iv) This thesis does not contain other persons' writing, unless specifically acknowledged as being sourced from other researchers. Where other written sources have been quoted, then:
 - (a) their words have been re-written but the general information attributed to them has been referenced;
 - (b) where their exact words have been used, their writing has been placed inside quotation marks, and referenced.
- (v) Where I have reproduced a publication of which I am an author, co-author or editor, I have indicated in detail which part of the publication was actually written by myself alone and have fully referenced such publications.
- (vi) This thesis does not contain text, graphics or tables copied and pasted from the Internet, unless specifically acknowledged, and the source being detailed in the thesis and in the References section.

Signed:

H. R. Tredgold (Candidate)

Signed:

C. H. Hunter (Supervisor)

ACKNOWLEDGEMENTS

My acknowledgements to the National Research Foundation (NRF) for their generous funding of this research project.

I would like to offer my gratitude and appreciation to the many technical and academic staff members and Postgraduate students who assisted, supported, and commiserated with me over the course of this research. The daily motivations and constant support of my friends Megan and Karis inspired me to find the strength to complete this work — and retain my sanity!

To Charles Hunter, my sincerest thanks for your guidance and continued support and encouragement. Thank you for always making time to discuss my work, and for your efforts throughout the editing process.

To Matthew, for the gentle nudges and pushes that kept me going. Thank you for your unfailing faith in me and constant presence at my side, and for your patience and encouraging words when I was at my lowest.

My heartfelt thanks go to my family for your abundant support during this journey:

Gran, Grandad, and Malcolm — My love and thanks to each of you for the support during this research and always.

To my Mom, I am so grateful for the quiet encouragement and unquestioning support during this work and always. Thank you for believing in me.

Finally, to my Uncle Derek — I am forever grateful to for giving me the opportunity and motivation to start down the path that has led me here. I hope that I have made you proud.

TABLE OF CONTENTS

ABSTRACT.....	i
DECLARATION	iii
ACKNOWLEDGEMENTS.....	iv
TABLE OF CONTENTS.....	v
LIST OF PLATES.....	viii
LIST OF FIGURES.....	ix
LIST OF TABLES.....	xi
LIST OF ABBREVIATIONS	xiii
INTRODUCTION.....	1
 CHAPTER ONE: Literature Review	 4
1.1. Introduction.....	4
1.2. The phyllosphere habitat and foliar biocontrol.....	6
1.3. <i>Bacillus</i> and related genera in plant health and disease control	8
1.3.1. <i>Bacillus</i> spp. lipopeptide compounds and their roles in plant disease control	11
1.4. Powdery mildew on cucurbits	14
1.4.1. Cucurbit powdery mildew life cycle and epidemiology	17
1.4.2. Control measures for powdery mildew of cucurbits	20
1.4.2.1. <i>Bacillus subtilis</i> and powdery mildew biocontrol	21
1.5. Screening methods for AEFB as BCAs of cucurbit powdery mildew	22
1.5.1. Isolation and characterisation of AEFB	24
1.5.2. Genetic fingerprinting to assess AEFB diversity	24
1.5.2.1. Fingerprinting of AEFB using RAPD-PCR	25
1.5.2.2. Fingerprinting of AEFB using ITS-PCR	27
1.5.3. DNA sequence polymorphisms for AEFB differentiation	27
1.5.4. Antifungal activity screening and assessment of powdery mildew antagonism	28
1.5.5. Lipopeptide compounds analysis and production potential in AEFB.....	31
1.5.5.1. Extraction and analysis of lipopeptide compounds.....	31
1.5.5.2. Gene marker PCR to determine lipopeptide production potential	32
1.5.6. MALDI-TOF-MS for bacterial identification.....	33
1.6. Conclusion	35
 CHAPTER TWO: Preliminary assessment of antifungal activity and diversity amongst AEFB isolated from the leaf material of various cucurbit species	 37
2.1. Introduction.....	37
2.2. Materials and Methods	40
2.2.1. Isolation of AEFB from cucurbit leaf material	40
2.2.2. Assessment of antifungal activity of AEFB using dual-culture bioassays.....	41

2.2.3. Genotyping and identification of AEFB isolates using DNA fingerprinting and gene fragment sequencing	42
2.2.4. DNA sequencing of 16S rRNA and gyrase subunit A gene fragments.....	45
2.2.5. AEFB classification using MALDI-TOF-MS.....	46
2.3. Results	48
2.3.1. <i>In vitro</i> screening for antifungal ability using dual-culture bioassays.....	48
2.3.2. Observations of AEFB isolate colony morphology, cell morphology, and sporangial characteristics	55
2.3.3. Fingerprinting of AEFB isolates using RAPD-PCR and ITS-PCR	56
2.3.4. RAPD-PCR differentiation of phylloplane-isolated AEFB isolates	58
2.3.5. ITS-PCR differentiation of phylloplane-isolated AEFB isolates.....	61
2.3.6. 16S rRNA and <i>gyrA</i> gene fragment sequencing	65
2.3.7. Sequencing of 16S rRNA gene fragment	65
2.3.8. Sequencing of <i>gyrA</i> gene fragment.....	69
2.3.9. Applying MALDI-TOF-MS to differentiate AEFB isolates.....	74
2.4. Discussion	80
CHAPTER THREE: Evaluation of lipopeptide production by <i>Bacillus</i> spp. isolates using gene marker PCR, TLC, and MALDI-TOF-MS analysis	88
3.1. Introduction.....	88
3.2. Materials and Methods	90
3.2.1. PCR detection of gene markers associated with lipopeptide production	90
3.2.2. Lipopeptide compound extraction from <i>Bacillus</i> cultures.....	92
3.2.3. Determination of antifungal activity of methanol extracts using a disc-diffusion bioassay	93
3.2.4. TLC analysis of lipopeptide-methanol extracts	94
3.2.5. MALDI-TOF-MS analysis of lipopeptide-methanol extracts.....	94
3.3. Results	96
3.3.1. PCR detection of gene markers associated with lipopeptide biosynthesis	96
3.3.2. Extraction and characterisation of lipopeptide compounds from <i>Bacillus</i> isolates.....	101
3.3.2.1. Disc-diffusion bioassay	101
3.3.2.2. Analysis of methanolic extracts using TLC.....	102
3.3.2.3. Detection of lipopeptide compounds using MALDI-TOF-MS.....	105
3.4. Discussion	117
CHAPTER FOUR: Screening of selected <i>Bacillus</i> spp. isolates for antagonism towards <i>Podosphaera fusca</i> using an agarised detached cotyledon assay and biocontrol pot trials	122
4.1. Introduction.....	122
4.2. Materials and Methods	123
4.2.1. Bacterial isolates	123

4.2.2.	Cultivation of powdery mildew disease and conidia harvesting.....	123
4.2.3.	Antagonism screening using an agarised detached cotyledon bioassay	124
4.2.4.	Biocontrol pot trial screening of <i>Bacillus</i> isolates against powdery mildew.....	127
4.2.5.	Impacts of inoculum preparation on cucurbit powdery mildew antagonism	128
4.3.	Results	130
4.3.1.	Agarised detached cotyledon assay.....	130
4.3.2.	Biocontrol pot trial of powdery mildew antagonism.....	133
4.3.3.	Impacts of bacterial preparation and culture age of <i>B. amyloliquefaciens</i> strain cce175 on cucurbit powdery mildew antagonism	136
4.4.	Discussion	139
CHAPTER FIVE:	General Overview and Conclusions	145
REFERENCES	150

LIST OF PLATES

Plate 1.1. A cucurbit powdery mildew infected 4-week-old greenhouse-grown zucchini displaying characteristic white spots of powdery mildew colonies visible (A) on the leaves (B) and stem (C), which eventually lead to leaf chlorosis (D) and senescence.....	16
Plate 2.1. Dual-culture antifungal bioassays illustrating varying levels of AEFB antagonism against <i>Botrytis cinerea</i> and <i>Rhizoctonia solani</i> on PDA after 4 d of incubation at 30°C. The rating system applied to measure antagonism was determined by the size of the zone of inhibition where: (+++) is greater than 5mm; (++) measures between 2–5mm; (+) measures less than 2mm; and a (-) rating indicated that no observable antagonism was evident.....	50
Plate 2.2. Influence of bioassay duration on fungal antagonism of <i>Rhizoctonia solani</i> by isolate ccc103 illustrating changes in mycelial appearance and colour over time. Dual-culture bioassays were performed on PDA and incubated at 30°C over a 14-d period.....	51
Plate 2.3. Influence of bioassay duration on fungal antagonism of <i>Botrytis cinerea</i> by isolate cce147 illustrating changes in mycelial appearance and colour over time. Dual-culture bioassays were performed on PDA and incubated at 30°C over a 14-d period.....	51
Plate 2.4. Effect of dual-culture antifungal bioassay duration on fungal antagonism of <i>Botrytis cinerea</i> by isolate bng119, illustrating the onset of fungistatic interactions over a 14-d period.	52
Plate 2.5. Dual-culture bioassay illustrating antifungal interaction between isolate bng216 and <i>Botrytis cinerea</i> in which the development of a red/pink colouration in the PDA medium (7 d) is evident.	52
Plate 2.6. Representative colony morphologies of selected AEFB isolates cultured on TSA after 48 h at 30°C. Colony morphology (A) was characterised a dry texture and matte appearance, whereas morphology (B) was highly mucoid and globose in appearance. Over time (B) type colonies dried out taking on a more rugose appearance with a firmer texture (C).	57
Plate 3.1. TLC plate showing marked bands of lipopeptide extracts in methanol after separation using a 70:30 (v/v) propan-1-ol : water mobile phase and visualised under UV illumination and/or atomisation with water.....	103
Plate 3.2. Sections of TLC plates of methanol extracts from <i>B. amyloliquefaciens</i> strains cce140, cce146, and cce175 showing band fluorescence as seen under UV illumination (A) and band hydrophobicity after atomisation with water (B).....	103
Plate 4.1. Agarised detached cotyledon assay demonstrating zucchini cotyledon embedded in basal agar medium.....	126
Plate 4.2. Examples of leaf area infected (l.a.i.) benchmarks used for rating of powdery mildew of cucurbits disease in the biocontrol pot trial. The images represent the leaf area infected values: (A) 10%, (B) 50%, (C) 70%, (D) 100%.	126
Plate 4.3. Development of powdery mildew disease on zucchini (Partenon hybrid F1, Starke-Ayres, South Africa) inoculated with <i>B. amyloliquefaciens</i> strain cce175 as seen at 7, 9, and 11 d post disease inoculation.	134

LIST OF FIGURES

Figure 1.1. Life cycle of <i>Podosphaera fusca</i> , the primary causal agent of cucurbit powdery mildew (Pérez-García <i>et al.</i> , 2009).	17
Figure 1.2. Asexual conidia of powdery mildew cucurbits pathogens <i>Podosphaera fusca</i> (left) and <i>Erysiphe cichoracearum</i> (right). Fibrosin bodies are observable in the <i>P. fusca</i> conidia as indicated by the arrows (Bruce Watt, University of Maine; Paul Bachi, University of Kentucky Research and Education Center).	19
Figure 1.3. Diagram of the detached leaf assay, adapted from Quinn and Powell (1982) showing: (A) the lower Petri dish containing nutrient solution; (B) the joined lower plate lid and upper plate bottom, through which the leaf petiole extrudes; and (C) the upper plate lid used to protect the system from cross-over contamination and to maintain the microclimate.	30
Figure 1.4. Diagrammatic representation of the process of intact cell MALDI-TOF-MS (IC-MS) analysis of bacterial isolates (Freiwald and Sauer, 2009).....	34
Figure 2.1. Fingerprint profiles of AEFB isolates from RAPD-PCR with primer OPG-11 as seen after electrophoresis using 1.5% agarose gel.....	59
Figure 2.2. UPGMA dendrogram demonstrating relationships between the representative banding patterns of RAPD-PCR profiles (a–n) of phyllosphere-isolated AEFB generated with primer OPG-11, as determined by GeneTools software (version 4.01.03, Syngene).....	60
Figure 2.3. RAPD-PCR fingerprint profiles of selected AEFB reference strains generated with primer OPG-11, as seen after electrophoresis using 1.5% agarose gel.....	61
Figure 2.4. Fingerprint profiles of AEFB isolates from ITS-PCR as seen after electrophoresis using 1.5% agarose gel.	62
Figure 2.5. UPGMA dendrogram showing the relationships between the representative ITS profiles derived from AEFB isolates screened in this study, as determined by GeneTools software (version 4.01.03, Syngene) using parameters of band molecular weight with a 1% tolerance.	63
Figure 2.6. ITS-PCR fingerprint profiles of selected AEFB reference strains, as seen after electrophoresis using 1.5% agarose gel.....	64
Figure 2.7. Examples of 16S rRNA gene fragment PCR amplicons (~1200 bp) as viewed after gel electrophoresis in 1.5% agarose gel.	65
Figure 2.8. Evolutionary relationships of phylloplane AEFB isolates and selected reference strains based on partial 16S rRNA gene sequences as inferred by the Neighbour-Joining method from bootstrap values from 1000 replicates (MEGA6). The scale bar represents 0.005 nucleotide substitutions per sequence position.....	68
Figure 2.9. Examples of <i>gyrA</i> gene fragment PCR amplicons (~1000 bp) as viewed after electrophoresis in 1.5% agarose gel.	69
Figure 2.10. Evolutionary relationships of phylloplane AEFB isolates and selected reference strains based on partial Gyrase subunit A gene sequences as inferred by the Neighbour-Joining method from bootstrap values from 1000 replicates (MEGA6). The scale bar represents 0.05 nucleotide substitutions per sequence position.....	72
Figure 2.11. Dendrogram depicting clustering of phylloplane AEFB isolates as determined from spectral variances after MALDI-TOF-MS analysis and MSP creation.....	77
Figure 2.12. Dendrogram depicting clustering between AEFB isolates as determined by variances in mass spectra after MSP creation, and compared to selected AEFB reference strains from the BDAL database.....	78

Figure 2.13. Dendrogram of mass spectra data representing clusters of AEFB isolated from the cucurbit phyllosphere. Cluster analysis was performed using SPECLUST online software, with the scale bar indicating the distance measure (d) applied during clustering.	79
Figure 3.1. Expected PCR product sizes for the respective lipopeptide gene markers in reference strain <i>B. amyloliquefaciens</i> R16, as viewed after gel electrophoresis using 1.5% (w/v) agarose.	97
Figure 3.2. Gel electrophoresis images demonstrating PCR products for lipopeptide gene marker primers <i>bacC</i> (A), <i>fenD</i> (B), <i>ituD</i> (C), and <i>sur3</i> (D) obtained for isolates bnd162 and bnd166, and <i>B. amyloliquefaciens</i> strains pkf167, cce175, cce183, and bng199. The presence of a band indicated a positive result for the gene marker, and band absence indicated a negative result.	101
Figure 3.3. Mass spectrum of reference standard surfactin (m/z 800–1150).	107
Figure 3.4. Mass spectrum of reference standard iturin A (m/z 800–1150).	107
Figure 3.5. MALDI-TOF-MS mass spectra of reference strain <i>B. amyloliquefaciens</i> R16. These demonstrate the peak profiles appearing in the m/z ranges 950–1150 (A) in which surfactins and bacillomycins were detected; and m/z 1400–1590 (B) in which fengycins were detected.	108
Figure 3.6. MALDI-TOF-MS mass spectra of reference strain <i>B. subtilis</i> strain B81. These demonstrate the peak profiles appearing in the m/z ranges 950–1150 (A) in which surfactins and bacillomycins were detected; and m/z 1400–1590 (B) in which fengycins were detected.	109
Figure 3.7. MALDI-TOF-MS mass spectra of reference strains <i>B. amyloliquefaciens</i> R16 (A) and <i>B. subtilis</i> B81 (B) demonstrating the peak clusters indicative of lipopeptide compounds appearing in the m/z range 717–1650.	111
Figure 3.8. MALDI-TOF-MS mass spectra of isolates bng241 (A), <i>B. subtilis</i> strain bnd134 (B), and <i>B. amyloliquefaciens</i> strain cce175 (C) demonstrating the peak clusters indicative of lipopeptide compounds appearing in the m/z range 717–1650.	113
Figure 3.9. Mass profiles of methanol extracts from <i>Bacillus</i> isolates, reference strains, and reference standards represented as a gel view generated using mMass software (m/z 750–1750).	115
Figure 4.1. AUDPC analysis of an agarised detached cotyledon assay evaluating nine AEFB isolates against powdery mildew of cucurbits. Error bars indicate standard deviation between replicates.	133
Figure 4.2. AUDPC analysis of a biocontrol pot trial evaluating nine AEFB isolates against powdery mildew of cucurbits. Error bars indicate standard deviation between replicates.	136
Figure 4.3. AUDPC analysis of a biocontrol pot trial assessing the performance of various formulations of <i>B. amyloliquefaciens</i> strain cce175 against powdery mildew of cucurbits disease, where: T1 Non-diseased Control; T2 Active Cells (48 h); T3 Supernatant (48 h); T4 Whole broth (48 h); T5 Whole broth (72 h); T6 Diseased Control; and T7 Folicur Control. Error bars indicate standard deviation between replicates.	139

LIST OF TABLES

Table 1.1. General characteristics of <i>Bacillus</i> species (Schleifer, 2009; Slepecky and Hemphill, 2006).	9
Table 2.1. PCR primers for diversity assessment and taxonomic classification of AEFB isolates.	43
Table 2.2. PCR reaction conditions for the primers used in DNA fingerprinting and gene fragment sequence analysis.	44
Table 2.3. Results for dual-culture antifungal bioassays of selected AEFB isolates against <i>Botrytis cinerea</i> and <i>Rhizoctonia solani</i> .	53
Table 2.4. Colony and Gram stain characteristics of AEFB isolates displaying high levels of fungal antagonism in dual-culture bioassay.	55
Table 2.5. Comparative matches of AEFB isolates after a BLAST search on GenBank of the 16S rRNA subunit gene fragment after sequencing (Date accessed: 20 March 2015).	67
Table 2.6. Comparative matches of AEFB isolates after a BLAST search on GenBank of the <i>gyrA</i> gene fragment after sequencing (Date accessed: 20 March 2015).	70
Table 2.7. Comparative data for DNA fingerprinting and gene sequence fragment with plant host and geographical sampling location for <i>Bacillus</i> spp. isolates.	73
Table 2.8. MALDI-TOF-MS identification of AEFB using the Bruker Daltonics Biotyper spectra database, as compared to the 16S rRNA partial gene sequence matches from GenBank.	76
Table 3.1. PCR primers used for lipopeptide gene marker detection in <i>Bacillus</i> isolates.	91
Table 3.2. PCR reaction conditions for the primers used for lipopeptide gene marker screening of <i>Bacillus</i> isolates.	91
Table 3.3. Sequence identities of lipopeptide gene markers derived from reference strain <i>B. amyloliquefaciens</i> R16 (Date accessed: 10 August 2013).	97
Table 3.4. Lipopeptide gene markers associated with fengycin (<i>fenD</i>), bacillomycin (<i>bacC</i>), surfactin (<i>sur3</i>), and iturin (<i>ituD</i>) biosynthesis amongst <i>Bacillus</i> isolates compared to RAPD fingerprint grouping.	99
Table 3.5. Disc-diffusion bioassay of methanol extracts from <i>Bacillus</i> isolates antagonistic towards <i>Rhizoctonia solani</i> .	102
Table 3.6. R _f values of all bands visible after TLC analysis of methanol extracts, recorded by colouration and after UV illumination and/or after atomising with water.	105
Table 3.7. <i>m/z</i> values of prominent peaks detected by MALDI-TOF-MS in duplicate mass spectra of surfactin and iturin A standards.	106
Table 3.8. <i>m/z</i> values of lipopeptide associated peaks from <i>Bacillus</i> spp. reference strain mass spectra.	110
Table 3.9. Detection of lipopeptide biomarkers in methanol extracts from <i>Bacillus</i> isolates using MALDI-TOF-MS analysis.	112
Table 3.10. Comparative data of lipopeptide PCR gene markers and MALDI-TOF-MS detection of lipopeptide compounds in methanol extracts from <i>Bacillus</i> isolates.	116
Table 4.1. Treatments used for a biocontrol pot trial determining effect of bacterial inoculum preparation of <i>B. amyloliquefaciens</i> strain cce175 against cucurbit powdery mildew.	129
Table 4.2. Results from agarised detached cotyledon assay of AEFB antagonism of cucurbit powdery mildew as generated by AUDPC and ANOVA using GenStat software.	132

Table 4.3. AUDPC statistical results from biocontrol pot trial of AEFB antagonism of cucurbit powdery mildew.	135
Table 4.4. AUDPC results from a biocontrol pot trial assessing the effects of inoculum preparation of <i>B. amyloliquefaciens</i> strain cce175 on antagonism of cucurbit powdery mildew.	138

LIST OF ABBREVIATIONS

AEFB	=	Aerobic endospore-forming bacteria
ANOVA	=	Analysis of variance
AUDPC	=	Area under disease progress curve
BCA	=	Biocontrol agent
DNA	=	Deoxyribonucleic acid
dNTP	=	Deoxyribnucleotide
<i>gyrA</i>	=	Gyrase subunit A
HCCA	=	α -cyano-hydroxycinnamic acid
IPM	=	Integrated pest management
ISR	=	Induced systemic resistance
ITS	=	Intergenic spacer region
MALDI-TOF-MS	=	Matrix-assisted laser deionisation-desorption time-of-flight mass spectrometry
MSP	=	Mass spectra profile
PCR	=	Polymerase chain reaction
PDA	=	Potato dextrose agar
PMB	=	Pietermaritzburg
RAPD	=	Randomly amplified polymorphic DNA
RH	=	Relative humidity
RNA	=	Ribonucleic acid
SAR	=	Systemic acquired resistance
TLC	=	Thin-layer chromatography
TSA	=	Tryptic soy agar
TSB	=	Tryptic soy broth
UPGMA	=	Unweighted pair group method with arithmetic mean
UV	=	Ultraviolet

INTRODUCTION

Disease control is an age-old challenge facing agriculture, which has relied heavily on chemical pesticides as the principle means of controlling crop pests. Dependence on pesticides has escalated the prevalence of pathogen resistance and poses risks to the health of the environment, which highlights the need to develop sustainable and environmentally compatible ways of controlling crop pests (Razdan and Gupta, 2009; Pal and McSpadden Gardener, 2006). Over the last few decades research into the development of more eco-friendly means of controlling plant diseases has expanded significantly (Heydari and Pessarakli, 2010). An avenue that has gained favour in recent years is the application of biocontrol agents, specifically amongst bacteria that exhibit antagonism towards plant pathogens (Heydari and Pessarakli, 2010; Mathre *et al.*, 1999). Such formulated biopesticide products are able to target a desired pest at lower levels of application and also offer lower levels of environmental persistence compared to traditional pesticides (Thakore, 2006).

The isolation and screening of potential biocontrol agents from the environment is a complex process and success in controlling a disease cannot be guaranteed (Schisler and Slininger, 1997). Screening strategies are inherently selective and there are always risks of excluding a potentially useful candidate. The key to discovering a successful biocontrol agent lies in implementing screening strategies which take into account ecological considerations as well as the modes of action linked to disease antagonism (Schisler and Slininger, 1997). Ideally, screening protocols should be able to deal with large numbers of candidates and achieve results within a relatively short space of time (Schisler and Slininger, 1997; Spurr, 1985). Knowledge of the ecological requirements of an antagonist and the modes of action it employs will also influence the screening approaches used (Jijakli and Lepoivre, 1998; Schisler and Slininger, 1997). In the field, a biocontrol agent will need to compete and establish within a targetted niche, and carry out antagonistic activities under the prevailing conditions associated with the intended habitat (Schisler and Slininger, 1997). The application of a streamlined approach to biocontrol agent screening prevents the squandering of time and resources. Furthermore, well thought out screening protocols reduce the likelihood of promising candidate isolate(s) being overlooked (Schisler and Slininger, 1997).

A study was initiated to develop screening protocols for selecting candidate biocontrol agents (BCAs) specifically targetting AEFB isolates antagonistic towards cucurbit powdery mildew. This group of bacteria were chosen as candidates for BCA screening since various species and strains have been associated with phytopathogen control (Borriss, 2011; Ongena *et al.*, 2010). A number of *Bacillus* and *Paenibacillus* species are antagonistic towards many fungal, oomycete and bacterial plant pathogens; and their significance in plant health maintenance and interactions with the plant host are widely recognised (Borriss, 2011; Govindasamy *et al.*, 2010; Ongena *et al.*, 2010; Nagórksa *et al.*, 2007; McSpadden Gardener, 2004).

Powdery mildew of cucurbits disease is caused by either of two biotrophic fungal pathogens, *Podosphaera fusca* (syn. *P. xanthii*) and *Golovinomyces cichoracearum* (Pérez-García *et al.*, 2009; Pérez-García *et al.*, 2001; Zitter *et al.*, 1996). Cucurbit powdery mildew is relevant to most species of cucurbits grown under both field and greenhouse conditions, and is found throughout South Africa, and indeed in all parts of the world where cucurbits are cultivated (Pérez-García *et al.*, 2009; Pérez-García *et al.*, 2001; Zitter *et al.*, 1996). Hundreds of thousands of tons of cucurbits are produced annually in South Africa (South African Department of Agriculture, Forestry and Fisheries, 2013). In 2007 alone, South African losses to powdery mildew were estimated at between R7 million to R11 million (Haupt, 2007). Historically fungicides were the primary means of controlling this disease, with alternative control methods including sulfur, mineral, and natural oil applications being used (Pérez-García *et al.*, 2009, Robinson and Decker-Walters, 1997, Bélanger *et al.*, 1998). Previous research has shown that *B. subtilis* isolates have potential as antagonists of *P. fusca*; and several *Bacillus* spp. strains have been commercialised for use against powdery mildew of cucurbits (Borriss, 2011; Pérez-García *et al.*, 2011; Ongena *et al.*, 2010; Romero *et al.*, 2004).

The aim of this study was to isolate and screen for phyllosphere-competent AEFB antagonistic towards cucurbit powdery mildew. Fungal antagonism was applied as the primary selection characteristic of AEFB isolates. However, due to the biotrophic nature of *P. fusca*, isolates were initially screened for fungal antagonism using surrogate fungal pathogens. The production of lipopeptide compounds was also investigated since compounds within the surfactin, iturin, and fengycin families have been shown to contribute to the success of AEFB in disease control activities and play an important role in facilitating plant colonisation (Ongena *et al.*, 2010; Ongena *et al.*, 2009; Ongena and Jacques, 2008; Nagórksa *et al.*, 2007; Romero *et al.*, 2007a).

The objectives of this research can be summarised as follows:-

1. The isolation of phyllosphere-dwelling AEFB from a range of cucurbit species.
2. Screening AEFB isolates for antifungal activity *in vitro* using surrogate fungal pathogens.
3. Use of genotyping methods to differentiate and group AEFB isolates.
4. Evaluating different screening methods for detecting lipopeptide compounds, including gene marker PCR and the use of MALDI-TOF-MS.
5. Assessing a detached cotyledon assay as a laboratory-based *in vivo* method for screening for antagonists of cucurbit powdery mildew.
6. Evaluating selected isolates against the *P. fusca* pathogen in biocontrol pot trials.

CHAPTER ONE

Literature Review

1.1. Introduction

It is estimated that at least 10% of global crop yields are lost to plant diseases annually, costing billions of US dollars (Cawoy *et al.*, 2011). With increased pressure on food production from a growing human population, crop management is crucial to increase yield. In recent years, alternative crop management programs have been developed to lessen the dependence on chemicals. This shift has been driven by a growing awareness of the environmental risks associated with the widespread application of synthetic chemical pesticides (Cawoy *et al.*, 2011). The emergence of pathogen resistance to many of the active chemical constituents is also a major concern (Heydari and Pessarakli, 2010). Biological control of plant diseases offers a viable alternative to traditional chemical disease control practices. In particular, many microbial biological control products are now being used in place of chemical pesticides (Cawoy *et al.*, 2011). Such biopesticides have many advantages over traditional chemical products. Aside from reduced environmental impacts, biopesticides are effective in smaller quantities, non-target effects on beneficial organisms are lower, and they decompose faster than traditional chemicals (Thakore, 2006).

In plant pathology, microbial biological control (or biocontrol) is defined as the use of either the beneficial microorganism itself or its separated metabolites to control plant disease (Pal and McSpadden Gardener, 2006; Thakore, 2006). For this review, the term biocontrol agent (BCA) refers to microbial antagonists of phytopathogens. The successful implementation of a biocontrol strategy is often dependent on the compatibility of the BCA with the habitat conditions (Schisler and Slininger, 1997). This has led to consumer distrust regarding the predictability and sustainability of biocontrol practices (Emmert and Handelsman, 1999; Jijakli and Lepoivre, 1998; Handelsman and Stabb, 1996). The microbial populations in a given habitat will constantly interact with each other and their host, with the activities of each species being influenced by the surrounding environment (Heydari and Pessarakli, 2010). Knowledge of the modes of action of an introduced antagonist, its interactions with the extant microbial community, and its ability to establish within the habitat will greatly increase the likelihood of successful disease control (Cawoy *et al.*, 2011; Schisler and Slininger, 1997). Microbial antagonists must therefore be screened for compatibility with both the intended habitat and targetted pathogen(s) (Cawoy *et al.*, 2011; Schisler and Slininger, 1997).

Various methods of formulating and applying a BCA are assessed and optimised in order to maximise the benefits of the biocontrol strategy (Heydari and Pessarakli, 2010; Schisler and Slininger, 1997). A substantial portion of the BCA development process involves screening the candidate antagonists under conditions mimicking the intended habitat. This is a change from the traditional *in vitro* assays performed on highly nutritious cultures, which often do not translate to performance in the field (Schisler and Slininger, 1997; Knudsen and Spurr, 1988; Spurr, 1985). Laboratory-based assays and intensive artificial culture practices can alter the wild-type characteristics of the microbe, which ultimately determine its survival as an introduced agent (Schisler and Slininger, 1997; Knudsen and Spurr, 1988).

Diseases affecting members of the plant family Cucurbitaceae are of great interest. Cucurbit fruits include squashes, melons, and cucumbers, making them an economically important group of crop plants worldwide. An estimated 600,000 tons of cucurbit fruits worth over R 3.5 billion were harvested in South Africa in 2012 (South African Department of Agriculture, Forestry and Fisheries, 2013). Cucurbits are prone to many diseases, the most recognisable and ubiquitous of which is powdery mildew (Pérez-García *et al.*, 2009). In cucurbits this disease is caused by either of two biotrophic fungal species, namely *Podosphaera fusca* (syn. *P. xanthii*) and *Golovinomyces cichoracearum* (Pérez-García *et al.*, 2009; Pérez-García *et al.*, 2001; Zitter *et al.*, 1996). The host ranges of these agents comprise most of the cucurbit species throughout the world that are grown in both greenhouse and field conditions (Glawe, 2008; Zitter *et al.*, 1996). The disease causes yield losses by severely damaging the plant's ability to photosynthesise and produce fruit (Zitter *et al.*, 1996). Like many phytopathogens, powdery mildews have developed fungicide resistant races, prompting growers to adopt alternative measures of disease control, such as integrated pest management (IPM) strategies, which often incorporate microbial BCAs. Several species of AEFB show antagonism towards powdery mildew of cucurbits, with certain strains having been developed commercially as biofungicides against a variety of crop diseases (Borriss, 2011; Cawoy *et al.*, 2011; Romero *et al.*, 2007a, Romero *et al.*, 2007b; Romero *et al.*, 2007c; Romero *et al.*, 2004; Bettiol *et al.*, 1997).

Ideally, antagonist screening protocols for powdery mildew in cucurbits should be amenable to screening large numbers of candidates with a high throughput, and allow for rapid differentiation between isolates (Schisler and Slininger, 1997). Screening of BCA candidates must take into account

not only the efficacy of antagonism, but also the modes of action, the ability of an isolate to survive and perform under the prevailing habitat conditions, and its interactions with the target pathogen on the desired plant host(s) (Schisler and Slininger, 1997; Spurr, 1985). The screening of bacterial isolates for antagonism of powdery mildew of cucurbits is complicated by the biotrophic nature of the causal fungal pathogens, which require live host tissue to survive (Pérez-García *et al.*, 2009).

This review focuses on topics pertinent to the screening and application of AEFB as biological control agents against powdery mildew of cucurbits and addresses the following elements:

- (i) The phyllosphere as a habitat for biological control of foliar diseases;
- (ii) Epidemiology of cucurbit powdery mildew pathogens and current disease control methods;
- (iii) Roles of AEFB species in disease control and their modes of action; and
- (iv) Screening approaches that can be used to select for AEFB as antagonists of cucurbit powdery mildew.

1.2. The phyllosphere habitat and foliar biocontrol

The size of the global phyllosphere habitat has been estimated at 6.4×10^8 km² of leaf surface area, where bacteria constitute the major component of microbial populations, averaging up to 10^8 cells per gram of leaf (Lindow and Brandl, 2003). Epiphytic bacterial populations are variable in size due to fluctuations in the physical and nutritional conditions experienced by the exposed leaf surface (Andrews, 1992). The phylloplane microclimate is defined by a translaminar boundary layer created by the release of stomatal water vapour, which serves as a buffer against the worst of the environmental extremes (Lindow and Brandl, 2003). However, the boundary layer is not rigid, and is affected by several environmental variables such as temperature, relative humidity, dew, rain, wind, and radiation (Lindow and Brandl, 2003). The boundary layer and leaf surface topography—defined by structures such as trichomes, hydathodes, leaf veins, and stomata—ultimately determine the successful establishment of a microorganism (Lindow and Brandl, 2003; Andrews, 1992).

Indeed, the phyllosphere is a harsh habitat for microorganisms, which must adapt to the shifting abiotic and biotic conditions in order to colonise a niche and survive there (Vorholt, 2012). Nutrients and water are unevenly distributed across the phylloplane and their availability is constantly

changing (Lindow 2006; Lindow and Brandl, 2003). Plant cell leakage and secretory organs such as trichomes and hydathodes provide most of the nutrients available to the microflora, though exogenous sources as pollen or honeydew are seasonally available (Blakeman and Fokkema, 1982). In addition to nutrients, the leaf may also secrete antimicrobial compounds—such as phenolics and terpenoids—which can negatively impact microbial survival (Blakeman and Fokkema, 1982). Microflora establishment is also influenced by the availability of free space and shelter which is determined by the leaf cuticle layer and surface topography (Vorholt, 2012).

The phyllosphere is considered a short-lived environment because the presence of leaves on many plants is variable. Annual plants complete their life cycle within one year, while perennial plants are constantly shedding and replacing leaves (Vorholt, 2012). Due to the more transitory and exposed nature of the phylloplane, biocontrol of plant diseases has generally been more successful in the rhizosphere than in the phyllosphere (Vorholt, 2012; Andrews, 1992). Above-ground plant biomass and the associated microbial populations are prone to spatial and temporal variability, which results in seasonal microbial successions (Knudsen and Spurr, 1988). Microbial community composition over time, the manner of BCA application, and the prevailing phyllosphere conditions influence the establishment and survival of an introduced antagonist (Lindow, 2006; Lindow and Brandl, 2003; Andrews, 1992; Andrews, 1990; Knudsen and Spurr, 1988).

The microflora of the above-ground biomass of plants is highly species rich, and complex interactions exist between bacteria and fungi, and between the microbial populations and the host plant (Vorholt, 2012). When selecting a BCA, an understanding of the epidemiology of the pathogen is required because this will ultimately determine which type of antagonist should be applied in a given situation (Andrews, 1992). The ability of a BCA to establish itself within a particular niche is essential for successful disease control. The mode(s) of action of a BCA and its ability to establish itself within a particular niche are essential for successful disease control (Schisler and Slininger, 1997). Several approaches to foliar biocontrol have been developed in order to promote BCA establishment and antagonistic activity, as outlined by Andrews (1992):

- (i) ensuring pre-emptive leaf colonisation by the BCA to exclude the establishment of pathogens;
- (ii) matching the agent to the intended environment;
- (iii) using foreign antagonists only where the habitat is conducive to their growth; and

(iv) relating the antagonist's mode of action to the pre-penetration requirements of the pathogen. For example: biotrophic rusts and mildews require little or no exogenous nutrient supply to penetrate the plant, thus antibiosis or mycoparasitism are effective in decreasing or inhibiting pathogen sporulation (Fokkema, 1996; Andrews, 1992). Alternately, necrotrophic pathogens are best repelled using saprophytic antagonists, whose actions will deplete exogenous nutrients before pathogen establishment (Blakeman and Fokkema, 1982).

The established community of non-pathogenic epiphytic microorganisms can exert a degree of background-level biocontrol against phytopathogens by outcompeting them for available resources (Lindow and Leveau, 2002; Andrews, 1990; Singh and Faull, 1988). Extant phylloplane microflora can be modified to promote the establishment of an introduced BCA through the application of foliar nutrients (Mercier and Lindow, 2000; Andrews, 1990; Blakeman and Fokkema 1982). For example, nutrients such as inosine, tyrosine, adenosine, and L-alanine are known to trigger endospore germination and have been used to revive dormant AEFB species (Knudsen and Spurr, 1988). Additionally, increasing nutrition stimulates metabolic activity in BCAs, rendering the bacterial antagonists more effective at disease suppression. Thus, keeping the BCAs in a metabolically active state will extend their usefulness (Schisler and Slininger, 1997; Andrews, 1992; Andrews, 1990; Knudsen and Spurr, 1988).

1.3. *Bacillus* and related genera in plant health and disease control

The AEFB are of the phylum Firmicutes, order Bacillales. The family Bacillaceae are comprised of the genus *Bacillus* and eighteen other related genera as defined by 16S rRNA gene phylogeny (Schleifer, 2009). The characteristics of the genus *Bacillus* according to Bergey's Manual of Systematic Bacteriology are briefly listed in Table 1.1. These bacteria are renowned for resistant endospore formation, synthesis of peptide and non-peptidal antibiotics, and the production of a wide range of extracellular enzymes. The diversity among *Bacillus* species—in terms of nutrient utilisation, motility, and physicochemical growth optima—allows them to occupy many different niches (McSpadden Gardener, 2004). The ecology of many *Bacillus* and *Paenibacillus* species in agriculture is widely recognised, as these saprophytes are commonly found in soil and in association with plants (Schleifer, 2009; McSpadden Gardener, 2004). Their pervasiveness throughout the agricultural ecosystem is considered to be the root of their competence in plant disease control and plant health maintenance (Jacques, 2011; Govindasamy *et al.*, 2010; Ongena *et al.*, 2010).

Table 1.1. General characteristics of *Bacillus* species (Schleifer, 2009; Slepecky and Hemphill, 2006).

Characteristic	Appearance
Cell morphology and Gram reaction	Gram positive rods.
	Rods have rounded ends, although squared ends define the <i>Bacillus cereus</i> group.
	Diameter 0.4–1.8 µm, length 0.9–10.0 µm.
Gas requirements	Aerobic or facultatively aerobic.
Metabolism	Chemo-organotrophic.
Endospore formation	Formed at the completion of the exponential phase of growth. Triggers include nutritional deprivation, temperature, pH, population density, and presence and concentrations of certain minerals.
Endospore location and morphology	Sporangium morphology can be indicative of species, sporangial swelling variable between strains.
	Spore shapes: cylindrical, ellipsoidal, spherical and, rarely, kidney-shaped.
	Spore positions frequently subterminal; although central, paracentral, and terminal locations are present in some species (position can be diagnostic).
Growth conditions	Variable tolerances to pH, salt and temperature.
Predominant environments	Highly ubiquitous.
	Predominantly associated with soil, or habitats contaminated by soil.
	Some obligate pathogens.
	Some animal or insect associations.
Colony morphology	Colony texture, margin, elevation and surface appearance are highly variable.
	Colouring ranges from buff, creamy grey to off-white; some pigmented colonies such as black, brown, orange, pink and yellow.

The ability to synthesise a spectrum of antimicrobial compounds is a desirable trait for microbial BCAs. Approximately 167 compounds have been identified among *Bacillus* spp. which are antagonistic towards bacteria, fungi, protozoa, and viruses (Bottone and Peluso, 2003). A range of antifungal peptides are produced by *Bacillus* spp. and these can be divided into cyclic lipopeptides, phosphono-oligopeptides, and dipeptides (Quan *et al.*, 2010). The production of lipopeptide

compounds, although not necessary for sporulation, has been linked to a bacterial survival response and advancement into specific ecological niches (Ongena and Jacques, 2008; Stein, 2005). Substantial portions of *Bacillus* spp. genomes are dedicated to the production of antimicrobial compounds, allowing for the synthesis of a range of structurally and functionally diverse compounds (Ongena and Jacques, 2008; Nagórksa *et al.*, 2007; Stein, 2005).

The ability to produce antifungal compounds has played a significant role in the application of AEFB species in biocontrol strategies. Phytopathogen antagonism has been described in a range of *Bacillus* and *Paenibacillus* species including *B. subtilis*, *B. amyloliquefaciens*, *B. cereus*, *B. licheniformis*, *B. megaterium*, *B. mycoides*, *B. pumilus*, *P. polymyxa*, and *P. macerans* (McSpadden Gardener, 2004; Shoda, 2000). No individual species or strain is able to produce an entire range of antibiotic compounds, and synthesis of these compounds is often strain-specific (Nagórksa *et al.*, 2007; Stein, 2005).

Plant-associated and free-living AEFB species may also be involved in other aspects of plant health maintenance besides antibiosis. These include nutrient competition and solubilisation (e.g. inorganic phosphates), extracellular enzyme secretion (including chitinases, glucanases, cellulases, and amylases), and plant growth stimulation through secretion of auxins, gibberellins and cytokinins (Kumar *et al.*, 2012; Laslo *et al.*, 2012; Heydari and Pessarakli, 2010; Quan *et al.*, 2010; McSpadden Gardener, 2004). Research has shown that *Bacillus* and *Paenibacillus* spp. are also involved in stimulating plant host resistance to pathogens (Govindasamy *et al.*, 2010). Induced resistance mechanisms in the plant can be defined as induced systemic resistance (ISR) and systemic acquired resistance (SAR) which are differentiated by their respective elicitor compounds and pathways (Choudhary and Johri, 2009). *Bacillus* species known to activate defence systems in the plant include *B. amyloliquefaciens*, *B. cereus*, *B. mycoides*, *B. pumilus*, *B. sphaericus*, *B. pasteurii*, *B. thuringiensis*, *B. cereus*, and *B. subtilis* (Choudhary and Johri, 2009; Kloepper *et al.*, 2004; McSpadden Gardener, 2004; Bargabus *et al.*, 2002; Raaijmakers *et al.*, 2002).

Bacillus spp. have been commercially developed for fungal disease control since 1990 (Quan *et al.*, 2010). They are among the most predominant microbes used in biopesticide formulations in North America, representing 9% of the market share (Borriss, 2011). The list of commercially formulated *Bacillus*-based BCAs is extensive, with some notable examples including: Serenade (*B. subtilis*

QST713), Kodiak (*B. subtilis* GB03), Phosphobacter (*B. megaterium* and *B. coagulans*), Ecoguard (*B. licheniformis*), Yield Shield (*B. pumilis* GB34), Bioyield (*B. amyloliquefaciens* and *B. subtilis* GB 122), HiStick and Subtilex (both *B. subtilis* MB1600), and Taegro (*B. amyloliquefaciens* subsp. *plantarum* FZB24) (Borriss, 2011; Pérez-García *et al.*, 2011; Govindasamy *et al.*, 2010; Ongena *et al.*, 2010). In particular, the biocontrol and plant health promotion capabilities of *B. subtilis* isolates have been extensively described against a range of crop diseases (Malfanova *et al.*, 2012; Zerrouh *et al.*, 2011; Baysal *et al.*, 2008; Cazorla *et al.*, 2007; Romero *et al.*, 2007b; Ongena *et al.*, 2005a; Bais *et al.*, 2004; Chitarra *et al.*, 2003; Collins and Jacobsen, 2003; Collins *et al.*, 2003; Bettiol *et al.*, 1997; Ferreira *et al.*, 1991; McKeen *et al.*, 1986). The United States Food and Drug Administration (USFDA) has categorised many of these *B. subtilis* strains as “generally regarded as safe” (GRAS) in their capacity as biopesticides (Cawoy *et al.*, 2011).

1.3.1. *Bacillus* spp. lipopeptide compounds and their roles in plant disease control

Lipopeptide compounds consist of a cyclic or short linear oligopeptide linked to a lipid tail (Raaijmakers *et al.*, 2010). These substances are renowned for their antimicrobial, antitumor, and general surfactant properties (Raaijmakers *et al.*, 2010; Ron and Rosenberg, 2008). Lipopeptide compounds are produced by certain fungi (e.g. *Aspergillus* spp.) and bacteria (e.g. *Streptomyces* spp., *Pseudomonas* spp., and many *Bacillus* spp.) (Raaijmakers *et al.*, 2010). Lipopeptides are among the antibiotic compounds most consistently produced by *B. subtilis*, with more than 30 variants discovered in various strains (Jacques, 2011; Stein, 2005). Recently, strains of *B. amyloliquefaciens* have also been found to synthesise cyclic lipopeptide compounds which are thought to play a role in their biocontrol abilities (Xun-Chao *et al.*, 2013; Alvarez *et al.*, 2011; Balhara *et al.*, 2011; Chen *et al.*, 2010; Alvindia and Natsuaki, 2009; Arguelles-Arias *et al.*, 2009; Yu *et al.*, 2002; Yoshida *et al.*, 2001).

Lipopeptides are low-molecular-mass surfactants that function as bio-emulsifiers through the modification of the physical and/or chemical properties at interfaces (Jacques, 2011; Stein, 2005). Stein (2005) suggests that lipopeptides offer three main advantages to general bacterial survival:

- (i) increasing the surface area of hydrophobic water-insoluble growth substrates;
- (ii) improving the bioavailability of hydrophobic substrates by improving their solubility; and
- (iii) assisting in bacterial detachment and attachment to or from surfaces.

In most cases, peptide antibiotics are produced at the early stages of sporulation, and it has been suggested that they may play roles in sporulation (Ron and Rosenberg, 2001).

The lipopeptides of *Bacillus* spp. are classified into four classes: surfactins, iturins, fengycins (or plipastatins), and kurstakins (Jacques, 2011; Ongena and Jacques, 2008; Hathout, 2000). Synthesis of lipopeptide compounds is ribosome-independent, using the multimodular enzymes non-ribosomal peptide synthetase (NRPS) and polyketide synthetase (PKS) (Fickers, 2012; Tapi *et al.*, 2010). Each lipopeptide family is synthesised by open reading frames (ORFs) which vary in number between compounds and code for the various modules of these compounds (Fickers 2012; Tapi *et al.*, 2010). These ribosome-independent synthesis systems are responsible for lipopeptide compound diversity in fatty acid and peptide amino acid constituency, chain lengths, branching, and cyclisation (Jacques, 2011; Ongena and Jacques, 2008; Nagórksa *et al.*, 2007; Stein, 2005). Such structural features ultimately determine biological activity, activity spectra, resistance to enzyme hydrolysis, and high temperature and pH tolerances of the lipopeptides (Nagórksa *et al.*, 2007).

The surfactin family variants are lipoheptapeptides characterised by a cyclic lactone ring structure, interlinked with a β -hydroxy fatty acid (Ongena and Jacques, 2007; Stein, 2005). Surfactins are amphiphilic in nature and readily link up to lipid layers. Their structures allow them to act antagonistically by altering biological membrane integrity in a dose-dependent manner (Jacques, 2011; Ongena and Jacques, 2008). The members of this family include esperin, lichenysin, pumilacidin, and surfactin (Ongena and Jacques, 2008). Surfactins are haemolytic, and display antiviral, antimycoplasma, and antibacterial properties (Stein, 2005). However, surfactins have limited antifungal ability owing to sensitivity to sterols (e.g. ergosterol) which interfere with the compounds' interaction with the phospholipid bilayer (Jacques, 2011).

The iturin family are comprised of heptapeptides linked to a β -amino fatty acid chain of variable length (C14–C17) (Jacques, 2011; Ongena and Jacques, 2007). Iturins possess haemolytic and *in vitro* antifungal and anti-yeast activities, yet exhibit neither antibacterial nor antiviral effects (Jacques, 2011; Ongena and Jacques; 2008, Latoud *et al.*, 1990). They cause osmotic imbalance in affected cells by creating ion-conducting pores in biomembranes, rather than direct membrane disruption as seen in surfactins (Ongena and Jacques, 2008). Their efficacy against filamentous fungi has shown dependence on membrane sterol composition, being more active against cholesterol-containing

membranes (Balhara *et al.*, 2011; Latoud *et al.*, 1990). The variants in this family are bacillomycin D, F, L and LC; iturin A, A_L, C; and mycosubtilin (Ongena and Jacques, 2008).

The third lipopeptide family are the fengycins, often referred to as plipastatins. These are lipodecapeptides, with an internal lactone ring in the peptidic moiety between the carboxyl terminal amino acid (Isoleucine) and the hydroxyl group in the side chain. The β -hydroxy fatty acid chain (C14–C17) can be saturated or unsaturated (Ongena and Jacques, 2007). Fengycin variants include fengycin A and B; and plipastatin A and B (Ongena and Jacques, 2008). The A and B forms differ in the amino acid residue in position 6, with alanine in form A and valine in form B (Jacques, 2011). Fengycins exhibit no haemolytic abilities, but they are toxic to a broad range of filamentous fungi (Jacques, 2011). This activity is believed to be linked to the compounds' interaction with lipid layers, which potentially modifies cell membrane packing and permeability in a dose-dependent fashion (Jacques, 2011; Ongena and Jacques, 2008).

Kurstakins were originally isolated from *B. thuringiensis kurstaki* HD-1 (Hathout *et al.*, 2000). Researchers suggest that kurstakin-related compounds may exist in other AEFB species (Price *et al.*, 2007; Madonna *et al.*, 2003). Kurstakins have also been implicated in the swarming growth on agar of *B. thuringiensis* strains able to produce it, and facilitate bacterial colonisation of the insect cadaver (Bechet *et al.*, 2012). Kurstakin acts similarly to its lipopeptide relatives as a pore-forming compound, though it exhibits a limited antifungal spectrum (Bechet *et al.*, 2012). Antagonism towards *Stachybotrys charatum* has been described, though whether this compound has activities in association with plants or against plant diseases in the wild habitat is as yet unknown (Hathout *et al.*, 2000).

Lipopeptide compounds have been shown to play various roles in association with plants (Pérez-García *et al.*, 2011). Surfactin is perhaps the most studied of the lipopeptides with regards to its capacity to facilitate bacterial swarming and biofilm formation, as well as inhibiting biofilm formation of other bacteria (Jacques, 2011; Nagórksa *et al.*, 2007). The surfactins also contribute directly to bacterial pathogen antagonism and signal mediation to plant cells (i.e. induced resistance mechanisms); iturins are involved in bacterial spreading and show antibacterial and antifungal activity; and fengycins are involved in signal mediation to plant cells and have antifungal activity (Ongena *et al.*, 2005a; Ongena *et al.*, 2005b). The lipopeptide families have been shown to interact

synergistically on the plant host, with partnerships including surfactin and iturin, surfactin and fengycin, and iturin and fengycin (Ongena and Jacques, 2008; Nagórksa *et al.*, 2007; Ongena *et al.*, 2007).

1.4. Powdery mildew on cucurbits

There are over 200 recognised cucurbit diseases, of which powdery mildew is considered to be the most recognisable and ubiquitous, appearing in a wide range of climates on various cucurbit species (Pérez-García *et al.*, 2009; Agrios, 2005; Robinson and Decker-Walters, 1997). Symptoms are characterised by white spots on the leaf surface, petioles and stems (Zitter *et al.*, 1996), as shown in Figure 1.1. These spots increase in size and coalesce over time, eventually covering the entire leaf surface as infection advances (Zitter *et al.*, 1996).

Powdery mildew on cucurbits is attributed either of two species of fungi belonging to the Ascomycete family, namely *Podosphaera fusca* (Fr.) U. Braun & Shishkoff (2000) (previously *P. fuliginea*, *P. xanthii*, *Sphaerotheca fuliginea*, *S. fusca*) and *Erysiphe cichoracearum* (DC.) (1805) (previously *E. orontii* or *Glovinomyces cichoracearum*) (Pérez-García *et al.*, 2009; Agrios, 2005; Pérez-García *et al.*, 2001; Zitter *et al.*, 1996). The taxonomy of these two organisms has been complicated due to the wide degree of natural variations and genetic plasticity found with each species, which has resulted in the multiple name modifications (Pérez-García *et al.*, 2009; Zitter *et al.*, 1996). It is now generally accepted that the genus *Sphaerotheca* has been incorporated into *Podosphaera* (Pérez-García *et al.*, 2009). Races of both pathogens have been recognised throughout the world (Zitter *et al.*, 1996). A lesser form of cucurbit powdery mildew is caused by *Leveillula taurica*, and is restricted to the Mediterranean and few other regions (Robinson and Decker-Walters, 1997). *Podosphaera fusca* is considered to be the main causal agent of cucurbit powdery mildew worldwide (Pérez-García *et al.*, 2009).

These fungi are obligate biotrophic parasites unable to be cultivated on conventional artificial laboratory media (Pérez-García *et al.*, 2009; Agrios, 2005). Mycelia remain external to the leaf tissue using penetrative haustoria to gain nutrients from plant cells (Agrios, 2005; Robinson and Decker-Walters, 1997). For research purposes, live plant host tissue is required to culture these fungi (Bardin *et al.*, 2007). Some success has been achieved in preserving conidia and inducing germination of

barley powdery mildew spores in the laboratory, although most species of biotrophic fungi cannot be induced to germinate without live host tissue (Bardin *et al.*, 2007; Pérez-García *et al.*, 2006; Arabi and Jawhar, 2002).

Powdery mildew seldom kills the host plant, but acts to the detriment of plant nutrition, photosynthetic capacity, growth, and yield by promoting early leaf senescence and defoliation (Bélanger *et al.*, 1998). Infected cucurbits produce lower yields, both in the number and size of fruit and in a lowered length of time over which the fruit can be harvested (Pérez-García *et al.*, 2009; Zitter *et al.*, 1996). The fruits of infected plants are not directly attacked by the disease but—as a consequence of infection—fruits have reduced quality due to sunscald, incomplete or premature ripening, and poor flavour and storability (Zitter *et al.*, 1996). Overall plant growth may show decreases of between 20–40%, with economic damage thresholds of 20% infected leaf area recorded (Agrios, 2005; Bélanger *et al.*, 1998).



Plate 1.1. A cucurbit powdery mildew infected 4-week-old greenhouse-grown zucchini displaying characteristic white spots of powdery mildew colonies visible (A) on the leaves (B) and stem (C), which eventually lead to leaf chlorosis (D) and senescence.

1.4.1. Cucurbit powdery mildew life cycle and epidemiology

The basic life cycle of the primary powdery mildew causal agent, *P. fusca*, is presented in Figure 1.1. Both *P. fusca* and *E. cichorearum* generally follow this life cycle, with some variation between each species as described below. In the asexual cycle of *P. fusca*, conidia produce short germ tubes when they come into contact with a susceptible host. A primary differentiated appressorium forms at the tip of a germ tube, from which a primary haustorium forms inside the host epidermal cell. A primary hypha then emerges which goes on to form secondary appressoria, eventually leading to secondary haustoria formation. At later stages, the primary hypha branches into secondary hyphae (Pérez-García *et al.*, 2009). The secondary hyphae give rise to conidiophores, which form chains of 5–10 circular, rectangular, or ovoid conidia at their tips (Pérez-García *et al.*, 2009; Agrios, 2005; Robinson and Decker-Walters, 1997). The mat of secondary hyphae and conidia creates the white mycelium on the leaf surface that is visible to the naked eye (Plate 1.1) (Pérez-García *et al.*, 2009). This external existence leaves both mycelia and spores exposed to the environment and susceptible to being washed away by heavy rains or spread by air movement (Agrios, 2005; Robinson and Decker-Walters, 1997).

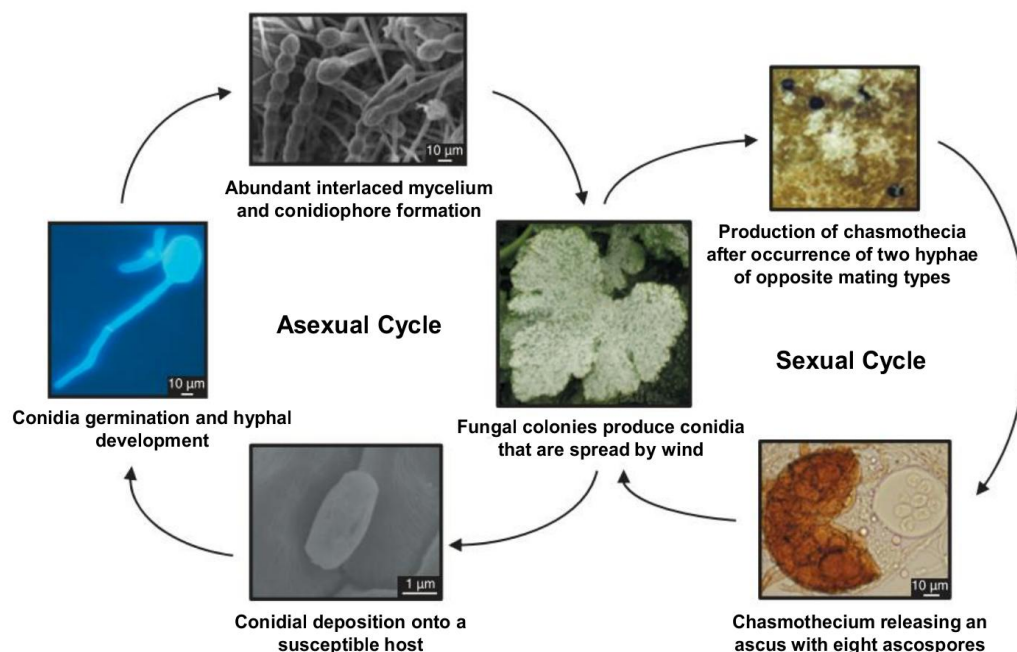


Figure 1.1. Life cycle of *Podosphaera fusca*, the primary causal agent of cucurbit powdery mildew (Pérez-García *et al.*, 2009).

The sexual cycle of cucurbit powdery mildew is initiated when a compatible mating type is found for the heterothallic *P. fusca*, while the sexual cycle of the homothallic *E. cichoracearum* involves self-compatible mating (Zitter *et al.*, 1996). A chasmothecium is the result of sexual reproduction in both fungi and are generally perceived as overwintering and oversummering sources of inoculum (Pérez-García *et al.*, 2009). The chasmothecium in *P. fusca* has branched appendages and contains one ascus bearing eight ascospores, whereas that of *E. cichoracearum* is unbranched with multiple asci (Zitter *et al.*, 1996). In the case of *P. fusca*, formation of a chasmothecium is a rare occurrence and has never been observed in the field, thus the prevalence of this sexual cycle is unknown (Pérez-García *et al.*, 2009; Robinson and Decker-Walters, 1997).

The time interval between infection and disease appearance ranges from 3–7 days and many spores will be released during this time (Zitter *et al.*, 1996). Symptoms of powdery mildew infection initially appear as pale yellow spots on the leaf, which evolve into the characteristic powdery white appearance with the onset of sporulation. In the case of *P. fusca*, infection may advance to a brown colouration (Pérez-García *et al.*, 2009). The small, white circular spots are visible on both leaf surfaces, particularly in shaded leaves, and will progressively enlarge and coalesce until they cover the entire leaf (Robinson and Decker-Walters, 1997; Cheah *et al.*, 1996). Initially symptoms appear on older leaves aged 7–8 weeks, thereafter symptoms appear progressively earlier with disease proliferation (Cheah *et al.*, 1996).

Powdery mildew inoculum enter an uninfected crop via windblown spores from infected areas, from out-of-season greenhouse cultivation of cucurbits, or from the pathogen overwintering through chasmothecia or bud perennation (dormancy within host plant buds) (Glawe, 2008; McGrath, 2001). Non-cucurbit plants are not considered to be major inoculum sources, due to the specialisation of the causal fungi to cucurbit hosts (Zitter *et al.*, 1996). Once established, dry conditions favour disease colonisation, sporulation, and dispersal (Zitter *et al.*, 1996). The conidia remain viable for up to 8 days under ambient conditions, and are spread to healthy leaves by air currents or water movement (Agrios, 2005; Zitter *et al.*, 1996). Germination occurs in wet conditions and high humidity, although in sufficiently high relative humidity conidia are able to germinate without a surface film of water (Agrios, 2005; Cheah *et al.*, 1996; Zitter *et al.*, 1996). The optimum temperature range for disease development is 20–27°C (Cheah *et al.*, 1996). Disease severity increases in shade,

where plants are closely spaced, and when luxuriant growth occurs due to high nitrogen levels (Zitter *et al.*, 1996).

The two primary causal agents of powdery mildew manifest on hosts almost identically, but can be distinguished by conidia morphology, inclusions that are detectable under bright field microscopy, and genetic studies (Pérez-García *et al.*, 2009; Glawe, 2008). Bright field microscopy can assist in rapid differentiation between these two fungi by the following characteristics (Zitter *et al.*, 1996):

- (i) Fibrosin bodies in conidia are unique to *P. fusca* and are visible in conidia treated with 3% potassium hydroxide solution (Figure 1.2). These bodies are straight to slightly curved, rodlike birefringent structures. Their presence is influenced by environmental conditions and do not appear in herbarium specimens.
- (ii) The edge line shapes between chained immature conidia appear sinuate (*viz.* wavy) in the genus *Erysiphe*, and crenate (*viz.* scalloped) in the genus *Podosphaera*.
- (iii) Germ tubes of *P. fusca* produces are forked, while those of *E. cichoracearum* are straight.

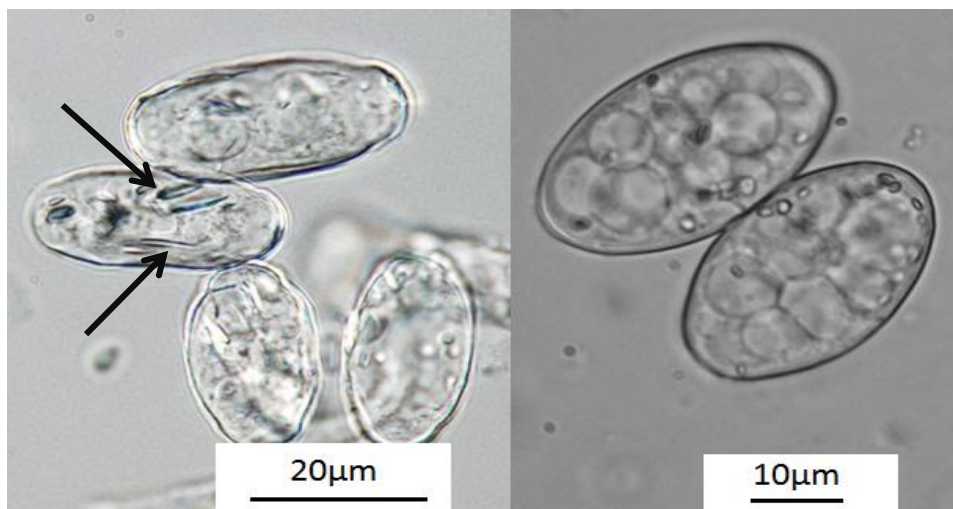


Figure 1.2. Asexual conidia of powdery mildew cucurbits pathogens *Podosphaera fusca* (left) and *Erysiphe cichoracearum* (right). Fibrosin bodies are observable in the *P. fusca* conidia as indicated by the arrows (Bruce Watt, University of Maine; Paul Bachi, University of Kentucky Research and Education Center).

1.4.2. Control measures for powdery mildew of cucurbits

Many fungicides are registered for use against cucurbit powdery mildew (Pérez-García *et al.*, 2009; McGrath, 2001; Bélanger *et al.*, 1998; Robinson and Decker-Walters, 1997). Repeated and excessive use of many of the commonly used, registered fungicides has led to the evolution of resistant races of the pathogen (McGrath, 2001; Zitter *et al.*, 1996). In the wake of fungicide resistance, a variety of alternative control methods for cucurbit powdery mildew have been investigated, including the employment of IPM strategies (Bélanger *et al.*, 1998; Reuvani *et al.*, 1995).

Management practices are important to the IPM approach because they break the disease cycle. For the IPM of cucurbit powdery mildew, such practices include alternative host eradication, deep ploughing, increased plant spacing (to lower relative humidity in the canopy), and plant monitoring for early detection (Razdan and Gupta, 2009). Resistant cultivars are currently seen as the best form of powdery mildew prevention and have been successfully bred in a variety of cucurbit species (Glawe, 2008; Robinson and Decker-Walters, 1997). Prophylactic methods for powdery mildew control include the application of unpasteurised milk, sulphur powder, plant extracts, compost extracts, salts, oils, clays, antitranspirants, or detergents to plant leaves (Pérez-García *et al.*, 2009; Tesfagiorgis, 2009; Bélanger *et al.*, 1998; Robinson and Decker-Walters, 1997).

The development of BCAs for cucurbit powdery mildew has focussed largely on hyperparasitic fungi and yeasts, rather than bacteria (Bélanger *et al.*, 1998). Fungal agents antagonistic towards cucurbit powdery mildew include: *Acremonium alternatum*, *Pseudozyma flocculosa*, *Sporothrix flocculose*, *Tilletiopsis* spp., *Ampelomyces quisqualis*, and *Verticillium lecanii* (Razdan and Gupta, 2009; Kiss, 2003; Romero *et al.*, 2003; Bélanger *et al.*, 1998). Antibiosis is the preferred method of biocontrol for powdery mildews, with research now shifting focus onto microorganisms such as *Agrobacterium radiobacter*, *Gliocladium virens*, *Trichoderma* spp., *Pseudomonas* spp., and *Bacillus* spp. (Bélanger *et al.*, 1998). Certain *Bacillus* strains have been commercialised as biofungicides, and some are also active against powdery mildew, these include: *B. subtilis* GB03 (Companion), *B. subtilis* QST713 (Rhapsody), *B. subtilis* QST713 (Serenade), *B. pumilus* QST2808 (Sonata), and *B. subtilis* CMB26 (Pomex) (Borriss, 2011; Cawoy *et al.*, 2011).

1.4.2.1. *Bacillus subtilis* and powdery mildew biocontrol

Bacillus subtilis isolates have been reported as successful antagonists of powdery mildew of cucurbits, whether live cells or extracted antifungal lipopeptides are applied against the disease (Romero *et al.*, 2007a; Romero *et al.*, 2007b; Romero *et al.*, 2007c; Romero *et al.*, 2004; Romero *et al.*, 2003; Bettiol *et al.*, 1997). Certain isolates obtained from the cucurbit phyllosphere and rhizosphere have displayed antagonistic activity toward *P. fusca*, with the establishment of the bacteria on the leaf surface and colonisation of fungal hyphae and conidia observed (Romero *et al.*, 2004). The biocontrol efficiency of the *B. subtilis* strains UMAF6614, UMAF6619, UMAF6639, and UMAF8561 were found to be determined by lipopeptide production (Romero *et al.*, 2007a; Romero *et al.*, 2007b; Romero *et al.*, 2007c; Romero *et al.*, 2004).

Romero *et al.* (2007a) reported reduced conidial germination and concomitant disruption of fungal leaf colonisation achieved with cell-free culture filtrates. These filtrates were found to contain surfactin, fengycin, iturin A, and bacillomycin, with the latter three compounds recognised for their antifungal activity (Ongena and Jacques, 2008). Disease antagonism persisted while lipopeptides could still be detected, and ceased with the absence of these compounds. The requirement of lipopeptides for the antagonism of cucurbit powdery mildew was further supported by an absence of disease antagonism after site-directed mutagenesis of a single locus in the bacterial genome controlling production of key lipopeptides (Romero *et al.*, 2007a). Furthermore, those mutants producing a combination of iturin A and surfactin continued to provide significant antifungal activity, which implies some degree of synergism between these two compounds (Romero *et al.*, 2007a). Based on previous findings, researchers have extrapolated that the powdery mildew fungus may show increased susceptibility to AEFB lipopeptides as these fungi contain lower amounts of sterols in their cell membranes (Jacques, 2011; Romero *et al.*, 2007a).

The ultrastructural damage caused to *P. fusca* after exposure to antagonistic *B. subtilis* isolates was further explored by Romero *et al.* (2007b). *Bacillus subtilis* strains UMAF6614 and UMAF6639 lowered *P. fusca* germination rates in assay, achieving decreases of 11% and 17% respectively. It was observed that exposure to lipopeptides caused conidia to shrink in size, and germ tube and first hypha development was diminished due to observable depressions in conidia and a loss of conidial turgidity. Other lipopeptide-mediated structural deformations included deformed appressoria, interlaced hyphae, and hyphal cell vacuolisation, cytoplasmic disorganisation, and granulation.

Despite no apparent damage to the fungal cell wall, the cell membrane and nuclear membrane showed indications of structural disruption. Certain fungal cells also showed an absence of key organelles, including the nucleus. These findings concur with previous observations of fungal structural disruption after exposure to antifungal compounds synthesised by *Bacillus* spp. (Arrebola *et al.*, 2010; Chaurasia *et al.*, 2005; Fiddaman and Rossall, 1993).

Bacillus subtilis strains UMAF6614, UMAF6639 and UMAF8561 showed antagonism towards *P. fusca* on a level comparable to an azoxystrobin fungicide and the commercialised mycoparasites AQ10 (*Ampelomyces quisqualis*) and Mycotal (*Lecanicillium lecanii*) (Romero *et al.*, 2007c). The application of the active vegetative bacteria was able to reduce disease incidence, and examinations of bacterial survival after 30 days showed populations of mostly vegetative cells. The researchers concluded that effective bacterial colonisation is the key to successful biocontrol of powdery mildew of cucurbits, and that active vegetative cells provided effective and continued antifungal activity (Romero *et al.*, 2007c).

Similar research was conducted by Bettiol *et al.* (1997) using the *B. subtilis* strain AP-3 against cucurbit powdery mildew, where a concentrated bacterial metabolite extract was applied to powdery mildew-infected leaves of cucumber and zucchini. Bacterial metabolite extracts at a concentration of 5,000 µg/ml achieved lesion reductions on cucumber of 90–99%, and 94.7–100% on zucchini. Total control of powdery mildew was achieved with a wettable powder formulation of bacterial cells and concentrated metabolites at 1000 and 10 000 µg/ml respectively. Furthermore, leaf weight was observed to increase with applications of either the metabolite or active cell formulations.

1.5. Screening methods for AEFB as BCAs of cucurbit powdery mildew

The performance of a candidate BCA in the laboratory is often not comparable to its field performance, and this limitation has been seen as a significant obstacle to the acceptance of biocontrol in agriculture (Jijakli and Lepoivre, 1998). A primary cause of BCA failure under field conditions has been attributed to *in vitro* culture practices. Extended periods of culturing on nutrient-rich media have been linked to the loss of important wild-type characteristics, such as pili, flagella and the glycocalyx, which are essential to bacterial survival in their native habitat (Andrews,

1990; Knudsen and Spurr, 1988). Despite microbial adaptability in gene expression, the maintenance of wild-type characteristics is essential in biocontrol to ensure the maximum degree of compatibility between the microbe and its environment, and will greatly increase the chances of isolating a stable BCA able to establish within the target habitat (Schisler and Slininger, 1997; Andrews, 1990). Schisler and Slininger (1997) summarise some key aspects which should be considered when isolating and evaluating BCA candidates:

- (i) Candidates should be isolated from areas where the disease can occur but is absent.
- (ii) The maximum numbers of isolates should be screened for biocontrol potential.
- (iii) Candidates should be isolated from appropriate plant parts grown under appropriate field conditions.
- (iv) *In vitro* assays and highly selective media should be avoided.
- (v) Bioassays should mimic field conditions.
- (vi) Isolate activity should be stable.
- (vii) Growth kinetics in liquid culture should favour formulation.

Preliminary screenings of large numbers of isolates for biocontrol suitability can be time-consuming and resource demanding. It is for this reason that dereplication steps are often included to streamline the numbers of isolates carried forward for further study (Ghyselinck *et al.*, 2011). Dereplication is a term commonly applied to natural product selection which involves separating previously studied organisms from a group of candidates (Dieckmann *et al.*, 2005). In microbiological terms a dereplication step involves separating “knowns” from “unknowns”, i.e. creating defined groupings from a large pool of isolates prior to further evaluation (Ghyselinck *et al.*, 2011). This step is seen to eliminate unnecessary time and resource expenditure by focussing further screenings on representatives of groupings defined by a dereplication step. Techniques applied for dereplication purposes should (Ghyselinck *et al.*, 2011):

- (i) Be universally applicable to all bacterial strains;
- (ii) Be robust;
- (iii) Yield data that is simple to process;
- (iv) Have high taxonomic resolution; and
- (v) Be high-throughput, have low operational costs and labour intensity.

The historical approach to achieve dereplication involved variations bacterial phenotypic characteristics. Due to several disadvantages of such methods and decreased costs and time

demands of newer technologies, alternative approaches have emerged as useful dereplication tools. Sequencing of genes to identify isolates can be applied for dereplication purposes; although cost and processing time requirements of gene sequencing have yielded to higher-throughput methods such as DNA fingerprinting and whole-cell analyses as techniques better suited for the purposes of preliminary study (Dieckmann *et al.*, 2005). Modern approaches applied to dereplication include repetitive element sequence based PCR (rep-PCR), RAPD-PCR, fatty acid methyl ester (FAME) analyses, and several mass spectrometry techniques including MALDI-TOF-MS (Ghyselinck *et al.*, 2011; Dieckmann *et al.*, 2005).

1.5.1. Isolation and characterisation of AEFB

The resilience of bacterial endospores makes AEFB relatively simple to target during isolation from their respective habitats. Heat treatment for the selection of endospores and the consequent plating of samples onto suitable medium is a common means of isolating AEFB (Schleifer, 2009). Media fortified with selective antimicrobial compounds can be employed, although the heat treatment method of endospore isolation remains the easiest and simplest method (Alvindia and Natsuaki, 2009; Zhang *et al.*, 2008; Yoshida *et al.*, 2001; Mizuki *et al.*, 1999).

Colonies which grow after heat treatment may then be selected randomly for screening, or by differentiating phenotypic characteristics or morphological traits (Schleifer, 2009). The evaluation of cell appearance can allow further discrimination between isolates to be made using bright field microscopy (*viz.* cell size, diameter, rod morphology, endospore location, and sporangial distension by the forming endospore). Metabolic phenotypic traits can also be used to differentiate between species and strains (Logan *et al.*, 2009; Schleifer, 2009).

1.5.2. Genetic fingerprinting to assess AEFB diversity

Reliability, time demands, and cost factors associated with phenotyping has resulted in bacterial differentiation based on metabolic characteristics being replaced by DNA-based means of bacterial strain differentiation (Li *et al.*, 2009; Olsen and Woese, 1993). Currently, genotyping is widely used to distinguish between closely related bacterial species and strains because it is able to provide the high resolution required (Li *et al.*, 2009). Methods of bacterial strain typing can be divided into three categories (Li *et al.*, 2009):

- (i) DNA banding patterns separate strains by their DNA fragment sizes after amplification protocols or restriction enzyme digest (i.e. DNA fingerprinting);
- (ii) DNA sequencing examines polymorphisms within a genomic DNA sequence; and
- (iii) DNA-DNA hybridisation uses DNA macro- and micro-array studies, whereby strains are differentiated by hybridisation of probes to known sequences in the genome.

In prokaryotes there exist repetitive sequences spread throughout the genome, whose length and frequency are exploited as a means of fingerprinting (van Belkum, 1994). Alternately, tRNA sequences, protein structure genes, and gene expression regulators which occur frequently in the genome may be selected for (van Belkum, 1994). PCR-based genotyping studies rely on separation by gel electrophoresis to resolve the amplified DNA segments into their respective fingerprints (Olive and Bean, 1999). The resultant PCR amplicons will arise from either the presence of the specific target site or the distance between sites of primer annealing, depending on the type of PCR-primer protocol applied (van Belkum, 1994).

Factors considered in selecting a genetic fingerprinting technique include ease of interpretation, ease of application, level of technical difficulty, cost, and time required (Olive and Bean, 1999). Within the scope of this study, methods applied for DNA fingerprinting of AEFB isolates were intergenic spacer region PCR (ITS-PCR) and randomly amplified polymorphic DNA PCR (RAPD-PCR), which will be further described below.

1.5.2.1. Fingerprinting of AEFB using RAPD-PCR

RAPD-PCR has been employed in microbiology for differentiation between bacterial isolates because it provides a high taxonomic resolution up to subspecies and strain levels. This technique has been successfully applied in the study of AEFB in both environmental and medical isolates (Kwon *et al.*, 2009; Li *et al.*, 2009; Rademaker *et al.*, 2005; Nilsson *et al.*, 1998; Tyler *et al.*, 1997). RAPD-PCR fingerprinting employs randomly sequenced, DNA oligonucleotide primers of 9–10 base pairs in length, which will anneal to sites throughout the genome aided by non-stringent annealing temperatures (Li *et al.*, 2009; Rademaker *et al.*, 2005; van Belkum, 1994).

Amplimers in RAPD protocols arise from two primers annealing at separate locations, resulting in a product the length between these two points (Li *et al.*, 2009; Olive and Bean, 1999). The number and location of these random sites of compatible annealing throughout the genome are variable between bacterial strains, representing a means by which to discriminate between close relatives (Li *et al.*, 2009; Ranjard *et al.*, 2000; Olive and Bean, 1999). The migration patterns of the variable-length products are visualised on agarose or acrylamide gels (Li *et al.*, 2009). In theory, the arbitrary primers will detect polymorphisms arising from deletions, mutations, or insertions to distinguish the strain or species by a distinct DNA fragment pattern (i.e. fingerprint) (Olive and Bean, 1999; Tyler *et al.*, 1997).

Compared to other PCR-based strain differentiation methods, RAPD-PCR is fast, sensitive and relatively inexpensive (Li *et al.*, 2009). Furthermore, the arbitrary primers are empirically designed and no previous knowledge of a target sequence is required (Rademaker *et al.*, 2005). However, as RAPD is not targetted at any specific locus in the genome, it is more easily influenced by DNA and primer concentration, to the extent that changes in these variables may see amplification of new targets or the reduced amplification of others (Li *et al.*, 2009; Olive and Bean, 1999; Tyler *et al.*, 1997). Furthermore, RAPD-PCR works best with a pure DNA template (Rademaker *et al.*, 2005).

The RAPD-PCR fingerprint patterns derived after electrophoresis may be complex and issues in interpretations may compromise the suitability of the method as a reliable and reproducible subtyping technique (Olive and Bean, 1999). Analysis of RAPD profiles has been greatly assisted by computer-aided analyses (Rademaker *et al.*, 2005). Methods used in genotyping for strain differentiation require reproducibility to be fully trusted, and the main disadvantage to RAPD protocols is low reproducibility, making comparison among laboratories difficult (Li *et al.*, 2009; Tyler *et al.*, 1997). However, there are commercially available kits for RAPD-PCR which may assist in addressing some of this variability (Li *et al.*, 2009). The worth of RAPD-PCR lies in its suitability for in-house comparisons of environmental bacterial strains, where resolution to strain level is highly valued for comparison and dereplication among a set of isolates (Logan *et al.*, 2009; Rademaker *et al.*, 2005).

1.5.2.2. Fingerprinting of AEFB using ITS-PCR

The 16S ribosomal RNA (rRNA) subunit sequence is highly conserved in bacteria and therefore exhibits limited variability for the purposes of bacterial strain differentiation (Shaver *et al.*, 2001). This invariability necessitates the utilisation of non-coding sequences under less selection pressure than coding genes (Li *et al.*, 2009). The intergenic spacers (ITS) (or intergenic spacer regions (ISR)) located between the 16S–23S rRNA subunit genes are sufficiently hypervariable in sequences and lengths to be suitable for bacterial strain typing (Daffonchio *et al.*, 2003; Shaver *et al.*, 2001; Mileham, 1997).

ITS-PCR employs universal primers with 3' ends facing outward from the 16S and 23S genes, resulting in a string of amplicons unique to a strain or species (Daffonchio *et al.*, 1998a). ITS-PCR shows great promise in the discrimination of AEFB species (Dingman, 2012; Martínez and Siñeriz, 2004; Xu and Cote, 2003; Shaver *et al.*, 2001). *Bacillus* and related genera have multiple ribosomal operons in their genomes, with members of the *B. cereus* group having as many as 12, and reference strain *B. subtilis* 168 possessing 10 operons (Daffonchio *et al.*, 2003; Shaver *et al.*, 2001). Within these operons the ITS lengths vary and, given variable mutations, the PCR amplification can generate species-specific banding patterns (i.e. fingerprints) after separation on low-resolution gel electrophoresis (Daffonchio *et al.*, 2003; Shaver *et al.*, 2001). However, this technique has been shown to fail to sufficiently differentiate between closely related species in a group, yet it is useful as a supplementary technique when different fingerprinting methods are being compared (Daffonchio *et al.*, 1998a).

1.5.3. DNA sequence polymorphisms for AEFB differentiation

16S rRNA gene sequencing is widely regarded as the benchmark for bacterial species identification (Maughan and Van der Avera, 2011). However, recent advances in bacterial strain typing have shown that 16S rRNA does not always differentiate between closely related species, as is the case for members of the *B. cereus* and *B. subtilis* groups of related taxa (Maughan and Van der Avera, 2011; Daffonchio *et al.*, 1998b). Consequently, alternate gene sequences have been used to distinguish these organisms at the species level. Genes used to differentiate AEFB species include: gyrase subunit A (*gyrA*) (Roberts *et al.*, 1994); gyrase subunit B (Dickinson *et al.*, 2004a); histidine kinase (*cheA*) (Borriss *et al.*, 2011); RNA polymerase subunit B (*rpoB*); DNA polymerase III subunit alpha (*polC*); heat-shock protein groEL (*groEL*); phosphoribosylaminoimidazolecarbox-amide

formyltransferase (*purH*) (Rooney *et al.*, 2009); alpha-amylase gene (*amyA* and *amyB*); and genes for antibiotic resistance (*tetB* and *tetL*) (Reva *et al.*, 2004). Gyrase subunit A sequences have shown sufficient sequence heterogeneity to allow closely related members of the *B. subtilis* group to be distinguished and was therefore chosen for the current study (Chun and Bae, 2000).

1.5.4. Antifungal activity screening and assessment of powdery mildew antagonism

Initial antagonism screenings of BCA candidates can assist in saving time and resources if performance in an assay can be directly translated to performance in the field (Anith *et al.*, 2003). Traditionally, plant disease BCAs have been discovered by applying empirical approaches to screening using simple *in vitro* bioassays (Spurr, 1985). These bioassays are typically designed around specific characteristics of the disease and antagonist mode of action, and serve as simple evaluation systems to screen potential antagonists in a regulated environment (Spurr, 1985). Primary bioassays are usually qualitative *in vitro* tests involving potential microbial agents and the target plant pathogen(s). However, secondary bioassays using the plant host and pathogen in a controlled environment (*in vivo*) strengthen the likelihood of antagonists being identified (Spurr, 1985).

In vitro dual-culture bioassays allow visualisation of broad-spectrum antimicrobial compound activity (Raaijmakers *et al.*, 2002). The primary means of screening an isolate for antifungal activity involves either an agar-based dual-culture technique, or the observation of pathogen development on glass slides (Blakeman and Fokkema, 1982). The former technique provides evidence of antagonism which may involve mechanisms such as hyperparasitism or antibiosis, whereas other mechanisms such as nutrient competition and stimulation of host resistance are excluded, which can lead to a potentially useful isolate being overlooked (Blakeman and Fokkema, 1982). Hence, it is recommended that more than one type of *in vitro* bioassay be applied in order to evaluate as many antagonistic mechanisms as possible to determine the most versatile antagonist for use in biocontrol (Spurr, 1985).

Laboratory conditions lack the stresses prevalent in the field (e.g. limited nutrient or water availability, competition with the indigenous microflora) and are not truly representative of a natural habitat (Schliser and Slininger, 1997; Spurr, 1985). Consequently, interactions *in vitro* may not necessarily correlate to the *in vivo* state. Antagonistic actions *in vitro* are influenced by external

factors—such as medium pH and nutrient concentration—which may introduce a bias into the isolate's performance (Schlisler and Slininger, 1997; Leifert *et al.*, 1995). This phenomenon has been demonstrated by Leifert *et al.* (1995), where isolates *B. subtilis* CL27 and *B. pumilus* CL45 both showed similar antagonism in dual-culture bioassays, but showed marked differences in their ability to prevent damping-off *in vivo*. Furthermore, bioassays alone cannot provide conclusive information on the exact mechanisms the bacteria employ in fungal antagonism because inhibition may arise from interplay of many factors, such as antibiotic compounds, extracellular enzymes, and siderophores (Leifert *et al.*, 1995). Hence, while laboratory-based bioassays remain rapid and efficient means of screening large numbers of candidate antagonists, these assays run the risk of neglecting such mechanisms as induced resistance as the plant is not present in the interaction (Schisler and Slininger, 1997; Spurr, 1985).

The dual-culture bioassay has proven useful in determining antifungal ability of AEFB *in vitro* (Alvindia and Natsuaki, 2009; Chaurasia *et al.*, 2005; Ongena *et al.*, 2005a; Ongena *et al.*, 2005b; Romero *et al.*, 2004; Touré *et al.*, 2004; Yoshida *et al.*, 2001; Fravel and Spurr, 1977; Leifert *et al.*, 1995; May *et al.*, 1997). Indications of antagonism from both diffusible and volatile compounds produced by bacteria are often visible to the naked eye as morphological changes in the fungus (Chaurasia, 2005). In the case of biotrophic fungi, where laboratory culture is not possible, surrogate pathogens may be applied for the purposes of bioassay. Fungal species *Botrytis cinerea*, *Fusarium oxysporum* f. sp. *lycopersici*, *Rosellinia necatrix*, *Phytophthora cinnamomi*, *Rhizoctonia solani* and *Penicillium digitatum* have been used in studies of cucurbit powdery mildew as laboratory-culturable substitutes for the biotrophic pathogen (Romero *et al.*, 2004).

Despite the valuable information that can be gleaned from performing *in vitro* bioassays with surrogate fungal species, a screening protocol which includes the host plant, pathogen and antagonist offers a more realistic extrapolation of biocontrol performance (Anith *et al.*, 2003). The biotrophic nature of powdery mildew causal agents necessitates the use of field trials or whole-plant assays to confirm *in vitro* findings under field conditions, but field-scale testing demands resources and time. Therefore, smaller-scale screenings incorporating live host plant tissue provide a means of assessing isolate antagonism against biotrophic phytopathogens. One commonly used bioassay is the detached leaf assay, which allows for the study of biotrophic disease progress and suppression in

a controlled environment at a smaller scale (Tesfagiorgis, 2009; Romero *et al.*, 2007a; Romero *et al.*, 2003; Shishkoff and McGrath, 2002; Quinn and Powell, 1982).

A conventional detached leaf assay uses two stacked Petri dishes, with a small hole made through the bottom of the upper plate into the lid of the lower plate (Figure 1.3). The petiole of the leaf protrudes through these holes, into plant nutrient solution in the lower plate. The leaf itself then rests within the upper plate where it can be inoculated and examined. The lid of the upper plate is closed over the leaf to ensure a closed environment, maintain humidity, and lessen cross-contamination between treatments (Quinn and Powell, 1982). A similar method, as used by Shishkoff and McGrath (2002), involves the uppermost lid (Figure 1.3.c) replaced by an inverted drinking cup of suitable diameter.

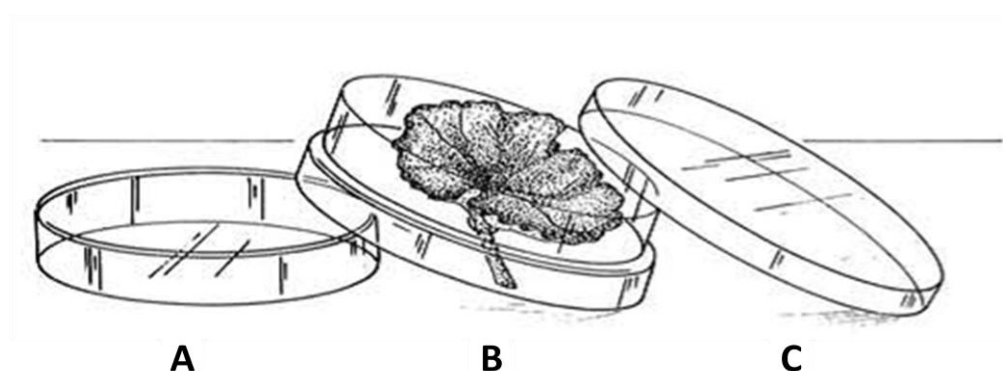


Figure 1.3. Diagram of the detached leaf assay, adapted from Quinn and Powell (1982) showing: (A) the lower Petri dish containing nutrient solution; (B) the joined lower plate lid and upper plate bottom, through which the leaf petiole extrudes; and (C) the upper plate lid used to protect the system from cross-over contamination and to maintain the microclimate.

Discs of cotyledonous tissue from a susceptible host plant species have been applied as an alternative to use of the adult leaf in the detached leaf assay (Fernández-Ortuño *et al.*, 2006; Romero *et al.*, 2004, Romero *et al.*, 2003). Discs are inoculated with the bacterial culture or extracted metabolites, and maintained on an agarised medium supplemented with carbohydrates and antimicrobial compounds to exclude contaminant microbes (Álvarez and Torés, 1997). The powdery mildew fungus can be applied by spraying a suspension of spores at a predetermined

concentration or by placing individual fungal spores onto the disc aided by a microscope (Fernández-Ortuño *et al.*, 2006; Shishkoff and McGrath, 2002). The treatments can then be examined microscopically and rated for disease presence and conidial germination incidence.

As discussed by Knudsen *et al.* (1997) a biocontrol pot trial presents a compromise between the laboratory-scale antagonism assays and full-scale field trials. Like field trials, biocontrol pot trials are carried out on susceptible host plants but on a more manageable scale under simulated field conditions. It has been found that antagonism potential on pot-scale screenings can be extrapolated to performance in the field (Teperi *et al.*, 1998). A biocontrol pot trial also lends itself to the evaluation of other disease control mechanisms and host–pathogen interactions (e.g. induced resistance in the host plant and BCA niche colonisation) and possible synergy between mechanisms (González-Sánchez *et al.*, 2010). Furthermore, the BCA may be able to colonise niches which may contribute to the protection of other parts of the plant biomass (Knudsen *et al.*, 1997). Factors such as culture age, growth medium, application method, and dosage can affect an antagonist’s efficacy in field and pot trials (Knudsen *et al.*, 1997). Hence, the impacts of some pertinent variables should be explored prior to full-scale field trials.

1.5.5. Lipopeptide compounds analysis and production potential in AEFB

1.5.5.1. Extraction and analysis of lipopeptide compounds

The spectrum of lipopeptide compounds that AEFB species produce has been reported extensively, along with the functions of these compounds in the bacteria–plant host relationship (Ongena *et al.*, 2010). Lipopeptide compounds, in particular, have attracted significant attention for their antagonistic potential against fungal phytopathogens and their functions in plant host colonisation and signalling (Jacques, 2011; Stein, 2005; Ongena and Jacques, 2008). There are various methods by which the extraction and analysis of lipopeptides can be carried out, as summarised by Gordillo and Maldonado (2012). Analysis techniques range from simple assays—such as drop collapse assay, tensiometry, haemolytic activity, turbidometric and spectrophotometric analysis, and thin-layer chromatography (TLC)—to advanced methods such as liquid chromatography, mass spectrometry, crystallography, nuclear magnetic resonance (NMR), Edman degradation, and ultraviolet (UV) and infrared spectrum analysis, (Gordillo and Maldonado, 2012; Athukorala *et al.*, 2009; Mukherjee *et al.*, 2009; Li *et al.*, 2008; Cazorla *et al.*, 2007; Raaijmakers *et al.*, 2006; Souto *et al.*, 2004; Wang *et al.*, 2004; Williams *et al.*, 2002; Razafindralambo *et al.*, 1993).

Methods of obtaining antimicrobial extracts from live cultures vary depending on the type of medium, culture optima, and medium constitution. For the biosurfactants produced by many AEFB species, the most common and perhaps simplest extraction involves acidifying the culture's cell-free supernatant and extracting the desired compounds using an appropriate solvent, or lyophilisation of the supernatant without solvent extraction (Das *et al.*, 2008; Hsieh *et al.*, 2008; Ji and Wilson, 2003; Leifert *et al.*, 1995). Extracted lipopeptides can be both qualified and quantified using TLC, and these can be achieved cost effectively using simple methods compared to other analysis techniques (Lin *et al.*, 1998b). Methods such as liquid chromatography and NMR likewise require pure compounds and, although demanding a higher degree of purity and costly equipment than TLC, the sensitivity and resolution achievable with these techniques is far higher (Souto *et al.*, 2004; Lin *et al.*, 1998b).

Mass spectrometry (MS) has also been widely applied in its various forms for lipopeptide analysis (Arguelles-Arias *et al.*, 2009; Li *et al.*, 2008; Price *et al.*, 2007; Tendulkar *et al.*, 2007; Madonna *et al.*, 2003; Vater *et al.*, 2002; Williams *et al.*, 2002; Leenders *et al.*, 1999). Mass spectrometry carries perhaps the most costly demand for specific equipment of all the methods which can be applied to lipopeptide identification. However the resolution of lipopeptide compound adducts and structures achievable with mass spectrometry is of great value (Price *et al.*, 1997). In particular MALDI-TOF-MS has proven to be effective in determining the presence of lipopeptide compounds produced by *Bacillus* spp. applying either compound extracts or whole cells (Price *et al.*, 2007; Koumoutsis *et al.*, 2004; Madonna *et al.*, 2003; Vater *et al.*, 2002; Leenders *et al.*, 1999).

1.5.5.2. Gene marker PCR to determine lipopeptide production potential

An alternative to laborious compound extraction and analysis is offered by the examination of genetic markers for lipopeptide synthesis, which may provide indications of production potential. These markers are contained within gene regions associated with the synthesis of lipopeptides, *viz.* within the non-ribosomal peptide synthetase (NRPS) or polyketide synthetase (PKS) genes (Fickers, 2012; Tapi *et al.*, 2010).

As discussed by Fickers (2012) and Tapi *et al.* (2010), each lipopeptide family is synthesised by open reading frames (ORFs) which vary in number between compounds and code for the various

modules. Surfactin comprises *srfA*-A, *srfA*-B, *srfA*-C, and *srfA*-D; plipastatins are encoded by *ppsA*, *ppsB*, *ppsC*, *ppsD* and *ppsE*; and fengycins by *fenC*, *fenD*, *fenE*, *fenA* and *fenB*. Iturins differ as they are created by a PKS–NRPS hybrid complex consisting of ORFs *ituD*, *ituA*, *ituB* and *ituC*. PCR-based targetting of these gene clusters can assist in screening large numbers of potentially antagonistic AEFB for lipopeptide synthesis capability, before performing compound extraction and analysis (Tapi *et al.*, 2010; Joshi and McSpadden Gardener, 2006). A number of genetic markers associated with lipopeptide biosynthesis in *Bacillus* spp. have been developed as a means of examining lipopeptide production capability, including *bmyB* (bacillomycin D), *fenD* and *fenB* (fengycin), *ituC* (iturin), and *srfA*-A and *srfA*-B (surfactin) (Athukorala *et al.*, 2009; Hsieh *et al.*, 2008; Joshi and McSpadden Gardener, 2006; Lin *et al.*, 1998a).

1.5.6. MALDI-TOF-MS for bacterial identification

MALDI-TOF-MS has been extensively applied in the field of microbiology to analyse microorganisms and their secondary metabolites, such as pigments and toxins (Carbonnelle *et al.*, 2011; Price *et al.*, 2007; Vater *et al.*, 2002; Lay, 2001; Wang *et al.*, 1998). Applications of MALDI-TOF-MS in proteomic microbial identification arose with the development of ‘intact-’ or ‘whole-cell’ mass spectrometry (IC-MS or WC-MS) which offers the advantage of analysing crude protein mixtures in cells without additional fractionation procedures (Welker and Moore, 2011; Wang *et al.*, 2004). Many of the peaks in IC-MS mass spectra represent ribosomal protein variants and fragments, detectable at the 3,000–20,000 Da range (Welker and Moore, 2011). The technique targets both internal and cell-surface proteins, with other less abundant structural proteins such as ribosomal modulation factors, carbon-storage regulators, cold-shock proteins, DNA binding proteins, and RNA chaperones also detectable (Welker and Moore, 2011; Dare, 2006).

For bacterial identification IC-MS applies as few as 10^5 – 10^6 whole bacterial cells to generate mass spectra (Welker and Moore, 2011). Typically, sample preparation for IC-MS is a simple protocol (Figure 1.4) involving the placement of the culture grown on agar onto a target plate and the addition of a matrix compound prior to ionisation. Additional extraction steps prior to target plate inoculation can be included to provide cleaner spectra for certain microorganisms (e.g. yeast, mycobacteria, and spore-formers) and commonly involve 80% TFA or ethanol–formic acid extraction procedures (Šedo *et al.*, 2011; Welker and Moore, 2011; Freiwald and Sauer, 2009).

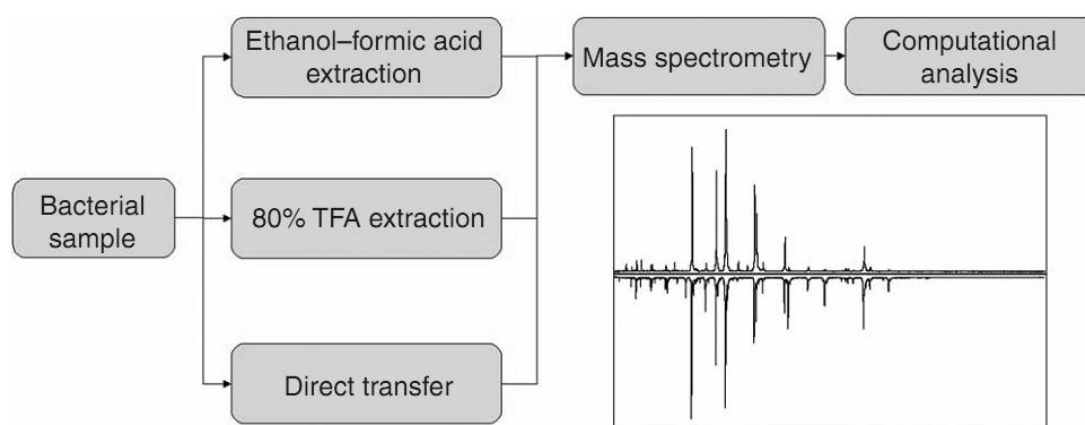


Figure 1.4. Diagrammatic representation of the process of intact cell MALDI-TOF-MS (IC-MS) analysis of bacterial isolates (Freiwald and Sauer, 2009).

Microbial identification using mass spectra involves spectral comparison to those in a reference database. This technique uses a list of the peaks' m/z values and intensities to produce a mass-fingerprint (Welker and Moore, 2011; Fox 2006). One or many peaks that remain conserved between different strains may be highlighted as protein biomarkers, which can be specifically applied in identifying bacteria at genus, species, and strain levels (Carbonnelle *et al.*, 2011; Lay, 2000; Wang *et al.*, 1998). Software-aided comparison to a database of reference strains generates a list of possible matches assigned a numerical value of similarity defined as the “score value” (MALDI Biotyper, Bruker Daltonics) or “confidence value” (SARAMIS, Anagnostec/BioMérieux) (Welker and Moore, 2011). Currently, a major restriction in the application of this technique to the characterisation of environmental isolates is the limited nature of standardised databases of reference strains (Welker and Moore, 2011; Dickinson *et al.*, 2004b). However, it is possible to generate supplementary mass spectra libraries of bacterial species and strains specifically relevant to the area of study (Welker and Moore, 2011). Patterns of protein masses in mass spectra can also be analysed by other methods, including cluster analysis, hierarchical clustering, and inter-spectra analysis to determine spectral diversity within a set of isolates, and as compared to reference strains (Fernández-No *et al.*, 2013; Freiwald and Sauer, 2009; Sauer *et al.*, 2008; Alm *et al.*, 2006).

Replicate mass spectra are required for accurate interpretation and pattern recognition, hence spectral reproducibility is important for microbial characterisation (Dare, 2006; Wunschel *et al.*, 2005; Keys *et al.*, 2004; Lay, 2001; Wang *et al.*, 1998). Standardisation of materials and protocols is critical because peaks are affected by the manner of sample preparation, culture growth phase and conditions, sample storage, sample numbers, specified mass range used, laser energy, instrumentation, and mass drift experienced during analysis (Carbonnelle *et al.*, 2011; Pavankumar *et al.*, 2011; Wunschel *et al.*, 2007; Dare, 2006; Valentine *et al.*, 2005; Keys *et al.*, 2004; Lay, 2000; Saenz *et al.*, 1999; Wang *et al.*, 1998). When applied to bacterial identification, MALDI-TOF MS represents a rapid and sensitive means of protein profiling with high resolution and reproducibility. Despite the requirement for expensive instruments and complex data handling, mass spectrometry-based bacterial fingerprinting and identification is rapid, simple to prepare, costs little to run, and can process large numbers of isolates (Ghyselinck *et al.*, 2011; Welker and Moore, 2011; Schleifer, 2009; Dare, 2006; Dickinson *et al.*, 2004b). Furthermore, the strain-level resolution achievable with MALDI-TOF-MS is higher than the more commonly used DNA electrophoresis or other protein profiling methods (Ghyselinck *et al.*, 2011; Welker and Moore, 2011).

1.6. Conclusion

The key to a successful biocontrol strategy lies in gaining as much information as possible about the candidate BCA and its capabilities to establish within the intended habitat and antagonise phytopathogens (Schisler and Slininger, 1997; Knudsen and Spurr, 1988). It is essential to screen large numbers of potential candidates against the target pathogen(s) under conditions representative of the intended habitat. A polyphasic screening approach applying high-throughput protocols is recommended to highlight candidates with the greatest potential prior to field-scale testing (Schisler and Slininger, 1997).

Several members of the AEFB are ideal candidates for application in biocontrol as their ecology in agriculture, genetics, and lipopeptide compounds have been intensively studied (Govindasamy *et al.*, 2010; Ongena and Jacques, 2008; Cawoy *et al.*, 2011; Jacobsen *et al.*, 2004; McSpadden Gardener and Diks, 2004). Furthermore, the success of some AEFB species BCAs has been widely established. Certain *Bacillus* spp. have been successfully commercialised for the control of a variety of phytopathogens, most notably strains of *B. subtilis* and *B. amyloliquefaciens* (Borriss, 2011; Cawoy *et al.*, 2011; Pérez-García *et al.*, 2011). *Bacillus subtilis* isolates have shown remarkable success in

antagonism toward *P. fusca*, a causal agent of powdery mildew on cucurbits (Romero *et al.*, 2007a; Romero *et al.*, 2007b; Romero *et al.*, 2004).

This study aims to isolate and screen for plant-associated, phyllosphere-competent AEFB that are antagonistic towards cucurbit powdery mildew. The screening of leaf-dwelling AEFB as antagonists of *P. fusca* represents an opportunity to apply a polyphasic approach to BCA selection against an obligately biotrophic disease which is not readily assayed *in vitro*. Since AEFB are easily isolated from a range of plant hosts, and are present in a variety of agricultural settings, the possibility of finding promising candidates for BCAs application is high. This situation therefore provides a basis from which to examine the ideal attributes of an AEFB isolate as a powdery mildew antagonist.

The objectives of this study can be summarised as follows:

- (i) Isolation of a pool of phyllosphere-dwelling AEFB from a range of cucurbit species.
- (ii) Screen AEFB isolates for antifungal activity *in vitro* against surrogate fungal pathogens.
- (iii) Differentiation and grouping of AEFB isolates using of genotyping methods.
- (iv) To characterise lipopeptide production amongst selected representative isolates using various screening methods.
- (v) Evaluating the detached leaf assay as a means of laboratory-based assessment of isolates antagonistic towards cucurbit powdery mildew.
- (vi) Evaluating biocontrol potential of selected isolates against *P. fusca* in *in vitro* and *in vivo* pot trials.

CHAPTER TWO

Preliminary assessment of antifungal activity and diversity amongst AEFB isolated from the leaf material of various cucurbit species

2.1. Introduction

Several members of the AEFB have gained prominence as potent BCAs due to their activities within the phytosphere, which have resulted in a number of strains being commercialised as biopesticides and biofertilisers (Jacobsen *et al.*, 2004; McSpadden Gardener, 2004). Many of these bacteria produce a range of antimicrobial compounds active against fungal, oomycete, and bacterial plant pathogens (Velho *et al.*, 2011; Govindasamy *et al.*, 2010; Nagórksa *et al.*, 2007; Pryor *et al.*, 2007; Emmert and Handelsman, 1999; Bélanger *et al.*, 1998). In addition, some plant-associated AEFB species are able to contribute to plant growth promotion through various mechanisms, such as: nutrient solubilisation, plant growth hormone production, and the stimulation of host plant resistance mechanisms (Heydari and Pessarakli, 2010; Choudhary *et al.*, 2009; Bargabus *et al.*, 2004; Kloepper *et al.*, 2004; McSpadden Gardener, 2004).

Much of the focus on AEFB as potential biocontrol agents has fallen on their activity within the rhizosphere. However, members of this grouping are also common residents of the phyllosphere, with some having been successfully applied as foliar disease antagonists (Collins *et al.*, 2003; Bargabus *et al.*, 2002; Nair *et al.*, 2002). A number of *Bacillus* spp. are able to establish in this habitat, and their activities within the phyllosphere have enabled their use as biocontrol agents against a range of foliar diseases, including: powdery mildew of cucurbits, *Cercospora* leaf spot on sugar beet, and *Colletotrichum dematium* on mulberry (Romero *et al.*, 2004; Collins and Jacobsen, 2003; Yoshida *et al.*, 2001; Bettiol, 1997). The successful colonisation of the leaf surface by introduced microbes is impacted by the manner in which biocontrol agents are applied as well as by the prevailing phyllosphere conditions (Lindow, 2006; Andrews, 1992; Andrews, 1990; Knudsen and Spurr, 1988).

Screening of candidate BCAs requires evaluation of a large pool of isolates to minimise the risk of excluding promising candidates. Dereplication steps are often included after initial isolate culture as

a means of streamlining candidate numbers and selecting representative isolates from groupings for further study (Ghyselinck *et al.*, 2011). Dereplication allows taxonomic-level differentiation and subsequent grouping of isolates with the aim of minimising time and resource wastage and unnecessary downstream analyses (Ghyselinck *et al.*, 2011). Phenotypic characterisation has, until recently, been the principal means by which bacteria were identified and their species-level diversity assessed. However, this approach does not readily distinguish between closely-related organisms, and thus is unsuitable for differentiation of closely-related isolates, and cannot resolve strain-level variations (van Belkum, 1994). Hence, molecular approaches have largely superseded phenotypic characterisation methods (Li *et al.*, 2009). Since dereplication is achieved by grouping isolates at a taxonomic level, the accessibility and resolution of genotyping methods greatly increases the ability to accurately differentiate and group bacterial isolates. There is a wide range of high-throughput PCR-based methods suitable for dereplication purposes, including commonly-used DNA fingerprinting approaches (Ghyselinck *et al.*, 2011).

DNA fingerprinting is often employed as a means of assessing strain diversity amongst a set of bacterial isolates (Ghyselinck *et al.*, 2011; van Belkum, 1994). This approach exploits genetic polymorphisms to differentiate between microorganisms based on differences in banding patterns generated by PCR amplicons after gel electrophoresis (Daffonchio *et al.*, 2003; Shaver *et al.*, 2001; Tyler *et al.*, 1997; van Belkum, 1994). Isolates displaying the same fingerprint can generally be assumed to belong to the same species or strain (Logan *et al.*, 2009). Randomly amplified polymorphic DNA PCR (RAPD-PCR) and intergenic transcribed spacer region PCR (ITS-PCR) fingerprinting methods were selected for use in the present study. RAPD-PCR applies a single short primer (~ 10 bp) that anneals to compatible sites throughout the genome, which results in a series of variably-sized fragments in the PCR product (Li *et al.*, 2009; Olive and Bean, 1999). In contrast, ITS-PCR targets polymorphic differences within the intergenic transcribed spacer (ITS) region located between the 16S–23S rRNA subunit operons, which are under less conservation pressure than the adjacent rRNA genes (Li *et al.*, 2009; Daffonchio *et al.*, 2003; Shaver *et al.*, 2001; Nagpal *et al.*, 1998). Both of these fingerprinting methods have been successfully applied in the differentiation of *Bacillus* spp., with some studies showing that RAPD-PCR offers a greater degree of resolution at strain-level compared to ITS-PCR (Logan *et al.*, 2009; Martínez and Siñeriz, 2004; Daffonchio *et al.*, 2000; Daffonchio *et al.*, 1998a; Daffonchio *et al.*, 1998b).

Identifying promising candidate BCAs at the taxonomic level is important when isolating and evaluating for biocontrol potential. This knowledge can offer insight into ecotypes amongst isolates, and can provide information as to the bacterial species extant in the chosen environment. Although 16S rRNA gene sequencing is widely regarded as the standard for bacterial characterisation, it is often insufficiently heterogeneous to allow differentiation between closely-related species; particularly in certain of the *Bacillus* groups of related taxa (Maughan and Van der Awerda, 2011; Daffonchio *et al.*, 1998b). A range of alternate gene sequences have been used to differentiate AEFB species (Borriss *et al.*, 2011; Rooney *et al.*, 2009; Dickinson *et al.*, 2004a; Reva *et al.*, 2004; Roberts *et al.*, 1994). Sequences of gyrase subunit A (*gyrA*) have shown sufficient sequence heterogeneity to allow closely-related members of the *B. subtilis* group to be distinguished and was therefore chosen for the current study (Chun and Bae, 2000).

Mass spectrometry has been widely used for the study of proteins and compounds produced by bacteria (Dare, 2006). Recently, MALDI-TOF-MS has been applied to the identification of bacteria (Lay, 2000). Whole bacterial cell preparations have been used to generate *m/z* peak lists to produce mass-fingerprints which have been used for identification purposes (Welker and Moore, 2011; Fox 2006). The mass spectrum is then compared to spectra within a database, using matching analysis software to provide an identity match (Welker and Moore, 2011). Conserved biomarker peaks in mass spectra can be specifically applied to identify bacteria at genus, species and strain levels (Carbonnelle *et al.*, 2011; Lay, 2000; Wang *et al.*, 1998). Cluster and inter-spectra analysis can also be applied to examine spectral diversity within an isolate set, or between isolates and reference strains (Fernández-No *et al.*, 2013; Welker and Moore, 2011). Its ease-of-use and high-throughput has seen MALDI-TOF-MS applied for dereplication of bacterial isolates, assessments of genus- and species-level diversity within a set of isolates, and utilisation in taxonomic studies in microbiology (Ghyselinck *et al.*, 2011; Welker and Moore, 2011).

Since *Podosphaera fusca*, is a biotrophic fungus, screening for BCA presents a challenge to researchers as the pathogen cannot be cultured under laboratory conditions without living host tissue. However, certain fungal species culturable on agar media have been applied as surrogates to screen for potential biocontrol candidates of cucurbit powdery mildew, and include: *Botrytis cinerea*, *Fusarium oxysporum* fsp. *lycopersici*, *Rosellinia necatrix*, *Phytophthora cinnamomi* and *Penicillium digitatum* (Romero *et al.*, 2004). Consequently, surrogate pathogens have been applied in *in vitro* screening as a means of selecting for potential antagonists (Romero *et al.*, 2004; Tewelde, 2004).

A study was undertaken with the aim of isolating AEFB extant in the cucurbit phyllosphere and to screen them for antagonism of the foliar disease powdery mildew of cucurbits. Candidate AEFB isolates were assessed for antifungal activity *in vitro* using surrogate pathogens *Rhizoctonia solani* and *Botrytis cinerea*. Diversity amongst the selected isolates was then determined using RAPD- and ITS-PCR fingerprinting. Partial 16S rRNA and *gyrA* gene sequences were used to identify and differentiate selected isolates. The use of MALDI-TOF-MS to determine isolate diversity was also assessed.

2.2. Materials and Methods

2.2.1. Isolation of AEFB from cucurbit leaf material

Leaves from representative cucurbit species showing diminished powdery mildew symptoms were harvested from mature plants of: butternut (*Cucurbita moschata*), cucumber (*Cucumis sativa*), chayote (*Sechium edule*), marrow, gem squash, squash, and pumpkin (*Cucurbita pepo*). These plants were grown in soil or growing media at various sites in the greater Msunduzi area in KwaZulu-Natal, South Africa. A minimum of two leaves per plant were harvested, and 1–5 plants were sampled from each location. The leaf material was transported to the laboratory in plastic bags to prevent cross-contamination and processed on the same day of harvesting.

Bacterial isolation was carried out using a procedure modified from de Jager *et al.* (2001), whereby leaf discs were punched out from representative regions of the leaf using an aluminium pipe borer (diameter 1 cm). The borer was disinfected with ethanol (70% v/v) between each sampling. Leaf discs from replicate leaves of each individual plant were pooled and added to 20 ml sterile quarter-strength Ringer's solution. In order to dislodge surface-attached bacteria, sample bottles were vortexed for 15–20 minutes, followed by sonication for 15–20 minutes. The leaf discs were then removed from each bottle with sterile forceps and the remaining liquid filtered (Sterile Whatman no. 1 filter paper, 150 mm diameter) into sterile centrifuge tubes (50 ml) (Beckman Coulter) and centrifuged for 15 minutes at 12,096 x *g* (Avanti Centrifuge, Beckman Coulter). The supernatants were discarded and the pellets resuspended in 1 ml sterile quarter-strength Ringer's solution before being transferred into sterile 1.5 ml microfuge tubes, and heated at 80°C for 15 minutes in order to eliminate vegetative cells. Each sample was serially diluted to 10⁻⁴ and aliquots (0.1 ml) from each dilution were inoculated onto duplicate sterile tryptic soy agar (TSA) plates (Biolab, Merck, Germany)

using the standard spread plate method. Plates were incubated at 30°C for 24–48 hours. If a sample could not be inoculated immediately, the heat-treated spore suspensions were stored at -20°C until use.

Colonies with representative morphologies were selected from each set of agar plates (i.e. from each individual plant sampled), and streaked onto fresh TSA and incubated overnight at 30°C. These cultures were used for observations of colony morphology, and then inoculated into 10ml tryptic soy broth (TSB) (Biolab, Merck, Germany) and incubated for 24 h at 28°C and 150 rpm, before Gram staining to confirm the presence of Gram positive rods. Slides were viewed using bright-field microscopy and cell dimensions were estimated using an ocular graticule. The broth cultures were incubated further for 48 h and then evaluated for endospore formation by Gram staining and viewing prepared slides using bright field microscopy. Endospores were distinguished as hyaline regions within the parent cell.

To ensure culture purity isolates were streaked onto 10% (w/w) TSA, containing: 13.8 g/l TSA premix supplemented with 11.7 g/l bacteriological agar (Biolab, Merck, Germany). In order to maintain wild-type characteristics glycerol stock cultures (20 % v/v) of each AEFB isolate were prepared for long-term storage at -80°C. Isolates were first cultured in 10ml TSB at 28°C and 150 rpm for 24 h before being dispensed into cryotubes containing appropriate aliquots of sterile glycerol.

2.2.2. Assessment of antifungal activity of AEFB using dual-culture bioassays

Two fungal species, *Rhizoctonia solani* and *Botrytis cinerea*, obtained from the Discipline of Plant Pathology (University of KwaZulu-Natal) culture collection, were used in the dual-culture antifungal assays (Romero *et al.*, 2007a; Tewelde, 2004). To ensure purity fungal cultures were initially cultured on water agar (15 g/l bacteriological agar) before being subcultured onto potato dextrose agar (PDA) (Biolab, Merck, Germany) and incubated at 30°C. Subculturing was performed every 7 d to ensure culture viability.

Antifungal potential of AEFB isolates was investigated using a dual-culture bioassay method modified from Tewelde (2004). Sterile antibiotic discs (diameter 9 mm) (Macherey-Nagal, Germany)

were placed onto PDA plates (4 discs per plate) and inoculated with 20 µl of 24 h TSB culture ($\sim 10^8$ cells/ml). Plates were incubated overnight at 30°C before a PDA plug (5x5 mm) fully colonised with fungal mycelium was placed onto the centre of each plate. Bioassays were incubated at 30°C and examined periodically over a 14 d period in order to rate the extent of antifungal activity.

The presence and extent of inhibition zones were measured from bacterial colony edge to the fungal mycelium boundary. Visible changes in each test fungus after exposure to a bacterial culture was also noted. A rating system was developed to rank antifungal activity, where: (+++) denoted a zone of inhibition greater than 5 mm; (++) denoted a zone of inhibition 2–5 mm; (+) denoted a zone of inhibition less than 2 mm; and (-) denoted an absence of antifungal activity. Based on this information, isolates showing the greatest zones of inhibition and/or antifungal activity against both test fungi were carried forward for further characterisation and evaluation.

2.2.3. Genotyping and identification of AEFB isolates using DNA fingerprinting and gene fragment sequencing

Based on their ability to inhibit fungi under dual-culture bioassay conditions, isolates were selected for DNA fingerprinting using ITS-PCR and RAPD-PCR. This data was used to group isolates, with gene sequence analysis and bacterial identifications subsequently carried out on representative isolates. Evolutionary relationships between isolates were inferred through the construction of phylogenetic trees based on the sequences of the 16S rRNA (Garbeva *et al.*, 2003; Heuer *et al.*, 1997) and gyrase subunit A (*gyrA*) gene fragments (Roberts *et al.*, 1994). Primers used for the above-mentioned PCR protocols are listed in Table 2.1. Primers were synthesised and supplied by Inqaba Biotech™ Hatfield, Pretoria, South Africa.

Template DNA used for ITS-PCR was obtained directly from vegetative cells picked off from 10% TSA using a freeze-thaw DNA extraction technique modified from Moré *et al.* (1994). Briefly, single colonies picked off from 24 h 10% TSA culture were suspended in 50 µl ultrapure water; and subjected to 2–3 cycles of freezing (-20°C) for 10 minutes and heating (95°C) for 10 minutes. For the remaining PCR protocols (*viz.* RAPD-PCR, *gyrA*, and 16S rRNA) template DNA was extracted from isolates cultured (24 h) in Luria-Bertani (LB) broth (10 ml) using a Nucleospin DNA Extraction Kit

(Macherey-Nagal, Germany). DNA extraction was carried out as per the manufacturer's instructions, following the protocol recommended for Gram positive bacteria.

Table 2.1. PCR primers for diversity assessment and taxonomic classification of AEFB isolates.

Protocol	Primers	Sequence (5' – 3')	Expected Product Size	Reference
ITS-PCR	ISR-1494	GTCGTAACAAGGTAGCCGTA	Variable	Martínez and Siñeriz (2004)
	ISR-35	CAAGGCATCCACCGT		
RAPD-PCR	OPG-11	TGCCCCGTCGT	Variable	Daffonchio <i>et al.</i> (1998b)
16S rRNA	BacF	GGGAAACCGGGGCTAATACCGGAT	1187 bp	Heuer <i>et al.</i> (1997) Garbeva <i>et al.</i> (2003)
	R1378	CGGTGTGTACAAGGCCCGGAACG		
<i>gyrA</i>	p- <i>gyrA</i> -f	CAGTCAGGAAATGCGTACGTCCTT	892 bp	Roberts <i>et al.</i> (1994)
	p- <i>gyrA</i> -r	CAACGTAATGCTCCAGGCATTGCT		

All PCR reaction protocols were carried out using Promega GoTaq® PCR reagents (Promega, Madison, USA). Each PCR reaction consisted of the following: 0.4 µM of the appropriate primer(s) (Table 2.1); 1x GoTaq® Flexi Buffer (without MgCl₂); 200 µM of each deoxyribonucleotide (dNTP); 2.5 U GoTaq® polymerase; 1.5 mM MgCl₂; and 1 µl template DNA; and nuclease-free water (Promega, Madison, USA) to bring the final volume to 25 µl. The thermal cycler used in all the protocols was a Bioer XP Cycler Model TC-XP-G (Bioer Technology Co. Ltd., China). Each PCR protocol was conducted using the conditions specified in Table 2.2. Holding temperature after the PCR run was 4°C for all PCR protocols.

For all of the PCR protocols a negative (template-DNA free) and positive (previously amplified template DNA) control were included. Several reference strains belonging to the *Bacillus* genus were included in the DNA fingerprinting for comparative purposes. These included the type strains *B. amyloliquefaciens* DSM 7^T and *B. subtilis* subsp. *subtilis* DSM 10^T; and plant-associated strains (isolated previously from rhizosphere material) which, based on 16S rRNA sequencing, were previously identified as *B. amyloliquefaciens* subsp. *plantarum* strains R51 and R43; *B. subtilis* strain B81; and *B. cereus* strain R73 (Personal communication: Hunter, C. H.; Discipline of Microbiology, School of Life Sciences, University of KwaZulu-Natal, Private bag X01, South Africa).

Table 2.2. PCR reaction conditions for the primers used in DNA fingerprinting and gene fragment sequence analysis.

Protocol	Initialisation	PCR cycle (Temperature and duration)				Cycles
		Denaturation	Annealing	Elongation	Final Extension	
ITS	95°C/ 4 min	94°C/ 1 min	55°C/ 2 min	72°C/ 2 min	72°C/ 10 min	30
RAPD	94°C/ 4 min	94°C/ 1 min	36°C/ 1 min	72°C/ 30 sec	72°C/ 5 min	40
16S rRNA	94°C/ 5 min	94°C/ 1 min	65°C/ 90 sec	72°C/ 2 min	72°C/ 10 min	35
<i>gyrA</i>	95°C/ 2 min	95°C/ 1 min	60°C*/ 30 sec	72°C/ 1 min	72°C/ 5 min	30

* Optimised to 58°C for certain isolates

The PCR products were separated and visualised by agarose gel electrophoresis using a 1.5% agarose gel (Laboroiois Conda, Madrid, Spain) prepared with 1x Tris-Borate-Ethylenediaminetetraacetic acid (TBE) buffer (89 mM Tris base, 89 mM Boric acid and 2 mM EDTA, adjusted to pH 8.0). Gels were pre-stained with 1x SYBR Safe (Invitrogen, California, USA). The PCR products were prepared in final volumes of 5 µl per lane, with a ratio of 3 µl DNA to 2 µl loading dye (6x blue-orange) (Promega, Madison, USA). A 1 kb molecular weight ladder (Promega, Madison, USA) was used to determine product band sizes. Gels were run at 90 V for 50–60 minutes and images of each gel electrophoresis were captured under ultra violet (UV) light on SynGene G:Box using the Syngene GeneSnap software (version 7.09) (Syngene, Cambridge, England).

Isolate banding profiles used for DNA fingerprinting purposes were grouped visually based on banding pattern similarities. Representatives of each grouping were combined on a single gel for comparative purposes. Dendograms were subsequently generated for both the ITS- and RAPD-PCR gels using Syngene GeneTools software (version 4.01). The ITS-PCR dendogram was generated using the Unweighted Pair Group Method with Arithmetic Mean (UPGMA) method with matching parameters based on profile, Jaccard similarity coefficient, alignment by molecular weight, and a 1% tolerance. The RAPD-PCR dendogram also used UPGMA with matching parameters using profile, Jaccard similarity coefficient, alignment by position, and a 1% tolerance.

2.2.4. DNA sequencing of 16S rRNA and gyrase subunit A gene fragments

Amplicons from the 16S rRNA and *gyrA* gene fragment PCRs were sequenced using an ABI 3500XL Genetic analyser (Applied Biosystems, California, USA) at Inqaba Biotec Laboratories (Hatfield, Pretoria, South Africa) in order to generate phylogenetic trees from sequence data. The 16S rRNA gene fragment was sequenced using only the forward (BacF) primer, and the *gyrA* gene fragment was sequenced using both the forward and reverse primers (see Table 2.1). Sequences were visualised and edited in Chromas Lite (version 2.01) and BioEdit (version 7.1.3.0) (Hall, 1999) and consensus sequences aligned using MAFFT online (<http://mafft.cbrc.jp/alignment/server>). Subsequently, the nucleotide sequences were submitted to NCBI Blast (<http://blast.ncbi.nlm.nih.gov/Blast.cgi>) (Zhang *et al.*, 2000) for comparison to existing 16S rRNA and *gyrA* gene sequences in the GenBank database using the Megablast algorithm and NCBI whole genome database.

16S rRNA and *gyrA* gene sequences for selected reference strains of significant *Bacillus* spp. were also obtained from the GenBank database for comparative purposes (Date accessed: 20 March 2015). The reference sequences used for 16S rRNA gene sequence phylogenetic comparisons were: *Bacillus* sp. JS (NC017743.1), *B. amyloliquefaciens* subsp. *plantarum* YAU B9601-Y2 (NC017061.1), *B. amyloliquefaciens* subsp. *plantarum* CAU B946 (NC016784.1), *B. amyloliquefaciens* subsp. *plantarum* FZB42 (NC009725.1), *B. amyloliquefaciens* subsp. *amyloliquefaciens* KHG19 (CP007242.1), *B. amyloliquefaciens* subsp. *amyloliquefaciens* DSM 7 (NC014551.1), *B. subtilis* BSn5 (CP002468.1), *B. subtilis* QB928 (NC018520.1), *B. subtilis* subsp. *subtilis* RO-NN-1 (CP002906.1), *B. subtilis* subsp. *subtilis* NCIB 3610 (NZCM000488.1), *B. subtilis* subsp. *subtilis* 168 (NC000964.3), *B. subtilis* subsp. *subtilis* 6051-HGW (NC020507.1), *B. subtilis* subsp. *spizizenii* NRRL B-23049 (NR024931.1), *B. subtilis* subsp. *spizizenii* TU-B-10 (CP002905.1), *B. subtilis* subsp. *spizizenii* W23 (CP002183.1), *B. subtilis* subsp. *spizizenii* NRS 231 (CP010434.1), *B. inaquosus* NRRL BD-571 (EU138495.1), *B. tequilensis* NRRL B-41771 (EU138487.1), *B. mojavensis* NRRL BD-600 (EU138506.1), *B. cereus* ATCC 14579 (NC004722.1), and *B. megaterium* DSM 319 (NC014103.1). The outgroup sequence for the 16S rRNA gene sequence phylogenetic tree was *Staphylococcus pasteurii* ATCC51129 (NR024669.1).

The reference sequences used for *gyrA* gene sequence phylogenetic comparisons were: *Bacillus* sp. A053 (NZJXAJ01000001.1), *Bacillus* sp. JS (NC017743.1), *B. amyloliquefaciens* subsp. *plantarum* FZB42 (NC009725.1), *B. amyloliquefaciens* subsp. *plantarum* CAU B946 (NC016784.1), *B.*

amyloliquefaciens subsp. *plantarum* YAU B9601-Y2 (NC017061.1), *B. amyloliquefaciens* subsp. *amyloliquefaciens* KHG19 (CP007242.1), *B. amyloliquefaciens* subsp. *amyloliquefaciens* DSM7 (NC014551.1), *B. amyloliquefaciens* L-H15 (CP010556.1), *B. amyloliquefaciens* IT-45 (NC020272.1), *B. amyloliquefaciens* X1 (NZJQNZ01000021.1), *B. amyloliquefaciens* SQR9 (CP006890.1), *B. amyloliquefaciens* LFB112 (NC023073.1), *B. subtilis* ATCC 19217 (CP009749.1), *B. subtilis* BSn5 (CP002468.1), *B. subtilis* XF-1 (CP004019.1), *B. subtilis* GXA-28 (NZJPNZ01000003.1), *B. subtilis* subsp. *subtilis* 168 (NC000964.3), *B. subtilis* subsp. *subtilis* BAB-1 (CP004405.1), *B. subtilis* subsp. *subtilis* 3NA (NZCP010314.1), *B. subtilis* subsp. *spizizenii* TU-B-10 (CP002905.1), *B. subtilis* subsp. *spizizenii* W23 (CP002183.1), *B. subtilis* subsp. *spizizenii* NRS 231 (CP010434.1), *B. atrophaeus* NRRL NRS-213 (EU138654.1), *B. mojavensis* NRRL BD-600 (EU138644.1), *B. inaquosus* NRRL BD-571 (EU138633.1), *B. tequilensis* NRRL B-41771 (EU138625.1), *B. megaterium* DSM 319 (NC014103.1), and *B. cereus* ATCC 14579 (NC004722.1). The outgroup sequence for the phylogenetic tree of the *gyrA* gene sequences was *Peptoclostridium difficile* 630 (NC009089.1).

Phylogenetic trees for 16S rRNA and *gyrA* gene fragment sequences were generated using MEGA6 software (version 6.0) (Tamura *et al.*, 2013) and aligned using MUSCLE in MEGA6 (Edgar, 2004). Evolutionary relationships between the isolates were inferred using the Neighbour-Joining method, incorporating a 1000 replicate bootstrap test (Tamura *et al.*, 2004; Saitou and Nei, 1987; Felsenstein, 1985) and evolutionary distances were computed using the Jukes-Cantor method (Jukes and Cantor, 1969). The trees were drawn to scale, with branch lengths in the same units as those of the evolutionary distances used to infer the phylogenetic tree. All positions containing gaps and missing data were eliminated.

2.2.5. AEFB classification using MALDI-TOF-MS

Analysis of selected AEFB isolates was carried out using a bench-top Bruker Microflex L20 MALDI-TOF mass spectrometer (Bruker Daltonics, Germany) equipped with an N₂ laser (337 nm). Mass spectra were generated, processed and analysed using FlexControl (version 2.4), and the laser energy level automatically optimised using the AutoX method (MBT_AutoX.axe) function of the FlexControl operation. For calibration purposes an *Escherichia coli* DH5 α Bacterial Test Standard (BTS) (Bruker Daltonics) (Mass range: 3637.8–16957.4 Da) (Bruker Daltonics, Germany) was included in each analytical run. The matrix solution used was α -cyano-hydroxycinnamic acid (HCCA) (Bruker Daltonics). The HCCA was dissolved in 50% (v/v) acetonitrile and 2.5% (v/v) trifluoroacetic acid to

provide a final concentration of 10 mg HCCA/ml. The protocol applied was as recommended and specified in the Bruker Daltonics operating manual.

AEFB cultures were prepared for MALDI-TOF-MS following an ethanol-formic acid extraction procedure outlined in the Bruker Daltonics operations manual; whereby bacterial colonies picked off from a 24 h TSA plate were suspended in 200 μ l of ultra-pure water dispensed into 1.5 ml microfuge tubes. Nine hundred microlitres of absolute ethanol was then added to each cell suspension before homogenisation. Each tube was centrifuged at 15,996 $\times g$ for 2 minutes after which the supernatants were removed, and the cell pellets air dried. Pellets were then resuspended in 10 μ l of 70% (v/v) aqueous formic acid and an equal volume of pure acetonitrile. Tubes were centrifuged again at 15,996 $\times g$ for 2 minutes and 1 μ l of each resultant supernatant was spotted onto a stainless steel target plate, air-dried and overlaid with an equal volume of HCCA matrix.

Spectra for bacterial identification purposes were acquired in positive reflector mode in the 1.9–20.1 kDa range were detected by measuring 40 laser shots from six different positions per spot. Spectra analysis was carried out using MALDI Biotyper (version 3.0) software (Bruker Daltonics, Germany). This software compared the spectra for each isolate to the spectra contained within the Biotyper Reference Library 1.0 (version 3.1.2 (2011)), and assigned each isolate an identity supported by a score value. The confidence of the isolate identity was denoted as follows: Highly probable genus and species identification (score 2.300–3.000); secure genus and probable species identification (score 2.000–2.299); probable genus identification (1.700–1.999); no consistency in genus or species (score 0.000–1.699).

Generation of phyloproteomic dendograms was achieved by the generation of a mass spectra profile (MSP) for each of the AEFB isolates. Bacterial samples were prepared for analysis as described above, with each bacterial sample spotted in ten replicate spots on the target plate, in addition to a single BTS calibrant spot per isolate set. The mass spectra were generated with the laser in positive linear mode, as the mean of 240 laser shots per spectrum (generated after 40 shots in six positions) at 60Hz in the mass range of 1.9–20.1 kDa. The ten test spots were analysed three times each for a total of 30 spectra per bacterial sample. Spectral processing and analysis was carried out using FlexControl (version 2.4), with MALDI Biotyper and FlexAnalysis software used for the creation of an MSP library, from which dendograms were created.

Independent cluster analysis of the MSPs was performed using SPECLUST (<http://bioinfo.thep.lu.se/speclust.html>) (Alm et al., 2006). Ten of the mass spectra profiles generated for each isolate underwent baseline subtraction (Precision set at 100, relative offset at 90), smoothing (Gaussian method, window size 0.3 m/z , with 2 cycles) and peak picking (S/N threshold 3.0, absolute intensity threshold 1.0, relative intensity threshold 5%, picking height at 80) using mMass open source software (version 5.5.0) (Niedermeyer and Strohm, 2012; Strohm et al., 2010; Strohm et al., 2008). The ten peak lists generated for each isolate were submitted to SPECLUST for the identification of common peaks. The parameters for the peaks-in-common SPECLUST function were defined as pairwise score cut-off of 0.7, measurement error of 5.0 Da, and multiple score cut-off of 0. From the SPECLUST consensus peak lists, peaks appearing nine or more times in an isolate's mass spectra were deemed sufficiently representative and retained for generation of the final peak list for that isolate. The final peak list for the 14 isolates underwent cluster analysis in SPECLUST to render a dendrogram of relatedness, with the parameters "metric" as liberal, "linkage" as average, and σ (sigma value) set to 1.0 Da.

2.3. Results

2.3.1. *In vitro* screening for antifungal ability using dual-culture bioassays

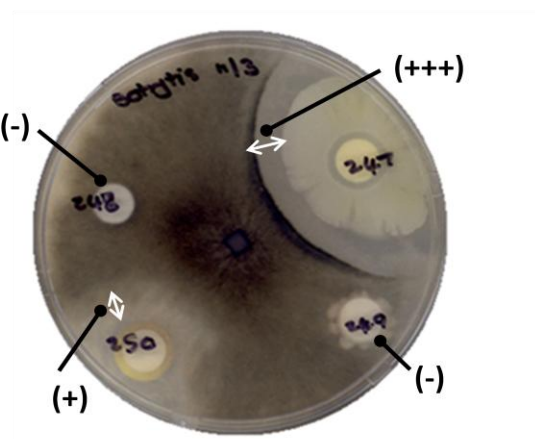
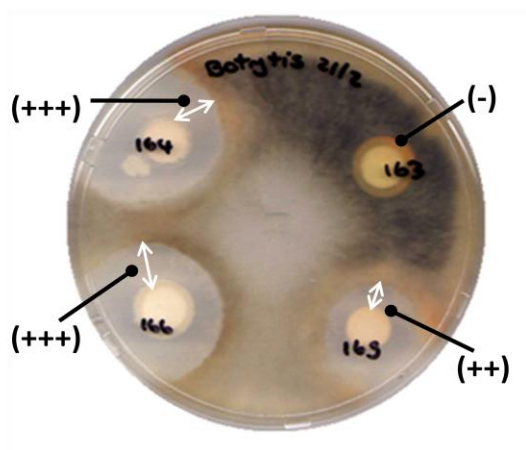
Of the 309 AEFB isolates screened, 151 isolates showed antifungal activity. Isolates antagonistic toward the test fungi were isolated from all the cucurbit host plant species sampled. For rating purposes the level of fungal antagonism was assessed at 2, 5, and 14 d; since these intervals were found to yield the most useful data. Examples of the rating system used to rank the degree of fungal antagonism observed, are presented in Plate 2.1. Control plates for both fungal species tested were fully colonised within 48 hours, though *R. solani* appeared to grow slightly faster than *B. cinerea*. Approximately 73% (110) of the isolates exhibiting antifungal capacity showed activity against both fungi. Specific antagonism towards *B. cinerea* was noted in 34 isolates (~23%); whereas only seven isolates (~4%) exhibited exclusive antagonism towards *R. solani*. *Botrytis cinerea* appeared to be more sensitive to bacterial antagonism than *R. solani* and generally produced larger, more sustained zones of inhibition over the incubation period. Of the antagonistic isolates screened, 54 were selected for further characterisation and evaluation (Table 2.3). These isolates were chosen based on an antagonism rating of (++) or greater at day 5 against *B. cinerea*, and where antifungal activity was still in evidence after 14 d of incubation.

Fungal antagonism was also characterised according changes in mycelium appearance, usually in the region adjacent to the zone of inhibition. These changes were evident in both fungi, and became more prominent over time. However, not all bacterial isolates screened produced the same antagonism response, and distinctions between dual-culture interactions could be made on this basis. For *R. solani* mycelial changes included mycelial thinning or thickening at the inhibition zone interface. In all but five of the isolates exhibiting antifungal activity *R. solani* mycelia exhibited a progressive “browning” which was evident from 3 d onwards (Plate 2.2). *Botrytis cinerea* mycelium showed mycelial thinning which was usually accompanied by “yellowing” of the hyphae and the appearance of a darkened ring at the periphery of the inhibition zone from 6 d onwards (Plate 2.3). For both fungi, colour changes became more prominent over time.

For most isolates antifungal activity was distinguished within 2–3 d post fungal inoculation. However, a significant number of isolates showed a fungistatic response from day 5 onwards, whereby the test fungi overgrow the zones of inhibition (Plate 2.4). Of the 54 antagonistic isolates selected for further characterisation (Table 2.1) 41 (~76%) showed a fungistatic response towards *R. solani* by day 14, whereas only 23 (~43%) isolates did so against *B. cinerea*. Overall, a greater number of isolates scored higher on the rating system for sustained, high levels of activity against *B. cinerea* than for *R. solani*.

A common occurrence associated with the *B. cinerea* dual-culture bioassay plates was the appearance of a pink to red colouration in the PDA medium adjacent to bacterial colonies after several days of incubation (Plate 2.5). This colour development was associated with isolates showing pronounced fungal antagonism that did not alter over time. The phenomenon was not observed in the *R. solani* dual-culture bioassays, or when isolates were cultured without fungus on TSA or 10% TSA.

Botrytis cinerea



Rhizoctonia solani

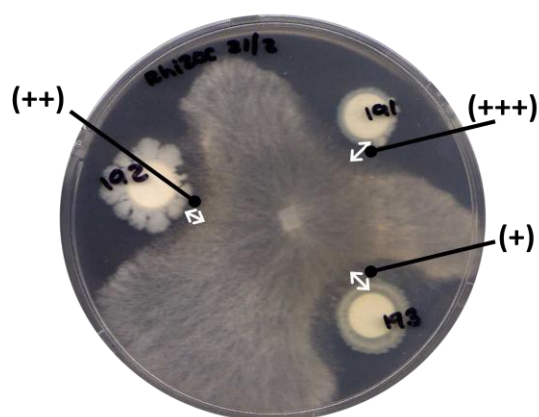
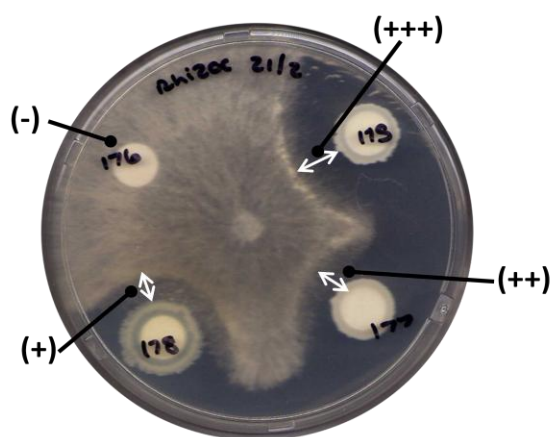


Plate 2.1. Dual-culture antifungal bioassays illustrating varying levels of AEFB antagonism against *Botrytis cinerea* and *Rhizoctonia solani* on PDA after 4 d of incubation at 30°C. The rating system applied to measure antagonism was determined by the size of the zone of inhibition where: (+++) is greater than 5mm; (++) measures between 2–5mm; (+) measures less than 2mm; and a (-) rating indicated that no observable antagonism was evident.

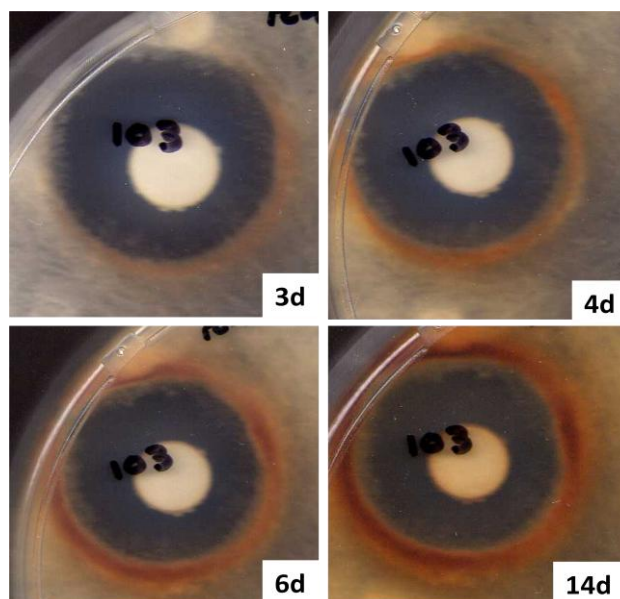


Plate 2.2. Influence of bioassay duration on fungal antagonism of *Rhizoctonia solani* by isolate ccc103 illustrating changes in mycelial appearance and colour over time. Dual-culture bioassays were performed on PDA and incubated at 30°C over a 14-d period.

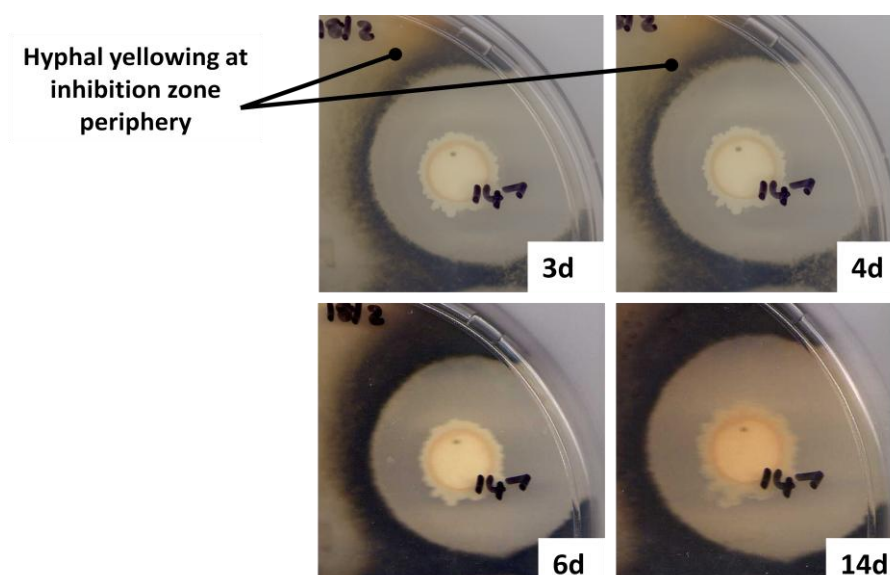


Plate 2.3. Influence of bioassay duration on fungal antagonism of *Botrytis cinerea* by isolate cce147 illustrating changes in mycelial appearance and colour over time. Dual-culture bioassays were performed on PDA and incubated at 30°C over a 14-d period.

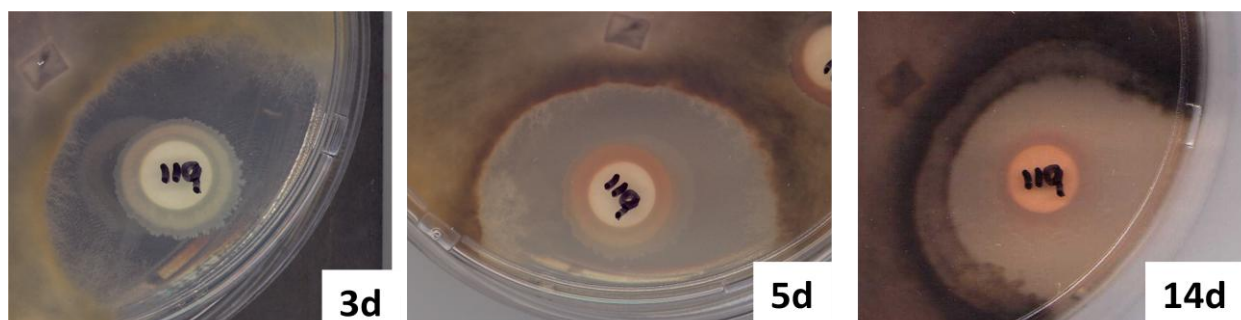


Plate 2.4. Effect of dual-culture antifungal bioassay duration on fungal antagonism of *Botrytis cinerea* by isolate bng119, illustrating the onset of fungistatic interactions over a 14-d period.



Plate 2.5. Dual-culture bioassay illustrating antifungal interaction between isolate bng216 and *Botrytis cinerea* in which the development of a red/pink colouration in the PDA medium (7 d) is evident.

Table 2.3. Results for dual-culture antifungal bioassays of selected AEFB isolates against *Botrytis cinerea* and *Rhizoctonia solani*.

Isolate	<i>B. cinerea</i> Antifungal Bioassay Rating				<i>R. solani</i> Antifungal Bioassay Rating				Host Plant	Sampling Location [#]
	2-day	5-day	14-day	Interaction	2-day	5-day	14-day	Interaction		
bna75	++	+++	+++	Fungicidal	++	++	++	Fungicidal	Butternut	PMB (Scottsville 1)
bna78	++	+++	++	Fungistatic	+++	++	++	Fungicidal	Butternut	PMB (Scottsville 1)
bna81	+++	+++	++	Fungistatic	++	+	+	Fungistatic	Butternut	PMB (Scottsville 1)
bna85	++	+++	+++	Fungicidal	++	++	++	Fungicidal	Butternut	PMB (Scottsville 1)
mwb86	+++	+++	+++	Fungicidal	+	+	+	Fungicidal	Zucchini	PMB (Scottsville 1)
mwb87	+++	+++	+++	Fungicidal	+	+	+	Fungicidal	Zucchini	PMB (Scottsville 1)
ccc103	+++	+++	+++	Fungicidal	+++	+++	+++	Fungicidal	Chayote	PMB (Scottsville 1)
bnd109	+++	+++	+++	Fungicidal	+++	+++	+	Fungistatic	Butternut	PMB (Epworth 1)
bnd115	+++	+++	+++	Fungicidal	+++	++	+	Fungistatic	Butternut	PMB (Epworth 1)
bnd116	+++	+++	+++	Fungicidal	++	++	+	Fungistatic	Butternut	PMB (Epworth 1)
bnd119	+++	+++	++	Fungistatic	++	+	+	Fungistatic	Butternut	PMB (Epworth 1)
bnd124	+++	+++	+++	Fungicidal	+++	+++	++	Fungistatic	Butternut	PMB (Epworth 1)
bnd125	+++	++	+++	Fungicidal	+++	+++	+++	Fungicidal	Butternut	PMB (Epworth 1)
bnd134	+++	+++	+++	Fungicidal	+	+	+	Fungicidal	Butternut	PMB (Epworth 1)
bnd136	+++	+++	++	Fungistatic	+++	++	+	Fungistatic	Butternut	PMB (Epworth 1)
bnd137	++	+++	+++	Fungicidal	+++	+++	++	Fungistatic	Butternut	PMB (Epworth 1)
bnd139	++	+++	+++	Fungicidal	+	+	+	Fungicidal	Butternut	PMB (Epworth 1)
cce140	++	+++	+++	Fungicidal	+	+	+	Fungicidal	Chayote	PMB (Chase Valley 1)
cce142	+++	+++	+++	Fungicidal	+++	+++	++	Fungistatic	Chayote	PMB (Chase Valley 1)
cce146	++	+++	+++	Fungicidal	++	++	+	Fungistatic	Chayote	PMB (Chase Valley 1)
cce147	+++	+++	+++	Fungicidal	++	++	+	Fungistatic	Chayote	PMB (Chase Valley 1)
bnd149	+++	+++	+++	Fungicidal	++	++	+	Fungistatic	Butternut	PMB (Epworth 2)
bnd150	+++	+++	+++	Fungicidal	+++	+	+	Fungistatic	Butternut	PMB (Epworth 2)
bnd154	++	+++	++	Fungistatic	+++	+++	+	Fungistatic	Butternut	PMB (Epworth 2)
bnd156	+++	+++	+++	Fungicidal	-	-	-	N/A	Butternut	PMB (Epworth 2)
bnd157	+++	+++	+++	Fungicidal	+	++	++	Fungicidal	Butternut	PMB (Epworth 2)
bnd160	+++	+++	+++	Fungicidal	++	++	++	Fungicidal	Butternut	PMB (Epworth 2)
bnd162	+++	+++	+++	Fungicidal	+++	++	++	Fungicidal	Butternut	PMB (Epworth 2)

Table 2.3. Continued.

Isolate	<i>B. cinerea</i> Antifungal Bioassay Rating				<i>R. solani</i> Antifungal Bioassay Rating				Host Plant	Sampling Location
	2-day	5-day	14-day	Interaction	2-day	5-day	14-day	Interaction		
bnd166	+++	+++	++	Fungistatic	+++	++	++	Fungicidal	Butternut	PMB (Epworth 2)
pkf167	+++	+++	+++	Fungicidal	++	++	++	Fungicidal	Pumpkin	PMB (Allan Wilson)
cce174	+++	+++	+++	Fungicidal	++	++	++	Fungicidal	Chayote	PMB (Chase Valley 2)
cce175	+++	+++	+++	Fungicidal	+++	+++	+++	Fungicidal	Chayote	PMB (Chase Valley 2)
cce183	++	+++	++	Fungistatic	+++	+++	+++	Fungicidal	Chayote	PMB (Chase Valley 2)
bng199	+++	+++	++	Fungistatic	++	+++	++	Fungistatic	Butternut	PMB (Voortrekker)
bng202	+++	+++	+	Fungistatic	+++	++	+	Fungistatic	Butternut	PMB (Voortrekker)
bng210	+++	+++	+++	Fungicidal	++	++	+	Fungistatic	Butternut	PMB (Voortrekker)
bng215	+++	+++	++	Fungistatic	+	+	-	Fungistatic	Butternut	PMB (Voortrekker)
bng216	+++	+++	++	Fungistatic	+	+	-	Fungistatic	Butternut	PMB (Voortrekker)
bng217	+++	+++	++	Fungistatic	+++	+++	++	Fungistatic	Butternut	PMB (Voortrekker)
bng218	+++	+++	++	Fungistatic	+++	++	+	Fungistatic	Butternut	PMB (Voortrekker)
bng221	++	+++	+	Fungistatic	++	++	+	Fungistatic	Butternut	PMB (Voortrekker)
bng224	++	+++	++	Fungistatic	+++	+++	++	Fungistatic	Butternut	PMB (Voortrekker)
bng227	+++	+++	+++	Fungicidal	++	++	+	Fungistatic	Butternut	PMB (Voortrekker)
bng230	+++	+++	++	Fungistatic	++	++	+	Fungistatic	Butternut	PMB (Voortrekker)
pkl242	+++	+++	+	Fungistatic	+++	+++	++	Fungistatic	Pumpkin	Wartberg
pkl247	+++	+++	+	Fungistatic	+++	++	++	Fungicidal	Pumpkin	Wartberg
pkk252	+++	+++	+	Fungistatic	+++	++	++	Fungicidal	Pumpkin	Wartberg
sqa271	+++	+++	++	Fungistatic	++	++	+	Fungistatic	Squash	Hilton
sqa272	+++	+++	++	Fungistatic	+++	+++	+	Fungistatic	Squash	Hilton
sqa275	+++	+++	+	Fungistatic	+++	+++	+	Fungistatic	Squash	Hilton
sqa277	+++	+++	++	Fungistatic	+++	+++	++	Fungistatic	Squash	Hilton
sqa279	+++	+++	+++	Fungicidal	+	+	+	Fungistatic	Squash	Hilton
bnn282	+++	+++	+++	Fungicidal	+++	+++	++	Fungistatic	Butternut	Wartberg
sqa298	+++	+++	++	Fungistatic	+	+	+	Fungistatic	Squash	PMB (Scottsville 2)

N/A = Not Applicable. # PMB = Pietermaritzburg

2.3.2. Observations of AEFB isolate colony morphology, cell morphology, and sporangial characteristics

AEFB isolates cultured on TSA were cream or white on colour; and gave rise to a range of different colony morphologies, including circular, punctiform or irregular colony shapes. Two colony types predominated (Table 2.4): one with a firm texture and matte appearance (Plate 2.6a); and the second comprising highly mucoid colonies, which displayed a tendency to swarm on TSA (Plate 2.6b). The surface appearance of the mucoid colonies altered with age, taking on a rugose appearance (Plate 2.6c). When isolates were cultured on 10% TSA colony morphologies arose which were different from those observed from full-strength TSA, being of a distinctly drier texture and with a puckered, matte appearance.

Table 2.4. Colony and Gram stain characteristics of AEFB isolates displaying high levels of fungal antagonism in dual-culture bioassay.

Isolate	Colony Characteristics			Cell Size (µm)	Endospore Characteristics	
	Colour	Appearance	Texture		Location	Sporangial Distension
bn75	White	Shiny	Mucoid	0.7x4	Subterminal	Slight
bn78	Cream	Shiny	Mucoid	0.7x3.5	Subterminal	Slight
bn81	White	Matte	Hard	0.7x3.5	Subterminal	Slight
bn85	Cream	Matte	Mucoid	0.7x3.5	Central	Slight
mwb86	White	Shiny	Mucoid	0.7x3.5	Subterminal	No
mwb87	Cream	Matte	Mucoid	0.7x3.5	Subterminal	Yes
ccc103	White	Shiny	Hard	0.7x4	Subterminal	Yes
bnd109	White	Matte	Mucoid	0.7x3	Central	Slight
bnd115	White	Matte	Hard	0.7x2	Central	No
bnd116	White	Matte	Mucoid	0.7x3	Subterminal	No
bnd119	White	Matte	Hard	0.7x3	Subterminal	Slight
bnd124	White	Shiny	Mucoid	0.7x2.5	Central	No
bnd125	White	Shiny	Mucoid	0.7x3	Subterminal	No
bnd134	White	Matte	Hard	0.7x3	Central	Slight
bnd136	White	Matte	Hard	0.7x2.5	Central	No
bnd137	White	Shiny	Mucoid	0.7x3	Central	No
bnd139	White	Matte	Mucoid	0.7x3	Subterminal	Slight
cce140	White	Matte	Hard	0.7x3.5	Subterminal	Slight
cce142	White	Matte	Mucoid	0.7x2.5	Central	Slight
cce146	White	Matte	Hard	0.7x3.5	Subterminal	No
cce147	White	Matte	Hard	0.7x3.5	Subterminal	Slight
bnd149	White	Shiny	Mucoid	0.7x3	Central	Yes
bnd150	White	Matte	Mucoid	0.7x3.5	Subterminal	No

Table 2.4. Continued.

Isolate	Colony Characteristics			Cell Size (μm)	Endospore Characteristics	
	Colour	Appearance	Texture		Location	Sporangial Distension
bnd154	White	Shiny	Mucoid	0.7x3.5	Central	No
bnd156	White	Matte	Hard	0.7x4	Central	No
bnd157	White	Matte	Hard	0.7.5x4	Subterminal	No
bnd160	White	Shiny	Mucoid	0.7x4	Subterminal	No
bnd162	White	Shiny	Hard	0.7x2.5	Central	No
bnd166	White	Matte	Hard	0.7x2.5	Subterminal	No
pkf167	White	Shiny	Mucoid	0.7x3	Central	No
cce174	White	Shiny	Mucoid	0.7x2.5	Central	No
cce175	White	Shiny	Mucoid	0.7x2.5	Central	Slight
cce183	White	Shiny	Mucoid	0.7x3	Subterminal	Yes
bng199	White	Matte	Mucoid	0.7x3.5	Subterminal	No
bng202	White	Matte	Hard	0.7x2.5	Subterminal	No
bng210	White	Shiny	Mucoid	0.7x2.5	Subterminal	No
bng215	Cream	Shiny	Mucoid	0.7x3.5	Central	Slight
bng216	Cream	Shiny	Hard	0.7x3.5	Central	Slight
bng217	White	Shiny	Mucoid	0.7x2.5	Subterminal	No
bng218	White	Matte	Hard	0.7x2.5	Subterminal	No
bng221	White	Matte	Hard	0.7x2.5	Subterminal	No
bng224	White	Matte	Mucoid	0.7x3	Subterminal	Slight
bng227	White	Matte	Mucoid	0.7x3	Subterminal	No
bng230	White	Matte	Mucoid	0.7x2.5	Subterminal	No
pk1242	White	Shiny	Mucoid	0.7x3.5	Subterminal	No
pk1247	White	Shiny	Mucoid	0.7x2.5	Subterminal	No
pkk252	White	Shiny	Mucoid	0.7x2.5	Subterminal	Slight
sqa271	White	Matte	Hard	0.7x2.5	Subterminal	Slight
sqa272	Cream	Shiny	Mucoid	0.7x2	Subterminal	Slight
sqa275	White	Matte	Mucoid	0.7x3.5	Central	No
sqa277	White	Matte	Mucoid	0.7x3	Subterminal	No
sqa279	White	Matte	Mucoid	0.7x3	Central	Slight
bnn282	White	Matte	Mucoid	0.7x2.5	Central	No
sqa298	White	Matte	Mucoid	0.7x2.5	Subterminal	No

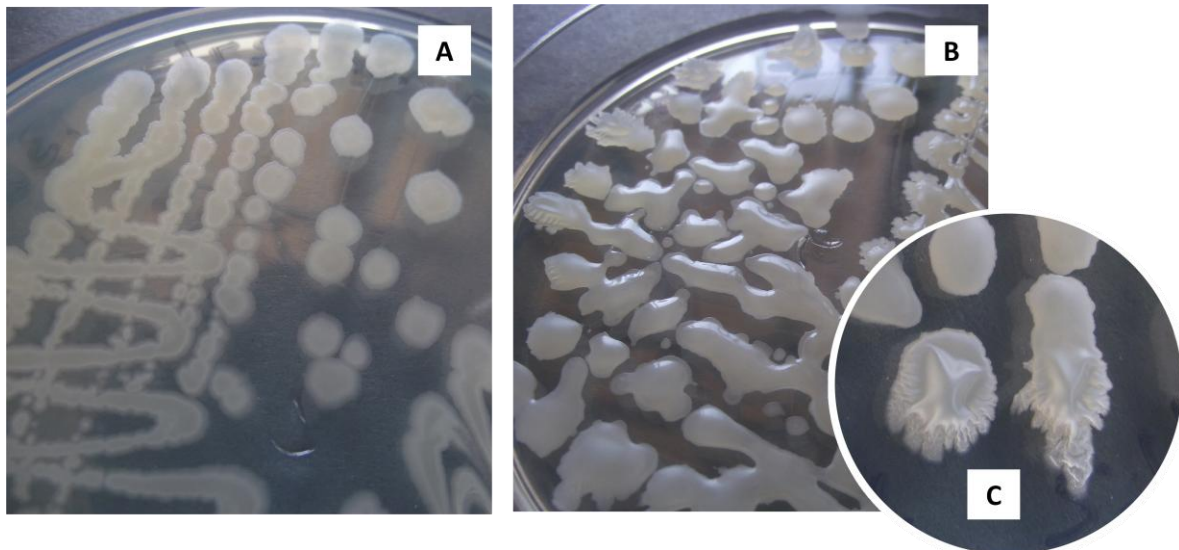


Plate 2.6. Representative colony morphologies of selected AEFB isolates cultured on TSA after 48 h at 30°C. Colony morphology (A) was characterised a dry texture and matte appearance, whereas morphology (B) was highly mucoid and globose in appearance. Over time (B) type colonies dried out taking on a more rugose appearance with a firmer texture (C).

Fifty five phyllosphere-isolated AEFB isolates from the initial dual-culture bioassays were carried forward for DNA fingerprinting using ITS-PCR and RAPD-PCR. These isolates were selected, primarily, on the basis of their antifungal activity against one or both test fungi screened in the dual-culture bioassays, and were representative of each location and cucurbit species sampled. The antifungal isolates chosen for DNA fingerprinting were: bna75, bna78, bna81, bna85, mwb86, mwb87, ccc103, bnd109, bnd115, bnd116, bnd119, bnd124, bnd125, bnd134, bnd136, bnd137, bnd139, cce140, cce142, cce146, cce147, bnd149, bnd150, bnd154, bnd156, bnd157, bnd160, bnd162, bnd166, pkf167, cce174, cce175, cce183, bng199, bng202, bng210, bng215, bng216, bng217, bng218, bng221, bng224, bng227, bng230, pkl242, pkl247, pkk252, sqo271, sqo272, sqo275, sqo277, sqo279, bnn282, and sqo298. Isolate bng241 was also included as a non-antifungal representative isolate.

2.3.4. RAPD-PCR differentiation of phylloplane-isolated AEFB isolates

Representative RAPD-PCR profiles obtained for the AEFB isolates are shown in Figure 2.1. Isolates could be grouped on a visual basis into 14 distinct RAPD fingerprint profiles (designated by letters a–n) based on the number, size, and intensity of the bands (Figure 2.2). Similarities between each of the RAPD profiles were determined using Syngene GeneSnap software (version 7.09) (Syngene, Cambridge, England) employing a UPGMA, taking into account the overall band profile of each isolate to a 1% tolerance (Figure 2.2).

Forty two percent of the AEFB isolates screened displayed RAPD fingerprint patterns consistent matching to profile a (Figure 2.2). Five isolates matched profiles c and f respectively; while profiles b and k comprised 4 isolates matches each. Profile g was matched to 3 isolates and profiles d, h and l were represented by 2 isolates each. The profiles e, i, j, m, n were each represented by a single isolate, namely bng199, bng241, bng216, sqo275, and bng230 respectively.

Four major groupings were discernable in the dendrogram. Group I comprised profiles a, b, f, g, e, and c; Group II comprised profiles n, k, l, and m. Profile d clustered separately from the remainder of the profiles (Group III), and whereas profiles i, h, and j clustered together (Group IV). The isolates corresponding to the fingerprint groupings in the dendrogram are presented in Table 2.7.

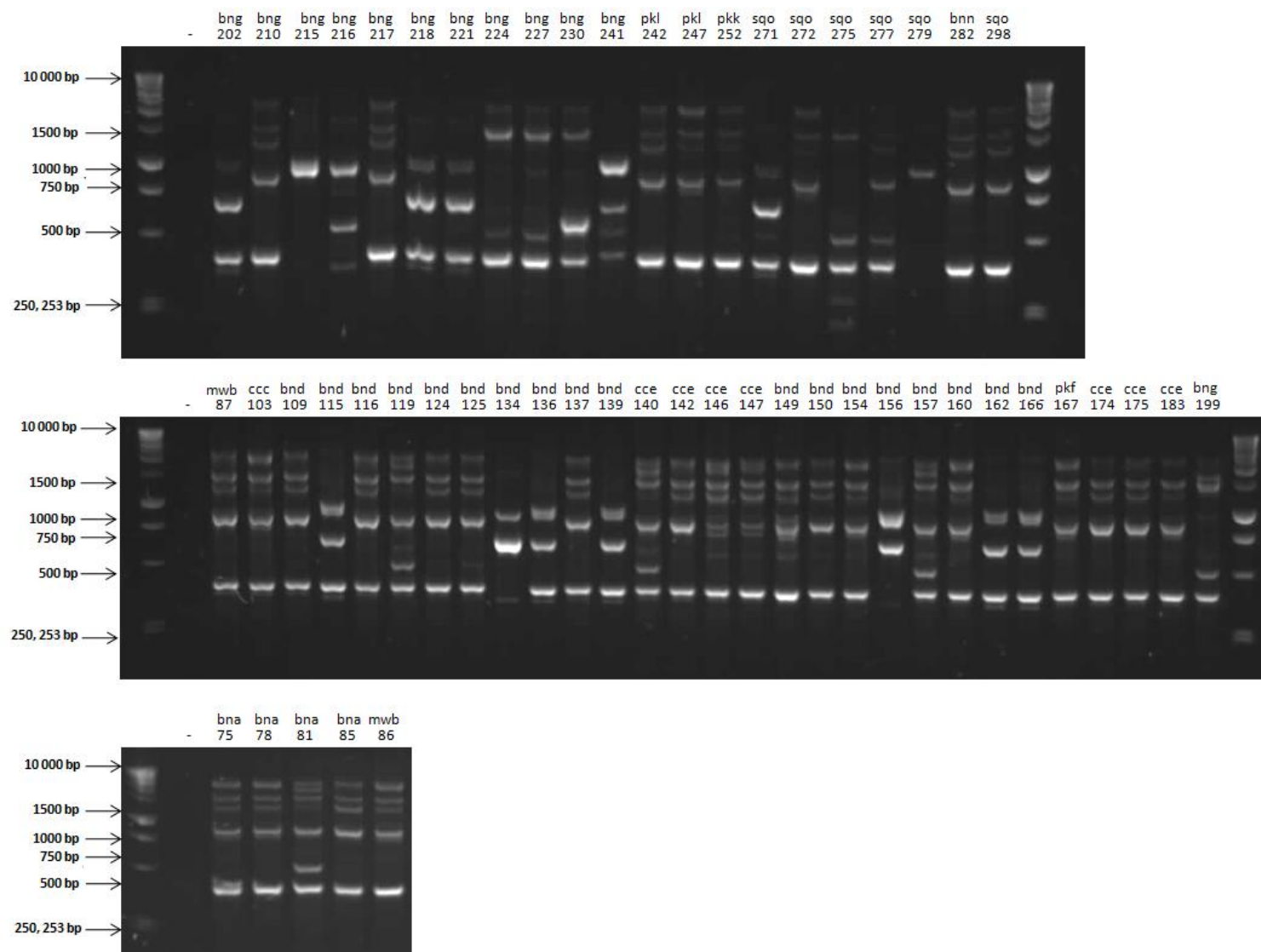


Figure 2.1. Fingerprint profiles of AEFB isolates from RAPD-PCR with primer OPG-11 as seen after electrophoresis using 1.5% agarose gel.

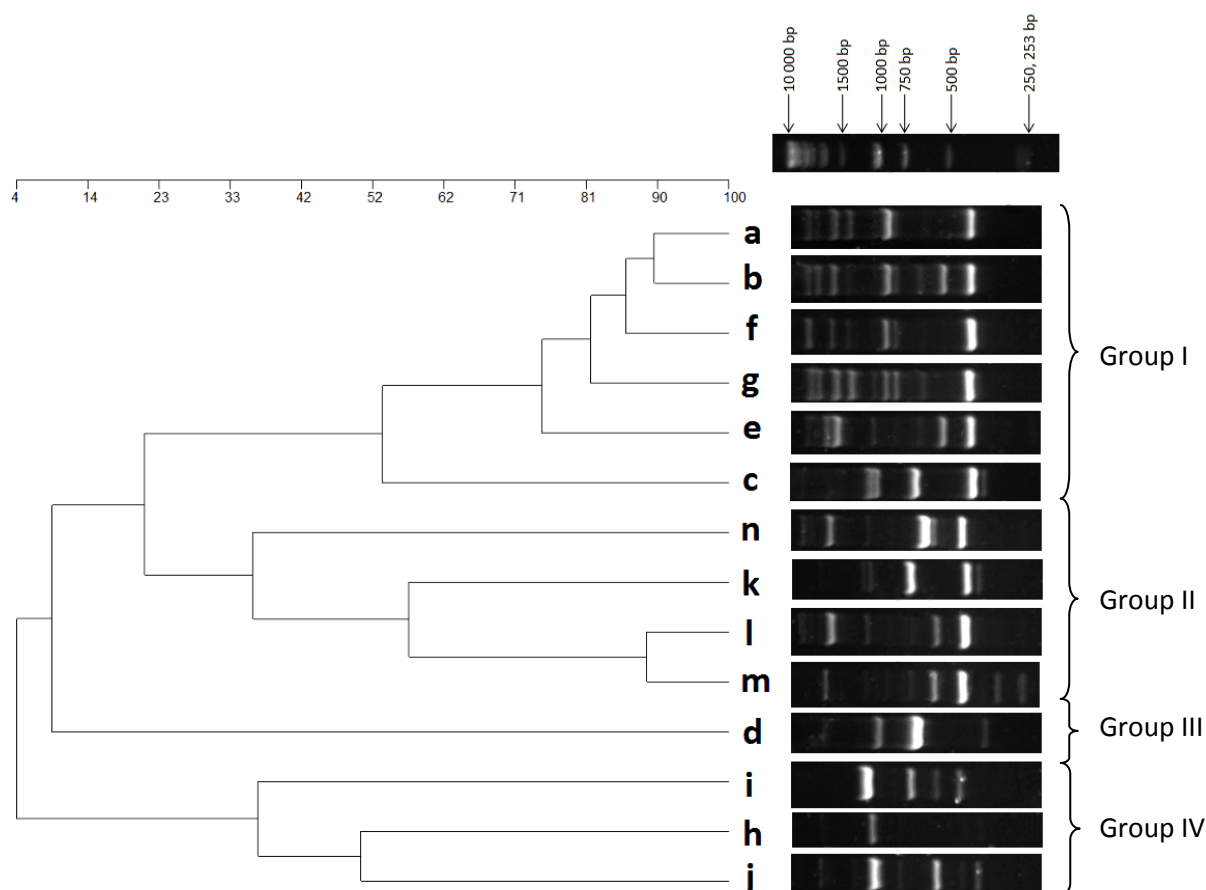


Figure 2.2. UPGMA dendrogram demonstrating relationships between the representative banding patterns of RAPD-PCR profiles (a–n) of phyllosphere-isolated AEFB generated with primer OPG-11, as determined by GeneTools software (version 4.01.03, Syngene).

RAPD-PCR fingerprints of each of the reference strains used in this study are shown in Figure 2.3. Each reference strain was found to have a unique fingerprint. Visual comparisons of RAPD profiles determined in this study indicated that reference strains *B. amyloliquefaciens* subsp. *plantarum* strains R43 and R51, and *B. subtilis* strain B81 could be matched to profiles a, b, and k respectively.

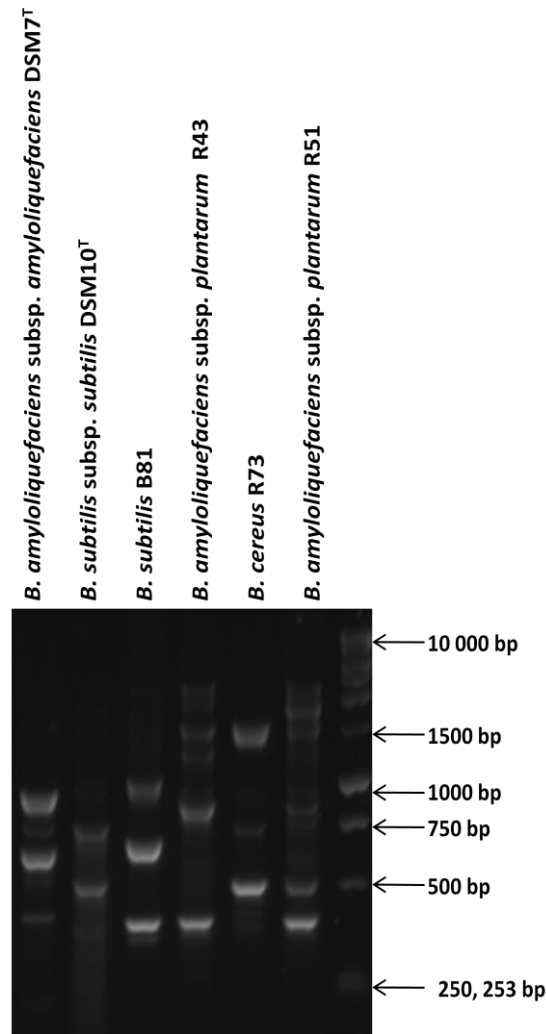


Figure 2.3. RAPD-PCR fingerprint profiles of selected AEFB reference strains generated with primer OPG-11, as seen after electrophoresis using 1.5% agarose gel.

2.3.5. ITS-PCR differentiation of phylloplane-isolated AEFB isolates

Representative ITS-PCR profiles obtained for the AEFB isolates are shown in Figure 2.4. Two major fingerprint groupings were distinguished, based on band number and size: Profile B had two fragments with band sizes at ~450 bp and ~250 bp; while similar fragments were noted for profile A, with additional bands ~300 bp and ~350 bp also distinguished. A third minor profile unique to isolate bng241 was observed (designated profile C). This also comprised two bands, ~240 bp and ~470 bp in size. Approximately 44% of isolates belonged to profile A, with the remainder (excepting isolate bng241) showing fingerprint profile B (Figure 2.5).

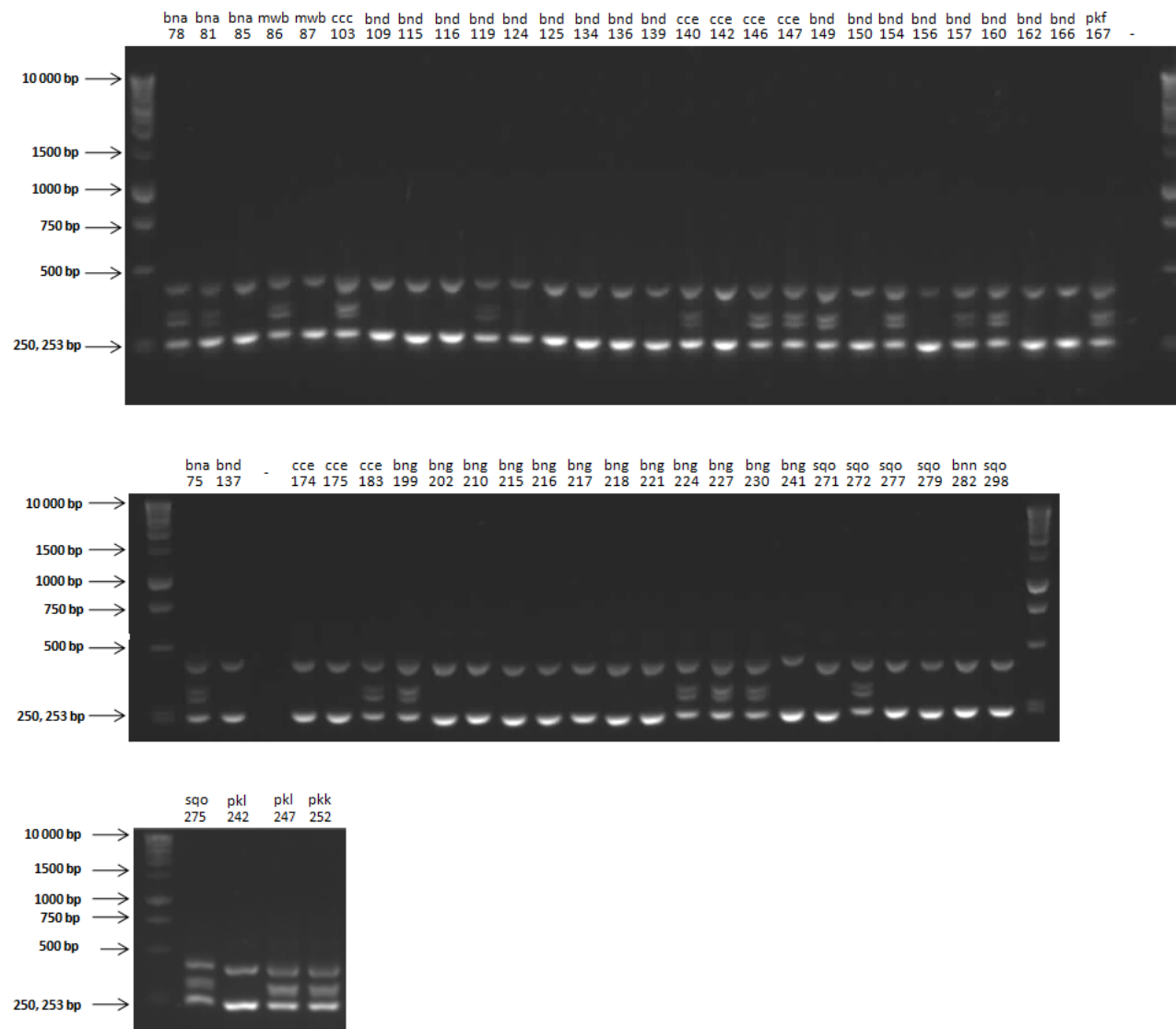


Figure 2.4. Fingerprint profiles of AEFB isolates from ITS-PCR as seen after electrophoresis using 1.5% agarose gel.

The relationships between these three profiles were determined using Syngene GeneSnap software (version 7.09) (Syngene, Cambridge, England). The relationships between these fingerprints showed a low level of diversity, the similarity of approximately 96% between profile A and bng241; and 86% between these and profile B (Figure 2.5).

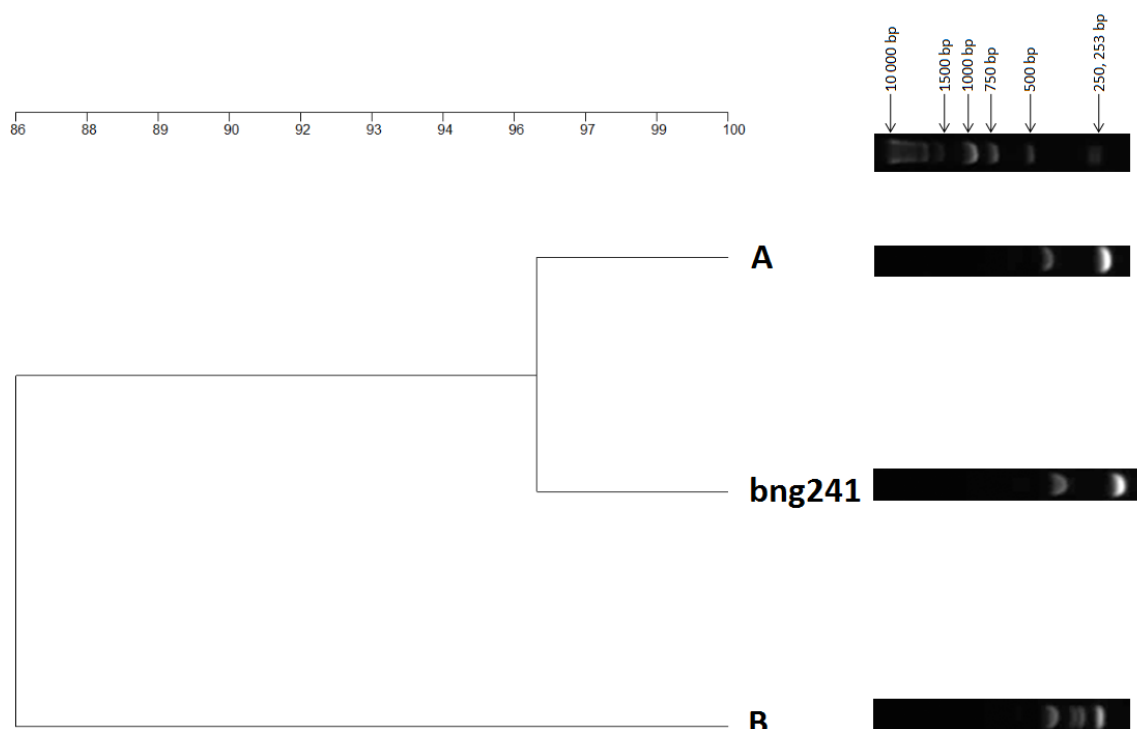


Figure 2.5. UPGMA dendrogram showing the relationships between the representative ITS profiles derived from AEFB isolates screened in this study, as determined by GeneTools software (version 4.01.03, Syngene) using parameters of band molecular weight with a 1% tolerance.

The ITS fingerprint profiles determined for the reference strains are shown in Figure 2.6. Intraspecific and interspecific variations in ITS-PCR banding profiles were evident amongst the reference strains evaluated, based on band molecular weight and intensities. The reference strains *B. subtilis* subsp. *subtilis* DSM10, *B. subtilis* B81, and *B. amyloliquefaciens* R43 visually match to profile B; while *B. amyloliquefaciens* subsp. *plantarum* R51 and *B. amyloliquefaciens* subsp. *amyloliquefaciens* DSM7 visually match profile A. Interestingly, profile C correlates to *B. cereus* R73.

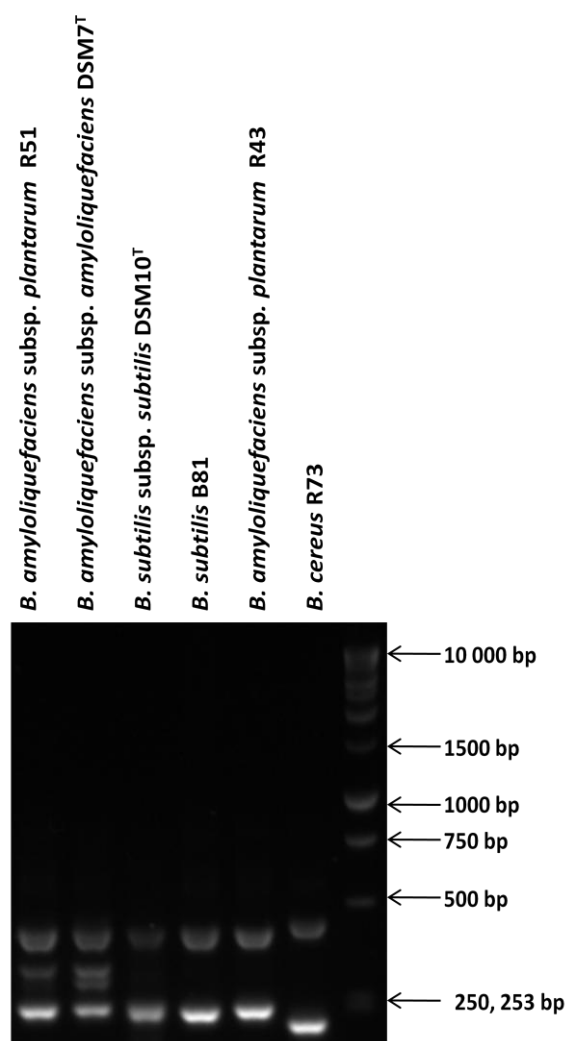


Figure 2.6. ITS-PCR fingerprint profiles of selected AEFB reference strains, as seen after electrophoresis using 1.5% agarose gel.

From RAPD- and ITS-PCR fingerprinting results (Table 2.7), it was observed that fingerprint profiles were neither host plant nor region specific. No apparent correlation between ITS and RAPD fingerprints could be determined, since isolates with similar RAPD profiles were found to have varied ITS profiles (e.g. within RAPD profile a, both ITS profiles A and B are represented).

2.3.6. 16S rRNA and *gyrA* gene fragment sequencing

Representative isolates were chosen for sequencing of 16S rRNA and *gyrA* gene fragments based on fingerprint grouping, cucurbit host species, and geographical sampling location. A total of 32 isolates were selected (*viz.* bna81, mwb86, mwb87, ccc103, bnd109, bnd134, bnd136, bnd137, cce140, cce142, cce146, bnd156, bnd160, pkf167, cce174, cce175, cce183, bng199, bng210, bng215, bng216, bng221, bng230, pkl242, pkl247, pkk252, sqo271, sqo275, sqo277, sqo279, bnn282, and sqo298).

2.3.7. Sequencing of 16S rRNA gene fragment

The 16S rRNA gene fragments amplified from the AEFB isolates resulted in PCR products ~1200 bp in size (Figure 2.7).

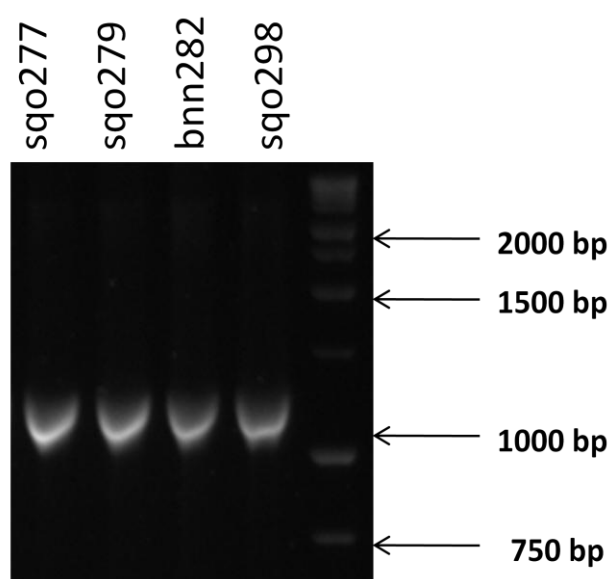


Figure 2.7. Examples of 16S rRNA gene fragment PCR amplicons (~1200 bp) as viewed after gel electrophoresis in 1.5% agarose gel.

After editing, the forward primer read 16S rRNA gene fragment sequences (~783 bp in length) were submitted to the NCBI BLAST whole genome database for comparative identification (Table 2.5). All the AEFB isolates gave >99% similarity matches for the top three 16S rRNA gene sequence matches identified from the GenBank database. The majority of isolates (75%) matched to strains of *B.*

amyloliquefaciens including the subspecies *B. amyloliquefaciens* subsp. *plantarum* (100% similarity). The remaining isolates were matched to strains of *B. subtilis* subsp. *subtilis* or *B. subtilis* subsp. *spizizenii* (99–100% similarity). The query cover for all sequences was 100% with an E-value of zero.

16S rRNA gene sequence data from the AEFB isolates and reference strains from GenBank were used to infer phylogenetic relationships (Figure 2.8). All isolates clustered within the *B. subtilis* group of closely-related taxa; the majority of which fall within one distinct sub-cluster grouping strains of *B. amyloliquefaciens* (Cluster A). The 16S rRNA gene sequence results revealed that there was a very high level of sequence similarity (>97%) amongst the isolates evaluated, although clear distinction between species and subspecies was not always evident.

Table 2.5. Comparative matches of AEFB isolates after a BLAST search on GenBank of the 16S rRNA subunit gene fragment after sequencing (Date accessed: 20 March 2015).

Isolate	BLAST Sequence Matches	Max score	Total score	Identity	Accession No.
bna81 mwb86 mwb87 ccc103 bnd109 bnd137 cce140 cce142 cce146 cce174 cce175 cce183 bnd160 pkf167 bng199 bng210 bng230 pkl242 pkl247 pkk252 sqo275 sqo277 sqo298	 <i>Bacillus amyloliquefaciens</i> DSM7 <i>B. amyloliquefaciens</i> subsp. <i>plantarum</i> FZB42 <i>B. subtilis</i> subsp. <i>subtilis</i> 168	 1476 1476 1465	 14765 13342 14522	 100% 100% 99%	 NC_014551.1 NC_009725.1 NZ_CP010052.1
bnd134 bnd156 sqo279	<i>B. subtilis</i> subsp. <i>subtilis</i> 168 <i>B. subtilis</i> subsp. <i>subtilis</i> 6051-HGW <i>B. subtilis</i> subsp. <i>subtilis</i> NCIB 3610	1476 1476 1476	14666 14642 14603	100% 100% 100%	NZ_CP010052.1 NC_020507.1 NZ_CM000488.1
bnd136 bng221 sqo271	<i>B. subtilis</i> subsp. <i>subtilis</i> 168 <i>B. subtilis</i> subsp. <i>subtilis</i> 6051-HGW <i>B. subtilis</i> subsp. <i>spizizenii</i> TU-B-10	1471 1471 1471	14655 14620 14693	99% 99% 99%	NZ_CP010052.1 NC_020507.1 NC_016047.1
bng215 bng216	<i>B. subtilis</i> subsp. <i>subtilis</i> 168 <i>B. subtilis</i> subsp. <i>spizizenii</i> TU-B-10 <i>B. subtilis</i> subsp. <i>subtilis</i> 6051-HGW	1476 1476 1471	14688 14749 14653	100% 100% 99%	NZ_CP010052.1 NC_016047.1 NC_020507.1
bnn282	<i>B. amyloliquefaciens</i> subsp. <i>plantarum</i> FZB42 <i>B. amyloliquefaciens</i> DSM7 <i>B. subtilis</i> subsp. <i>subtilis</i> 168	1476 1471 1459	13336 14710 14555	100% 99% 99%	NC_009725.1 NC_014551.1 NZ_CP010052.1

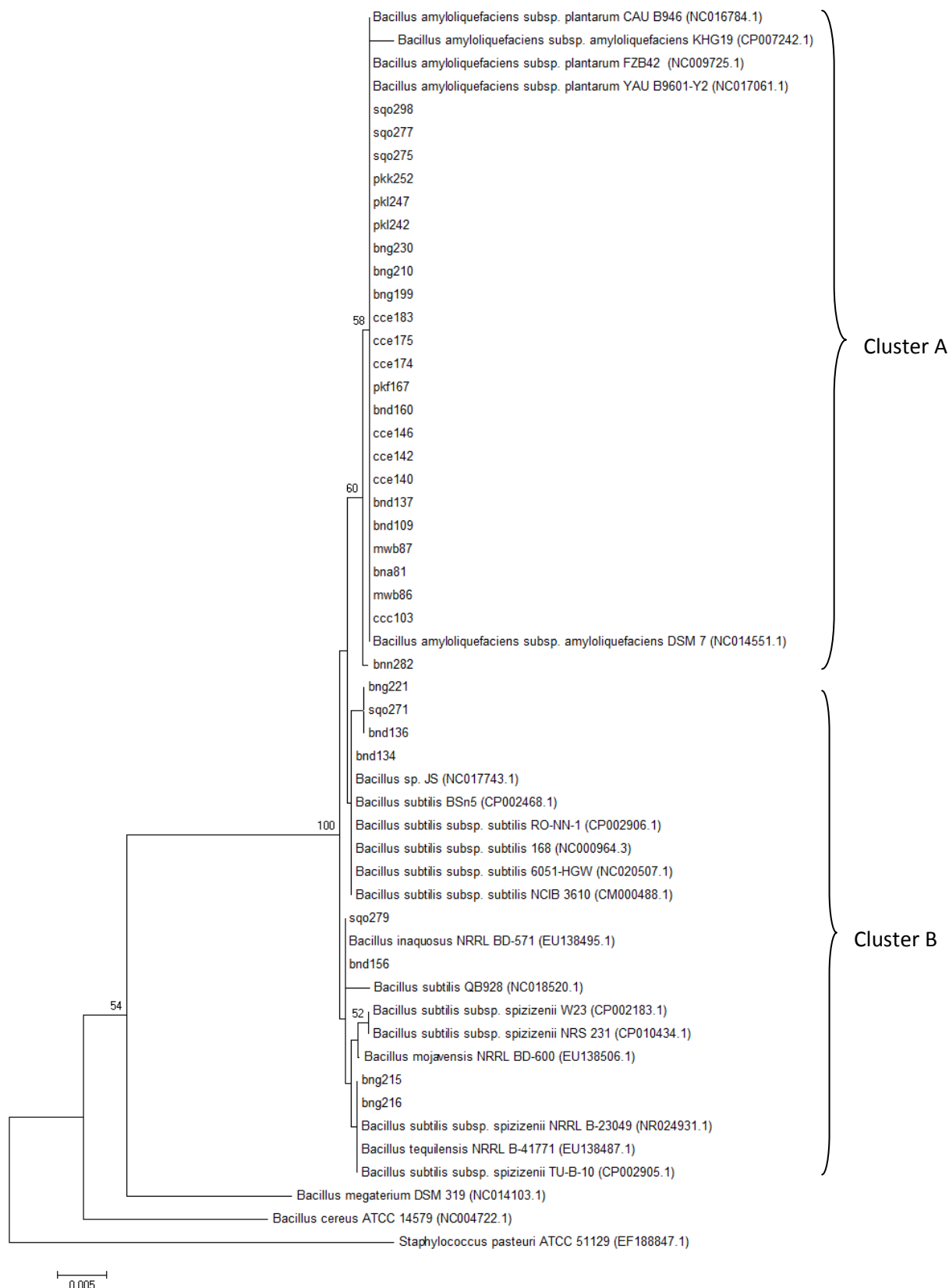


Figure 2.8. Evolutionary relationships of phylloplane AEFB isolates and selected reference strains based on partial 16S rRNA gene sequences as inferred by the Neighbour-Joining method from bootstrap values from 1000 replicates (MEGA6). The scale bar represents 0.005 nucleotide substitutions per sequence position.

2.3.8. Sequencing of *gyrA* gene fragment

To differentiate between the AEFB isolates further, *gyrA* gene fragment amplification and sequencing was undertaken. Within the *B. subtilis* group this gene marker has been shown to display a greater degree of sequence variation than the 16S rRNA gene and has been used to differentiate closely related strains (Borriss *et al.*, 2011; Chun and Bae, 2000). Amplicons resulting from *gyrA* PCR yielded fragments ~1000 bp in size (Figure 2.9).

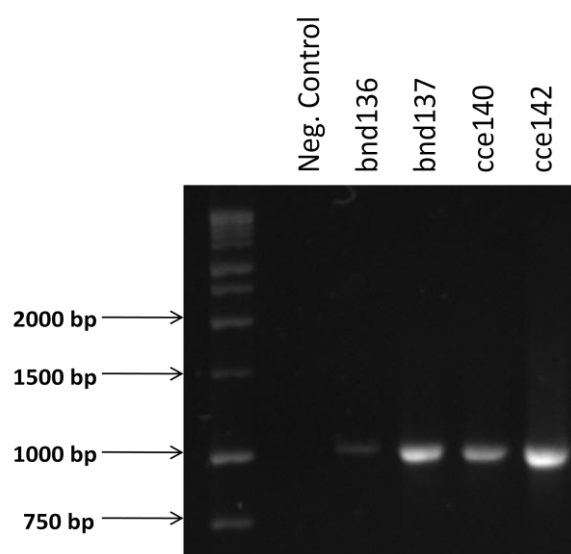


Figure 2.9. Examples of *gyrA* gene fragment PCR amplicons (~1000 bp) as viewed after electrophoresis in 1.5% agarose gel.

After editing and the generation of consensus sequences generated from reads of both forward and reverse primers, these sequences (~896 bp in length) were compared with reference sequences contained within the GenBank BLAST-N whole genome database (Table 2.6). The *gyrA* gene fragments of the AEFB isolates were assigned high levels of similarity (99–100%) to NCBI whole genome reference strains. The bulk (75%) of the isolates showed high levels of sequence similarities that could be matched to strains of *B. amyloliquefaciens*. Three isolates (*viz.* bnd136, bng221, and sqo271) were found to be similar to an unidentified AEFB *Bacillus* sp. JS. The whole genome of this particular strain has been sequenced due to interest in its biocontrol attributes (Song *et al.*, 2012). The remaining isolates were all matched to *B. subtilis* strains (99%). The query cover for all sequences was 99–100% and the E-value for all sequences was zero.

The GenBank database matches for the *gyrA* sequences were consistent with those obtained for the 16S rRNA sequence fragments, but revealed a greater sensitivity to intraspecific variation between the isolates and showed additional strain variation. In particular this was observed amongst those isolates matched to *B. amyloliquefaciens* based on 16S rRNA partial gene sequence analysis. A summary of the RAPD- and ITS-PCR profile groupings is presented in Table 2.7. Interestingly, the *gyrA* sequences revealed identity matches that were consistent with RAPD fingerprints, with profiles a, b, f, e, g, h, n, and m being associated with *B. amyloliquefaciens*; and the profiles c, d, i, j, and k being associated with *B. subtilis* strains.

Table 2.6. Comparative matches of AEFB isolates after a BLAST search on GenBank of the *gyrA* gene fragment after sequencing (Date accessed: 20 March 2015).

Isolate	BLAST Sequence Matches	Max score	Total score	Identity	Accession No.
bna81	<i>Bacillus amyloliquefaciens</i> SQR9	1580	1580	99%	NZ_CP006890.1
cce140		1580	1580	99%	NZ_CP009749.1
		1580	1580	99%	NZ_JQNZ01000021.1
mwb86	<i>B. amyloliquefaciens</i> SQR9	1576	1576	99%	NZ_CP006890.1
ccc103					
bnd160					
pkf167	<i>B. subtilis</i> ATCC 19217	1576	1576	99%	NZ_CP009749.1
cce183	<i>B. amyloliquefaciens</i> X1	1576	1576	99%	NZ_JQNZ01000021.1
pk1247					
pkk252					
mwb87	<i>B. amyloliquefaciens</i> SQR9	1585	1585	99%	NZ_CP006890.1
bnd109					
bnd137					
cce142	<i>B. subtilis</i> ATCC 19217	1585	1585	99%	NZ_CP009749.1
cce174					
cce175					
bng210	<i>B. amyloliquefaciens</i> X1	1585	1585	99%	NZ_JQNZ01000021.1
pk1242					
sqo277					
sqo298					
bnn282					
cce146	<i>B. amyloliquefaciens</i> SQR9	1602	1602	100%	NZ_CP006890.1
	<i>B. subtilis</i> ATCC 19217	1602	1602	100%	NZ_CP009749.1
	<i>B. amyloliquefaciens</i> X1	1602	1602	100%	NZ_JQNZ01000021.1
bng199	<i>B. amyloliquefaciens</i> L-H15	1585	1585	99%	NZ_CP010556.1
	<i>B. amyloliquefaciens</i> IT-45	1580	1580	99%	NC_020272.1
	<i>B. amyloliquefaciens</i> LFB112	1591	1591	99%	NC_023073.1

Table 2.6. Continued.

Isolate	Description	Max score	Total score	Identity	Accession No.
bng230	<i>B. amyloliquefaciens</i> L-H15	1602	1602	100%	NZ_CP010556.1
	<i>B. amyloliquefaciens</i> IT-45	1596	1596	99%	NC_020272.1
	<i>B. amyloliquefaciens</i> LFB112	1574	1574	99%	NC_023073.1
sqo275	<i>B. amyloliquefaciens</i> L-H15	1596	1596	100%	NZ_CP010556.1
	<i>B. amyloliquefaciens</i> LFB112	1596	1596	99%	NC_023073.1
	<i>B. amyloliquefaciens</i> subsp. <i>plantarum</i> CAU B946	1596	1596	99%	NC_016784.1
bnd134	<i>B. subtilis</i> subsp. <i>subtilis</i> BAB-1	1596	1596	99%	NC_020832.1
	<i>B. subtilis</i> XF-1	1596	1596	99%	NC_020244.1
	<i>B. subtilis</i> subsp. <i>subtilis</i> 3NA	1585	1585	99%	NZ_CP010314.1
bng215	<i>B. subtilis</i> subsp. <i>subtilis</i> BAB-1	1591	1591	99%	NC_020832.1
bng216	<i>B. subtilis</i> XF-1	1591	1591	99%	NC_020244.1
sqo279	<i>B. subtilis</i> subsp. <i>subtilis</i> 3NA	1568	1568	99%	NZ_CP010314.1
bnd156	<i>B. subtilis</i> subsp. <i>subtilis</i> BAB-1	1574	1574	99%	NC_020832.1
	<i>B. subtilis</i> XF-1	1574	1574	99%	NC_020244.1
	<i>B. subtilis</i> GXA-28	1557	1557	99%	NZ_JPNZ01000003.1
bnd136	<i>Bacillus</i> sp. JS	1574	1574	99%	NC_017743.1
bng221	<i>Bacillus</i> sp. A053	1568	1568	99%	NZ_JXAJ01000001.1
sqo271	<i>B. subtilis</i> subsp. <i>subtilis</i> BAB-1	1382	1382	95%	NC_020832.1

The *gyrA* gene sequence data from the AEFB isolates and reference strains obtained from GenBank were used to infer phylogenetic relationships (Figure 2.10). A greater degree of sequence heterogeneity was evident in the *gyrA* phylogenetic tree than for the 16S rRNA sequence phylogenetic tree (Figure 2.8). The majority of the isolates grouped with *B. amyloliquefaciens* strains, with reference strains of *B. amyloliquefaciens* subsp. *plantarum* grouping throughout this clade (Cluster A). The remaining isolates were grouped separately from other representatives of the *B. subtilis* group (Cluster B). The *gyrA* sequences overall proved better able to illustrate both inter- and intra-species variability than 16S rRNA gene sequences.



Figure 2.10. Evolutionary relationships of phylloplane AEFB isolates and selected reference strains based on partial Gyrase subunit A gene sequences as inferred by the Neighbour-Joining method from bootstrap values from 1000 replicates (MEGA6). The scale bar represents 0.05 nucleotide substitutions per sequence position.

The combined data obtained from DNA fingerprinting and partial gene sequence analysis is presented in Table 2.7. Those RAPD profiles included in the Group I of Figure 2.2 are largely matched by gene sequencing to *B. amyloliquefaciens*; while profiles c, n, and k matched to *Bacillus* sp. JS or *B. subtilis*. Comparing the ITS profiles, those isolates closely related to *B. subtilis* possessed profile B, while profile A occurs amongst both *B. amyloliquefaciens* and *B. subtilis* related isolates. The data highlights that similar fingerprint profiles and *Bacillus* spp. were found throughout the sampling areas on various cucurbit host species.

Table 2.7. Comparative data for DNA fingerprinting and gene sequence fragment with plant host and geographical sampling location for *Bacillus* spp. isolates.

Isolate	Fingerprint		RAPD Group ^y	Sequence Matches*		Plant	Sampling Location [#]
	ITS	RAPD		16S rRNA	gyrA		
bn75	A	a	I	ND	ND	Butternut	PMB (Scottsville 1)
bn78	A	a	I	ND	ND	Butternut	PMB (Scottsville 1)
bn81	A	b	I	<i>B. amyloliquefaciens</i>	<i>B. amyloliquefaciens</i>	Butternut	PMB (Scottsville 1)
bn85	B	a	I	ND	ND	Butternut	PMB (Scottsville 1)
mwb86	A	a	I	<i>B. amyloliquefaciens</i>	<i>B. amyloliquefaciens</i>	Marrow	PMB (Scottsville 1)
mwb87	B	a	I	<i>B. amyloliquefaciens</i>	<i>B. amyloliquefaciens</i>	Marrow	PMB (Scottsville 1)
ccc103	A	a	I	<i>B. amyloliquefaciens</i>	<i>B. amyloliquefaciens</i>	Chayote	PMB (Scottsville 1)
bnd109	A	a	I	<i>B. amyloliquefaciens</i>	<i>B. amyloliquefaciens</i>	Butternut	PMB (Epworth 1)
bnd115	B	c	I	ND	ND	Butternut	PMB (Epworth 1)
bnd116	B	a	I	ND	ND	Butternut	PMB (Epworth 1)
bnd119	A	b	I	ND	ND	Butternut	PMB (Epworth 1)
bnd124	B	a	I	ND	ND	Butternut	PMB (Epworth 1)
bnd125	B	a	I	ND	ND	Butternut	PMB (Epworth 1)
bnd134	B	d	III	<i>B. subtilis</i>	<i>B. subtilis</i>	Butternut	PMB (Epworth 1)
bnd136	B	k	I	<i>B. subtilis</i>	<i>Bacillus</i> sp. JS	Butternut	PMB (Epworth 1)
bnd137	B	a	I	<i>B. amyloliquefaciens</i>	<i>B. amyloliquefaciens</i>	Butternut	PMB (Epworth 1)
bnd139	B	c	I	ND	ND	Butternut	PMB (Epworth 1)
cce140	A	b	I	<i>B. amyloliquefaciens</i>	<i>B. amyloliquefaciens</i>	Chayote	PMB (Chase Valley 1)
cce142	B	a	I	<i>B. amyloliquefaciens</i>	<i>B. amyloliquefaciens</i>	Chayote	PMB (Chase Valley 1)
cce146	A	g	I	<i>B. amyloliquefaciens</i>	<i>B. amyloliquefaciens</i>	Butternut	PMB (Chase Valley 1)
cce147	A	g	I	ND	ND	Butternut	PMB (Chase Valley 1)
bnd149	A	g	I	ND	ND	Butternut	PMB (Epworth 2)
bnd150	B	a	I	ND	ND	Butternut	PMB (Epworth 2)
bnd154	A	a	I	ND	ND	Butternut	PMB (Epworth 2)
bnd156	B	d	III	<i>B. subtilis</i>	<i>B. subtilis</i>	Butternut	PMB (Epworth 2)
bnd157	A	b	I	ND	ND	Butternut	PMB (Epworth 2)
bnd160	A	a	I	<i>B. amyloliquefaciens</i>	<i>B. amyloliquefaciens</i>	Butternut	PMB (Epworth 2)
bnd162	B	c	I	ND	ND	Butternut	PMB (Epworth 2)

Table 2.7. Continued.

Isolate	Fingerprint		RAPD Group [†]	Sequence Matches*		Plant	Sampling Location [#]
	ITS	RAPD		16S rRNA	<i>gyrA</i>		
bnd166	B	c	I	ND	ND	Butternut	PMB (Epworth 2)
pkf167	A	a	I	<i>B. amyloliquefaciens</i>	<i>B. amyloliquefaciens</i>	Pumpkin	PMB (Allan Wilson)
cce174	B	a	I	<i>B. amyloliquefaciens</i>	<i>B. amyloliquefaciens</i>	Pumpkin	PMB (Allan Wilson)
cce175	B	a	I	<i>B. amyloliquefaciens</i>	<i>B. amyloliquefaciens</i>	Pumpkin	PMB (Allan Wilson)
cce183	A	a	I	<i>B. amyloliquefaciens</i>	<i>B. amyloliquefaciens</i>	Chayote	PMB (Chase Valley 2)
bng199	A	e	I	<i>B. amyloliquefaciens</i>	<i>B. amyloliquefaciens</i>	Butternut	PMB (Voortrekker)
bng202	B	k	II	ND	ND	Butternut	PMB (Voortrekker)
bng210	B	a	I	<i>B. amyloliquefaciens</i>	<i>B. amyloliquefaciens</i>	Butternut	PMB (Voortrekker)
bng215	B	h	IV	<i>B. subtilis</i>	<i>B. subtilis</i>	Butternut	PMB (Voortrekker)
bng216	B	j	IV	<i>B. subtilis</i>	<i>B. subtilis</i>	Butternut	PMB (Voortrekker)
bng217	B	a	I	ND	ND	Butternut	PMB (Voortrekker)
bng218	B	k	II	ND	ND	Butternut	PMB (Voortrekker)
bng221	B	k	II	<i>B. subtilis</i>	<i>Bacillus</i> sp. JS	Butternut	PMB (Voortrekker)
bng224	A	l	II	ND	ND	Butternut	PMB (Voortrekker)
bng227	A	l	II	ND	ND	Butternut	PMB (Voortrekker)
bng230	A	n	II	<i>B. amyloliquefaciens</i>	<i>B. amyloliquefaciens</i>	Butternut	PMB (Voortrekker)
bng241	C	i	IV	ND	ND	Butternut	PMB (Voortrekker)
pkf242	B	f	I	<i>B. amyloliquefaciens</i>	<i>B. amyloliquefaciens</i>	Pumpkin	Wartberg
pkf247	A	f	I	<i>B. amyloliquefaciens</i>	<i>B. amyloliquefaciens</i>	Pumpkin	Wartberg
pkk252	A	f	I	<i>B. amyloliquefaciens</i>	<i>B. amyloliquefaciens</i>	Pumpkin	Wartberg
sqa271	B	k	I	<i>B. subtilis</i>	<i>Bacillus</i> sp. JS	Squash	Hilton
sqa272	A	f	I	ND	ND	Squash	Hilton
sqa275	A	m	II	<i>B. amyloliquefaciens</i>	<i>B. amyloliquefaciens</i>	Squash	Hilton
sqa277	B	f	I	<i>B. amyloliquefaciens</i>	<i>B. amyloliquefaciens</i>	Squash	Hilton
sqa279	B	h	IV	<i>B. subtilis</i>	<i>B. subtilis</i>	Squash	Hilton
bnn282	B	a	I	<i>B. amyloliquefaciens</i>	<i>B. amyloliquefaciens</i>	Butternut	Wartberg
sqa298	B	a	I	<i>B. amyloliquefaciens</i>	<i>B. amyloliquefaciens</i>	Squash	PMB (Scottsville 2)

* ND = not determined. [#] PMB = Pietermaritzburg. [†] Clusters of RAPD-PCR fingerprint profiles detailed in Figure 2.2 *
Sequence matches from 16S rRNA and *gyrA* gene fragment sequencing.

2.3.9. Applying MALDI-TOF-MS to differentiate AEFB isolates

A study to differentiate AEFB isolates using MALDI-TOF-MS was carried out on 14 isolates in conjunction with Bruker Biotyper software (Bruker Daltonics, Germany). These isolates were selected on the basis of their identities from 16S rRNA and *gyrA* gene fragment sequences, and as representatives from RAPD fingerprint profile groups distinguished in the study. These isolates included *B. amyloliquefaciens* strains mwb86, ccc103, cce140, cce146, cce175, bng199, sqa275, sqa277, and bnn282; *B. subtilis* strains bnd134, bnd136, bng216, sqa279; and unidentified isolate bng241. Mass spectra were determined for each of the isolates and compared to reference strains

contained within the Bruker Daltonics (BDAL) bacterial strain library (Bruker Daltonics, Germany). Dendograms were generated using the Biotyper software to establish relationships between the AEFB isolates themselves (Figure 2.16), and in relation to selected AEFB reference strains in the BDAL library (Figure 2.17). The mass spectra were also processed using mMass and analysed using SPECLUST for additional cluster analysis (Figure 2.13).

The results for Biotyper identification of the AEFB isolates are presented in Table 2.8. *Bacillus amyloliquefaciens* strain ccc103 was omitted from this analysis owing to insufficient culture growth. The similarity of the isolates' spectra to those in the BDAL library was ranked according to confidence levels reflecting overall identity match at the genus or species level. *Bacillus subtilis* strains bnd134, bng216 and sqo279 were assigned confidence rankings to the genus and species levels. The remaining isolates all scored with confidence in genus only, with *B. amyloliquefaciens* strain sqo277 scoring an unreliable identification.

Table 2.8. MALDI-TOF-MS identification of AEFB using the Bruker Daltonics Biotyper spectra database, as compared to the 16S rRNA partial gene sequence matches from GenBank.

Isolate	16S rRNA GenBank Match	BDAL Match	Score Value [#]
mwb86	<i>B. amyloliquefaciens</i> subsp. <i>plantarum</i>	<i>Bacillus</i> sp.	1.706
bnd134	<i>B. subtilis</i>	<i>B. subtilis</i>	2.069
bnd136	<i>B. subtilis</i>	<i>Bacillus</i> sp.	1.972
cce140	<i>B. amyloliquefaciens</i> subsp. <i>plantarum</i>	<i>Bacillus</i> sp.	1.793
cce146	<i>B. amyloliquefaciens</i> subsp. <i>plantarum</i>	<i>Bacillus</i> sp.	1.806
cce175	<i>B. amyloliquefaciens</i> subsp. <i>plantarum</i>	<i>Bacillus</i> sp.	1.733
bng199	<i>B. amyloliquefaciens</i> subsp. <i>plantarum</i>	<i>Bacillus</i> sp.	1.824
bng216	<i>B. subtilis</i>	<i>B. subtilis</i>	2.081
bng241	ND	<i>Bacillus</i> sp.	1.863
sqa275	<i>B. amyloliquefaciens</i> subsp. <i>plantarum</i>	<i>Bacillus</i> sp.	1.765
sqa277	<i>B. amyloliquefaciens</i> subsp. <i>plantarum</i>	Not reliable	1.663
sqa279	<i>B. subtilis</i>	<i>B. subtilis</i>	2.045
bnn282	<i>B. amyloliquefaciens</i>	<i>Bacillus</i> sp.	1.749

ND = not determined. # Confidence of isolate identity in Bruker Daltonics Biotyper database where: Highly probable genus and species identification (score 2.300–3.000); secure genus and probable species identification (score 2.000–2.299); probable genus identification (1.700–1.999); no consistency in genus or species (score 0.000–1.699).

Owing to the disparity between the 16S rRNA partial gene sequence matches and the Biotyper matches, a mass spectra profile (MSP) was generated for each isolate. From these MSPs a dendrogram was generated to reflect the relationships between the isolates based on variances in their mass spectra (Figure 2.10). *Bacillus amyloliquefaciens* strains ccc103 and sqa277, *B. subtilis* strain bng216, and unidentified isolate bng241 were clearly distinguished from the remainder of the isolates which clustered closely together and display high levels of similarity.

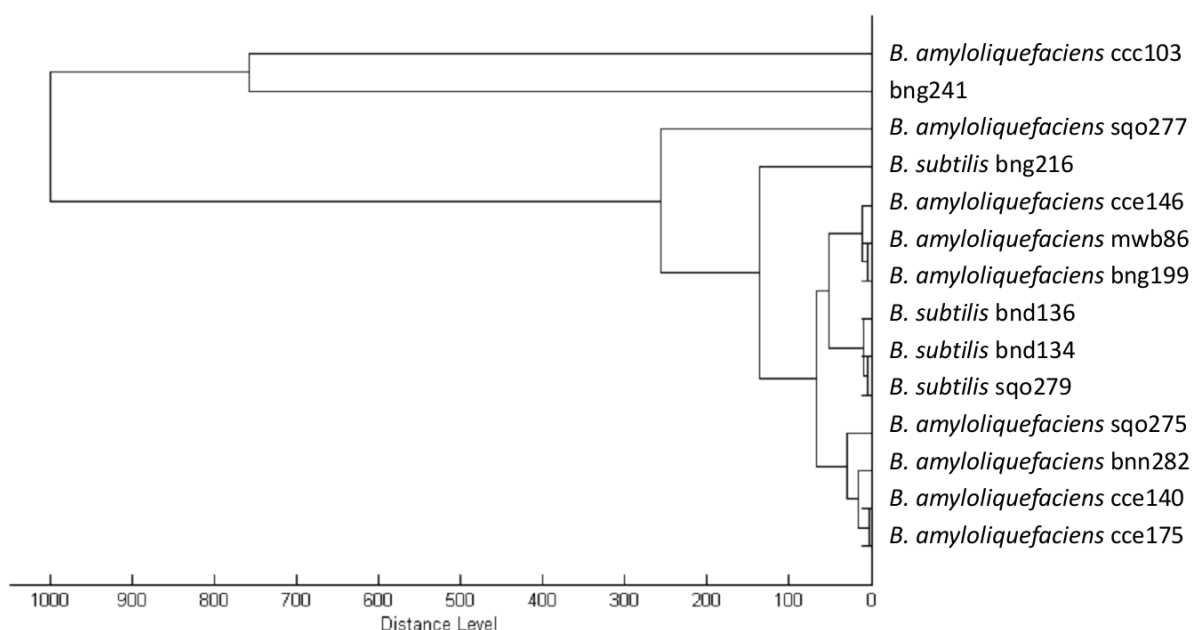


Figure 2.11. Dendrogram depicting clustering of phylloplane AEFB isolates as determined from spectral variances after MALDI-TOF-MS analysis and MSP creation.

A second dendrogram was generated incorporating AEFB reference strains from the Biotyper database, as shown by Figure 2.12. The majority of the AEFB isolates grouped closely with a *B. amyloliquefaciens* strain in the BDAL database, which is in agreement with the sequence matches to this species obtained from the 16S rRNA partial gene sequence BLAST searches (see Table 2.6). Exceptions within this grouping were *B. subtilis* strains bnd134, bnd136, and bng216; and *B. amyloliquefaciens* strains sqo277 and sqo279 which were matched based on 16S rRNA partial gene sequences to strains of *B. subtilis*. As seen previously in Figure 2.10, the MSPs for isolate bng241 and *B. amyloliquefaciens* strain ccc103 clustered separately from the other isolates. Isolate bng241 groups with *B. subtilis* and related taxa, while *B. amyloliquefaciens* strain ccc103 groups instead with *B. megaterium* and *P. ehimensis*.

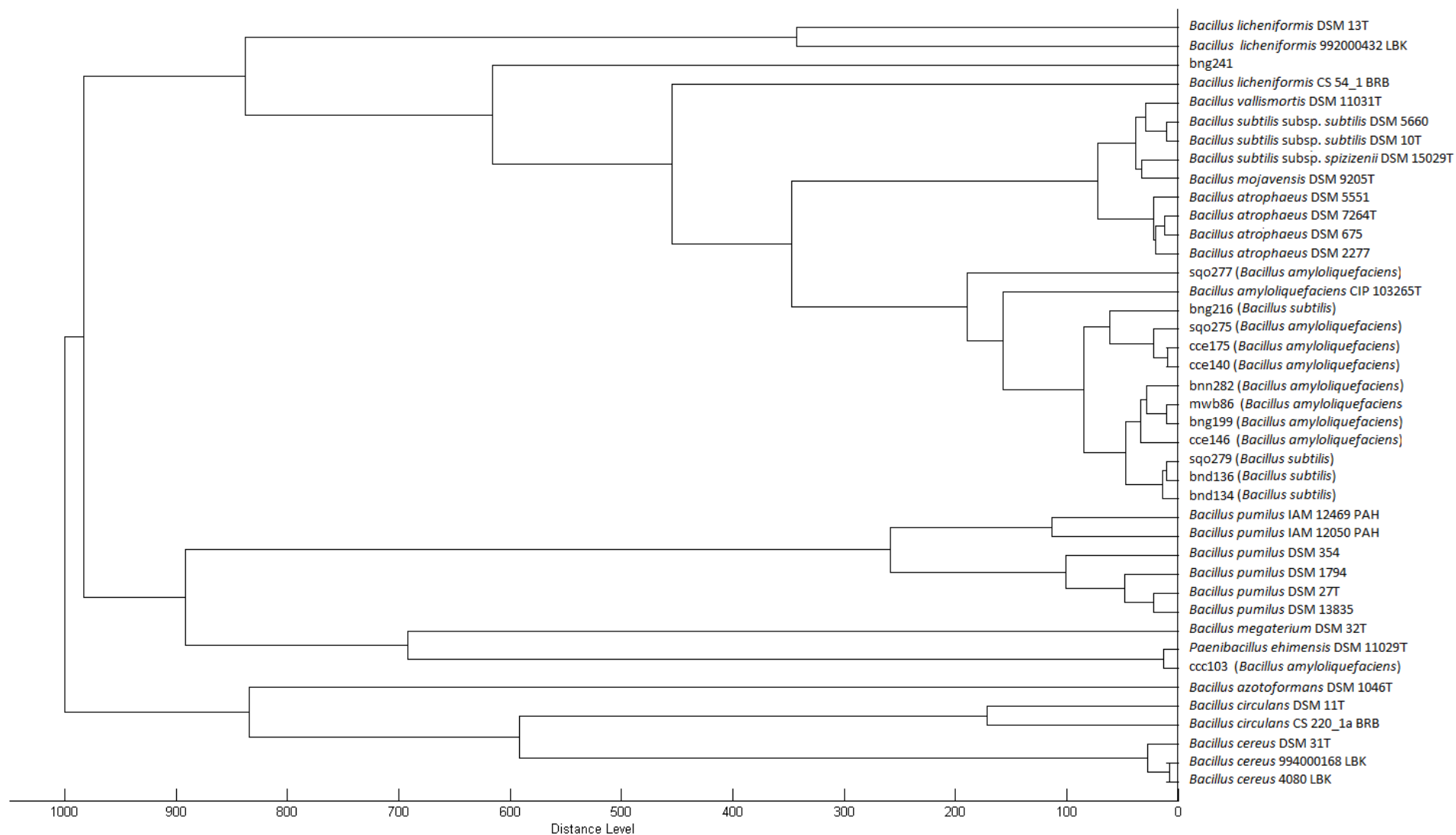


Figure 2.12. Dendrogram depicting clustering between AEFB isolates as determined by variances in mass spectra after MSP creation, and compared to selected AEFB reference strains from the BDAL database.

The dendrogram generated from the MSP peak lists using the online clustering tool SPECLUST (Figure 2.13) grouped isolates along similar lines to those achieved with the dendrogram generated using MALDI Biotyper (Figure 2.10). Isolate bng241 and *B. amyloliquefaciens* strain ccc103 were again found to be clearly differentiated from the other isolates, as were *B. subtilis* strain bng216 and *B. amyloliquefaciens* strain sqo277. The remaining isolates display high similarity and cluster closely together. Closely-related isolates such as *B. subtilis* strains bnd134 and bnd136, and *B. amyloliquefaciens* strain sqo279 appear together in both dendrograms. However, *B. amyloliquefaciens* strains mwb86 and cce140, and bnn282 and cce175 are not clustered as closely as in the Biotyper-generated dendrogram (Figure 2.11). These slight variations in clustering may be attributed to the parameters applied in dendrogram creation between the Biotyper and SPECLUST software.

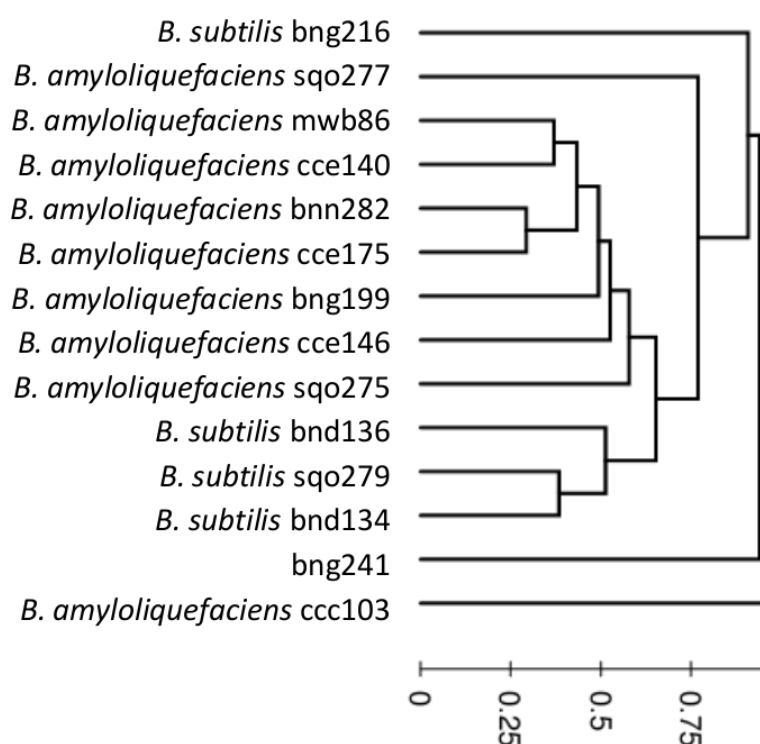


Figure 2.13. Dendrogram of mass spectra data representing clusters of AEFB isolated from the cucurbit phyllosphere. Cluster analysis was performed using SPECLUST online software, with the scale bar indicating the distance measure (d) applied during clustering.

In summary, PCR-based DNA fingerprinting allowed for isolates to be differentiated and groupings to be determined for dereplication purposes. The analysis of the 16S rRNA gene fragment sequences confirmed the identities of representatives of the isolate groupings. Higher levels of species variations were resolved when analysis of the *gyrA* gene fragment sequence was performed. The taxonomic resolution of the MALDI-TOF-MS Biotyper system was limited owing to poor reference strain representation in the BDAL database. Yet, the MSP dendograms and SPECLUST analysis were able to group isolates based on spectral variances, though limited correlation between these groupings and DNA fingerprint profiles was noted.

2.4. Discussion

Powdery mildew of cucurbits infects a range of cucurbit species grown under both field and greenhouse conditions. Cucurbit production in South Africa contributes millions of Rands towards the national agricultural output (South African Department of Agriculture, Forestry and Fisheries, 2013). In light of the ecological issues and expense associated with pesticide use, BCAs have been advocated as promising alternatives against various crop diseases. In several studies, strains of *Bacillus* spp. have shown promise as antagonists of cucurbit powdery mildew (Romero *et al.*, 2007b; Romero *et al.*, 2004; Bettiol *et al.*, 1997). The present study was undertaken with the aim of isolating phyllosphere AEFB from various cucurbit species and screening them for fungal antagonism *in vitro*; and establishing the diversity of antagonistic organisms selected using DNA fingerprinting, gene fragment sequencing, and MALDI-TOF-MS.

Since powdery mildews are biotrophic, and require live host tissue to survive, they are not amenable to conventional agar-based dual-culture bioassay screening approaches (Pérez-García *et al.*, 2009). For the purposes of assessing antifungal activity in this study, *B. cinerea* and *Rhizoctonia solani* were chosen as surrogate test organisms. Over half of the AEFB isolates obtained from cucurbit leaves showed *in vitro* antifungal activity against *Rhizoctonia solani* and/or *B. cinerea*. Approximately 73% of antagonistic isolates displayed activity against both fungal species, and representatives of these were selected for further evaluation. The incidence of antifungal activity observed during screening was regarded to be high, considering that similar studies reported that only 8–10% of isolates showed fungal antagonism *in vitro* (Ghyselinck *et al.*, 2013; Mari *et al.*, 1996).

In general, *B. cinerea* exhibited higher levels of sensitivity to antagonism by the AEFB isolates than did *R. solani* (Table 2.3). The inhibitory effect of antifungal lipopeptide compounds, such as iturin and fengycin, are known to be influenced by sterol composition of fungal cell membranes (Balhara *et al.*, 2011; Ongena and Jacques, 2008; Latoud *et al.*, 1990). The observed browning (*R. solani*) and/or darkening (*B. cinerea*) of fungal mycelia on bioassay plates may be attributed to a fungal response to compounds produced by the antagonistic bacteria, as has been reported previously (Fiddaman and Rossall, 1993; Ferreira *et al.*, 1991). In addition, extracellular cell wall degrading enzymes (*viz.* cellulases, glucanases, and chitinases) can also contribute to antagonistic activity and induce fungal morphology aberrations which can be detected with the naked eye (Cantu *et al.*, 2009; Pal and McSpadden Gardener, 2006; Shoda, 2000). Given the variations in sensitivity of these two fungal species to the actions of antagonistic AEFB isolates, it is recommended that a range of surrogate fungi be used when screening for potential antagonists of unculturable biotrophic fungi *in vitro*.

In some instances dual-culture interactions were found to be fungistatic, whereby test fungi overgrew the initial zone of inhibition formed by AEFB isolates (Table 2.4). This phenomenon was attributed to various factors, such as: a decrease in active compound concentration due to degradation or diffusion; discontinued bacterial production of antifungal compounds due to sporulation or depleted nutrients; or the possible development of fungal resistance to the antibiotic compounds (Tewelde, 2004; Leifert *et al.*, 1995; Fiddaman and Rossall, 1994; Fiddaman and Rossall, 1993; Ferreira *et al.*, 1991). Isolates which displayed sustained antifungal activity for the duration of the bioassay suggest that the active compound(s) are produced in sufficiently high concentrations or are more stable over longer periods. Alternatively, the production of synergistic mixtures of active compounds may account for the sustained antifungal activity observed.

Laboratory-based *in vitro* antifungal bioassays are economical and rapidly yield results; hence they are considered important in the initial evaluation of fungal antagonism (Spurr, 1985). They are convenient for screening large numbers of isolates and provide insights into antimicrobial compound or extracellular enzyme activity (Raaijmakers *et al.*, 2002). Dual-culture bioassays have been widely used to determine the antifungal ability of AEFB *in vitro* (Alvindia and Natsuaki, 2009; Chaurasia *et al.*, 2005; Ongena *et al.*, 2005b; Romero *et al.*, 2004; Touré *et al.*, 2004; Yoshida *et al.*, 2001; May *et al.*, 1997; Leifert *et al.*, 1995; Ferreira *et al.*, 1991; Fravel and Spurr, 1977). Despite the valuable data that can be gleaned from *in vitro* studies, the *in vivo* performance of antagonistic strains selected on

this basis is not guaranteed (Schisler and Slininger, 1997; Leifert *et al.*, 1995). The laboratory conditions under which *in vitro* bioassays are carried out are not representative of those found in the field, and lack stresses such as nutrient and water limitation, and competition from indigenous microbial communities (Schisler and Slininger, 1997; Leifert *et al.*, 1995; Spurr, 1985). The antagonism evidenced in the *in vitro* bioassays is influenced by factors such as medium composition, pH, and incubation temperature (Yoshida *et al.*, 2001; Leifert *et al.*, 1995). Furthermore, fungi vary in their sensitivity to diffusible or volatile compounds (Fiddaman and Rossall, 1994; Fiddaman and Rossall, 1993). Thus, antagonism *in vitro* should not be the sole criterion by which an isolate's biocontrol suitability is determined. In the present study, the dual-culture bioassay formed an integral part of selecting potential powdery-mildew antagonists, if only for the purpose of determining promising fungal antagonists from amongst the isolate set.

Morphology and phenotypic characteristics alone are no longer considered viable for the dereplication and identification of bacterial isolates. This is largely due to reproducibility issues, insufficient strain-level resolution, and high resource and time demands incurred when phenotyping large numbers of isolates (Li *et al.*, 2009; Olsen and Woese, 1993). Consequently, these methods have been largely superseded by genomic approaches which offer more informative results within a relatively short time period (Li *et al.*, 2009). The use of morphological characteristics to distinguish AEFB is complicated, as there are few distinctive traits amongst these species that can be consistently applied to this end (Maughan and Van der Auwera, 2011). Although such characteristics have been applied as selection criteria by other researchers (Savadogo *et al.*, 2011; Tewelde *et al.*, 2004; Reva *et al.*, 2001); in the present study colony characteristics and cell morphology (Table 2.4) were inadequate criteria for isolate differentiation. For this reason DNA fingerprinting was applied for dereplication purposes, and to establish the distribution of related strains from different geographical locations and cucurbit host species.

Despite the accessibility of DNA-sequencing, sequencing of all the gene fragments from a large pool of isolates remains expensive and time-consuming. For this reason, the present study chose to include a DNA fingerprinting dereplication step prior to gene fragment sequence analysis. The fingerprint profiles generated using ITS- and RAPD-PCRs both allowed the differentiation of distinct groupings amongst isolates to be achieved; however RAPD-PCR proved to be more valuable of the two approaches as it generated more profile variants (Figure 2.2). A significant percentage (~42%) of

isolates could be ascribed to one RAPD profile (variant a), with representatives isolated from various cucurbit host species and locations. The ITS-PCR provided lower diversity levels but still proved useful in distinguishing isolate bng241 as an outgroup (Figure 2.4). It should be noted that it was not possible to use either fingerprinting method alone as a means to group isolates, as some isolates with different ITS-PCR profiles possessed similar RAPD-PCR profiles and *vice versa* (Table 2.7).

RAPD-PCR fingerprinting proved to be a fast, sensitive and relatively inexpensive method to use, as has been previously reported in the literature (Li *et al.*, 2009; Olive and Bean, 1999; Tyler *et al.*, 1997). RAPD-PCR requires good quality DNA template, which adds to the overall time and resource investment, whereas the ITS-PCR works well with the crude DNA template material obtained using the freeze-thaw DNA extraction method. Pre-treatment of crude DNA extracts with proteinase K has been shown to provide more distinct banding patterns in RAPD-PCR (Damiani *et al.*, 1996). This approach may prove to be a cost-effective alternative to the use of DNA extraction kits for obtaining good quality RAPD profiles. To improve the resolving power of RAPD-PCR, it is recommended that multiple RAPD primers be used to assure an accurate reflection of isolate variation within a sample set (Rademaker *et al.*, 2006). The fingerprint profiles of the included *Bacillus* spp. reference strains did not allow for conclusive comparative identification of the isolates, thus gene sequence analysis was used to determine the identities of the isolates.

Sequence analysis of the 16S rRNA gene is considered a benchmark for bacterial isolate identification and diversity assessment (Woo *et al.*, 2008; Goto *et al.*, 2000). The isolates chosen for gene sequencing in the current study were identified as members of the *B. subtilis* group of related taxa. Analysis of 16S rRNA gene fragment sequences revealed that the majority of AEFB isolates applied in this study were strains of *B. amyloliquefaciens*; the remainder of the isolates were identified as strains of *B. subtilis* (Table 2.5). The differentiation of members of the *B. subtilis* group of related taxa using 16S rRNA sequences has proven difficult, particularly owing to limited variations present within the 16S rRNA gene between *B. subtilis* group members (Borriss *et al.*, 2011; Logan *et al.*, 2009; Reva *et al.*, 2004; Chun and Bae, 2000). This led to the inclusion of *gyrA* sequences as a means by which to further differentiate strains. Analysis of the *gyrA* gene sequences confirmed the finding of 16S rRNA subunit gene analysis. Most of the isolates (75%) were found to be closely related to strains of *B. amyloliquefaciens*, including the subspecies *B. amyloliquefaciens* subsp. *plantarum* which is known to be active in plant growth promotion (Table 2.6). The *gyrA*

sequence fragments offered greater levels of sequence heterogeneity within subspecies and strains and showed some correlation with the RAPD fingerprint profile groupings. Further divisions were made possible when the ITS-PCR fingerprint profiles and 16S rRNA sequence matches are included (Table 2.7).

In previous studies involving AEFB antagonism toward powdery mildew of cucurbits, Romero *et al.* (2004) determined that four candidate isolates showed 93–97% sequence homology to *B. subtilis* based on partial 16S rRNA gene sequencing. Representative strains of both *B. amyloliquefaciens* and *B. subtilis* species have been described as plant-associated, and many are capable of acting as disease antagonists and plant-health-promoting bacteria (Borriss, 2011; Nagórska *et al.*, 2007). Several plant-associated strains of these species are known to produce a range of lipopeptide compounds which are considered essential to their niche establishment and antagonistic actions (Jacques, 2011).

Sequencing of 16S rRNA gene fragments confirmed that representatives from each RAPD grouping were closely related (Table 2.7). Eight of the RAPD fingerprint profiles were distinguished as strains of *B. amyloliquefaciens* strains when 16S rRNA and *gyrA* gene fragment sequences were analysed. These findings are indicative of strain-level resolution achievable with the RAPD primer OPG-11. A number of these profiles grouped together when UPGMA analysis of the profiles was performed (Figure 2.2). The *B. subtilis* isolates showed greater levels of profile heterogeneity and were separated into several distinct RAPD banding profiles, and were present in all four clusters identified in Figure 2.2. Hence, the inclusion of genotyping methods as a dereplication step—in particular the RAPD-PCR—saved time and resources. By aiding in the grouping of related isolates, the dereplication step eliminated additional unnecessary and costly steps to taxonomically identify each of the individual isolates.

Compared to gene sequencing as a means of bacterial identification and dereplication, MALDI-TOF-MS has great potential as a “one-stop” dereplication and identification system. Whole-cell MALDI-TOF-MS bacterial identification is simpler and faster than PCR or gene sequencing, with data interpretation easily achieved by comparison to an adequately representative strain library (Dare, 2006). Furthermore, MALDI-TOF-MS is well-suited for microbial identifications as the analysis time is less than a minute, requires very little sample, provides resolution to strain level, and is easily

standardised for maximum reproducibility from a large pool of unknown isolates (Sauer, 2008; Dickinson *et al.*, 2004a). MALDI-TOF-MS was evaluated in the present study as a means of rapidly identifying isolates, since its resolution is considered to be similar to that achievable by 16S rRNA gene sequence analysis and RAPD-PCR fingerprinting (Welker and Moore, 2011; Dickinson *et al.*, 2004b).

Applying MALDI-TOF-MS has been reported to provide a simpler and faster method of characterising isolates than sequencing and is capable of achieving levels of sensitivity comparable 16S rRNA sequence analysis (Ghyselinck *et al.*, 2011). The MALDI Biotyper system was able to confidently identify all but one isolate as belonging to the genus *Bacillus* (Table 2.8). A confident match to species level was only possible for *B. subtilis* strains bnd134, bng216 and sqo279, which were all accurately assigned as strains of *B. subtilis*. However, the Biotyper system was unable to accurately distinguish the eight isolates identified by 16S rRNA gene sequencing as *B. amyloliquefaciens*. It is possible that isolate identification using the Biotyper library would be more accurate if the database possessed a more representative range of AEFB subspecies and strains, particularly of the environmentally-relevant *Bacillus* spp. and related genera.

The MSP dendrogram (Figure 2.11) shows that the majority of the isolates grouped closely together and showed a close association with *B. amyloliquefaciens* CIP103265T. Several isolates (*viz.* bng241, *B. amyloliquefaciens* strains ccc103 and sqo277, and *B. subtilis* strain bng216) were grouped separately in both mass spectra dendrograms (Figures 2.11 and 2.13), which was contrary to the 16S rRNA gene sequence findings. This disparity could be attributed to slight variations in culture growth stage—including sporulation—or sample handling when the mass spectra were generated (Carbonnelle *et al.*, 2011; Šedo, 2009; Valentine *et al.*, 2005; Wunschel *et al.*, 2005).

The existence of plant-associated ecotypes amongst *Bacillus* spp. strains has been reported by Reva *et al.*, (2004). Cohan (2001) describes an ecotype as a population of cells in the same ecological niche, and which can be out-competed by any adaptive mutant arising within the population. Both Chen *et al.* (2009b) and Reva *et al.* (2004) report that phylogenetic analysis of *gyrA* and *cheA* gene sequences in *Bacillus* spp. suggest that strains exhibiting biocontrol and plant growth promotion activity such as *B. amyloliquefaciens* FZB42 and FZB24 (RhizoPlus), and *B. subtilis* strains GB03 (Kodiak) and QST713 (Serenade), form a closely-related group that is distinct from the *B.*

amyloliquefaciens type strain DSM7^T. In the current study the strains of *B. amyloliquefaciens* identified from 16S rRNA and *gyrA* gene sequence data showed high levels of similarity to plant-associated strains, suggesting that they were probable ecotypes. Borriss *et al.* (2011) suggests the existence of the *B. amyloliquefaciens* subsp. *plantarum*, based on genetic variations between the plant-colonising *B. amyloliquefaciens* strains and the type strain *B. amyloliquefaciens* DSM7^T. In order to investigate the possible existence of AEFB ecotypes on the cucurbit phyllosphere, more in-depth studies of population diversity would be valuable. These can include such techniques as gradient gel electrophoresis (DGGE), terminal restriction fragment length polymorphism (T-RFLP), and multiple locus sequence typing (MLST) (Prabhakar and Bishop, 2014; Kim *et al.*, 2010; Schütte *et al.*, 2008).

The incidence of fungal antagonism amongst the isolates assessed using the dual-culture bioassays was found to be high. Although limited discrimination between the isolates could be determined from colony and cell morphologies, the dual-culture bioassays identified certain isolates as promising candidates for further study of powdery mildew antagonism. Representatives of these antifungal isolates were carried forward for genotyping using DNA fingerprinting. RAPD-PCR proved very useful for the generation of taxonomic groupings of isolates for dereplication purposes. While the 16S rRNA gene fragment sequencing remains useful in separating AEFB species and assigning taxonomic affiliations, sequence analysis of *gyrA* fragments were better able to resolve interspecies variation, particularly in the case of isolates identified as strains of *B. amyloliquefaciens*.

MALDI-TOF-MS is considered to be a bacterial identification technique that circumvents many of the complexities associated with PCR-based genotypic strain identification methods; and is able to offer fast, sensitive and higher resolution profiling than offered by gel electrophoresis or protein profiling (Ghyselinck *et al.*, 2011; Carbonnelle *et al.*, 2011; Schleifer, 2009; Dare, 2006; Dickinson *et al.*, 2004a). However, due to inadequate representation of environmental strains in the BDAL library, many of the AEFB isolates analysed in this study were not confidently identified to species level by the Biotyper system. The dendograms generated from the mass spectra showed some correlations to the phylogenetic trees obtained from 16S rRNA sequences. Yet, the inclusion of *gyrA* sequence analysis data combined with RAPD-PCR fingerprinting was able to offer a greater level of resolution to distinguish between closely-related isolates. Many of the AEFB isolates were found to be related to plant-associated and/or biocontrol strains on the basis of gene sequence analyses. Hence there is potential for applying these bacterial isolates as antagonists of cucurbit powdery mildew. Further

investigation into isolate modes of action, antifungal compound biosynthesis, and evaluation against the *P. fusca* pathogen is required.

CHAPTER THREE

Evaluation of lipopeptide production by *Bacillus* spp. isolates using gene marker PCR, TLC, and MALDI-TOF-MS analysis

3.1. Introduction

Many species of AEFB—specifically members of the genus *Bacillus*—are well known for their ability to produce antimicrobial compounds; with over 167 different compounds being identified to date (Bottone and Peluso, 2003). Many of range of diverse compounds synthesised by *Bacillus* spp. have shown activity against a variety of fungal, oomycete, and bacterial plant pathogens (Govindasamy *et al.*, 2010; Nagórksa *et al.*, 2007; Pryor *et al.*, 2007; Emmert and Handelsman, 1999; Bélanger *et al.*, 1998). The ability to produce antifungal compounds has contributed to the commercialisation of a number of AEFB strains, particularly amongst members of the *B. subtilis* group, as BCA of plant diseases (Borriss, 2011; Pérez-García *et al.*, 2011; Govindasamy *et al.*, 2010; Ongena *et al.*, 2010).

Lipopeptides are an important group of bioactive compounds produced by many *Bacillus* spp. which have gained prominence for their role in biocontrol mechanisms (Ongena *et al.*, 2010). They comprise a group of low molecular-mass surfactants which have a lipid tail linked to a short linear or cyclic oligopeptide (Raaijmakers *et al.*, 2010; Stein, 2005). The lipopeptides commonly produced by AEFB have been divided into four major classes: surfactins, iturins, fengycins, and kurstakins (Ongena and Jacques, 2008; Hathout *et al.*, 2000). The members of the surfactin family include esperin, lichenysin, pumilacidin, and surfactin (Ongena and Jacques, 2008). Iturin variants include bacillomycin D, F, L and LC; iturin A, A_L, C; and mycosubtilin (Ongena and Jacques, 2008). The fengycin family is comprised of fengycin A and B; and plipastatin A and B (Ongena and Jacques, 2008). A fourth lipopeptide variant named kurstakins was isolated from *B. thuringiensis*, though the relevance of this compound to biocontrol activities has not as yet been established (Bechet *et al.*, 2012; Hathout *et al.*, 2000).

Ribosome-independent biosynthesis involving multi-modular enzyme systems accounts for the diversity evident in lipopeptide structures, chemical properties, and modes of action (Jacques, 2011; Ongena and Jacques, 2008; Nagórksa *et al.*, 2007; Stein, 2005). Surfactins are able to alter biological

membrane integrity in bacteria, but exhibit no or limited antifungal activity due to the mitigating effect of sterols located in the phospholipid bilayer (Jacques, 2011; Ongena and Jacques, 2008; Stein, 2005). Iturins create ion-conducting pores in membranes, which results in an osmotic imbalance in the affected cell (Ongena and Jacques, 2008). The iturins have antifungal properties, but are neither antibacterial nor antiviral (Jacques, 2011; Ongena and Jacques, 2008; Latoud *et al.*, 1990). Fengycins are toxic to a range of filamentous fungi through interaction with membrane lipid layers by interference with cell membrane packing and permeability (Ongena and Jacques, 2008).

Many AEFB lipopeptide variants are thought to play a range of roles within the plant-associated environment (Ongena *et al.*, 2010; Ongena *et al.*, 2009; Ongena and Jacques, 2008). Surfactin production has been linked to the swarming activities of bacteria which facilitate niche colonisation; it has also been shown to interfere with biofilm formation by competing bacteria, and to play a role as an elicitor of host plant resistance mechanisms (Jacques, 2011; Jourdan *et al.*, 2009; Ongena *et al.*, 2009; Ongena *et al.*, 2007; Nagórksa *et al.*, 2007). Iturins are thought to play important roles in bacterial spreading; antifungal activity, and plant host resistance stimulation (Ongena *et al.*, 2009; Ongena and Jacques, 2008). The fengycins are believed to play a role in plant host resistance stimulation, and exhibit antifungal abilities (Ongena and Jacques, 2008; Ongena *et al.*, 2007; Ongena *et al.*, 2005b).

In light of the contribution of these compounds to biocontrol activities, the determination of lipopeptide synthesis ability is considered an important criterion when screening AEFB as candidate BCAs. Several simple direct-detection assays have been developed to determine the presence of lipopeptides (Raaijmakers *et al.*, 2010; Mukherjee *et al.*, 2009). However, conclusive identification of lipopeptides is best achieved using more complex methods such chromatography and mass spectrometry (Gordillo and Maldonado, 2012; Raaijmakers *et al.*, 2006; Razafindralambo *et al.*, 1993). PCR-based detection of gene markers associated with lipopeptide biosynthesis has been applied as an approach for determining production potential prior to compound analysis (Joshi and McSpadden Gardener, 2006). This study was undertaken to examine the lipopeptide production potential of selected *Bacillus* spp. isolates using PCR to detect gene markers, and to analyse lipopeptide extracts using TLC and MALDI-TOF-MS.

3.2. Materials and Methods

3.2.1. PCR detection of gene markers associated with lipopeptide production

PCR-based screening of *Bacillus* isolates for lipopeptide production targetted genetic markers associated with lipopeptide biosynthesis. The primers used in this study are listed in Table 3.1; and included: *fenD* F/R, targetting the fengycin synthetase *fenD* gene which activates the third and the fourth amino acids of fengycin (Lin *et al.*, 2005); *bacC* F/R targeting *bmyC*, the synthetase C gene involved in bacillomycin D synthesis (Moyne *et al.*, 2004); *sur3* F/R, targetting the *srfDB3* gene proposed to be involved in the biosynthesis of a putative thioesterase (Ramarathnam, 2007); and *ituD* F/R, which encodes a malonyl coenzyme A transacylase involved in iturin A biosynthesis (Tsuge *et al.*, 2001). Primers were synthesised and supplied by Inqaba Biotech™ Hatfield, Pretoria, South Africa. *Bacillus amyloliquefaciens* strain R16, a rhizosphere-associated isolate, was used as a positive control reference strain. This strain has been shown to produce lipopeptide compounds in previous studies (Personal communication: Hunter, C. H.; Discipline of Microbiology, School of Life Sciences, University of KwaZulu-Natal, Private bag X01, South Africa).

Template DNA was extracted from bacterial isolates using a Nucleospin DNA Extraction Kit (Macherey-Nagal, Germany). Isolates were cultured (150 rpm at 30°C for 24 h) in Luria-Bertani (LB) broth (10 ml), which contained: tryptone, 10.0 g, yeast extract, 5.0 g, NaCl, 10.0 g and deionised water 1000 ml; adjusted to pH 7.5 and autoclaved at 121°C (103.4 kPa) for 15 minutes. DNA extraction was carried out according to the manufacturer's instructions, following the protocol recommended for Gram positive bacteria. For all PCR protocols a negative (template-DNA free) and a positive control (template DNA of reference strain *B. amyloliquefaciens* R16) were included. The template DNA was stored in cryotubes at -20°C until use.

Table 3.1. PCR primers used for lipopeptide gene marker detection in *Bacillus* isolates.

Lipopeptide	Primers	Sequence (5' – 3')	Reference
Iturin	<i>ituD</i> - F	ATGAACAATCTTGCCTTTTTA	Hsieh <i>et al.</i> (2008)
	<i>ituD</i> - R	TTATTTTAAAATCCGCAATT	
Surfactin	<i>sur3</i> – F	ACAGTATGGAGGCATGGTC	Ramarathnam (2007)
	<i>sur3</i> – R	TTCCGCCACTTTTTTCAGTTT	
Bacillomycin	<i>bacC1</i> – F	GAAGGACACGGCAGAGAGTC	Ramarathnam <i>et al.</i> (2007) Athukorala <i>et al.</i> (2009)
	<i>bacC1</i> – R	CGCTGATGACTGTTCATGCT	
Fengycin	<i>fenD1</i> – F	TTTGGCAGCAGGAGAAGTTT	Ramarathnam <i>et al.</i> (2007) Athukorala <i>et al.</i> (2009)
	<i>fenD1</i> – R	GCTGTCCGTTCTGCTTTTTC	

PCR reactions were carried out using Promega GoTaq® PCR reagents (Promega, Madison, USA) with each PCR reaction consisting of the following: 0.4 µM of the appropriate primer (Table 3.1); 1x GoTaq® Flexi Buffer (without MgCl₂); 200µM of each deoxyribonucleotide (dNTP); 1.5 mM MgCl₂; 2.5 U of GoTaq® polymerase; 1 µl template DNA; and nuclease-free water to bring the final volume to 25 µl. A Bioer XP thermocycler (Model TC-XP-G, Bioer Technology Co. Ltd., China) was used to run each PCR protocol. The reaction conditions are specified in Table 3.2; and were adapted from Ramarathnam *et al.* (2007) for surfactin, fengycin and bacillomycin primers; and Hsieh *et al.*, (2008) for the iturin primer. After completion of the PCR run, the holding temperature for all protocols was 4°C.

Table 3.2. PCR reaction conditions for the primers used for lipopeptide gene marker screening of *Bacillus* isolates.

Protocol	PCR cycling (Temperature and duration)					Cycles
	Initialisation	Denaturation	Annealing	Elongation	Final Extension	
<i>ituD</i>	94°C / 2 min	94°C / 1 min	50°C / 1 min	72°C / 90 sec	72°C / 7 min	30
<i>sur3</i>	94°C / 4 min	94°C / 1 min	60°C / 30 sec	72°C / 1 min	72°C / 10 min	35
<i>bacC1</i>	94°C / 4 min	94°C / 1 min	60°C / 30 sec	72°C / 1 min	72°C / 10 min	25
<i>fenD1</i>	94°C / 4 min	94°C / 1 min	60°C / 30 sec	72°C / 1 min	72°C / 10 min	25

PCR products were analysed and visualised by agarose gel electrophoresis using 1.5% (w/v) agarose gel (Laboratoriois Conda, Madrid, Spain) prepared with 1x Tris-Borate-Ethylenediaminetetraacetic acid (TBE) buffer (89 mM Tris base, 89 mM Boric acid and 2 mM EDTA, adjusted to pH 8.0). Gels were pre-stained with SYBR Safe (1x) (Invitrogen, California, USA). The PCR products were prepared in final volumes of 5 µl per lane, with a ratio of 3 µl amplicon to 2 µl loading dye (6x blue-orange) (Promega, Madison, USA). A 1 kb molecular weight ladder (Promega, Madison, USA) was included to estimate the molecular weight of each PCR product. Gels were run at 90 V for 50–60 minutes and images of each gel electrophoresis were captured under ultra violet (UV) light on a SynGene G:Box imaging system (Syngene, Cambridge, England) using the Syngene GeneSnap software (version 7.09).

To confirm the sequence homology of PCR products obtained from the positive control *B. amyloliquefaciens* R16, each of the four gene marker amplicons were sequenced using an ABI 3500XL Genetic analyser (Applied Biosystems, California, USA) at Inqaba Biotec Laboratories (Pretoria, South Africa). Consensus sequences were visualised and edited using Chromas Lite (version 2.01) and BioEdit (version 7.1.3.0.) (Hall, 1999) software and aligned using MAFFT online (<http://mafft.cbrc.jp/alignment/server>). Sequences were then submitted to the BLAST-N database (<http://blast.ncbi.nlm.nih.gov/Blast.cgi>) for comparison to existing sequences within the EMBL/GenBank/DDBJ database.

3.2.2. Lipopeptide compound extraction from *Bacillus* cultures

For the purposes of lipopeptide compound extraction, selected *Bacillus* isolates were cultured in a defined antibiotic production medium (McKeen *et al.*, 1986). The medium comprised (per litre of deionised water): D-glucose, 15.0 g; L-glutamic acid, 5.0 g; MgSO₄·7H₂O, 1.02 g; K₂HPO₄·3H₂O, 1.0 g; and KCl, 0.5 g; and 1 ml of a trace element solution. The trace element solution consisted of: CuSO₄·5H₂O, 0.16 g; MnSO₄·7H₂O, 0.1 g; and FeSO₄·7H₂O, 0.015 g in 100 ml deionized water. The medium pH was adjusted to pH 6.0-6.2 using 1 N NaOH before decanting and autoclaving at 121°C (103.4 kPa) for 15 minutes.

Starter cultures were established by inoculating a single colony from a 10% TSA culture (24 h at 30°C) into 10 ml of antibiotic production medium and incubating at 30°C at 150 rpm for 18 h. Three

millilitres of the starter culture was then aseptically inoculated into 50 ml of the antibiotic production medium, and incubated for a further 48 h (30°C at 150 rpm).

Lipopeptide extraction was performed following an acid precipitation method modified from Vater *et al.* (2002) and McKeen *et al.*, (1986). The broth cultures were centrifuged at 12,096 x *g* (Avanti centrifuge, Beckman Coulter) for 30 minutes at 4°C after which the supernatant was transferred into sterile glass bottles and acidified to pH 2.0–2.2 using 1 M HCl. The solution was refrigerated (4°C) for 3–4 h to encourage the precipitation of any lipopeptide compounds present. The contents of the bottle were centrifuged as before, and the supernatant discarded. The precipitate was resuspended in 1 ml methanol and decanted into a microfuge tube. The centrifuge tube was washed out with an additional 1 ml methanol, and this decanted into a separate microfuge tube. Both of the tubes from each respective isolate were centrifuged at 15,996 x *g* for 5 minutes, after which the two supernatants were combined and filter-sterilized (GxP 0.45 µm GHP Acrodisc, Pall Life Sciences) into sterile 10 ml glass polytop vials, and stored at -20°C.

3.2.3. Determination of antifungal activity of methanol extracts using a disc-diffusion bioassay

To determine the antifungal activity of the methanol extracts, disc-diffusion bioassays were performed using *Rhizoctonia solani* obtained from the Discipline of Plant Pathology (University of KwaZulu-Natal) culture collection. To ensure purity the fungus was initially cultured on water agar (15 g/l bacteriological agar) before being subcultured onto potato dextrose agar (PDA) (Biolab, Merck, Germany) and incubated at 30°C. Subculturing was performed every 7 d to ensure culture viability.

Sterile filter-paper discs (9 mm diameter) (Macherey-Nagel, Germany) were placed onto PDA plates and inoculated with 20 µl of methanol extract, with each extract being tested in triplicate (i.e. three discs per plate). Methanol-inoculated discs (20 µl) were included as a control. Colonised *R. solani* agar plugs (5 x 5 mm) were taken from PDA cultures (4 d), and aseptically transferred to the centre of each assay plate. Incubation was carried out at 30°C, and the plates were examined and rated after 72 h for signs of antifungal activity. Observations were recorded as measurements of the zone

of inhibition, measured from the disc edge to fungal mycelium boundary. The degree of antifungal activity was rated as described previously (Section 2.2.2).

3.2.4. TLC analysis of lipopeptide-methanol extracts

TLC analysis of the methanol extracts was carried out on an oven-dried TLC Silica Gel 60 F254 aluminium plate (20 cm x 20 cm) (Merck, Germany). The plate was spotted with 20 µl of each methanol extract approximately 1 cm from the bottom edge. For comparative purposes lipopeptide standards surfactin and iturin A (20 ppm in methanol) (Sigma-Aldrich, Chemie GmbH, Munich, Germany) were included.

The TLC plate was placed into a glass tank containing a 70:30 (v/v) propan-1-ol : water mobile phase (Tewelde, 2004). After sealing the tank, the TLC was allowed to proceed until the solvent front reached approximately 1 cm from the plate edge (~ 3 h). Where after the plate was removed from the tank, the solvent front marked, and the plate air-dried. Bands were visualised under UV illumination (260 nm) for UV-active regions; and hydrophobic regions were determined by misting the plate with water. In each instance visible bands were marked and the relative mobility (R_f) values of each band were calculated using the following formula (Kowalska *et al.*, 2003):

$$R_f = \frac{\text{distance of the chromatographic band centre from the spotted region (mm)}}{\text{distance between the spotted region and the solvent front (mm)}}$$

3.2.5. MALDI-TOF-MS analysis of lipopeptide-methanol extracts

MALDI-TOF-MS analysis of methanol extracts was carried out using a bench-top Bruker Microflex L20 MALDI-TOF mass spectrometer (Bruker Daltonics, Germany) equipped with an N₂ laser (337 nm). Spectral processing and analysis was carried out using FlexControl software (version 2.4) (Bruker Daltonics). The matrix solution used was α-cyano-hydroxycinnamic acid (HCCA) (Bruker Daltonics) dissolved in 50% (v/v) acetonitrile and 2.5% (v/v) trifluoroacetic acid (TFA) to provide a final concentration of 10 mg HCCA/ml. For calibration purposes a Bovine Serum Albumin Digest standard (tryptic digest of bovine serum albumin, ~500 pmol/tube) (Bruker Daltonics, Germany) was used, which contained peptide fragments with a mass range of 927.493 Da to 2045.029 Da.

Included in the analysis were surfactin and iturin A standards (20 ppm in methanol) (Sigma-Aldrich, Chemie GmbH, Munich, Germany). Methanol extracts from two plant-associated reference strains (*B. amyloliquefaciens* R16 and *B. subtilis* B81) were also included as examples of previously characterised lipopeptide-producing *Bacillus* spp. (Personal communication: Hunter, C. H.; Discipline of Microbiology, School of Life Sciences, University of KwaZulu-Natal, Private bag X01, South Africa).

Aliquots (0.5 µl) of each methanol extract were spotted, in duplicate, onto a stainless steel target plate and allowed to air-dry before being overlaid with 0.5 µl of HCCA matrix. The co-crystallized complex was then allowed to air-dry prior to analysis. Mass spectra of the lipopeptide extracts were generated with the laser in positive linear mode at 60 Hz (with laser power at 12%), as an average of 300 laser shots per spectrum (50 shots in 6 positions) in the mass range of 750–2500 Da. Post processing utilised the snap-peak detection algorithm with averaging.

For the differentiation and identification of peaks associated with lipopeptide compounds, the mass spectra were exported to mMass open source software (version 5.5.0) (Niedermeyer and Strohm, 2012; Strohm *et al.*, 2010; Strohm *et al.*, 2008) and SPECLUST (<http://bioinfo.thep.lu.se/speclust.html>) (Alm *et al.*, 2006). Using mMass, the duplicated mass spectra from each sample were subjected to spectral processing which involved baseline subtraction (Precision set at 100, relative offset at 90); smoothing (Gaussian method, window size 0.3 *m/z*, with 2 cycles); and peak picking (S/N threshold 3.0, absolute intensity threshold 1.0, relative intensity threshold 5%, and picking height at 100). The spectra peak data generated was used to create a gel view for visual comparisons between the mass spectra using mMass.

The duplicate peak lists of the lipopeptide standards and reference strains were also submitted to SPECLUST for the identification of common peaks between the replicate spectra for each isolate. The parameters for the peaks-in-common SPECLUST function were defined as pairwise score cut-off of 0.7, measurement error of 5.0 Da, and multiple score cut-off of 0. Those peaks common to both peak lists per isolate comprised the final peak list from which lipopeptide-associated peaks were identified using the *m/z* values previously published in literature (Price *et al.*, 2007; Koumoutsis *et al.*, 2004; Vater *et al.*, 2002; Leenders *et al.*, 1999).

3.3. Results

3.3.1. PCR detection of gene markers associated with lipopeptide biosynthesis

Fifty five isolates were selected for PCR screening based on their performance in the dual-culture antifungal assays and data obtained from DNA fingerprinting and gene fragment sequencing. The isolates chosen were: *B. amyloliquefaciens* strains bna75, bna78, bna81, mwb86, mwb87, ccc103, bnd109, bnd137, cce140, cce142, cce146, bnd160, pkf167, cce174, cce175, cce183, bng199, bng210, bng230, pkl242, pkl247, pkk252, sqo275, sqo277, bnn282, and sqo298; *B. subtilis* strains bnd134, bnd136, bnd156, bng215, bng216, bng221, sqo271, and sqo279; and unidentified isolates bna85, bnd115, bnd116, bnd119, bnd124, bnd125, bnd139, cce147, bnd149, bnd150, bnd154, bnd157, bnd162, bnd166, bng202, bng217, bng218, bng224, bng227, and sqo272. Isolate bng241 was also included as a negative control, as this isolate that did not exhibit any antifungal activity in the initial dual-culture bioassays.

The gene markers used to detect the functional genes involved in lipopeptide synthesis were those associated with fengycin (*fenD*), bacillomycin (*bacC*), surfactin (*sur3*) and iturin (*ituD*). Each of these gene markers were detected in the reference strain *B. amyloliquefaciens* R16. The approximate product sizes for each PCR are visualised in Figure 3.1.

The four gene marker amplicons from reference strain *B. amyloliquefaciens* R16 from were sequenced and submitted to GenBank for a BLAST search to confirm sequence identity (Table 3.3). The surfactin, bacillomycin and fengycin sequences were found to be homologous to their respective markers. However, the *ituD* amplicon showed sequence homology to *bmyD*, a malonyl CoA-acyl carrier protein associated with the production of bacillomycin D, an iturin variant. Compound analysis previously undertaken has shown that *B. amyloliquefaciens* R16 is not known to produce iturin A, but does synthesise bacillomycin D (Personal communication: Hunter, C. H.; Discipline of Microbiology, School of Life Sciences, University of KwaZulu-Natal, Private bag X01, South Africa).

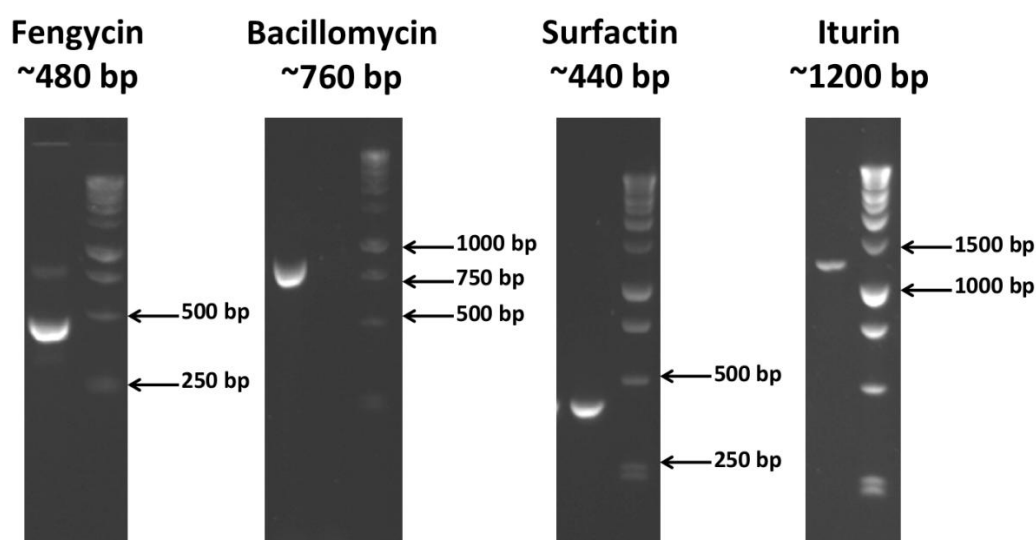


Figure 3.1. Expected PCR product sizes for the respective lipopeptide gene markers in reference strain *B. amyloliquefaciens* R16, as viewed after gel electrophoresis using 1.5% (w/v) agarose.

Table 3.3. Sequence identities of lipopeptide gene markers derived from reference strain *B. amyloliquefaciens* R16 (Date accessed: 10 August 2013).

Primer	Product Size (bp)	BLAST Sequence Match	Accession Number	Similarity
<i>fenD</i>	431	Fengycin synthetase (<i>fenD</i>) <i>B. amyloliquefaciens</i> subsp. <i>plantarum</i> YAU B9601-Y2	NC017061.1	99
<i>ituD</i>	1115	Malonyl CoA-acyl carrier protein associated with bacillomycin D synthesis (<i>bmyD</i>) <i>B. amyloliquefaciens</i> FZB42	NC009725.1	100
<i>sur3</i>	361	Surfactin synthase thioesterase subunit (<i>srfA-D</i>) <i>B. amyloliquefaciens</i> subsp. <i>plantarum</i> UCMB5036	NC020410.1	100
<i>bacC</i>	763	Bacillomycin D synthetase C (<i>bmyC</i>) <i>B. amyloliquefaciens</i> FZB42	NC009725.1	99

Results for the screening of isolates for lipopeptide gene markers are shown in Table 3.4, with examples of positive banding shown in Figure 3.2. Isolates that yielded PCR fragments consistent with the expected amplicon size of each gene markers were recorded as positive. The absence of a PCR product was considered a negative result. Positive marker bands for fengycin and iturin were detected in 41 isolates; 39 isolates were distinguished as positive for surfactin; and 22 isolates had positive banding for the bacillomycin primer. For comparative purposes Table 3.4 also includes the RAPD-PCR fingerprint groupings of the isolates and their sequence matches to the GenBank database for 16S rRNA and *gyrA* gene sequence fragments.

Eighteen isolates were positive for all markers screened for, and many had been identified to be closely-related to strains of *B. amyloliquefaciens* (Table 3.4). These isolates included *B. amyloliquefaciens* strains mwb86, mwb87, bnd109, bnd137, cce142, cce174, cce175, pkl242, sqo277, and sqo298; as well as unidentified isolates bna85, bnd116, bnd119, bnd124, bnd125, bnd150, bnd157, and bng217. Isolate bng241 did not produce any positive results for the gene markers screened, which was not unexpected owing to this isolate's lack of antifungal activity. A further thirteen isolates showed negative results for all gene markers screened, and included *B. subtilis* strains bnd134, bnd136, bnd156, bng216, bng221, and sqo271; as well as unidentified isolates bnd115, bnd139, bnd157, bnd162, bnd166, bng202, and bng218. Interestingly, representatives from the group of marker-negative isolates (*viz.* *B. subtilis* strains bnd134, bnd136, bnd156, bng216, bng221, and sqo271) comprise RAPD fingerprint groupings c, d, j, and k (Table 3.4), which showed high levels of gene sequence homology to strains of *Bacillus* sp. JS and *B. subtilis*. Additionally, *B. subtilis* strains bng215 and sqo279 showed a positive result for the surfactin marker only; and comprised RAPD fingerprint grouping h, which also closely matched to *B. subtilis*. Owing to the lack of specificity of the *ituD* primer, it is difficult to determine which isolates were able to produce iturin, and which were co-producing iturin and bacillomycin.

Table 3.4. Lipopeptide gene markers associated with fengycin (*fenD*), bacillomycin (*bacC*), surfactin (*sur3*), and iturin (*ituD*) biosynthesis amongst *Bacillus* isolates compared to RAPD fingerprint grouping.

Isolate ^x	RAPD Group ^x	Lipopeptide Gene Markers*			
		Fengycin	Bacillomycin	Surfactin	Iturin
bn75	a	+	-	+	+
bn78	a	+	-	+	+
<i>B. amyloliquefaciens</i> bnb85	a	+	+	+	+
<i>B. amyloliquefaciens</i> mwb86	a	+	+	+	+
<i>B. amyloliquefaciens</i> mwb87	a	+	+	+	+
<i>B. amyloliquefaciens</i> ccc103	a	+	-	+	+
<i>B. amyloliquefaciens</i> bnd109	a	+	+	+	+
bnd116	a	+	+	+	+
bnd124	a	+	+	+	+
bnd125	a	+	+	+	+
<i>B. amyloliquefaciens</i> bnd137	a	+	+	+	+
<i>B. amyloliquefaciens</i> cce142	a	+	+	+	+
bnd150	a	+	+	+	+
bnd154	a	+	-	+	+
<i>B. amyloliquefaciens</i> bnd160	a	+	-	+	+
<i>B. amyloliquefaciens</i> pkf167	a	+	-	+	+
<i>B. amyloliquefaciens</i> cce174	a	+	+	+	+
<i>B. amyloliquefaciens</i> cce175	a	+	+	+	+
<i>B. amyloliquefaciens</i> cce183	a	+	-	+	+
<i>B. amyloliquefaciens</i> bng210	a	-	+	+	+
bng217	a	+	+	+	+
<i>B. amyloliquefaciens</i> bnn282	a	-	+	+	+
<i>B. amyloliquefaciens</i> sqo298	a	+	+	+	+
bn81	b	+	+	-	+
bnd119	b	+	+	+	+
<i>B. amyloliquefaciens</i> cce140	b	+	+	-	+
<i>B. subtilis</i> bnd157	b	+	+	+	+
bnd115	c	-	-	-	-
<i>B. subtilis</i> bnd136	c	-	-	-	-
<i>B. subtilis</i> bnd139	c	-	-	-	-
bnd162	c	-	-	-	-
bnd166	c	-	-	-	-
<i>B. subtilis</i> bnd134	d	-	-	-	-
<i>B. subtilis</i> bnd156	d	-	-	-	-
<i>B. amyloliquefaciens</i> bng199	e	+	-	+	+
<i>B. amyloliquefaciens</i> pkl242	f	+	+	+	+
<i>B. amyloliquefaciens</i> pkl247	f	+	-	+	+

Table 3.4. Continued.

Isolate [†]	RAPD Group ^x	Lipopeptide Gene Markers*			
		Fengycin	Bacillomycin	Surfactin	Iturin
<i>B. amyloliquefaciens</i> bng199	e	+	-	+	+
<i>B. amyloliquefaciens</i> pkl242	f	+	+	+	+
<i>B. amyloliquefaciens</i> pkl247	f	+	-	+	+
<i>B. amyloliquefaciens</i> pkk252	f	+	-	+	+
sqa272	f	+	-	+	+
<i>B. amyloliquefaciens</i> sqa277	f	+	+	+	+
<i>B. amyloliquefaciens</i> cce146	g	+	-	+	+
cce147	g	+	-	+	+
bnd149	g	+	-	+	+
<i>B. subtilis</i> bng215	h	+	-	-	-
<i>B. subtilis</i> sqa279	h	+	-	-	-
<i>B. subtilis</i> bng216	j	-	-	-	-
bng202	k	-	-	-	-
bng218	k	-	-	-	-
<i>B. subtilis</i> bng221	k	-	-	-	-
<i>B. subtilis</i> sqa271	k	-	-	-	-
bng224	l	+	-	+	+
bng227	l	+	-	+	+
<i>B. amyloliquefaciens</i> sqa275	m	+	-	+	+
<i>B. amyloliquefaciens</i> bng230	n	+	-	+	+
bng241 [§]	i	-	-	-	-
<i>B. amyloliquefaciens</i> R16 [#]	a	+	+	+	+

* (+) positive band after PCR, (-) no band present after PCR. ^x OPG-11 RAPD-PCR fingerprint groupings. [†] Sequence homology based on 16S rRNA and *gyrA* partial gene sequences. [§] Negative control isolate bng241. [#] Reference strain *B. amyloliquefaciens* R16.

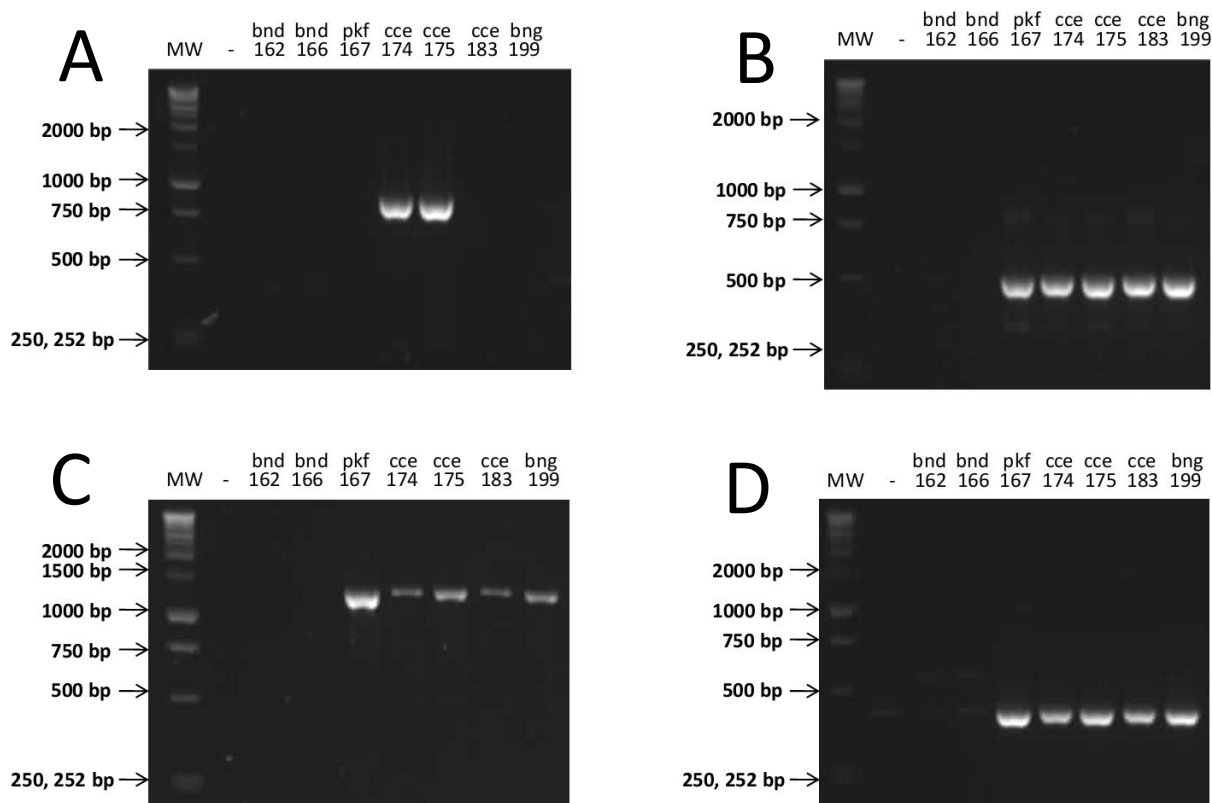


Figure 3.2. Gel electrophoresis images demonstrating PCR products for lipopeptide gene marker primers *bacC* (A), *fenD* (B), *ituD* (C), and *sur3* (D) obtained for isolates bnd162 and bnd166, and *B. amyloliquefaciens* strains pkf167, cce175, cce183, and bng199. The presence of a band indicated a positive result for the gene marker, and band absence indicated a negative result.

3.3.2. Extraction and characterisation of lipopeptide compounds from *Bacillus* isolates

3.3.2.1. Disc-diffusion bioassay

Fourteen isolates were selected for lipopeptide compound extraction analysis based on their antifungal rating in the initial dual-culture bioassays, and as representatives of the groupings from DNA fingerprint and phylogenetic groupings distinguished previously (Chapter 2). The isolates selected that had provided positive results for one or more gene marker PCR were *B. amyloliquefaciens* strains mwb86, ccc103, cce140, cce146, cce175, bng199, sqo275, sqo277, and bnn282; *B. subtilis* strain sqo279. *Bacillus subtilis* strains bnd134, bnd136, and bng216 were included as representatives of those isolates providing negative results for all lipopeptide gene markers. The inclusion of isolate bng241 served as a negative control, as this isolate exhibited

neither antifungal activity nor any positive results for lipopeptide gene marker PCR. The methanol extracts from all the isolates displayed antagonism towards *R. solani*, excepting the negative control isolate bng241 (Table 3.5). The methanol control did not appreciably affect fungal growth.

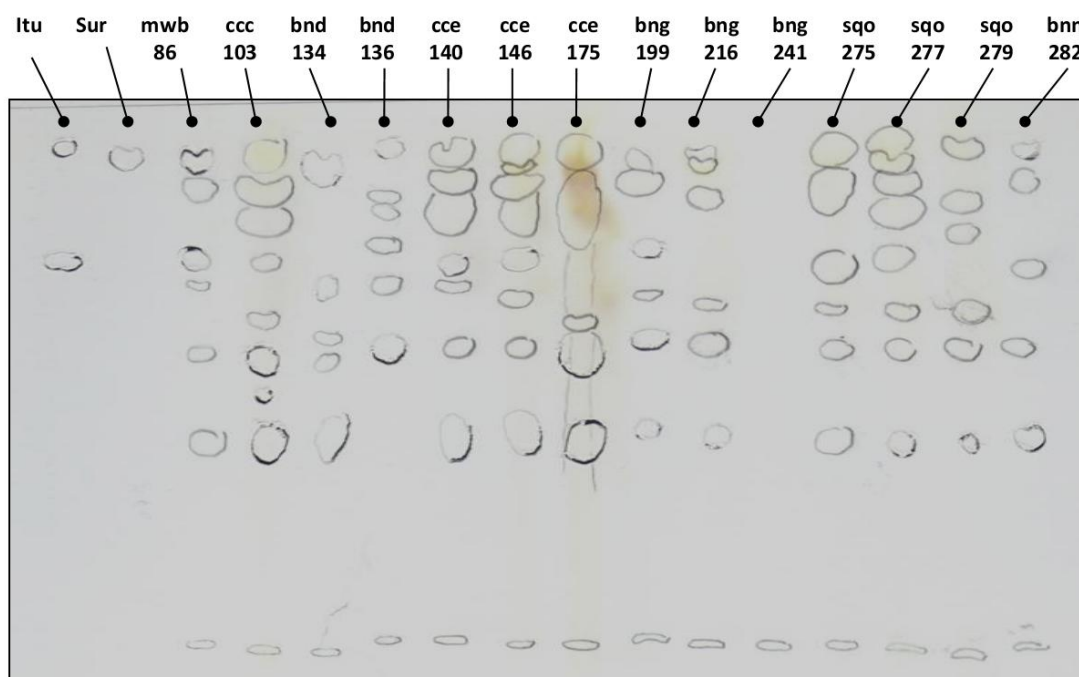
Table 3.5. Disc-diffusion bioassay of methanol extracts from *Bacillus* isolates antagonistic towards *Rhizoctonia solani*.

Isolate	Antifungal Activity Rating*
<i>B. amyloliquefaciens</i> mwb86	+++
<i>B. amyloliquefaciens</i> ccc103	+++
<i>B. subtilis</i> bnd134	++
<i>B. subtilis</i> bnd136	++
<i>B. amyloliquefaciens</i> cce140	+++
<i>B. amyloliquefaciens</i> cce146	+++
<i>B. amyloliquefaciens</i> cce175	+++
<i>B. amyloliquefaciens</i> bng199	+++
<i>B. subtilis</i> bng216	++
<i>B. amyloliquefaciens</i> sqo275	+++
<i>B. amyloliquefaciens</i> sqo277	+
<i>B. subtilis</i> sqo279	+++
<i>B. amyloliquefaciens</i> bnn282	+++
bng241 ^s	-
Methanol control	-

* Rating system of zone of inhibition 72 h post fungal inoculation: (+++) greater than 5 mm; (++) 2–5 mm; and (+) less than 2 mm; (-) no zone observed. ^s Negative control isolate.

3.3.2.2. Analysis of methanolic extracts using TLC

TLC analysis of the methanolic extracts resolved several bands for the thirteen antifungal isolates when the plate was viewed under UV light and after wetting (Plate 3.1). After exposure to both visualisation methods the R_f values of all the visible bands were marked and calculated (Table 3.6). Many of the UV-fluorescent bands also exhibited hydrophobic properties; though in some instances hydrophobic regions did not fluoresce under UV, as was noted for *B. amyloliquefaciens* strain cce140 and the lipopeptide standards (Plate 3.2).



* Purified standards : Itu = iturin A, Sur = surfactin.

Plate 3.1. TLC plate showing marked bands of lipopeptide extracts in methanol after separation using a 70:30 (v/v) propan-1-ol : water mobile phase and visualised under UV illumination and/or atomisation with water.

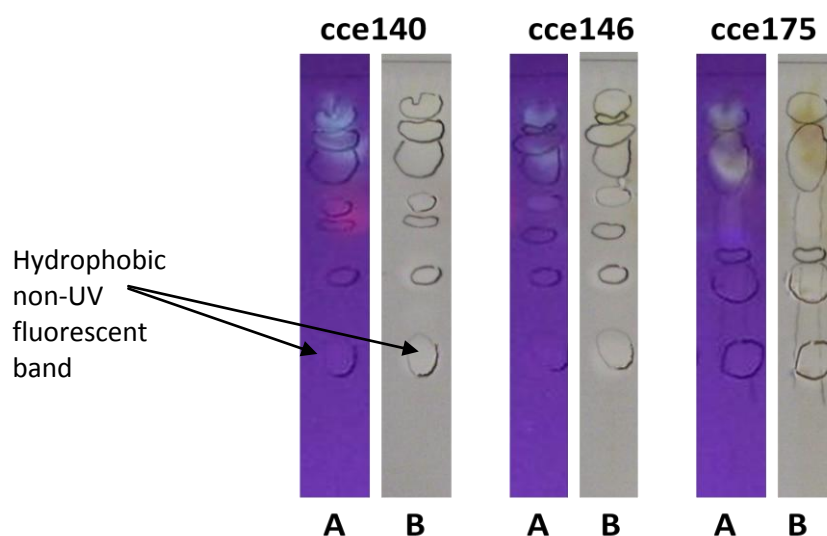


Plate 3.2. Sections of TLC plates of methanol extracts from *B. amyloliquefaciens* strains cce140, cce146, and cce175 showing band fluorescence as seen under UV illumination (A) and band hydrophobicity after atomisation with water (B).

In all of the fourteen methanol extracts analysed, a faint brown-coloured band was observed just above the region spotted at R_f 0.35–0.37 which possessed neither UV-activity nor hydrophobicity, and was not present in the lipopeptide standards. This is the only band noted for negative control isolate bng241. Though recorded, other coloured bands without fluorescence or hydrophobic properties appeared at locations in other profiles (Table 3.6). Owing to their lack of any lipopeptide-associated characteristic these bands were disregarded.

With the exception of isolate bng241, all methanol extracts showed a band corresponding to that of surfactin at R_f 0.94. The iturin A standard showed a prominent band at R_f 0.82, with an additional band also present with an R_f value of 0.94. A band corresponding closely to the R_f 0.82 band of the iturin A standard was not resolved in *B. amyloliquefaciens* strains cce175, sqo275, and bnn282; and *B. subtilis* strains bnd134, bng216, and sqo279.

Table 3.6. R_f values of all bands visible after TLC analysis of methanol extracts, recorded by colouration and after UV illumination and/or after atomising with water.

Sample	R _f Values*									
Iturin A	<u>0.82</u>	<u>0.95</u>								
Surfactin	<u>0.94</u>									
<i>B. amyloliquefaciens</i> mwb86	0.36	<u>0.61</u>	<u>0.71</u>	0.79	0.82	0.9	0.94			
<i>B. amyloliquefaciens</i> ccc103	0.36	<u>0.6</u>	<u>0.66</u>	<u>0.7</u>	0.74	<u>0.81</u>	<u>0.86</u>	0.88	0.94	
<i>B. subtilis</i> bnd134	0.35	0.61	<u>0.7</u>	<u>0.73</u>	<u>0.79</u>	<u>0.92</u>				
<i>B. subtilis</i> bnd136	0.37	<u>0.71</u>	<u>0.78</u>	0.83	0.87	0.88	0.9			
<i>B. amyloliquefaciens</i> cce140	0.37	<u>0.61</u>	<u>0.71</u>	0.78	0.81	<u>0.87</u>	0.9	0.93		
<i>B. amyloliquefaciens</i> cce146	0.36	<u>0.61</u>	<u>0.71</u>	0.76	<u>0.81</u>	<u>0.86</u>	<u>0.9</u>	0.91	0.93	
<i>B. amyloliquefaciens</i> cce175	0.37	<u>0.6</u>	<u>0.7</u>	0.74	0.87	0.9				
<i>B. amyloliquefaciens</i> bng199	0.37	<u>0.61</u>	<u>0.71</u>	0.77	<u>0.82</u>	0.9	<u>0.91</u>			
<i>B. subtilis</i> bng216	0.36	<u>0.61</u>	<u>0.71</u>	0.76	0.88	0.92	0.94			
<i>B. amyloliquefaciens</i> sqo275	0.35	<u>0.59</u>	<u>0.7</u>	0.75	0.79	0.89	0.93			
<i>B. amyloliquefaciens</i> sqo277	0.35	<u>0.59</u>	<u>0.7</u>	0.74	<u>0.81</u>	<u>0.86</u>	0.9	0.91	0.94	
<i>B. subtilis</i> sqo279	0.35	<u>0.59</u>	<u>0.7</u>	0.75	0.76	0.87	<u>0.94</u>			
<i>B. amyloliquefaciens</i> bnn282	0.35	<u>0.59</u>	<u>0.7</u>	<u>0.79</u>	0.9	0.93				
bng241 [§]	0.36									

* Values marked in **bold** indicate fluorescence under UV illumination. Underlined values denote hydrophobicity. Plain text values represent those bands visible by colouration only, and possessed neither UV-fluorescence nor hydrophobicity.

[§] Negative control isolate bng241.

3.3.2.3. Detection of lipopeptide compounds using MALDI-TOF-MS

Methanolic extracts from the selected isolates were also analysed with MALDI-TOF-MS to screen for lipopeptide biomarkers. Only thirteen extracts were analysed, as the extract of *B. subtilis* strain sqo279 was omitted from analysis due to excessive production of extracellular matter during culture in the antibiotic production medium, which hampered lipopeptide recovery and interfered with detection using MALDI-TOF-MS.

To accurately define the presence of lipopeptide peaks, purified standards of iturin A and surfactin were analysed. The *m/z* values obtained from the mass spectra were assigned to specific lipopeptide

isoforms based on m/z values in literature (Price *et al.*, 2007; Koumoutsis *et al.*, 2004; Vater *et al.*, 2002; Leenders *et al.*, 1999). It was then possible to assign peaks to protonated species; as well as to sodium and potassium adducts of known isoforms, indicated by ions detected respectively as 22 or 38 mass units larger than the protonated species (Table 3.7) (Price *et al.*, 2007; Koumoutsis *et al.*, 2004). The iturin A standard provided prominent peaks from m/z 1043.72–1071.71; and the surfactin standard main peaks appeared at the m/z range 994.46–1059.11. The averaged mass spectrum of the duplicate mass spectra for each of the surfactin and iturin A standards are presented in Figures 3.3 and 3.4 respectively.

Table 3.7. m/z values of prominent peaks detected by MALDI-TOF-MS in duplicate mass spectra of surfactin and iturin A standards.

Peak Assignment	m/z	Std.Dev.
Iturin Species		
C14 [M+H ⁺]	1043.72	0.0003
C14 [M+K ⁺]	1082.63	0.04
C14 [M+Na ⁺]	1065.74	0.11
C15 [M+H ⁺]	1057.72	0.47
C15 [M+K ⁺]	1079.69	0.04
C16 [M+H ⁺]	1071.71	0.02
Surfactin Species		
C12 [M+H ⁺]	994.96	0.5
C13 [M+H ⁺]	1009.53	0.13
C14 [M+H ⁺]	1023.08	0.07
C14 [M+K ⁺]	1061.04	0.10
C14 [M+Na ⁺]	1047.27	0.88
C15 [M+H ⁺]	1037.10	0.08
C15 [M+K ⁺]	1075.07	0.10
C15 [M+Na ⁺]	1059.11	0.08

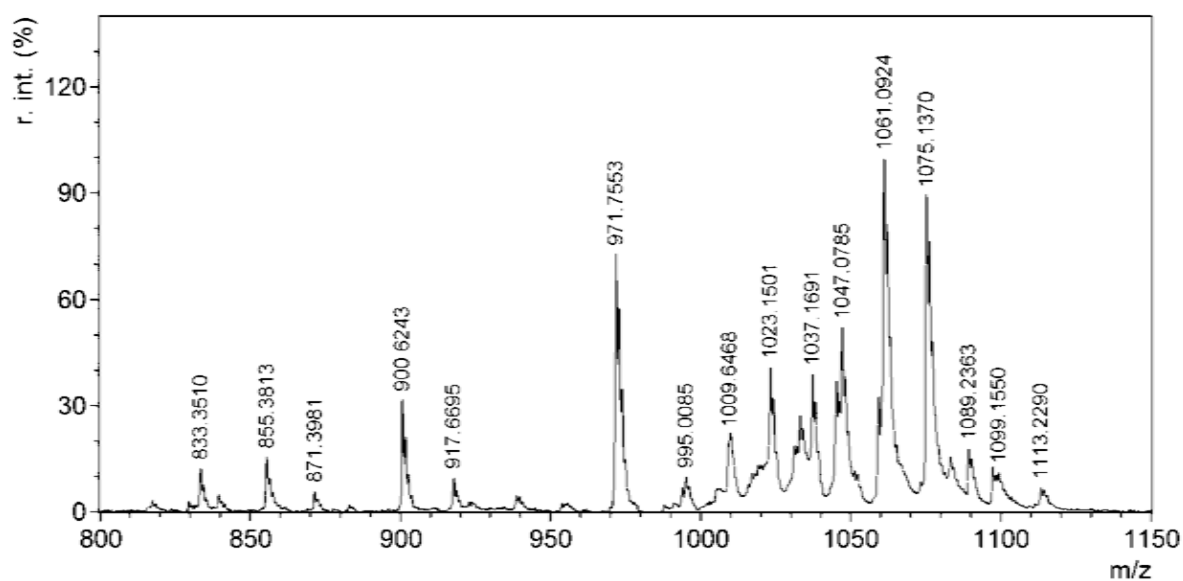


Figure 3.3. Mass spectrum of reference standard surfactin (m/z 800–1150).

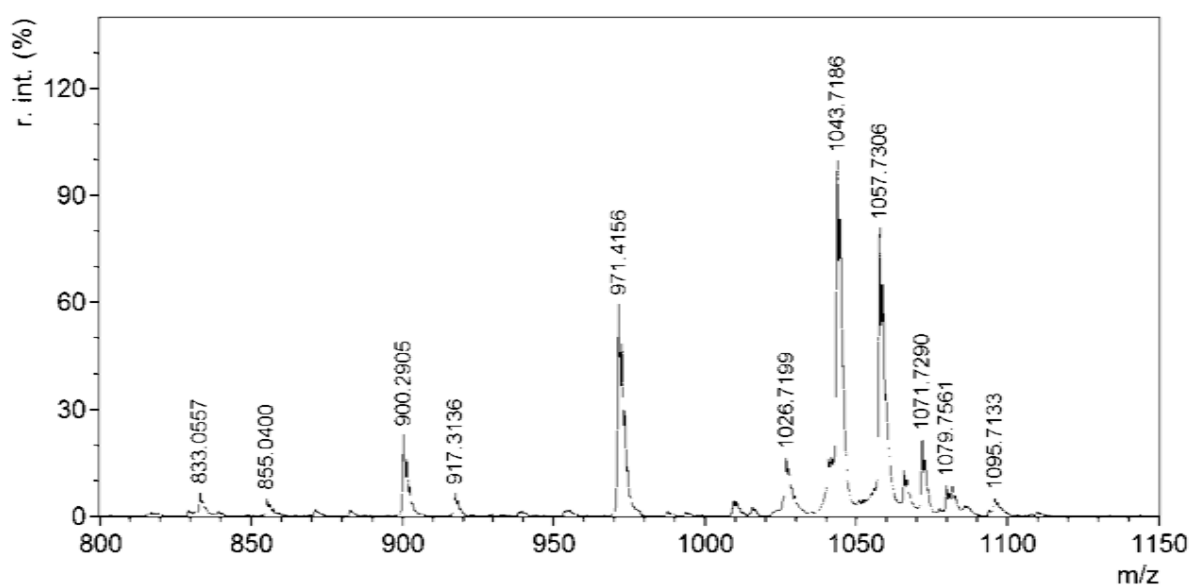


Figure 3.4. Mass spectrum of reference standard iturin A (m/z 800–1150).

The mass spectra for the methanol extracts of reference strains *B. amyloliquefaciens* R16 and *B. subtilis* B81 are shown in Figures 3.5 and 3.6 respectively. In both cases lipopeptide compounds were distinguished and identified based on similarities to the spectra derived from the surfactin and iturin

standards, and from the m/z values of lipopeptides previously described in the literature (Price *et al.*, 2007; Koumoutsis *et al.*, 2004; Vater *et al.*, 2002; Leenders *et al.*, 1999).

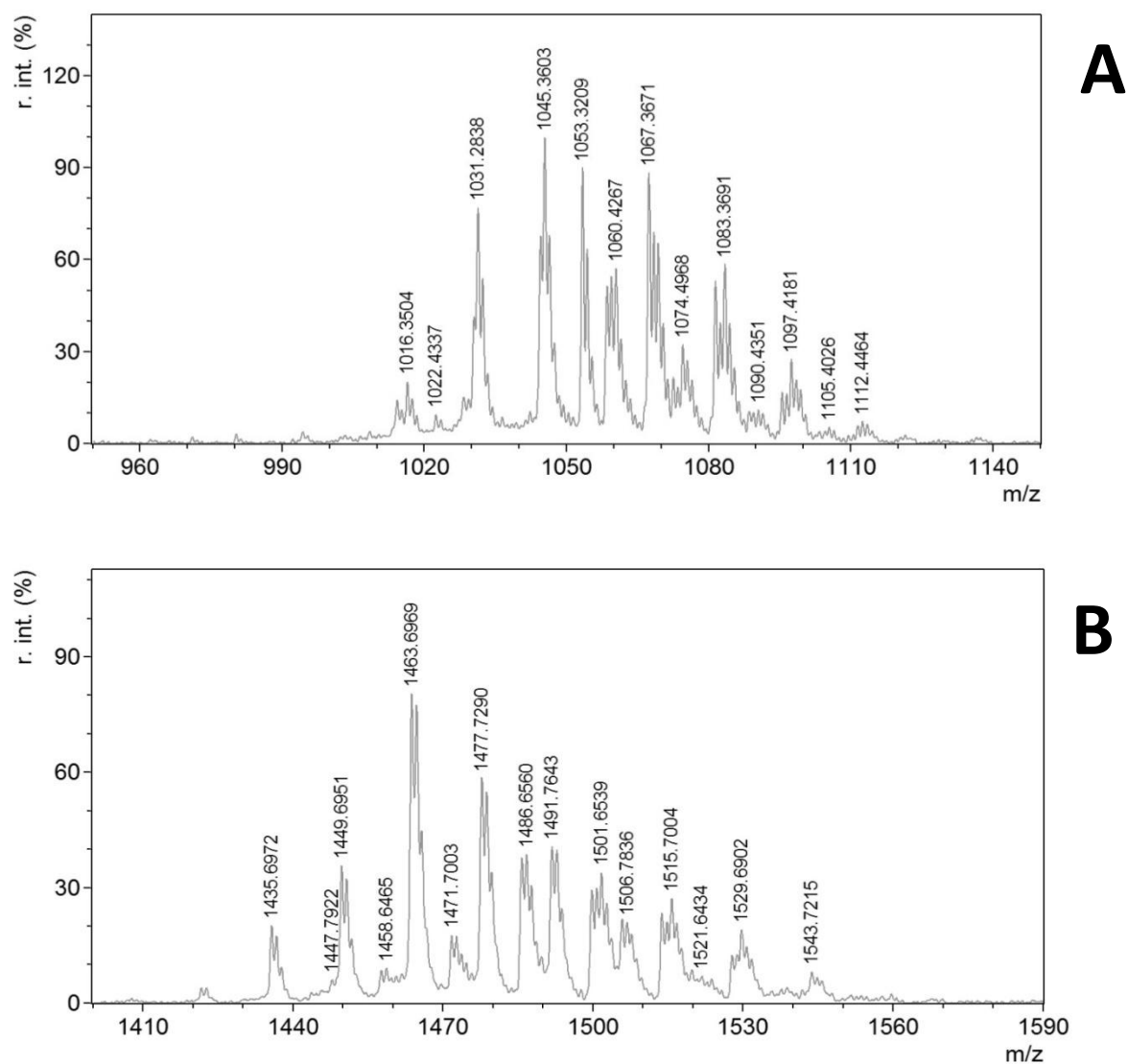


Figure 3.5. MALDI-TOF-MS mass spectra of reference strain *B. amyloliquefaciens* R16. These demonstrate the peak profiles appearing in the m/z ranges 950–1150 (A) in which surfactins and bacillomycins were detected; and m/z 1400–1590 (B) in which fengycins were detected.

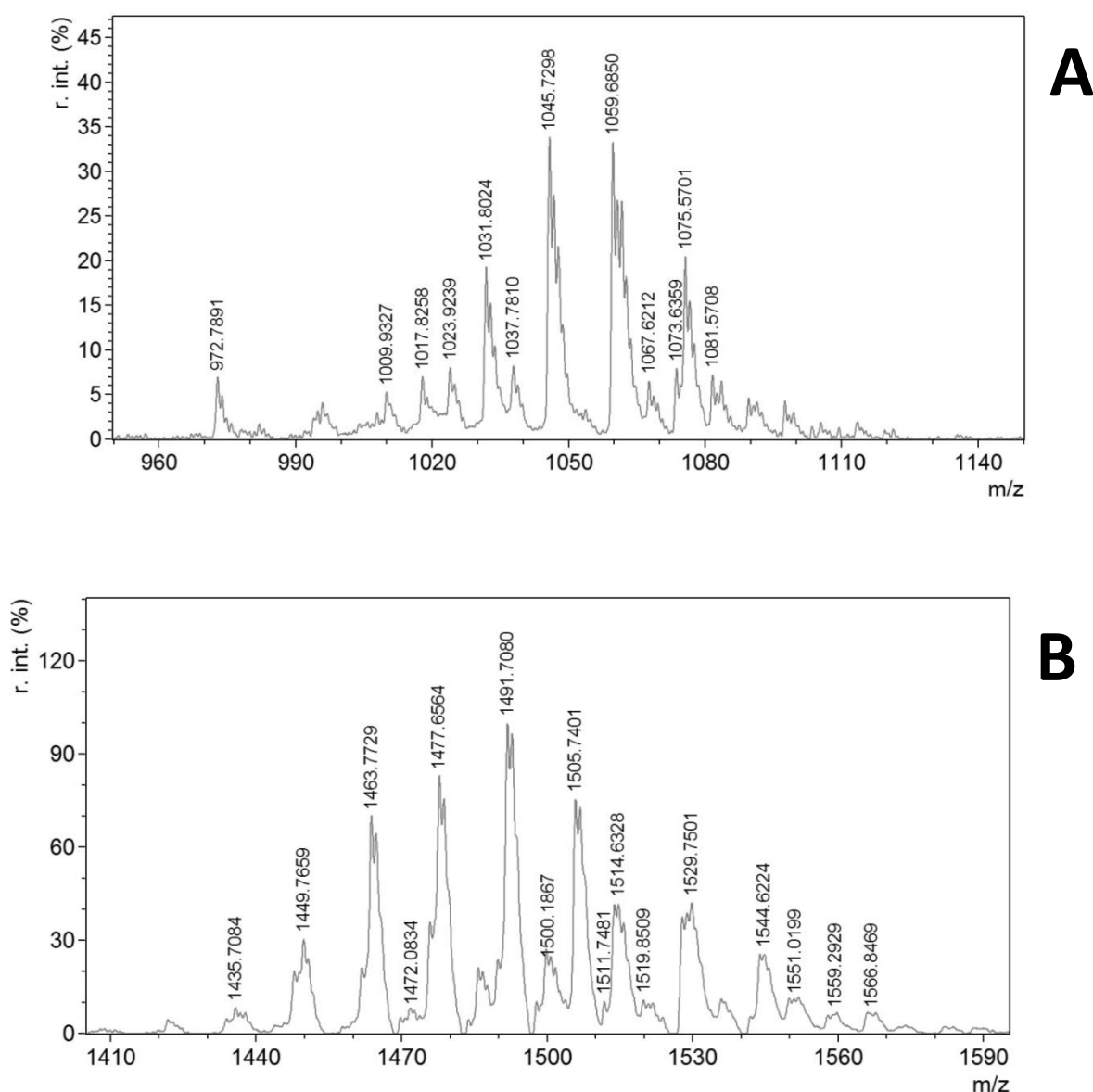


Figure 3.6. MALDI-TOF-MS mass spectra of reference strain *B. subtilis* strain B81. These demonstrate the peak profiles appearing in the m/z ranges 950–1150 (A) in which surfactins and bacillomycins were detected; and m/z 1400–1590 (B) in which fengycins were detected.

Peaks corresponding to isoforms of surfactin were distinguished for both reference strains *B. amyloliquefaciens* R16 and *B. subtilis* B81 (Table 3.8). Peaks correlating to isoforms for the fengycin family were also distinguished in both of these strains (Price *et al.*, 2007; Koumoutsi *et al.*, 2004; Vater *et al.*, 2002; Leenders *et al.*, 1999). However, iturin isoforms were not distinguishable in the extracts of either reference strain, although a suite of peaks corresponding to isoforms of bacillomycin D, an iturin variant, were detected in *B. amyloliquefaciens* R16 (Koumoutsi *et al.*, 2004).

The peak clustering indicative of the various lipopeptide families detected for these two reference strains is presented in Figure 3.7.

Table 3.8. m/z values of lipopeptide associated peaks from *Bacillus* spp. reference strain mass spectra.

Peak Assignment	m/z *
<i>B. amyloliquefaciens</i> strain R16	
Surfactin	
Surfactin C13 [M+Na, K] ⁺	1029.32, 1045.37
Surfactin C14 [M+K] ⁺	1060.47
Surfactin C15 [M+K] ⁺	1074.46
Bacillomycin D	
Bacillomycin D C14 [M+H, Na, K] ⁺	1031.28, 1053.33, 1069.34
Bacillomycin D C15 [M+Na, K] ⁺	1067.38, 1083.35
Bacillomycin D C16 [M+Na, K] ⁺	1081.41, 1097.37
Fengycin	
Ala-6-C15 Fengycin [M+H, Na, K] ⁺	1435.68, 1487.64, 1471.65
Ala-6-C16 Fengycin [M+H, Na, K] ⁺	1463.62, 1485.63, 1500.16
Ala-6-C17 Fengycin [M+H, K] ⁺	1477.69, 1516.18
Val-6-C15 Fengycin [M+H, Na, K] ⁺	1491.22, 1513.66, 1529.66
Val-6-C17 Fengycin [M+H, Na] ⁺	1505.7, 1528.2
<i>B. subtilis</i> strain B81	
Surfactin	
Surfactin C13 [M+Na, K] ⁺	1031.81, 1047.22
Surfactin C14 [M+H, Na] ⁺	1023.89, 1045.69
Surfactin C15 [M+H, Na, K] ⁺	1037.78, 1060.14, 1075.54
Fengycin	
Ala-6-C15 Fengycin [M+H, K] ⁺	1449.72, 1487.16
Ala-6-C16 Fengycin [M+H, K] ⁺	1463.72, 1502.23
Ala-6-C17 Fengycin [M+H, Na] ⁺	1478.22, 1500.25
Val-6-C15 Fengycin [M+H, Na, K] ⁺	1491.75, 1515.25, 1530.24
Val-6-C17 Fengycin [M+H, Na, K] ⁺	1505.78, 1527.8, 1543.79

* m/z values represent averaged values from duplicate mass spectra.

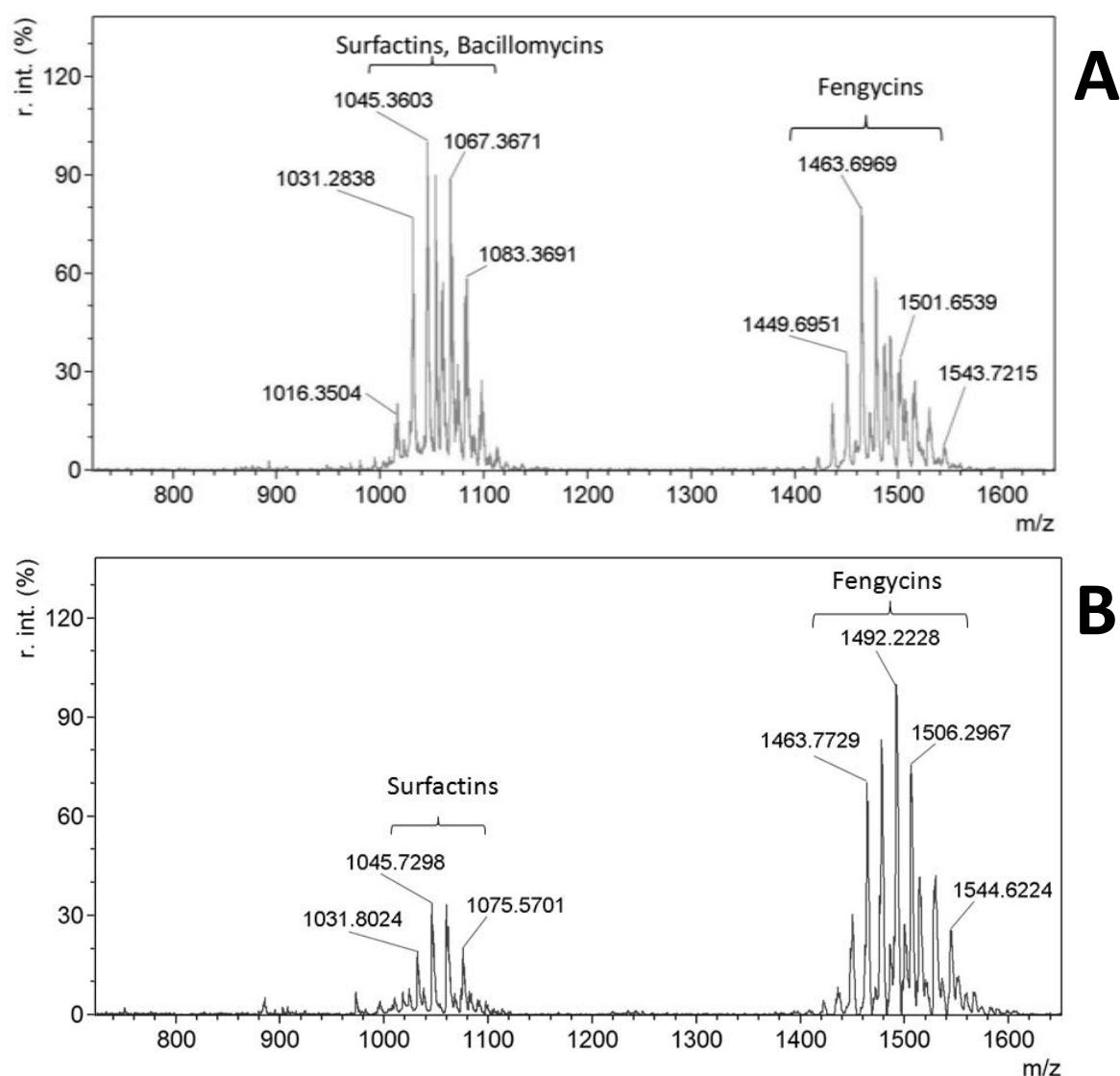


Figure 3.7. MALDI-TOF-MS mass spectra of reference strains *B. amyloliquefaciens* R16 (A) and *B. subtilis* B81 (B) demonstrating the peak clusters indicative of lipopeptide compounds appearing in the m/z range 717–1650.

Results for the detection of lipopeptide biomarkers amongst *Bacillus* isolates screened are presented in Figure 3.8 and Table 3.9. Lipopeptide biomarkers in the mass spectra obtained from methanol extracts were distinguished using the m/z values from the iturin A and surfactin standards (Table 3.7), reference strains (Table 3.8), and literature values. The lack of lipopeptide peaks for isolate bng241 was not unexpected (Figure 3.10a), as this isolate did not exhibit any antifungal ability, possessed none of the lipopeptide gene markers targetted in PCR screening, and did not resolve any lipopeptide-associated bands after TLC analysis (Figure 3.10a and Table 3.6). Of the remaining

samples, all were found to contain peaks corresponding to surfactin and fengycin isoforms. Most of the isolates screened produced isoforms of all three lipopeptide classes; although *B. subtilis* strains bnd134, bnd136, and bng216 did not produce peaks indicative of iturins or bacillomycins. Interestingly, these three isolates had yielded negative results for the gene markers screened, but were found to produce surfactin and fengycin under MALDI-TOF-MS analysis.

Table 3.9. Detection of lipopeptide biomarkers in methanol extracts from *Bacillus* isolates using MALDI-TOF-MS analysis.

Isolate	Surfactins	Bacillomycins	Iturins	Fengycins
<i>B. amyloliquefaciens</i> strain mwb86	+	+	+	+
<i>B. amyloliquefaciens</i> strain ccc103	+	+	-	+
<i>B. subtilis</i> strain bnd134	+	-	-	+
<i>B. subtilis</i> strain bnd136	+	-	-	+
<i>B. amyloliquefaciens</i> strain cce140	+	+	+	+
<i>B. amyloliquefaciens</i> strain cce146	+	+	+	+
<i>B. amyloliquefaciens</i> strain cce175	+	+	+	+
<i>B. amyloliquefaciens</i> strain bng199	+	+	+	+
<i>B. subtilis</i> strain bng216	+	-	-	+
<i>B. amyloliquefaciens</i> strain sqo275	+	+	+	+
<i>B. amyloliquefaciens</i> strain sqo277	+	+	+	+
<i>B. amyloliquefaciens</i> strain bnn282	+	+	+	+
bng241 [§]	-	-	-	-
<i>B. amyloliquefaciens</i> strain R16 [#]	+	+	-	+
<i>B. subtilis</i> strain B81 [#]	+	-	-	+

(+) presence of band indicating marker; (-) no band present and no marker detected. [§] Negative control isolate bng241.

[#] Reference strains *B. amyloliquefaciens* R16 and *B. subtilis* B81.

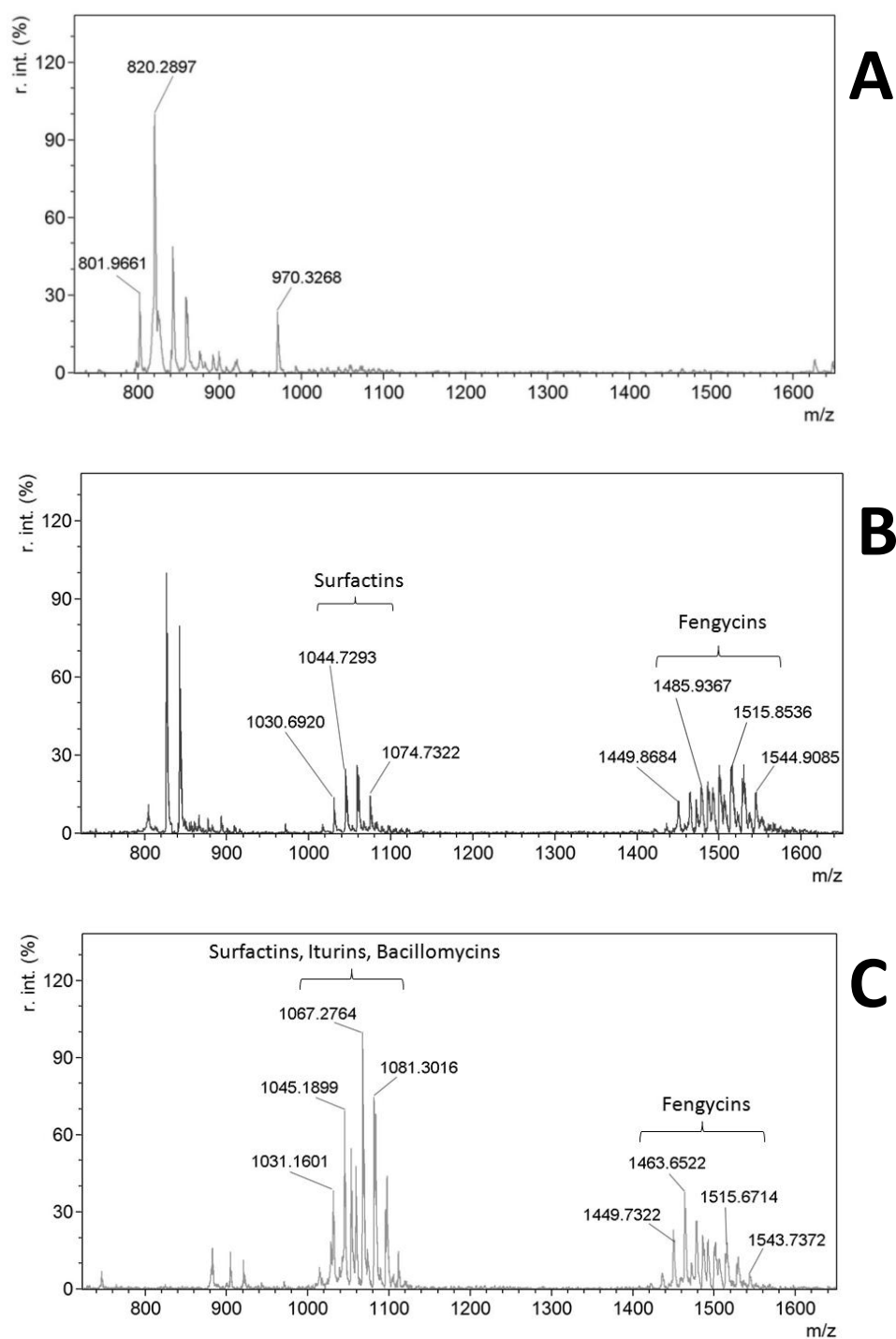


Figure 3.8. MALDI-TOF-MS mass spectra of isolates bng241 (A), *B. subtilis* strain bnd134 (B), and *B. amyloliquefaciens* strain cce175 (C) demonstrating the peak clusters indicative of lipopeptide compounds appearing in the m/z range 717–1650.

For comparative purposes, these mass spectra were also transformed using mMass software (version 5.5.0) to generate a gel view of the mass spectra (Figure 3.9). The m/z values were converted into vertical lines and the peak intensity represented as a function of greyscale lightening (low intensity) or darkening (high intensity). The *B. amyloliquefaciens* grouping of isolates (*viz.* mwb86, ccc103, cce140, cce146, cce175, bng199, sqo275, sqo277, and bnn282) produced all three compound families, while the three isolates belonging to the *B. subtilis* grouping (*viz.* bnd134, bnd136, and bng216) produced only fengycin and surfactin. *Bacillus subtilis* strain bnd134 and isolate bng241 produce peaks of high intensity at approximately m/z 825 which are not, to our knowledge, associated with the lipopeptides being screened for.

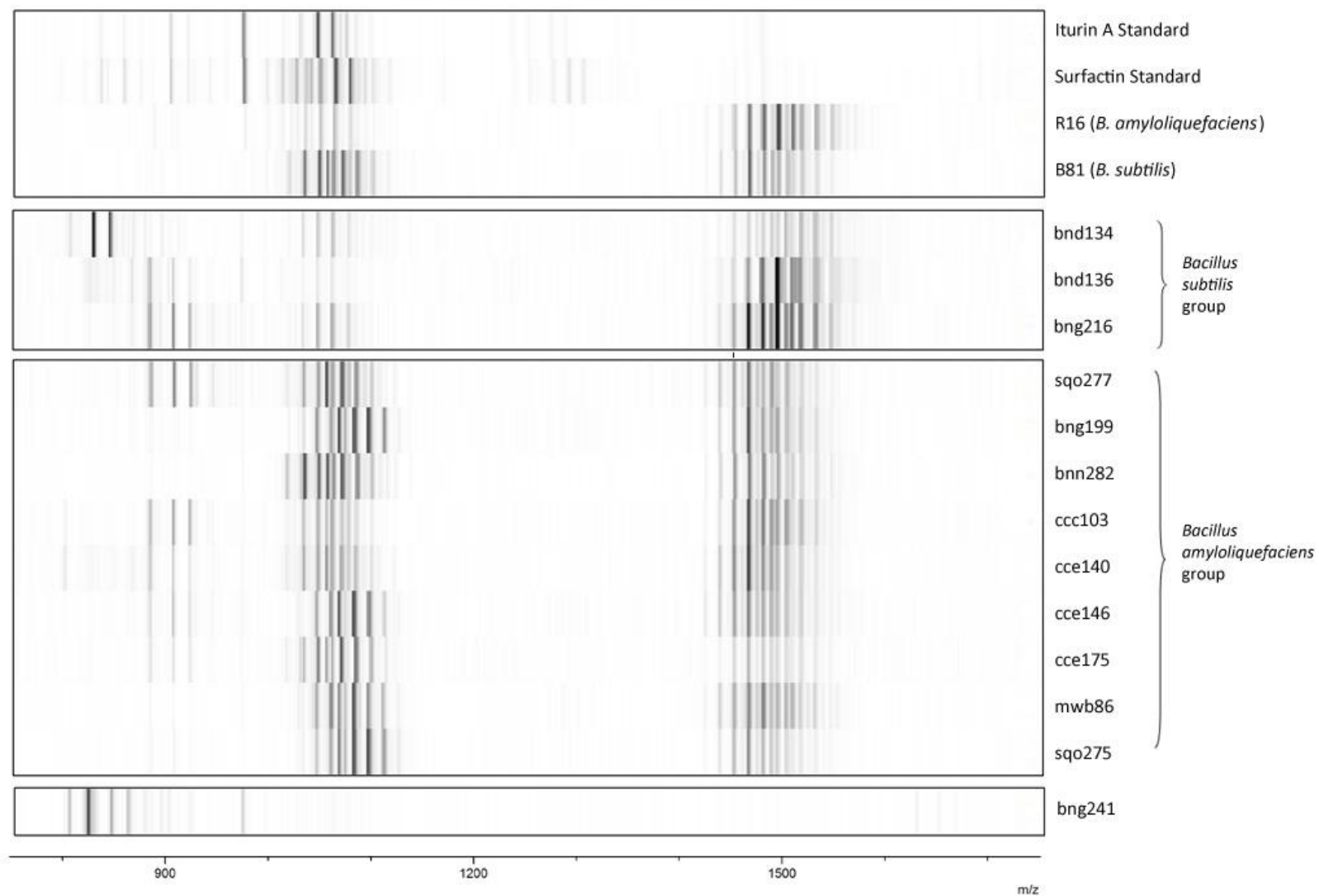


Figure 3.9. Mass profiles of methanol extracts from *Bacillus* isolates, reference strains, and reference standards represented as a gel view generated using mMass software (m/z 750–1750).

Some disparity was observed when the results for MALDI-TOF-MS analysis and lipopeptide gene markers were compared (Table 3.10). Though there are no instances where a gene marker positive result was not confirmed by MALDI-TOF-MS. Fengycin and surfactin are widely produced, with MALDI-TOF-MS also detecting these compounds in the three gene marker negative isolates (*viz.* *B. subtilis* strains bnd134, bnd136, and bng216). Iturin and bacillomycin production was variable amongst the isolates. Excluding the three gene marker negative isolates discussed above, there are some instances where MALDI-TOF-MS detected compound isoforms for a negative PCR result. However, these instances are only for one lipopeptide class each: *B. amyloliquefaciens* strain ccc103 for bacillomycin; *B. amyloliquefaciens* strain cce140 for surfactin; *B. amyloliquefaciens* strain bng199 for bacillomycin; *B. amyloliquefaciens* strain sqo275 for bacillomycin; and *B. amyloliquefaciens* strain bnn282 for fengycin. Only in *B. amyloliquefaciens* strains mwb86, cce175, and sqo277 do MALDI-TOF-MS and PCR results correlate for all lipopeptides screened for.

Table 3.10. Comparative data of lipopeptide PCR gene markers and MALDI-TOF-MS detection of lipopeptide compounds in methanol extracts from *Bacillus* isolates.

Isolate	Surfactin		Bacillomycin		Iturin		Fengycin	
	MALDI	PCR	MALDI	PCR	MALDI	PCR	MALDI	PCR
<i>B. amyloliquefaciens</i> mwb86	+	+	+	+	+	+	+	+
<i>B. amyloliquefaciens</i> ccc103	+	+	+	-	+	+	+	+
<i>B. subtilis</i> bnd134	+	-	-	-	-	-	+	-
<i>B. subtilis</i> bnd136	+	-	-	-	-	-	+	-
<i>B. amyloliquefaciens</i> cce140	+	-	+	+	+	+	+	+
<i>B. amyloliquefaciens</i> cce146	+	+	+	-	+	+	+	+
<i>B. amyloliquefaciens</i> cce175	+	+	+	+	+	+	+	+
<i>B. amyloliquefaciens</i> bng199	+	+	+	-	+	+	+	+
<i>B. subtilis</i> bng216	+	-	-	-	-	-	+	-
<i>B. amyloliquefaciens</i> sqo275	+	+	+	-	+	+	+	+
<i>B. amyloliquefaciens</i> sqo277	+	+	+	+	+	+	+	+
<i>B. amyloliquefaciens</i> bnn282	+	+	+	+	+	+	+	-
bng241 ^s	-	-	-	-	-	-	-	-

(+) lipopeptide isoforms detected; (-) no lipopeptide isoforms present. ^s Negative control isolate bng241.

3.4. Discussion

Several strains of *Bacillus* spp. have been commercially formulated for the control of a variety of fungal crop diseases, with some of these products also effective against cucurbit powdery mildew (Borriss, 2011; Cawoy *et al.*, 2011). Biosynthesis of lipopeptide compounds has shown to be a major determinant of the biocontrol potential of many AEFB strains (Alvarez *et al.*, 2011; Arguelles-Arias *et al.*, 2009; Chen *et al.*, 2009a; Ongena *et al.*, 2008). Applications of live cells of *B. subtilis* or extracted lipopeptide metabolites have both been found to be effective in reducing the severity of powdery mildew on cucurbits (Romero *et al.*, 2007a; Romero *et al.*, 2007b; Romero *et al.*, 2004; Romero *et al.*, 2003; Bettiol *et al.*, 1997). Furthermore, Romero *et al.* (2007a) found that powdery mildew antagonism of *P. fusca* by several strains of *B. subtilis* was directly linked to the synthesis of fengycin and iturin. The research presented in this chapter was undertaken with the aim of screening the lipopeptide production capabilities of selected *Bacillus* isolates as candidate BCA of *P. fusca*. Three screening approaches were applied and evaluated, namely PCR screening of gene markers, and analysis of lipopeptide extracts using TLC and MALDI-TOF-MS.

When evaluating *Bacillus* spp. as BCA, lipopeptide biosynthesis is an important consideration, as these compounds play many roles the bacteria–plant host relationship, and are considered to be crucial to the success of many *Bacillus* spp. as biocontrol agents (Nagórska *et al.*, 2007). Not only are lipopeptide compounds known to directly antagonise fungi (fengycins and iturins), they assist in niche colonisation and biofilm establishment (surfactins), and stimulate plant host resistance mechanisms (surfactins and fengycins) (Ongena *et al.*, 2009). The *Bacillus* isolates screened in the present study were able to produce a range of lipopeptide compounds, with biosynthetic capability variable between *B. amyloliquefaciens* and *B. subtilis* isolates. PCR gene marker screening and MALDI-TOF-MS analysis provided the most useful data of lipopeptide production. The detection capability of TLC was found to be insufficiently sensitive without additional band analysis techniques. Fengycin and surfactin lipopeptide classes were most widely produced by the isolates, while synthesis of compounds within the iturin family was found to be variable. The negative control isolate bng241 had not shown any antifungal activity in prior dual-culture bioassays, and no evidence of lipopeptide production was detected from this isolate by any of the three evaluation methods applied.

PCR gene marker screening determined differences in the biosynthetic capabilities between isolates belonging to the *B. amyloliquefaciens* and *B. subtilis* species. Isolates which had been placed into different groups based on RAPD fingerprints generally displayed similar gene marker PCR profiles (Table 3.4). Those isolates which grouped together as *B. amyloliquefaciens* strains were found to be positive for surfactin and fengycin markers, barring negative marker results for *B. amyloliquefaciens* strains bng210 and bnn282 for fengycin, and *B. amyloliquefaciens* strains bna81 and cce140 for surfactin. Amongst this species the iturin marker was present in many cases, bacillomycin marker presence was variable. Thirteen isolates (24%) grouped together as strains of *B. subtilis* and were negative for all markers screened for. *Bacillus subtilis* strains bng199, bng215, and sqo279; and isolates bng224 and bng227 were the only isolates to possess any of the markers screened for (Table 3.4). However, MALDI-TOF-MS analysis of methanolic extracts from twelve antifungal isolates—representative of both species—found that all of these were able to produce surfactin and fengycin. MALDI-TOF-MS showed that the only isolates which did not produce bacillomycin and/or iturin compounds were *B. amyloliquefaciens* strain ccc103, and *B. subtilis* strains bnd134, bnd136, and bng216. Banding was detected in all extracts after TLC analysis, with bands correlating to R_f values of the surfactin and iturin reference standards widely observed (Table 3.6). Fengycin presence could not be determined by TLC owing to a lack of reference standard.

Gene marker PCR screening for lipopeptide production is considered a useful method of evaluating *Bacillus* spp. candidates for biocontrol applications (Joshi and McSpadden Gardener, 2006). This is also convenient method of evaluating lipopeptide synthesis potential prior to field testing and can provide information on the lipopeptide production potential without compound extraction (Hsieh *et al.*, 2008; Hsieh *et al.*, 2004). Hence, a number of genetic markers associated with lipopeptide biosynthesis in *Bacillus* spp. have been developed as a means of examining lipopeptide production capability (Alvarez *et al.*, 2011; Mora *et al.*, 2011; Velho *et al.*, 2011; Hsieh *et al.*, 2008; Ramarathnam *et al.*, 2007; Joshi and McSpadden Gardener, 2006; Abushady *et al.*, 2005; Hsieh *et al.*, 2004; Koumoutsis *et al.*, 2004). A potential shortfall in the use of PCR screening in this study was observed when sequencing data from reference strain *B. amyloliquefaciens* R16 gene marker amplicons identified the *ituD* PCR product as a region of the bacillomycin synthetase (Table 3.3). This demonstrates that this

primer set was unable to distinguish between the biosynthetic genes of these closely-related compounds, and the lack of specificity highlights the limitations of the *ituD* primer set used. Hence, in order to be fully trusted, the *ituD* primer set requires some level of refinement, or the inclusion additional primers for iturin-associated markers (Alvarez *et al.*, 2011; Mora *et al.*, 2011; Tsuge *et al.*, 2001).

Disparity between the iturin and bacillomycin gene marker PCR data was further highlighted by MALDI-TOF-MS analysis data (Table 3.8). All isolates positive for the bacillomycin gene marker were confirmed to be bacillomycin producers when extracts were analysed using MALDI-TOF-MS extract analysis. Interestingly, the bacillomycin primer failed to detect bacillomycin synthesis in four instances (*viz.* *B. amyloliquefaciens* strains ccc103, cce146, bng199, and sqo275) (Table 3.10). Detection of the co-production of bacillomycin and iturin with gene marker PCR was limited, as isolates showing positive results for both the *ituD* and *bmyC* regions may not necessarily indicate the co-production of these two compounds. Although MALDI-TOF-MS revealed instances of concurrent iturin and bacillomycin biosynthesis in some isolates which had returned positive results for both of these gene markers (*viz.* *B. amyloliquefaciens* strains mwb86, cce140, cce175, and sqo277). All isolates which provided positive results for the iturin marker were found to produce iturin under MALDI-TOF-MS analysis; though positive results for the *ituD* marker using PCR data alone need to be interpreted with caution as they may not necessarily indicate the production potential of iturin but possibly also that of bacillomycin.

Differences in primer sensitivity between *Bacillus* species was observed amongst the gene marker primers. It is unlikely that the negative results for some of the *B. subtilis* isolates were indicative of a lack of biosynthetic ability as this species is known as a prolific lipopeptide producer (Stein, 2005). Given that MALDI-TOF-MS confirmed the presence of lipopeptide biomarkers in all *B. subtilis* isolates screened, a more likely scenario is that the gene marker primers used in the current study lacked specificity. This is an unexpected outcome as these primer sets had been successfully applied to a variety of *Bacillus* spp. by other researchers (Athukorala *et al.*, 2009; Hsieh *et al.*, 2008; Ramarathnam *et al.*, 2007). Yet, differences in the synthetic capability of these two species were revealed by MALDI-TOF-MS analysis of

reference strains *B. amyloliquefaciens* R16 and *B. subtilis* B81. Both reference species were found to synthesise surfactin and fengycin variants; though *B. subtilis* B81 did not produce any of the iturin family variants and *B. amyloliquefaciens* R16 was only able to synthesise bacillomycin D (Table 3.8). In light of these findings, future prospects for the use of lipopeptide gene marker PCR screenings would require either the inclusion of additional primer sets, or the synthesis of new primers better able to detect markers in both *B. subtilis* and *B. amyloliquefaciens* groupings.

Chromatographic methods such as ion exchange chromatography, TLC, and gel permeation chromatography have been frequently-used techniques for the analysis of biosurfactant compounds from *Bacillus* spp. (Gordillo and Maldonado, 2012). In the present study, TLC was applied to detect the presence of UV-active hydrophobic bands indicative of amphiphilic compounds in the methanol extracts. Isolate bng241 notwithstanding, multiple bands were detected in all of the extracts analysed, and bands showing correlation to the two reference standards in hydrophobicity and R_f values were widely detected (Table 3.3). In agreement with MALDI-TOF-MS and PCR results, bands of R_f values correlating to surfactin were detected in all antifungal isolates. R_f values correlating to iturin were less commonly observed, and detection of iturin by TLC did not entirely correlate with the PCR and MALDI-TOF-MS findings. UV-fluorescence was of little assistance in discriminating related bands.

The purified iturin A standard displayed two bands after TLC separation (Plate 3.1), which could be attributed to iturin isoforms (Price *et al.*, 2007). Alternately, the standard might have possessed low levels of a contaminant lipopeptide—which matched the R_f values of surfactin—although MALDI-TOF-MS data from these reference standards could not confirm this (Table 3.7). The data obtained from extract analysis using TLC highlights the need for a full complement of purified lipopeptide reference standards in order for banding comparisons to be considered reliable without including individual band analyses (Gordillo and Maldonado, 2012). Additional band-qualification methods after TLC would have required considerably more of a time investment than other techniques available (e.g. MALDI-TOF-MS), and were therefore not pursued further for the purposes of this study.

Despite the convenience PCR offers in the evaluation of lipopeptide production potential, the findings of the present study, and those of other researchers, have determined that lipopeptide production *in situ* is not guaranteed by the presence of a gene marker (Alvarez *et al.*, 2011; Savadogo *et al.*, 2011; Athorkurala *et al.*, 2009; Leenders *et al.*, 1999). Gene marker PCR for the purposes of this study requires the inclusion of more gene marker primer sets, or the refinement of the existing *ituD* primer, in order to offer accurate extrapolations of compound synthesis. MALDI-TOF-MS is able to yield data much faster and with a lower resource demand than PCR, and is highly sensitive to compositional variations amongst compounds in a mixture, which TLC does not offer. Nevertheless, as MALDI-TOF-MS hardware is expensive and often unavailable TLC presents a “low-tech” means of both separation and qualification of biosurfactant compounds, that is able to be carried out with minimal sample purification (Gordillo and Maldonado, 2012). TLC can form a useful part of a polyphasic lipopeptide screening approach should a suite of reference standards be included (Tewelde, 2004; Poole, 2003; Lin *et al.*, 1998b). Of the three methods used to determine lipopeptide production potential, MALDI-TOF-MS proved to be a rapid, powerful, and effective tool for detecting lipopeptides in methanolic extracts. Nevertheless, both PCR and MALDI-TOF-MS have proven to be valuable tools when used in conjunction to screen for lipopeptide-producing *Bacillus* strains (Athukorala *et al.*, 2009).

All of the antifungal isolates screened in this study were found to be able to produce variants of some, if not all, of the three major lipopeptide compound families known to be synthesised by AEFB. Overall, those isolates related to *B. amyloliquefaciens* were found to be the most consistent producers of the three lipopeptide compound families assayed for. The fact that surfactin and fengycin classes were produced by all of the isolates screened is two compounds are known to play roles in bacterial establishment on the host plant (Ongena *et al.*, 2008). Antibiosis is an easily assayed mechanism involved in biocontrol activity, though it is not the only mechanism by which *Bacillus* spp. act as BCAs, nor can it be a guarantee of successful disease antagonism in the field. However, preliminary screening evaluating candidate BCAs that is based on antibiosis has shown this ability to be highly valuable (Athukorala *et al.*, 2009). On the basis of the data presented here those isolates exhibiting an ability to produce lipopeptide compounds were considered promising candidates warranting further evaluation.

CHAPTER FOUR

Screening of selected *Bacillus* spp. isolates for antagonism towards *Podosphaera fusca* using an agarised detached cotyledon assay and biocontrol pot trials

4.1. Introduction

A polyphasic screening approach applied prior to field trials provides a strong basis from which to select candidate biocontrol agents most likely to be successful against a target pathogen (Pliego *et al.*, 2010; Knudsen *et al.*, 1997). This strategy has been shown to be useful in selecting antagonistic bacterial isolates against a variety of plant diseases (Pliego *et al.*, 2011; Anith *et al.*, 2003; Knudsen *et al.*, 1997). *In vivo* screening is an important aspect of biocontrol screening programs. Despite the valuable information that can be gleaned from performing laboratory-based *in vitro* bioassays for large numbers of isolates, a screening protocol which includes the host plant, pathogen, and antagonist offers a more realistic extrapolation of biocontrol performance in the field (Anith *et al.*, 2003). Due to the biotrophic nature of *P. fusca* preliminary *in vitro* screenings rely on surrogate fungal species. This necessitates the use of *in planta* assays to confirm *in vitro* findings under conditions reflective of natural growing conditions.

The detached cotyledon assay represents a laboratory-scale technique for the evaluation of antagonism for biotrophic species. The protocol involves the artificial maintenance of leaf or cotyledonous tissue, thereby allowing the study of pathogen antagonism in a controlled environment, and has been applied for *P. fusca* with some success (Tsfagiorgis, 2009; Bardin *et al.*, 2007; Romero *et al.*, 2007a; Romero *et al.*, 2003; Shishkoff and McGrath, 2002; Álvarez and Torés, 1997; Quinn and Powell, 1982). Biocontrol pot trials represent a means of evaluating plant–pathogen–antagonist interactions under conditions that approximate normal growing conditions (Anith *et al.*, 2003). Since biocontrol pot trials are usually carried out in greenhouses under controlled growth conditions the influence of environmental variables associated with the field environment are minimised. Pot trials are useful for assessing an organisms' ability to colonise its host and compete with the existing microflora (Pliego *et al.*, 2011). Additional mechanisms contributing to antagonism are also afforded opportunity to be

revealed (e.g. induced plant host resistance, siderophore production, and competitive exclusion) (González-Sánchez *et al.*, 2010).

In this study nine *Bacillus* isolates, selected previously from preliminary screening assays, were evaluated for powdery mildew antagonism. Two methods, namely an agarised detached cotyledon assay and a biocontrol pot trial, were used to evaluate disease antagonism. A subsequent pot trial was conducted to assess the impacts of inoculum preparation of isolate cce175 on the targetted pathogen.

4.2. Materials and Methods

4.2.1. Bacterial isolates

Nine *Bacillus* isolates (*viz.* *B. amyloliquefaciens* strains mwb86, ccc103, cce140, cce175, bng199, sqo275, and bnn282; and *B. subtilis* strains bnd136 and sqo279) were chosen for *in vivo* screening of cucurbit powdery mildew antagonism. These isolates were selected on the basis of their antagonism towards surrogate test fungi in *Botrytis cinerea* and *Rhizoctonia solani* *in vitro*, their lipopeptide profiles determined by MALDI-TOF-MS, and genomic fingerprint profiles determined by RAPD-PCR (Chapters 2 and 3). Isolates were stored as glycerol stock cultures at -80°C and cultured on TSA (30°C) prior to use.

4.2.2. Cultivation of powdery mildew disease and conidia harvesting

A source of cucurbit powdery mildew inoculum was established and maintained on susceptible zucchini plants (*Cucurbita pepo*) (Partenon hybrid F1, Starke-Ayres (Pty) Ltd., South Africa) grown under greenhouse conditions. The plants were initially inoculated from diseased plant material. The powdery mildew pathogen was identified as *P. fusca* based in conidia morphology and evidence of fibrosin bodies present in conidia when treated with 3% (w/v) KOH solution and viewed under bright-field microscopy (Zitter *et al.*, 1996). The host plants were grown in pots (25 cm diameter) filled with ~8 L of a composted pine bark medium, and the pots placed 30 cm apart in rows. The plants were drench-fertigated every 3 d using 1 g/l of a commercial fertilizer preparation Dr. Fisher's Multifeed Classic (N 19 : P 8 : K 16) (Plaaskem

(Pty) Ltd., South Africa). This formulation contained (per kg): nitrogen, 190 g; phosphorus, 82 g; potassium, 158 g; magnesium, 900 mg; zinc, 350 mg; boron, 1000 mg; molybdenum, 70 mg; iron, 750 mg; manganese, 900 mg; and copper, 75 mg. The plants were watered as required between fertigations. The disease was allowed to advance unimpeded and new host plants were added to the collection every 4–6 weeks as dictated by disease progress.

For disease inoculation purposes fungal conidia were harvested from infected 6-week old plants. Diseased leaves were collected and placed into 250 ml sterile deionised water, before being agitated by hand for 2 minutes to promote conidial removal. The leaf material was removed and conidia counted within 2–3 h of harvesting using a haemocytometer (0.1 mm depth, counting area 0.0025 mm²) (Thoma, Marienfield) with each sample counted in triplicate. Conidial suspensions were adjusted to the required concentration by dilution with sterile deionised water. An ethanol-disinfected polyethylene terephthalate (PET) plastic atomiser (capacity 250 ml) was used to apply the conidial suspension over the whole plant until runoff was visible.

4.2.3. Antagonism screening using an agarised detached cotyledon bioassay

A modified detached leaf assay was adapted from Álvarez and Torés (1997) and Bardin *et al.* (2007) using zucchini cotyledons which were embedded into an agar-based medium. The agarised basal medium used was adapted from Álvarez and Torés (1997) and consisted of (per litre): mannitol, 0.1 M; sucrose, 0.02 M; and bacteriological agar, 10 g. The medium was autoclaved at 121°C (103.4 kPa) for 15 minutes.

Zucchini cotyledons (14 d old) (Partenon F1 hybrid) (Starke-Ayres, South Africa) were removed from the plant at the petiole using ethanol-disinfected scissors. Cotyledons were surface-sterilised by soaking for 15–20 minutes in an aqueous solution of 0.5% (v/v) bleach and 0.1% (v/v) Tween80. This was followed by three successive rinse steps in sterile deionised water, at 1 minute each. Transfers between beakers were carried out aseptically using ethanol-flamed forceps. The leaves were blotted dry using disinfected paper towel (18 h oven incubation at

70°C) before placement onto the agarised medium (one cotyledon per plate) as demonstrated in Plate 4.1. Three cotyledons were used per treatment, including diseased and non-diseased controls.

Single colonies taken from TSA cultures (18 h at 30°C) of each selected isolate were inoculated into 10 ml TSB (Merck, Biolab) and incubated for 36 h (30°C at 150 rpm). Thereafter, 5 ml aliquots were removed and centrifuged for 30 minutes at 17,969 x *g* (Avanti centrifuge, Beckman Coulter). Supernatant was removed and the bacterial pellets resuspended in 5 ml quarter-strength Ringer's solution. Bacterial cells were enumerated using a bacterial counting chamber, counting the number of cells within five squares over three replicates (0.02 mm depth, counting area 0.0025 mm²) (Thoma, Marienfield) and the samples kept on ice to arrest cell division until completion of counting. The suspensions were adjusted to ~10⁸ cells/ml using sterile quarter-strength Ringer's solution, and applied to sterile cotton wool swabs until saturated. Each cotyledon on the agar medium was then aseptically swabbed with the saturated cotton wool. Petri dish lids were closed, and the plates dried for 1–2 h in a laminar flow bench before transfer into a controlled environment growth chamber (PGI-500H Growth Chamber, MRC Labs, Israel). Incubation conditions were a constant temperature of 21°C, with 16 h of illumination (~2,000 lux) per day at 65% relative humidity (RH). Each treatment was performed in triplicate and included diseased and non-diseased controls. The plates were arranged in the incubator in a randomised block design.

After 72 h of incubation the cotyledons (excepting the negative controls) were inoculated with ~10⁵ powdery mildew conidia/ml as described above (Section 4.2.1). The cotyledons were visually rated for leaf area infected (l.a.i.) at 4, 6, 9, 11, and 12 d post inoculation (Plate 4.2). Statistical analysis of leaf area infected was carried out using Area Under Disease Progress Curve (AUDPC) (Shaner and Finney, 1977) and one-way analysis of variance (ANOVA) carried out on Genstat software (Version 14, VSN International Ltd.). Disease reduction percentages were expressed as a function of the treatment AUDPC value and the diseased control AUDPC value.

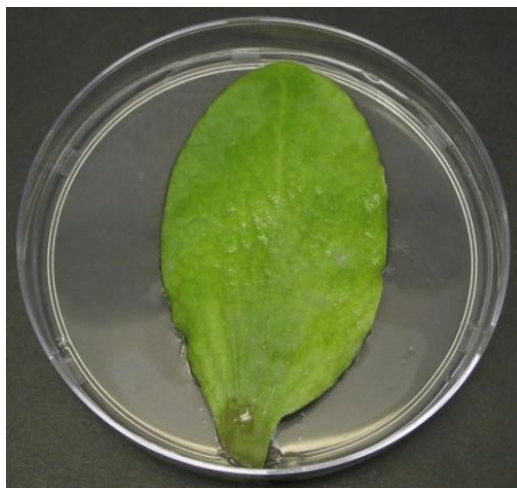


Plate 4.1. Agarised detached cotyledon assay demonstrating zucchini cotyledon embedded in basal agar medium.

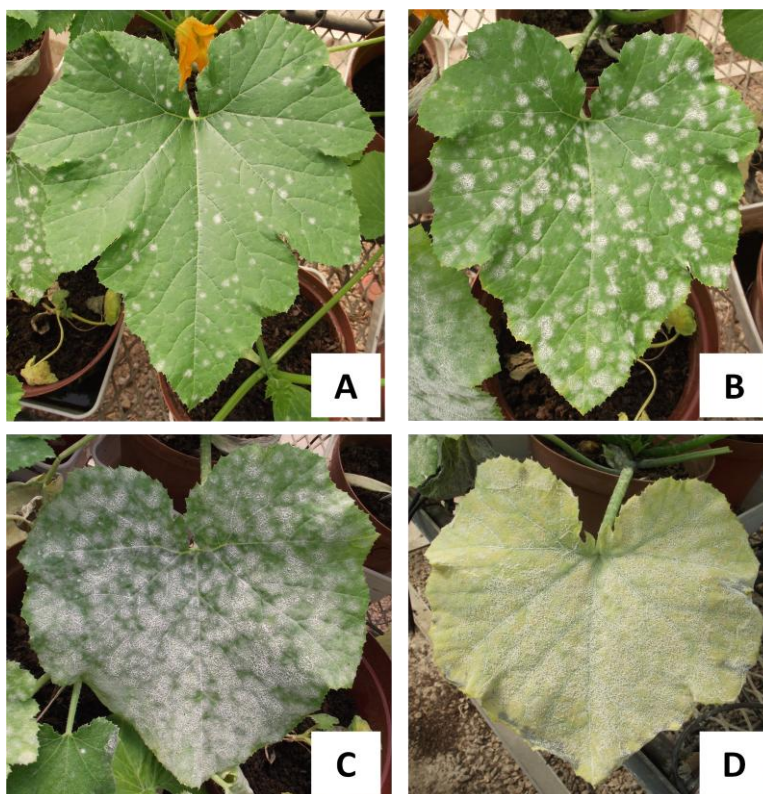


Plate 4.2. Examples of leaf area infected (l.a.i.) benchmarks used for rating of powdery mildew of cucurbits disease in the biocontrol pot trial. The images represent the leaf area infected values: (A) 10%, (B) 50%, (C) 70%, (D) 100%.

4.2.4. Biocontrol pot trial screening of *Bacillus* isolates against powdery mildew

Potted zucchini host plants (Partenon hybrid F1) (Starke-Ayres (Pty) Ltd., South Africa) were grown in pots (18 cm diameter) containing composted pine bark medium (~2.3 L volume) and maintained in a controlled environment growth chamber (Controlled Environment Research Unit, University of KwaZulu-Natal, Pietermaritzburg, South Africa). The growth chamber was illuminated (~3,500 lux) for 16 h per day, with a day temperature of 25°C, night temperature of 20°C, and 70% RH. The plants were drench-fertigated and watered as described above (Section 4.2.1).

Bacterial inoculum was prepared as described previously (Section 4.2.3). The bacterial suspensions were adjusted to $\sim 10^8$ cells/ml using sterile quarter-strength Ringer's solution. Each suspension was sprayed onto the 14 d old zucchini plants (Partenon hybrid F1) (Starke-Ayres (Pty) Ltd., South Africa) with 3–4 adult leaves present. The whole plant was sprayed with the bacterial suspension until runoff was visible. The plants were maintained in a growth chamber (Controlled Environment Research Unit, University of KwaZulu-Natal, Pietermaritzburg, South Africa) at 70% RH, illuminated for 16 h per day, with a day temperature of 25°C, and a night temperature of 20°C. The powdery mildew disease was inoculated 72 h later using powdery mildew spores (of $\sim 10^5$ spores/ml) harvested and applied to the whole plant, following the method previously described (Section 4.2.1). The treatments were performed in triplicate, and arranged in a randomised block design. Both diseased and non-diseased control plants were included. The non-diseased plants were placed in a separate unit, and housed under the same conditions as the biocontrol pot trial.

The second adult leaf on each plant was marked for the purpose of rating disease progress. Disease levels were rated by means of visual estimates of infected leaf area at 2, 9, 11, and 13 d post fungal inoculation. Examples of benchmarks used for rating infected leaves are shown in Plate 4.2 (adapted from Tesfagiorgis, 2009 and Haupt, 2007). Statistical analysis of I.a.i. was carried out using AUDPC (Shaner and Finney, 1977) and one-way ANOVA analysis carried out on Genstat software (Version 14, VSN International Ltd). Disease reduction percentages were expressed as a function of the treatment AUDPC value and the diseased control AUDPC value.

4.2.5. Impacts of inoculum preparation on cucurbit powdery mildew antagonism

The impacts of bacterial inoculum preparation of *P. fusca* antagonism was carried out using a biocontrol pot trial with *B. amyloliquefaciens* strain cce175; which was chosen based on data obtained from previous screenings. Powdery mildew susceptible patty pan host plants (Yellow Scallop hybrid STAR 8081) (Starke-Ayres (Pty) Ltd., South Africa) were grown in pots (18 cm diameter) filled with composted pine bark medium (~2.3 L volume). The plants were maintained in a growth chamber (Controlled Environment Research Unit, University of KwaZulu-Natal, Pietermaritzburg, South Africa) at 70% RH with illuminated (~3,500 lux) for 16 h per day, day temperature at 25°C, and dark temperature at 20°C. The plants were drench-fertigated and watered as required between fertigations as described above (Section 4.2.1).

Bacillus amyloliquefaciens strain cce175 was cultured in antibiotic production medium (McKeen *et al.*, 1986). The medium comprised (per litre of deionised water): D-glucose, 15.0 g; L-glutamic acid, 5.0 g; MgSO₄·7H₂O, 1.02 g; K₂HPO₄·3H₂O, 1.0 g; and KCl, 0.5 g; and 1 ml of a trace element solution. The trace element solution consisted of: CuSO₄·5H₂O, 0.16 g; MnSO₄·7H₂O, 0.1 g; and FeSO₄·7H₂O, 0.015 g in 100 ml deionised water. The medium pH was adjusted to pH 6.0–6.2 using 1 N NaOH before decanting and autoclaving at 121°C (103.4 kPa) for 15 minutes.

Single bacterial colonies taken from TSA culture (18 h at 30°C) were inoculated into 10 ml of antibiotic production medium to create starter cultures, which were incubated for 48 h in a rotary shaker (30°C at 150 rpm). Thereafter, these starter cultures were aseptically added to 100 ml sterile antibiotic production medium in sufficient quantity to achieve A₅₅₀ 0.5. Broth cultures were incubated in a rotary shaker (30°C at 150 rpm) for 48 h or 72 h as dictated by the experimental treatment protocol. A summary of the various inoculum preparations applied in the pot trial are shown in Table 4.1.

Table 4.1. Treatments used for a biocontrol pot trial determining effect of bacterial inoculum preparation of *B. amyloliquefaciens* strain cce175 against cucurbit powdery mildew.

Treatment	Powdery Mildew	Inoculum Preparation
T1 (Uninoculated Control)	None	None
T2	10 ² conidia/ml	Live cells, 10 ⁸ cells/ml (48 h)
T3	10 ² conidia/ml	Cell-free supernatant (48 h)
T4	10 ² conidia /ml	Whole broth, 10 ⁸ cells/ml (48 h)
T5	10 ² conidia /ml	Whole broth, 10 ⁸ cells/ml (72 h)
T6 (Diseased Control)	10 ² conidia /ml	None
T7 (Fungicide Control)	10 ² conidia /ml	Tebuconazole 430 g/l

Treatment 1 comprised a non-diseased control, and was housed in a separate unit under the same conditions as the biocontrol pot trial. For Treatments 2 and 3, bacterial cultures were incubated for 48 h; thereafter, 100 ml of broth culture was centrifuged for 30 minutes at 17,969 x *g* (Avanti centrifuge, Beckman Coulter). The supernatant was decanted and placed into an ethanol-disinfected PET atomiser (250 ml capacity) prior to inoculation. The cell pellets were resuspended in 100 ml sterile quarter-strength Ringer's solution and cell enumeration was carried out (five squares per view, in triplicate) using a bacterial counting chamber (0.02 mm depth, counting area 0.0025 mm²) (Thoma, Marienfield). The cell number was corrected to ~3 x 10⁸ cells/ml and the solution placed into a disinfected atomiser. The broth culture for Treatments 4 and 5 were sampled and cells enumerated and numbers adjusted as described above, before being decanted into disinfected PET atomisers. Treatment 6 consisted of sterile deionised water only, and Treatment 7 comprised a fungicide control Folicur 430 SC (active ingredient 430 g/l Tebuconazole) (Bayer CropScience, Monheim, Germany) mixed at 1 ml/l.

Each treatment was atomised onto patty pan host plants (14 d old) with a minimum of 5 adult leaves present. The whole plant was sprayed with the treatment suspension until runoff was visible. Treatments 2–7 were re-applied at 10 d post fungal inoculation. The powdery mildew disease was inoculated 72 h after bacterial treatments were applied. Powdery mildew spores were harvested and applied to the plants (barring Treatment 1) following the method previously described (Section 4.2.1.) at a concentration of ~10² spores/ml.

The treatments were performed in triplicate, and arranged in a randomised block design. The non-diseased control was housed in a separate growth chamber under the same conditions of the experimental treatments. Five leaves on each of replicate plant were randomly marked for the purposes of disease rating. Disease levels were rated by means of visual estimates of infected leaf area; examples of the I.a.i. benchmarks used for rating infected leaves are shown in Figure 4.2. Initial ratings were taken 10 d after powdery mildew inoculation; and thereafter at 72 h intervals 10 d after the re-applications of each experimental treatment. Statistical analysis of leaf area infected was carried out using AUDPC (Shaner and Finney, 1977) and one-way ANOVA using Genstat software (Version 14, VSN International Ltd). Disease reduction percentages were expressed as a function of the treatment AUDPC value and the diseased control AUDPC value.

On the day of final rating, the trial plants were assessed for numbers of fungal spores per centimetre (cm²) of leaf material in a procedure adapted from Romero *et al.* (2004). The five rated leaves from each plant were removed, and three leaf discs were taken from each leaf (1 cm diameter) using a disinfected aluminium pipe borer. The fifteen discs from each replicate plant were pooled in 10 ml deionised water amended with 0.02% (v/v) Tween80. The bottles were placed on a rolling bench agitator for 2 h, and samples removed for conidia enumeration using a counting chamber (0.1 mm depth, counting area 0.0025 mm²) (Thoma, Marienfield) with each sample counted in triplicate and the conidia numbers averaged. The spore numbers were averaged between the three plants per treatment, and calculated to express the number of conidia/cm² of leaf material.

4.3. Results

4.3.1. Agarised detached cotyledon assay

During cell enumeration using phase-contrast microscopy, bacterial cells were observed as motile rods in a vegetative state. In some instances forming endospores were observed as refractile areas in the cells, though no free endospores were observed.

The diseased controls for the agarised detached cotyledon assay showed initial symptoms of powdery mildew infection within 5 d of fungal inoculation, after which symptoms progressed rapidly. All of the bacterial treatments showed disease symptoms by 6 d, though some replicates showed slight signs of infection at 5 d. At the first disease rating (5 d post disease inoculation) the I.a.i. was estimated at between 10–20% between treatments, but rose to 40–50% at the second rating 3 d later. The cotyledon tissue on all assays survived a total of 11 d on the medium after disease inoculation, before fungal infection overwhelmed the cotyledon.

Statistical data or the treatment ratings are presented in Figure 4.1 and Table 4.2. Experimental treatments were all found to be statistically significant ($p \leq 0.05$). The only bacterial treatments to be statistically different from the diseased control were *B. amyloliquefaciens* strains sqo275, bng199, and cce175; and *B. subtilis* strain sqo279. *Bacillus subtilis* strain sqo279 gave the greatest degree of disease retardation at 16.2%, followed closely by *B. amyloliquefaciens* strains sqo275, bng199, and cce175 (Table 4.2). *Bacillus amyloliquefaciens* strains mwb86, cce140, bnd136, bnn282 and ccc103 all performed poorly, with disease reductions of less than 9% over the experimental period (Figure 4.1) but were not significantly different from the diseased control.

Table 4.2. Results from agarised detached cotyledon assay of AEFB antagonism of cucurbit powdery mildew as generated by AUDPC and ANOVA using GenStat software.

Treatment	AUDPC Mean*	Disease Reduction % [#]
Control: Non-diseased	0 ^a	
<i>B. subtilis</i> strain sqo279	427.5 ^b	16.2
<i>B. amyloliquefaciens</i> strain sqo275	449.2 ^{bc}	11.9
<i>B. amyloliquefaciens</i> strain bng199	460.0 ^{bc}	9.8
<i>B. amyloliquefaciens</i> strain cce175	461.7 ^{bc}	9.5
<i>B. amyloliquefaciens</i> strain mwb86	467.5 ^{bcd}	8.3
<i>B. amyloliquefaciens</i> strain cce140	473.3 ^{cd}	7.2
<i>B. subtilis</i> strain bnd136	482.7 ^{cd}	5.4
<i>B. amyloliquefaciens</i> strain bnn282	487.5 ^{cd}	4.4
<i>B. amyloliquefaciens</i> strain ccc103	489.2 ^{cd}	4.1
Control: Diseased	510.0 ^d	-
<i>p</i> -value	<0.001	
L.S.D.	42.53	
C.V. %	5.9	
F-ratio	20.45	
S.E.	25.04	

* Treatment mean values followed by the same letter(s) are not significantly different according to Fischer's LSD test ($P \leq 0.05$). [#] Percentage calculated between treatment AUDPC value and the diseased control AUDPC value.

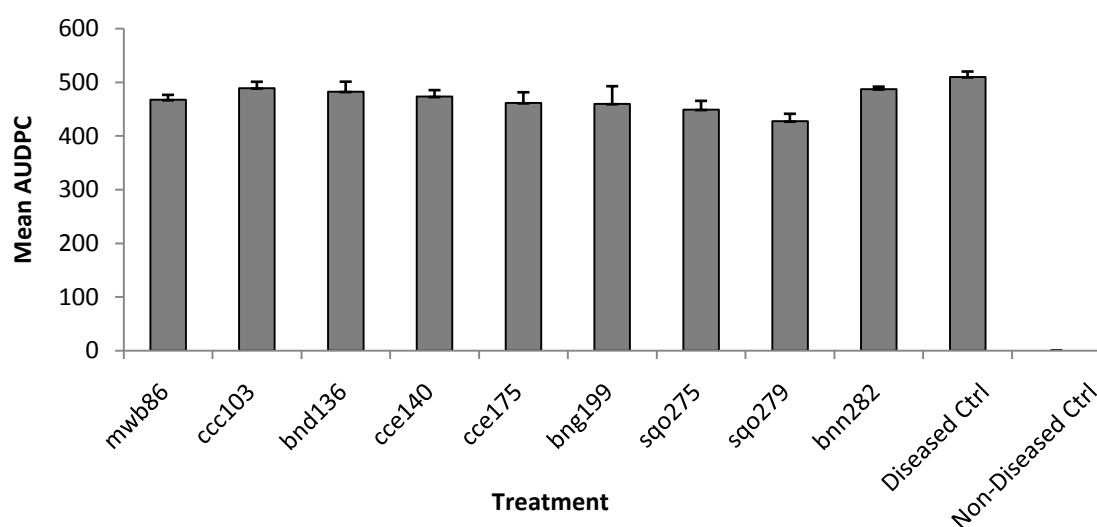
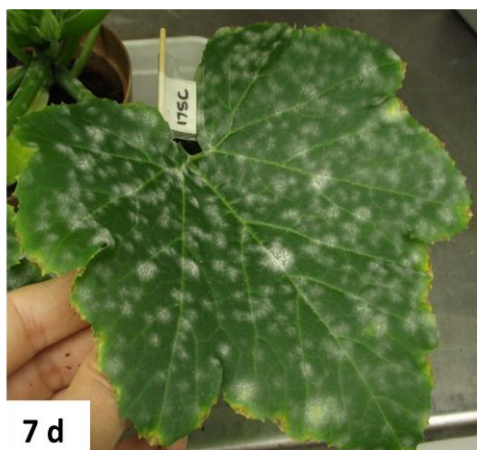


Figure 4.1. AUDPC analysis of an agarised detached cotyledon assay evaluating nine AEFB isolates against powdery mildew of cucurbits. Error bars indicate standard deviation between replicates.

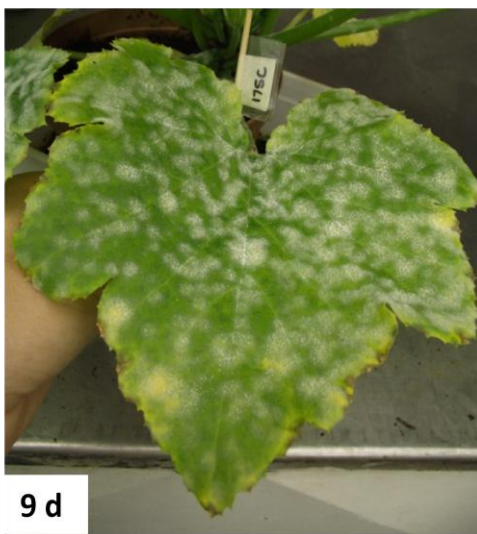
4.3.2. Biocontrol pot trial of powdery mildew antagonism

During enumeration using phase-contrast microscopy bacterial cells were observed to be motile rods in a vegetative state, with some evidence of endospore formation observed as refractile areas within the cells. No free endospores were observed in any of the samples.

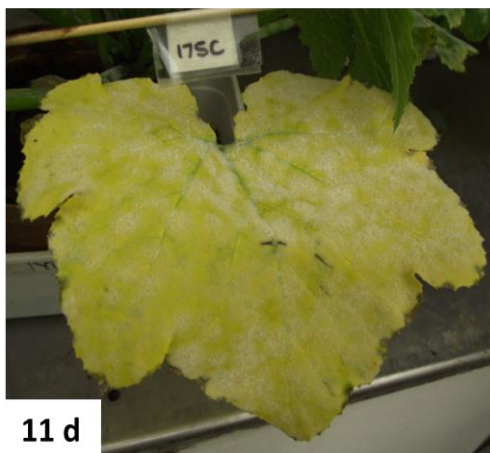
The powdery mildew disease applied at $\sim 10^5$ spores/ml resulted in a rapid and severe disease progression over the 13 d experimental period. Initial infection symptoms were evident on the plants from 2 d post fungal inoculation. In some replicates chlorosis and mild necrosis began to appear on certain leaves 9 d post disease inoculation (Plate 4.3), though this did not appear to have been as a result of nutrient or water stress or other diseases. The plants survived in excess of 16 d under artificially controlled conditions before the disease began to induce leaf senescence. Most of the marked leaves rated throughout the trial had senesced after 13 d. Those marked leaves that had died during rating were assigned a rating equal to the mean value ascribed to that leaf number from previous ratings (Marroni *et al.*, 2006).



7 d



9 d



11 d

Plate 4.3. Development of powdery mildew disease on zucchini (Partenon hybrid F1, Starke-Ayres, South Africa) inoculated with *B. amyloliquefaciens* strain cce175 as seen at 7, 9, and 11 d post disease inoculation.

Statistical data and treatment AUDPC values are presented in Table 4.3 and Figure 4.2. No bacterial treatments provided disease reductions that were statistically significant compared to the diseased control. Although *B. amyloliquefaciens* strain cce175 provided the lowest AUDPC value (Figure 4.5). *B. subtilis* strain sqo279, and *B. amyloliquefaciens* strains cce140, bng199, and sqo275 had disease levels exceeding those of the diseased control treatments. Overall, disease reduction percentages were low, with all isolates achieving less than 10% disease reduction over the period of assay (Table 4.3).

Table 4.3. AUDPC statistical results from biocontrol pot trial of AEFB antagonism of cucurbit powdery mildew.

Treatment	AUDPC Mean*	Disease Reduction % [#]
Control: Non-diseased	0 ^a	
<i>B. amyloliquefaciens</i> strain cce175	726.7 ^b	8.6
<i>B. amyloliquefaciens</i> strain bnn282	768.3 ^{bc}	3.4
<i>B. amyloliquefaciens</i> strain mwb86	768.3 ^{bc}	3.4
<i>B. subtilis</i> strain bnd136	771.7 ^{bc}	3.0
<i>B. amyloliquefaciens</i> strain ccc103	786.7 ^{bcd}	1.0
Control: Diseased	795.0 ^{bcd}	-
<i>B. subtilis</i> strain sqo279	816.7 ^{bcd}	-
<i>B. amyloliquefaciens</i> strain cce140	856.7 ^{cd}	-
<i>B. amyloliquefaciens</i> strain bng199	858.3 ^{cd}	-
<i>B. amyloliquefaciens</i> strain sqo275	870.0 ^d	-
<i>p</i> -value	<0.001	
L.S.D.	97.6	
C.V. %	7.9	
F-ratio	47.0	
S.E.	57.6	

* Treatment mean values followed by the same letter(s) are not significantly different according to Fischer's LSD test ($P \leq 0.05$). [#] Percentage calculated between treatment AUDPC value and the diseased control AUDPC value.

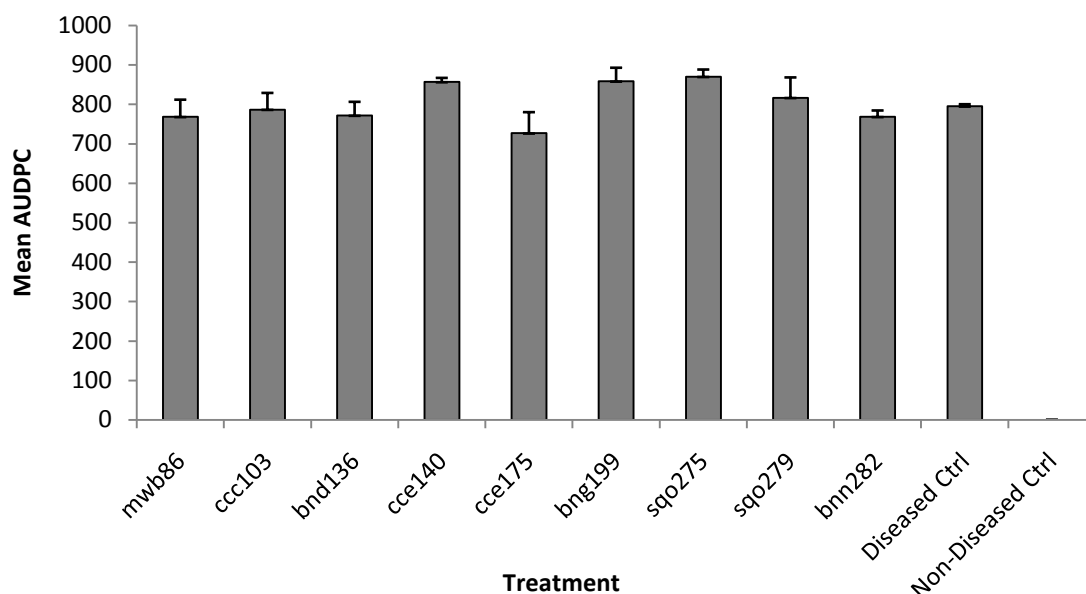


Figure 4.2. AUDPC analysis of a biocontrol pot trial evaluating nine AEFB isolates against powdery mildew of cucurbits. Error bars indicate standard deviation between replicates.

4.3.3. Impacts of bacterial preparation and culture age of *B. amyloliquefaciens* strain cce175 on cucurbit powdery mildew antagonism

The bacterial cells of *B. amyloliquefaciens* strain cce175 were examined under phase contrast microscopy during cell enumeration. The bacterial cells in Treatments 2 and 4 (48 h old live cells and whole broth respectively) were predominantly vegetative motile cells. In some instances forming endospores were observed as refractile areas within cells, although free endospores were rarely observed. In contrast Treatment 5 (72 h whole broth) was found to comprise predominantly sporulating cells and free endospores.

Symptoms of powdery mildew infection appeared on the diseased control plants at 7 d post-disease inoculation. Some of the replicates for the other treatments also showed symptoms of initial infection at this time, though disease was mostly observed at 9 d. Little incidence of disease was noted on the Treatment 7 (Folicur control) replicates until after 22 d. Overall, the progression of the disease was slower than the previous pot trial, owing to the lower concentration of *P. fusca* conidia in the suspension applied. Ratings carried out 10 d after

disease inoculation revealed I.a.i estimates between 2–20%. The rating conducted 10 d later showed a progression of disease in the treated plants, with I.a.i. estimates doubling from the 10 d rating figures.

The statistical data obtained from the AUDPC values is presented in Table 4.4 and Figure 4.3. No statistical difference was found between the experimental cce175 treatments and the diseased control. Overall, the Folicur fungicide control gave the greatest degree of disease control. Only Treatments 3 and 4 offered any reduction in disease, though these disease reductions were substantially lower than that achieved by the fungicide control at 8.14% and 1.34% respectively. Some leaf senescence had occurred from 28 days post-disease inoculation, hence for AUDPC purposes these leaves were rated equal to the mean value ascribed to that leaf from previous ratings (Marroni *et al.*, 2006).

The numbers of conidia/cm² of leaf material varied between treatments and did not correlate the AUDPC figures calculated (Table 4.4). Interestingly, Treatment 3 (48 h cell-free supernatant) provided the highest fungal spore count at 3.91 x10⁵ spores/cm² of leaf material. Treatment 2 gave the lowest conidia count (1.30 x10⁵ conidia/cm²), followed by the Folicur control (1.49 x10⁵ conidia/cm²).

Table 4.4. AUDPC results from a biocontrol pot trial assessing the effects of inoculum preparation of *B. amyloliquefaciens* strain cce175 on antagonism of cucurbit powdery mildew.

Treatment	AUDPC Mean*	Disease Reduction %[#]	Conidia/cm² (std.dev)
T1 Control: Non-diseased	0 ^a		0
T7 Control: Follicur	229.9 ^a	66.1	1.49 (±0.183) ×10 ⁵
T3 Supernatant (48 h)	622.9 ^b	8.14	3.91 (±0.183) ×10 ⁵
T4 Whole broth (48 h)	669.0 ^b	1.34	2.23 (±0.323) ×10 ⁵
T6 Control: Diseased	678.1 ^b	-	2.60 (±0.190) ×10 ⁵
T2 Active Cells (48 h)	771.1 ^b	-	1.30 (±0.183) ×10 ⁵
T5 Whole broth (72 h)	794.0 ^b	-	1.67 (±0.318) ×10 ⁵
<i>p</i> -value	<0.001		
L.S.D.	332.85		
C.V. %	35.3		
F-ratio	155.19		
S.E.	155.2		

* Treatment mean values followed by the same letter(s) are not significantly different according to Fischer's LSD test ($P \leq 0.05$). [#] Percentage calculated between treatment AUDPC value and the diseased control AUDPC value.

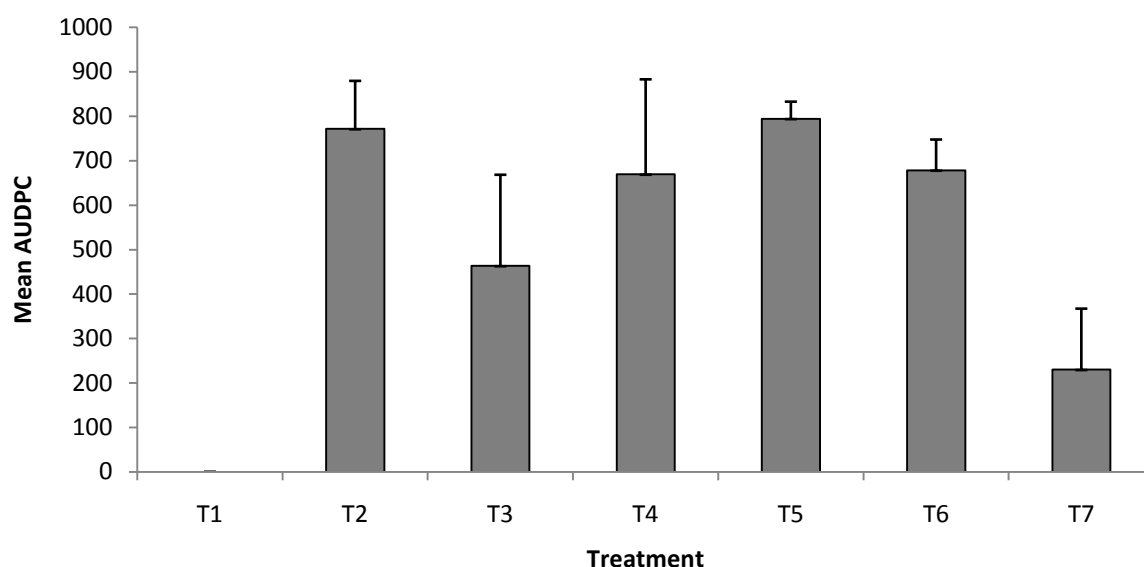


Figure 4.3. AUDPC analysis of a biocontrol pot trial assessing the performance of various formulations of *B. amyloliquefaciens* strain cce175 against powdery mildew of cucurbits disease, where: T1 Non-diseased Control; T2 Active Cells (48 h); T3 Supernatant (48 h); T4 Whole broth (48 h); T5 Whole broth (72 h); T6 Diseased Control; and T7 Folicur Control. Error bars indicate standard deviation between replicates.

4.4. Discussion

When screening candidate BCAs, pathogen antagonism assessments should ideally be carried out in the field. However, antifungal screening is impractical when evaluating large numbers of isolates due to labour, time, and resource constraints (Pliego *et al.*, 2010). For this reason *in vitro* bioassays are commonly used to screen and select candidate BCAs prior to undertaking lengthy assessments of field performance (Spurr, 1985). However, *in vitro* dual-culture bioassays risk overlooking certain interactions with the plant, hence *in planta* assays—which incorporate the host plant, pathogen, and antagonist—are considered to provide a more relevant evaluation of disease antagonism (Anith *et al.*, 2003). The present study was undertaken to evaluate the performance of nine AEFB isolates against cucurbit powdery mildew using a detached cotyledon assay and biocontrol pot trials.

Disease reductions observed for the nine isolates in the detached cotyledon assays and the pot trial were marginal, with reductions in the agarised cotyledon assay ranging between 9.5–16.2% (Table 4.2), and a maximum of 8.6% disease reduction recorded in the pot trial (Table 4.3). The detached cotyledon assay and biocontrol pot trial data yielded conflicting results with regards to the performance of individual isolates in antagonising *P. fusca*. Results obtained from the assessment of different inoculum preparations are disappointing, with some possible trends apparent, but overall the AUDPC values of experimental treatments are not significantly different from diseased control. All of the candidate isolates were effective in antagonising surrogate fungi in the dual-culture antifungal bioassays and able to synthesise antifungal lipopeptides. Ultimately, many treatments failed to achieve statistically significant levels of powdery mildew disease reduction in either assay method.

Previous studies report high incidences of disease reduction after application of *B. subtilis* vegetative cells or extracted metabolites. Romero *et al.* (2007c) reported that *B. subtilis* strains applied negatively impacted *P. fusca* conidia production, achieving conidial number reductions of 83–94%, which was statistically indistinguishable to that achieved using the fungicide azoxystrobin. The numbers of bacterial cells were found to persist on the leaf at levels comparable to those at application. Additionally, the bacteria were found to have established on the leaf surface at regions associated with higher nutrient availability, which indicated their capacity to establish vegetative microcolonies on the leaf. Bettiol *et al.* (1997) report disease reductions greater than 90% achieved from concentrated *B. subtilis* metabolites (5000 µg/ml). Detached leaf assays conducted by Romero *et al.* (2004) reported reduced conidial germination by over 80% and overall and disease reductions over 40%.

Disparity between BCA performance *in vitro* and *in vivo* is not uncommon (Folman *et al.*, 2003; Leifert *et al.*, 1995; Merriman and Russel 1990). There are several parameters which could account for the lacklustre performance of the chosen AEFB isolates against *P. fusca* in the present study. These include conditions favouring pathogen over-infestation; interactions with the extant microflora which may impede isolate establishment; pathogen and treatment application protocols; and inoculum preparation of the bacterial treatments (Pliego *et al.*, 2010; Knudsen *et al.*, 1997; Schisler and Slininger, 1997; Leifert *et al.*, 1995; Spurr, 1985).

Manipulation of environmental variables has been shown to influence the establishment and activity of both mycoparasites and *Bacillus* spp. against powdery mildew of cucurbits (Romero *et al.*, 2004; Dik *et al.*, 1998). The environmental parameters applied in the current study were very similar to those applied by Romero *et al.* (2007c), Romero *et al.* (2004), and Gilardi *et al.* (2008). However, the present study applied RH 70%, while Romero *et al.* (2007c) and Romero *et al.* (2004) found better performance by isolates was achieved at RH 75–90%. Although RH 90–95% offered greater isolate performance for Romero *et al.* (2007c).

Pathogen loading was found to be largely consistent between detached leaf assays and greenhouse trials in published literature, ranging from 10^4 – 10^5 conidia/ml (Romero *et al.*, 2007c; Perez-Garcia *et al.*, 2001; Romero *et al.*, 2004; Romero *et al.*, 2003; Bettiol *et al.*, 1997). In the present study conidia were applied in similar concentrations. Owing to the rapid progress of the disease in the biocontrol pot trial, the pot trial undertaken to assess the impacts of inoculum preparation on disease antagonism applied disease at $\sim 10^2$ conidia/ml. Disease progress in the latter trial was found to be slower, and offered a greater window of time over which to rate disease incidence. A concern with the use of growth chambers and small greenhouses for disease trials is the potential for continued disease inoculation of the plants owing to air currents generated by fan-driven ventilation systems, which may exacerbate the artificially high disease pressure already present in enclosed growing areas.

Biocontrol strategies can be broadly grouped into two categories: applying BCA in a preventative capacity, to persist within the introduced environment; or applying a curative approach, whereby the BCA or its metabolites are used as a short-term remedy (i.e. biopesticides) (Pliego *et al.*, 2010). The choice of strategy will have a direct bearing on the screening approach used, as the focus of each strategy is on different activities of the candidates. Hence, the timing of fungal and bacterial inoculations is an important factor in disease reduction, as bacterial cells require time to establish on the leaf in order to carry out their antagonistic activities and hence should be applied before the pathogen (Andrews, 1992; Andrews, 1990). However, when metabolites are being applied it could be argued that the pathogen be applied before the treatment to prevent compound decay and digestion by resident microflora. Bettiol *et al.* (1997) compared metabolite extracts applied at 1 h before

pathogen application, 1 h after the pathogen, and 24 h after the pathogen and reported disease reductions of 99.4%, 98.1%, and 99.5% respectively. Romero *et al.* (2007c) applied *P. fusca* after *B. subtilis* (3–4 d after bacteria, repeated 10 d later); Romero *et al.* (2004) applied *P. fusca* 4 h after the bacteria; and Gilhardi *et al.* (2008) applied *P. fusca* 24 h after fungicide treatments. The present study applied the disease 72 h after the bacterial treatments in all cases. This approach intended not only to allow the bacteria time to establish and colonise the leaf, but also to initiate lipopeptide synthesis prior to arrival of the pathogen. However, in order to establish the validity of this approach, further experiments to determine the prevalence of endospore numbers versus the populations of active cells are required.

Lipopeptide compounds synthesised by *Bacillus* spp. are generally produced during the stationary growth phase, therefore the age of the bacterial culture at the time of application has been shown to influence the efficacy of powdery mildew disease control (Romero *et al.*, 2004). In the present study much higher bacterial numbers were applied ($\sim 10^8$ cells/ml) than those reported previously in the literature were applied. Furthermore, the 36 h old culture previously been shown to have lipopeptides present in the supernatant. Various preparations of *B. amyloliquefaciens* strain cce175 were applied to assess the impact of inoculum preparation on cucurbit powdery mildew antagonism in a biocontrol pot trial (Table 4.1). Unfortunately, all treatments performed poorly when compared to disease control levels achieved by the Folicur fungicide control (Table 4.4). Romero *et al.* (2004) observed that *B. subtilis* cells applied in stationary growth phase (48 h old) achieved disease reductions of up to 69%. Nevertheless, bacterial cells applied at the log phase of growth were still shown to negatively impact disease. Romero *et al.* (2007c) report that cells applied at the log phase of growth (27–30 h old), achieved disease reductions of 80–97%. Both Romero *et al.* (2007c) and Romero *et al.* (2004) report stable bacterial population numbers at 10^4 – 10^5 cfu/cm² regardless of growth phase at the time of application. Furthermore, previous studies examining the influence of lipopeptides against *P. fusca* have included concentrated purified extracts, which can be argued to offer more concentrated levels of active compounds than a simple cell-free supernatant (Romero *et al.*, 2007a; Romero *et al.*, 2007b; Bettiol *et al.*, 1997). Hence, it can be concluded that the application of *P. fusca* 72 h post bacterial treatment inoculation may have been too long.

Conidia enumeration conducted at the close of the inoculum preparation pot trial found that conidial numbers did not correlate with the AUDPC data of the experimental treatments (Table 4.4). The highest numbers of spores were found for Treatment 3 (48 h cell-free supernatant). Although no conidial abnormalities were noted during enumeration, it is possible for the conidia to have been negatively affected by exposure to the activities of lipopeptide compounds present in Treatments 3, 4, and 5. Compounds produced by *Bacillus* spp.—particularly those of the lipopeptide families—have been shown to impact the reproductive capability of fungal conidia (Chaurasia *et al.*, 2005). Conidiophore aberrations and conidial malformation in *P. fusca* has been reported after exposure to lipopeptide compounds (Romero *et al.*, 2007b). However, the present study did not examine the harvested conidia any further, hence it was not conclusively established whether conidia were structurally intact and reproductively functional.

The evaluation of disease antagonism potential using *in vitro* bioassays alone are often of little extrapolative value, as the interplay of many mechanisms determines an isolates' ability to survive and thrive in a niche on the host plant (Folman *et al.*, 2003). Nevertheless, *in vitro* assessments such as the dual-culture bioassay, and small-scale *in planta* methods such as detached cotyledon assays can contribute to narrowing the field of prospective antagonists prior to field testing. Despite employing a polyphasic screening approach to BCA selection, the present study was unable to identify *Bacillus* spp. candidates warranting further evaluation on the basis of the detached cotyledon assay and biocontrol pot trial. The detached cotyledon assay represents a rapid and simplified means of assessing antagonism on a laboratory-scale, but offers only a small area of which to evaluate antagonism potential. In contrast, a biocontrol pot trial is considered to be a reasonable compromise between *in vitro* screening methods and full-scale field trials (Pliego *et al.*, 2010). A pot trial retains indigenous microflora, and is considered a more accurate representation of the natural habitat conditions and interactions with the plant host and extant microflora than the detached cotyledon assay (Anith *et al.*, 2003). Nevertheless, optimising the agarised detached cotyledon assay to ensure greater statistical rigour would be beneficial, as this assay has the potential to be implemented earlier in the screening process and possibly in place of the *in vitro* dual-culture bioassay. Investigation into the influence of bacterial inoculum preparation on powdery mildew antagonism yielded no conclusive results in the present study, yet bacterial establishment in

the introduced environment and the biosynthesis of lipopeptide compounds contribute to the efficacy of *B. subtilis* against *P. fusca*, and hence merit further consideration and investigation (Romero *et al.*, 2007a; Romero *et al.*, 2007c; Romero *et al.*, 2004).

CHAPTER FIVE

General Overview and Conclusions

Bacterial biocontrol agents have been extensively researched as potential alternatives to conventional chemical-based plant disease control methods (Heydari and Pessarakli, 2010; Pal and McSpadden Gardener, 2006). Of the bacterial species evaluated for biocontrol and plant growth promotion capabilities, applications of various strains of *Bacillus* and *Paenibacillus* spp. have demonstrated great potential in this regard (McSpadden Gardener and Diks, 2004; McSpadden Gardener, 2004). Previous studies have shown that strains of *B. subtilis* are promising as antagonists of powdery mildew of cucurbits (Romero *et al.*, 2007a; Romero *et al.*, 2007b; Romero *et al.*, 2004; Bettiol *et al.*, 1997). Much of the antagonistic potential demonstrated by these bacteria has been traced to the biosynthesis of lipopeptide compounds (Borriss, 2011; Jacques, 2011; Ongena *et al.*, 2010; Ongena *et al.*, 2008).

This study was undertaken with the aim of isolating AEFB from cucurbit species showing diminished powdery mildew symptoms grown in various locations in the greater Msunduzi area of KwaZulu-Natal. Isolates were assessed for antifungal capability against surrogate pathogens *in vitro*, and ultimately against cucurbit powdery mildew *in vivo*. This research also explored means of identifying and distinguishing between isolates using MALDI-TOF-MS, DNA fingerprinting (ITS-PCR and RAPD-PCR), and analysing 16S rRNA and *gyrA* gene fragment sequence analyses to establish species- and strain-level diversity amongst the isolates. Lipopeptide compound biosynthesis by selected isolates was evaluated using TLC and MALDI-TOF-MS and lipopeptide gene marker PCR. The findings of this study established that:

- More than 70% of the AEFB isolated were antagonistic towards *Rhizoctonia solani* and/or *Botrytis cinerea* in *in vitro* dual-culture bioassays. These isolates originated from various geographical locations and cucurbit species, viz. pumpkin, chayote, butternut, squash, and marrow. Colony morphology and endospore location characteristics did not provide sufficient grounds for discrimination or dereplication amongst the isolates. Hence DNA fingerprinting methods RAPD-PCR and ITS-PCR were compared for isolate

differentiation and dereplication purposes. Among the 55 isolates examined, RAPD-PCR was able to distinguish 14 distinct RAPD fingerprint profiles, while ITS-PCR was able to determine two variants, with a third minor profile exclusive to one isolate. These two methods were able to give insights into the levels of genetic diversity amongst the isolates, and showed that certain profiles were widespread amongst cucurbit species and geographical location of isolation. This finding may indicate the existence of ecotypes, which suggests that these strains would exhibit some degree of adaptation enabling them to colonise and survive on the cucurbit phylloplane. Analysis of 16S rRNA and *gyrA* gene fragment sequences was undertaken to distinguish and identify AEFB species. The *gyrA* partial gene sequences showed greater sequence heterogeneity than 16S rRNA gene sequences; and were able to distinguish isolates to the subspecies and strain levels. Antagonistic AEFB isolates were found to be closely related to either *B. amyloliquefaciens* or *B. subtilis*. MALDI-TOF-MS showed promise as a rapid means of identifying environmental isolates. The Bruker Daltonics MALDI Biotyper library was of limited use in identifying isolates by comparison to the existing reference spectra database, due to a lack of environmentally relevant subspecies and strains within the BDAL database. However, the generation of dendograms demonstrated spectral variances amongst the pool of isolates, which was reflected after cluster analysis with SPECLUST was employed. Both dendograms allowed the grouping of isolates, though variations in the parameters used for dendogram construction created some differences between the respective dendograms generated. MALDI-TOF-MS proved a very useful tool in distinguishing isolates. However, further optimisation and expansion of the Biotyper spectral library is needed.

- MALDI-TOF-MS was a rapid and powerful tool for determining the presence of lipopeptide compounds from methanol extracts of culture supernatants. The m/z values from the mass spectra generated were compared to values ascribed in literature, from reference strains, and purified standards of iturin and surfactin. Biomarker peak data were able to provide information not only of the lipopeptide variants present, but also of compound isoforms and adducts. All of the antifungal extracts tested were found to contain surfactins and fengycins; though the prevalence of iturin- and bacillomycin-associated peaks was found to vary between isolates. The isolates which showed the most prolific lipopeptide production were found to be

related to *B. amyloliquefaciens*. *Podosphaera fusca* is known to be sensitive to these lipopeptides, therefore MALDI-TOF-MS is a very convenient method for the screening of potential candidate BCAs against this fungus. TLC analysis of the methanol extracts provided a crude means of detecting the presence of compounds when bands were compared to the iturin and surfactin purified standards. However, little information could be gathered as to the isoforms of the lipopeptide compound families present in the bands. Compared to MALDI-TOF-MS, TLC appears to be an outdated approach as it allows only the separation of compounds present within a mixture. Further characterisation of the constituents of individual bands was not possible with TLC alone; and would require additional extraction and analysis to determine individual band constituents. The application of gene marker PCR to detect lipopeptide production potential demonstrated a wide distribution of lipopeptide markers amongst the isolates; with markers indicative of iturin, fengycin, and surfactin synthesis prevalent amongst the isolate set. However, gene sequence data for reference strain *B. amyloliquefaciens* R16 suggests that the *ituD* gene marker primer may have been non-specific, as this amplicon was identified after sequencing as a marker for bacillomycin D synthesis (*BmyD*). Certain isolates related to *B. subtilis* displayed negative results for all gene markers, yet MALDI-TOF-MS analysis detected biomarker peaks associated to some—if not all—of the lipopeptide families in methanol extracts from these isolates. Further investigation of the accuracy of the gene marker PCR primers is therefore required before this method can be considered a fully reliable assessment of lipopeptide production potential.

- Based on the *in vitro* screening and selection criteria used in this study, nine isolates were selected as potential antagonists of powdery mildew of cucurbits. These isolates were assessed using a simple agarised detached cotyledon assay and a biocontrol pot trial, both applying live bacterial cells. Statistical analysis showed that both of these methods would benefit some level of optimisation. The detached cotyledon assay is attractive as a simplified screening method for candidate BCAs of biotrophic pathogens. The biocontrol pot trial remains the cornerstone for evaluation of isolate performance under field-representative conditions. Overall, any of the methods of *in planta* assay are dependent on many factors, which need to be addressed and refined to establish a reliable disease antagonism-assessment assay. Hence, isolate cce175 was

selected for assessment of the effects of inoculum preparation against powdery mildew. This isolate was selected on the basis of its antifungal activity, the production of lipopeptide compounds, and its relation to strains of *B. amyloliquefaciens*. Unfortunately no statistical differences between the performance of the experimental treatments and the diseased control were found. This suggests that some degree of optimisation and refinement of the biocontrol pot trial conditions could benefit the outcomes of this trial.

Screening a large pool of isolates for antagonistic potential is a complicated process and requires the examination of many biocontrol traits. This is achievable with use of multiple high-throughput methods without extensive resource demands. In this study it was demonstrated that a large pool of isolates can be successfully rationalised during the early stages of screening, and that DNA fingerprinting is useful for dereplication purposes and establishing diversity levels amongst candidate isolates. MALDI-TOF-MS presents a very promising high-throughput approach for both characterising isolates and evaluating lipopeptide production potential. Field trials remain the basis for the evaluation and development of isolates for commercial products. However, due to the resource intensive nature of field trials only limited numbers of candidates can be assessed. Hence preliminary screening and selection criteria play an essential role in short-listing suitable isolates for field trial evaluation.

The performance of an isolate under field conditions remains the final criterion by which a candidate antagonist is judged as a biocontrol agent, though laboratory-scale assays and biocontrol pot trials present manageable options to this end. Screening and selection protocols which investigate multiple aspects contributing to the survival of that agent can assist a researcher in selecting the candidate most likely to survive and remain active before lengthy field trials are embarked upon.

Additional research into the population diversity, ecology, and prevalence of AEFB within the cucurbit phyllosphere and is warranted in order to identify ecotypes and establish which traits are associated with phyllosphere competence. In order to improve and expand on the DNA

fingerprinting techniques used in this study, different RAPD-PCR primers could be evaluated to further differentiate between closely-related strains of AEFB. In addition, sequence analysis of alternative house-keeping genes (e.g. gyrase subunit B (*gyrB*), histidine kinase (*cheA*), and RNA polymerase subunit B (*rpoB*)) would aid in distinguishing and identifying plant-associated species of the *B. subtilis* group of related taxa; as isolates proved difficult to distinguish based on conventional 16S rRNA sequence analysis methods. MALDI-TOF-MS proved to be a valuable tool for the rapid identification of isolates, however there is a pressing need to create MSPs for environmentally-relevant AEFB strains. In addition, MALDI-TOF-MS is also an effective for resolving the presence of lipopeptide compounds produced by the AEFB isolates. This is an avenue that needs to be expanded upon, for example there is the potential to apply whole-cell material for a high-throughput determination of lipopeptide production by antifungal isolates. The biocontrol pot trials evaluating powdery mildew antagonism by AEFB isolates require some optimisation of parameters such as the age of bacterial cells at application, and further analysis of the impacts of bacterial inoculum preparation. The detached cotyledon assay also merits further investigation, as this technique has potential as a means of distinguishing AEFB isolates antagonistic to powdery mildew at an earlier stage in the screening process.

REFERENCES

- Abushady, H., Bashandy, A., Aziz, N. & Ibrahim, H. (2005).** Molecular characterization of *Bacillus subtilis* surfactin producing strain and the factors affecting its production. *International Journal of Agriculture and Biology* **3**, 337–344.
- Agrios, G. N. (2005).** *Plant Pathology*. 5 edn: pp. 196–197, 200–201. Elsevier Academic Press.
- Alm, R., Johansson, P., Hjernø, K., Emanuelsson, C., Ringnér, M. & Häkkinen, J. (2006).** Detection and identification of protein isoforms using cluster analysis of MALDI-MS mass spectra. *Journal of Proteome Research* **5**, 785–792.
- Álvarez, B. & Torés, J. A. (1997).** Cultivo *in vitro* de *Sphaerotheca fuliginea* (Schlecht. Ex. Fr.), efecto de diferentes fuentes de carbono sobre su desarrollo. *Boletín de Sanidad Vegetal* **23**, 283–288.
- Alvarez, F., Castro, M., Príncipe, A., Borioli, A., Fischer, S., Mori, G. & Jofré, E. (2011).** The plant-associated *Bacillus amyloliquefaciens* strains MEP₂18 and ARP₂3 capable of producing the cyclic lipopeptides iturin or surfactin and fengycin are effective in biocontrol of sclerotinia stem rot disease. *Journal of Applied Microbiology* **112**, 159–174.
- Alvindia, D. G. & Natsuaki, K. T. (2009).** Biocontrol of *Bacillus amyloliquefaciens* DGA14 isolated from banana fruit surface against banana crown rot-causing pathogens. *Crop Protection* **28**, 236–242.
- Andrews, J. H. (1990).** Biological control in the phyllosphere: Realistic goal or false hope? *Canadian Journal of Plant Pathology* **12**, 300–307.
- Andrews, J. H. (1992).** Biological control in the phyllosphere. *Annual Review of Phytopathology* **30**, 603–635.

- Anith, K. N., Radhakrishnan, N. V. & Manomohandas, T. P. (2003).** Screening of antagonistic bacteria for biological control of nursery wilt of black pepper (*Piper nigrum*). *Microbiological Research* **158**, 91–97.
- Arabi, M. I. E. & Jawhar, M. (2002).** The ability of barley powdery mildew to grow *in vitro*. *Journal of Phytopathology* **150**, 305–307.
- Arguelles-Arias, A., Ongena, M., Halimi, B., Lara, Y., Brans, A., Joris, B. & Fickers, P. (2009).** *Bacillus amyloliquefaciens* GA1 as a source of potent antibiotics and other secondary metabolites for biocontrol of plant pathogens. *Microbial cell factories* **8**, 63.
- Arrebola, E., Sivakumar, D. & Korsten, L. (2010).** Effect of volatile compounds produced by *Bacillus* strains on postharvest decay in citrus. *Biological Control* **53**, 122–128.
- Athukorala, S. P., Fernando, W. G. D. & Rashid, K. Y. (2009).** Identification of antifungal antibiotics of *Bacillus* species isolated from different microhabitats using polymerase chain reaction and MALDI-TOF mass spectrometry. *Canadian Journal of Microbiology* **55**, 1021–1032.
- Bais, H. P., Fall, R. & Vivanco, J. M. (2004).** Biocontrol of *Bacillus subtilis* against infection of *Arabidopsis* roots by *Pseudomonas syringae* is facilitated by biofilm formation and surfactin production. *Plant Physiology* **134**, 307–319.
- Balhara, M., Ruhil, S., SDhankar, S. & Chhillar, A. K. (2011).** Bioactive compounds hold up *Bacillus amyloliquefaciens* as a potent bio-control agent. *The Natural Products Journal* **1**, 20–28.
- Bardin, M., Suliman, M. E., Sage-Palloix, A.-M., Mohamed, Y. F. & Nicot, P. C. (2007).** Inoculum production and long-term conservation methods for cucurbits and tomato powdery mildews. *Mycological Research* **111**, 740–747.
- Bargabus, R. L., Zidack, N. K., Sherwood, J. E. & Jacobsen, B. J. (2002).** Characterisation of systemic resistance in sugar beet elicited by a non-pathogenic phyllosphere-colonizing *Bacillus mycoides*, biological control agent. *Physiological and Molecular Plant Pathology* **61**, 289–298.

Bargabus, R. L., Zidack, N. K., Sherwood, J. E. & Jacobsen, B. J. (2004). Screening for the identification of potential biological control agents that induce systemic acquired resistance in sugar beet. *Biological Control* **30**, 342–350.

Baysal, Ö., Çalışkan, M. & Yeşilova, Ö. (2008). An inhibitory effect of a new *Bacillus subtilis* strain (EU07) against *Fusarium oxysporum* f. sp. *radicis-lycopersici*. *Physiological and Molecular Plant Pathology* **73**, 25–32.

Bechet, M., Caradec, T., Hussein, W., Abderrahmani, A., Chollet, M., Leclere, V., Dubois, T., Lereclus, D., Pupin, M. & Jacques, P. (2012). Structure, biosynthesis, and properties of kurstakins, nonribosomal lipopeptides from *Bacillus* spp. *Applied microbiology and Biotechnology* **95**, 593–600.

Bélangier, R. R., Dik, A. J. & Menzies, J. G. (1998). Powdery mildews: recent advances toward integrated control. In *Plant–Microbe Interactions and Biocontrol*, pp. 89–104. Edited by G. J. Boland and L. Kuykendall. New York: Marcel Dekker, Inc.

Bettiol, W., Garibaldi, A. & Migheli, Q. (1997). *Bacillus subtilis* for the control of powdery mildew on cucumber and zucchini squash. *Bragantia* **56**.

Blakeman, J. P. & Fokkema, N. J. (1982). Potential for biological control of plant diseases on the phylloplane. *Annual Review of Phytopathology* **20**, 167–192.

Borriss, R. (2011). Use of plant-associated *Bacillus* strains as biofertilizers and biocontrol agents in agriculture. In *Bacteria in Agrobiolgy: Plant Growth Responses*, pp. 41–76. Edited by D. K. Maheshwari. Berlin Heidelberg: Springer-Verlag.

Borriss, R., Chen, X.-H., Rueckert, C., Blom, J., Becker, A., Baumgarth, B., Fan, B., Pukall, R., Schumann, P., Spröer, C., Junge, H., Vater, J., Pühler, A. & Klenk, H.-P. (2011). Relationship of *Bacillus amyloliquefaciens* clades associated with strains DSM 7T and FZB42T: a proposal for *Bacillus amyloliquefaciens* subsp. *amyloliquefaciens* subsp. nov. and *Bacillus amyloliquefaciens* subsp. *plantarum* subsp. nov. based on complete genome sequence comparisons. *International Journal of Systematic and Evolutionary Microbiology* **61**, 1786–1801.

Bottone, E. J. & Peluso, R. W. (2003). Production by *Bacillus pumilus* (MSH) of an antifungal compound that is active against *Mucoraceae* and *Aspergillus* species: preliminary report. *Journal of Medical Microbiology* **52**, 69–74.

Cantu, D., Greve, L. C., Labavitch, J. M. & Powell, A. L. (2009). Characterization of the cell wall of the ubiquitous plant pathogen *Botrytis cinerea*. *Mycological Research* **113**, 1396–1403.

Carbonnelle, E., Mesquita, C., Bille, E., Day, N., Dauphin, B., Beretti, J.-L., Ferroni, A., Gutmann, L. & Nassif, X. (2011). MALDI-TOF mass spectrometry tools for bacterial identification in clinical microbiology laboratory. *Clinical Biochemistry* **44**, 104–109.

Cawoy, H., Bettiol, W., Fickers, P. & Ongena, M. (2011). *Bacillus*-based biological control of plant diseases. In *Pesticides in the Modern World: Pesticides Use and Management*, pp. 273–302. Edited by M. Stoytcheva. InTech.

Cazorla, F. M., Romero, D., Pérez-García, A., Lugtenberg, B. J. J., de Vicente, A. & Bloemberg, G. (2007). Isolation and characterization of antagonistic *Bacillus subtilis* strains from the avocado rhizoplane displaying biocontrol activity. *Journal of Applied Microbiology* **103**, 1950–1959.

Chaurasia, B., Pandey, A., Palni, L. M. S., Trivedi, P., Kumar, B. & Colvin, N. (2005). Diffusible and volatile compounds produced by an antagonistic *Bacillus subtilis* strain cause structural deformations in pathogenic fungi *in vitro*. *Microbiological Research* **160**, 75–81.

Cheah, L. H., Page, B. B. C. & Cox, J. K. (1996). Epidemiology of powdery mildew (*Sphaerotheca fuliginea*) of squash. In *Proceedings of 49th New Zealand Plant Protection Conference*, pp. 147–151.

Chen, L., Wang, N., Wang, X., Hu, J. & Wang, S. (2010). Characterization of two anti-fungal lipopeptides produced by *Bacillus amyloliquefaciens* SH-B10. *Bioresource Technology* **101**, 8822–8827.

Chen, X. H., Koumoutsis, A., Scholz, R. & Borriss, R. (2009a). More than anticipated – production of antibiotics and other secondary metabolites by *Bacillus amyloliquefaciens* FZB42. *Journal of Molecular Microbiology and Biotechnology* **16**, 14–24.

Chen, X. H., Koumoutsis, A., Scholz, R., Schneider, K., Vater, J., Süssmuth, R., Piel, J. & Borriss, R. (2009b). Genome analysis of *Bacillus amyloliquefaciens* FZB42 reveals its potential for biocontrol of plant pathogens. *Journal of Biotechnology* **140**, 27–37.

Chitarra, G. S., Breeuwer, P., Nout, M. J. R., van Aelst, A. C., Rombouts, F. M. & Abee, T. (2003). An antifungal compound produced by *Bacillus subtilis* YM 10–20 inhibits germination of *Penicillium roqueforti* conidiospores. *Journal of Applied Microbiology* **94**, 159–166.

Choudhary, D. K. & Johri, B. N. (2009). Interactions of *Bacillus* spp. and plants – with special reference to induced systemic resistance (ISR). *Microbiological Research* **164**, 493–513.

Chun, J. & Bae, K. S. (2000). Phylogenetic analysis of *Bacillus subtilis* and related taxa based on partial *gyrA* gene sequences. *Antonie van Leeuwenhoek* **78**, 123–127.

Cohan, F. M. (2001). Bacterial Species and Speciation. *Systematic Biology* **50**, 513–524.

Collins, D. P. & Jacobsen, B. J. (2003). Optimizing a *Bacillus subtilis* isolate for biological control of sugar beet *Cercospora* leaf spot. *Biological Control* **26**, 153–161.

Collins, D. P., Jacobsen, B. J. & Maxwell, B. (2003). Spatial and temporal population dynamics of a phyllosphere colonizing *Bacillus subtilis* biocontrol agent of sugar beet *Cercospora* leaf spot. *Biological Control* **26**, 224–232.

Daffonchio, D., Borin, S., Consolandi, A., Mora, D., Manachini, P. L. & Sorlini, C. (1998a). 16S–23S rRNA internal transcribed spacers as molecular markers for the species of the 16S rRNA group I of the genus *Bacillus*. *FEMS Microbiology Letters* **163**, 229–236.

Daffonchio, D., Borin, S., Frova, G., Manachini, P. L. & Sorlini, C. (1998b). PCR fingerprinting of whole genomes: the spacers between the 16S and 23S rRNA genes and of intergenic tRNA

gene regions reveal a different intraspecific genomic variability of *Bacillus cereus* and *Bacillus licheniformis*. *International Journal of Systematic Bacteriology* **48**, 107–116.

Daffonchio, D., Cherif, A. & Borin, S. (2000). Homoduplex and heteroduplex polymorphisms of the amplified ribosomal 16S–23S internal transcribed spacers describe genetic relationships in the “*Bacillus cereus* group”. *Applied and Environmental Microbiology* **66**, 5460–5468.

Daffonchio, D., Cherif, A., Brusetti, L., Rizzi, A., Mora, D., Boudabous, A. & Borin, S. (2003). Nature of polymorphisms in 16S–23S rRNA gene Intergenic transcribed spacer fingerprinting of *Bacillus* and related genera. *Applied and Environmental Microbiology* **69**, 5128–5137.

Damiani, G., Amedeo, P., Bandi, C., Fani, R., Bellizzi, D. & Sgaramella, V. (1996). Bacteria identification by PCR-based techniques. In *Microbial Genome Methods*, pp. 167–178. Edited by K. W. Adolph: CRC Press, Inc.

Dare, D. (2006). Rapid bacterial characterization and identification by MALDI-TOF mass spectrometry. In *Advanced Techniques in Diagnostic Microbiology*, pp. 117–133. Edited by Y.-W. Tang and C. W. Stratton. United States of America: Springer.

Das, P., Mukherjee, S. & Sen, R. (2008). Antimicrobial potential of a lipopeptide biosurfactant derived from a marine *Bacillus circulans*. *Journal of Applied Microbiology* **104**, 1675–1684.

de Jager, E. S., Wehner, F. C. & L., K. (2001). Microbial ecology of the mango phylloplane. *Microbial Ecology* **42**, 201–207.

Dickinson, D. N., La Duc, M. T., Haskins, W. E., Gornushkin, I., Winefordner, J. D., Powell, D. H. & Venkateswaran, K. (2004b). Species differentiation of a diverse suite of *Bacillus* spores by mass spectrometry-based protein profiling. *Applied and Environmental Microbiology* **70**, 475–482.

Dickinson, D. N., La Duc, M. T., Satomi, M., Winefordner, J. D., Powell, D. H. & Venkateswaran, K. (2004a). MALDI-TOF-MS compared with other polyphasic taxonomy

approaches for the identification and classification of *Bacillus pumilus* spores. *Journal of Microbiological Methods* **58**, 1–12.

Dieckmann, R., Graeber, I., Kaesler, I., Szewzyk, U. & Döhren, H. (2005). Rapid screening and dereplication of bacterial isolates from marine sponges of the Sula Ridge by Intact-Cell-MALDI-TOF mass spectrometry (ICM-MS). *Applied Microbiology and Biotechnology* **67**, 539–548.

Dik, A. J., Verhaar, M. A. & Bélanger, R. R. (1998). Comparison of three biological control agents against cucumber powdery mildew (*Sphaerotheca fuliginea*) in semi-commercial-scale glasshouse trials. *European Journal of Plant Pathology* **104**, 413–423.

Edgar, R. C. (2004). MUSCLE: Multiple alignment with high accuracy and high throughput. *Nucleic Acids Research* **32**, 1792–1797.

Dingman, D. W. (2012). *Paenibacillus larvae* 16S–23S rDNA intergenic transcribed spacer (ITS) regions: DNA fingerprinting and characterization. *Journal of Invertebrate Pathology* **110**, 352–358.

Emmert, E. A. B. & Handelsman, J. (1999). Biocontrol of plant disease: a (Gram-) positive perspective. *FEMS Microbiology Letters* **171**, 1–9.

Felsenstein, J. (1985). Confidence limits on phylogenies: An approach using the bootstrap. *Evolution* **39**, 783–791.

Fernández-No, I. C., Böhme, K., Díaz-Bao, M., Cepeda, A., Barros-Velázquez, J. & Calo-Mata, P. (2013). Characterisation and profiling of *Bacillus subtilis*, *Bacillus cereus* and *Bacillus licheniformis* by MALDI-TOF mass fingerprinting. *Food Microbiology* **33**, 235–242.

Fernández-Ortuño, D., Pérez-García, A., López-Ruiz, F., Romero, D., de Vicente, A. & Torís, J. A. (2006). Occurrence and distribution of resistance to QoI fungicides in populations of *Podosphaera fusca* in south central Spain. *European Journal of Plant Pathology* **115**, 215–222.

Ferreira, J. H. S., Matthee, F. N. & Thomas, A. C. (1991). Biological control of *Eutypa lata* on grapevine by an antagonistic strain of *Bacillus subtilis*. *Phytopathology* **81**, 283–287.

Fickers, P. (2012). Antibiotic compounds from *Bacillus*: Why are they so amazing? *American Journal of Biochemistry and Biotechnology* **8**, 40–46.

Fiddaman, P. J. & Rossall, S. (1993). The production of antifungal volatiles by *Bacillus subtilis*. *Journal of Applied Bacteriology* **74**, 119–126.

Fiddaman, P. J. & Rossall, S. (1994). Effect of substrate on the production of antifungal volatiles from *Bacillus subtilis*. *Journal of Applied Bacteriology* **76**, 395–405.

Fokkema, N. J. (1996). Biological control of fungal plant diseases. *Entomophaga* **41**, 333–342.

Folman, L. B., Postma, J. & Van Veen, J. A. (2003). Inability to find consistent bacterial biocontrol agents of *pythium aphanidermatum* in cucumber using screens based on ecophysiological traits. *Microbial Ecology* **45**, 72–87.

Fox, A. (2006). Mass spectrometry for species or strain identification after culture or without culture: Past, present, and future. *Journal of Clinical Microbiology* **44**, 2677–2680.

Fravel, D. R. & Spurr, H., W. Jr. (1977). Biocontrol of tobacco brown-spot disease by *Bacillus cereus* subsp. *mycoides* in a controlled environment. *Phytopathology* **67**, 930–932.

Freiwald, A. & Sauer, S. (2009). Phylogenetic classification and identification of bacteria by mass spectrometry. *Nature Protocols* **4**, 732–742.

Garbeva, P., van Veen, J. A. & van Elsas, J. D. (2003). Predominant *Bacillus* spp. in agricultural soil under different management regimes detected via PCR-DGGE. *Microbial Ecology* **25**, 302–316.

Ghyselinck, J., Van Hoorde, K., B., H., Heylen, K. & De Vos, P. (2011). Evaluation of MALDI-TOF MS as a tool for high-throughput dereplication. *Journal of Microbiological Methods* **86**, 327–336.

Ghyselinck, J., Velivelli, S. L. S., Heylen, K., O’Herlihy, E., Franco, J., Rojas, M., De Vos, P. & Doyle Prestwich, B. (2013). Bioprospecting in potato fields in the Central Andean Highlands: Screening of rhizobacteria for plant growth-promoting properties. *Systematic and Applied Microbiology* **36**, 116–127.

Gilardi, G., Manker, D. C., Garibaldi, A. & Gullino, M. L. (2008). Efficacy of the biocontrol agents *Bacillus subtilis* and *Ampelomyces quisqualis* applied in combination with fungicides against powdery mildew of zucchini. *Journal of Plant Diseases and Protection* **115**, 208–213.

Glawe, D. A. (2008). The powdery mildews: A review of the world’s most familiar (yet poorly known) plant pathogens. *Annual Review of Phytopathology* **46**, 27–51.

González-Sánchez, M. A., M., P.-J. R., Pliego, C., Ramos, C., de Vicente, A. & Cazorla, F. M. (2010). Biocontrol bacteria selected by a direct plant protection strategy against avocado white root rot show antagonism as a prevalent trait. *Journal of Applied Microbiology* **109**, 65–78.

Gordillo, M. A. & Maldonado, M. C. (2012). Purification of peptides from *Bacillus* strains with biological activity. In *Chromatography and Its Applications*, pp. 201–224. Edited by S. Dhanarasu: InTech.

Goto, K., Omura, T., Hara, Y. & Sadaie, Y. (2000). Application of the partial 16S rDNA sequence as an index for rapid identification of species in the genus *Bacillus*. *Journal of General Applied Microbiology* **46**, 1–8.

Govindasamy, V., Senthilkumar, M., Magheshwaran, V., Kumar, U., Bose, P., Sharma, V. & Annapurna, K. (2010). *Bacillus* and *Paenibacillus* spp.: potential PGPR for sustainable agriculture. In *Plant Growth and Health Promoting Bacteria*, pp. 333–364. Edited by D. K. Maheshwari. Heidelberg: Springer-Verlag.

Hall, T. A. (1999). BioEdit: A user-friendly biological sequence alignment editor and analysis program for Windows 95/98/NT. *Nucleic Acids Symposium Series* **41**, 95–98.

Handelsman, J. & Stabb, E. V. (1996). Biocontrol of soilborne plant pathogens. *The Plant Cell* **8**, 1855–1869.

Hathout, Y., Ho, Y.-P., Ryzhov, V., Demirev, P. & Fenselau, C. (2000). Kurstakins: A new class of lipopeptides isolated from *Bacillus thuringiensis*. *Journal of Natural Products* **63**, 1492–1496.

Haupt, M. R. (2007). An investigation into the use of biological control agents as a sustainable alternative to synthetic fungicides in treating powdery mildew in tunnel cucumbers. Department of Nature Conservation, pp. 1–131: University of South Africa.

Heuer, H., Krsek, M., Baker, P., Smalla, K. & Wellington, E. M. (1997). Analysis of actinomycete communities by specific amplification of genes encoding 16S rRNA and gel-electrophoretic separation in denaturing gradients. *Applied and Environmental Microbiology* **63**, 3233–3241.

Heydari, A. & Pessarakli, M. (2010). A review on biological control of fungal plant pathogens using microbial antagonists. *Journal of Biological Sciences* **10**, 273–290.

Hsieh, F.-C., Li, M.-C., Lin, T.-C. & Kao, S. S. (2004). Rapid detection and characterization of surfactin-producing *Bacillus subtilis* and closely related species based on PCR. *Current Microbiology* **49**, 186–191.

Hsieh, F.-C., Lin, T.-C., Meng, M. & Kao, S.-S. (2008). Comparing methods for identifying *Bacillus subtilis* strains capable of producing the antifungal lipopeptide iturin A. *Current Microbiology* **56**, 1–5.

Jacobsen, B. J., Zidack, N. K. & Larson, B. J. (2004). The role of *Bacillus*-based biological control agents in integrated pest management systems: Plant diseases. *Phytopathology* **94**, 1272–1275.

Jacques, P. (2011). Surfactin and other lipopeptides from *Bacillus* spp. In *Biosurfactants: from Genes To Applications*, pp. 58–91. Edited by G. Soberón-Chávez. Berlin Heidelberg: Springer-Verlag

Ji, P. & Wilson, M. (2003). Enhancement of population size of a biological control agent and efficacy in control of bacterial speck of tomato through salicylate and ammonium sulfate amendments. *Applied and Environmental Microbiology* **69**, 1290–1294.

Jijakli, M. H. & Lepoivre, P. (1998). Development of biocontrol agents: Opportunities and challenges for their practical application. *Revista Corpoica* **2**, 16–17.

Joshi, R. & McSpadden Gardener, B. B. (2006). Identification and characterization of novel genetic markers associated with biological control activities of *Bacillus subtilis*. *Phytopathology* **96**, 145–154.

Jourdan, E., Henry, G., Duby, F., Dommes, J., Barthélemy, J. P., Thonart, P. & Ongena, M. (2009). Insights into the defense-related events occurring in plant cells following perception of surfactin-type lipopeptide from *Bacillus subtilis*. *Molecular Plant–Microbe Interactions* **22**, 456–468.

Jukes, T. H. & Cantor, C. R. (1969). *Evolution of protein molecules*. New York: Academic Press.

Keys, C. J., Dare, D. J., Sutton, H., Wells, G., Lunt, M., McKenna, T., McDowall, M. & Shah, H. N. (2004). Compilation of a MALDI-TOF mass spectral database for the rapid screening and characterisation of bacteria implicated in human infectious diseases. *Infection, Genetics and Evolution* **4**, 221–242.

Kim, Y. T., Cho, M., Jeong, J. Y., Lee, H. B. & Kim, S. B. (2010). Application of terminal restriction fragment length polymorphism (T-RFLP) analysis to monitor effect of biocontrol agents on rhizosphere microbial community of hot pepper (*Capsicum annuum* L.). *The Journal of Microbiology* **48**, 566–572.

Kiss, L. (2003). A review of fungal antagonists of powdery mildews and their potential as biocontrol agents. *Pest Management Science* **59**, 475–483.

Kloepper, J. W., Ryu, C.-M. & Zhang, S. (2004). Induced systemic resistance and promotion of plant growth by *Bacillus* spp. *Phytopathology* **94**, 1259–1266.

Knudsen, G. R. & Spurr, H. W. (1988). Management of bacterial populations for foliar disease biocontrol. In *Biocontrol of Plant Diseases*, pp. 83–91. Edited by K. G. Mukerji and K. L. Garg. Florida: CRC Press, Inc.

Knudsen, I. M. B., Hockenhull, J., Funck Jensen, D., Gerhardson, B., Hökeberg, M., Tahvonen, R., Teperi, E., Sundheim, L. & Henriksen, B. (1997). Selection of biological control agents for controlling soil and seed-borne diseases in the field. *European Journal of Plant Pathology* **103**, 775–784.

Koumoutsis, A., Chen, X. H., Henne, A., Liesegang, H., Hitzeroth, G., Franke, P., Vater, J. & Borriß, R. (2004). Structural and functional characterization of gene clusters directing nonribosomal synthesis of bioactive cyclic lipopeptides in *Bacillus amyloliquefaciens* strain FZB42. *Journal of Bacteriology* **186**, 1084–1096.

Kowalska, T., Kaczmariski, K. & Prus, W. (2003). Theory and mechanism of thin-layer chromatography. In *Handbook of Thin-layer Chromatography*, pp. 62–105. Edited by J. Sherma and B. Fried. USA: Marcel-Dekker, Inc.

Kumar, P., Dubey, R. C. & Maheshwari, D. K. (2012). *Bacillus* strains isolated from rhizosphere showed plant growth promoting and antagonistic activity against phytopathogens. *Microbiological Research* **167**, 493–499.

Kwon, G.-H., Lee, H.-A., Park, J.-Y., S., K. J., Lim, J., Park, C.-S., Kwon, D.-Y., Kim, Y.-S. & Kim, J. H. (2009). Development of a RAPD-PCR method for identification of *Bacillus* species isolated from Cheonggukjang. *International Journal of Food Microbiology* **129**, 282–287.

Laslo, É., György, É., Mara, G., Tamás, É., Ábrahám, B. & Lányi, S. (2012). Screening of plant growth promoting rhizobacteria as potential microbial inoculants. *Crop Protection* **40**, 43–48.

Latoud, C., Peypoux, F. & Michel, G. (1990). Interaction of iturin A, a lipopeptide antibiotic, with *Saccharomyces cerevisiae* cells: Influence of the sterol membrane composition. *Canadian Journal of Microbiology* **36**, 384–389.

Lay, J. O. (2000). MALDI-TOF mass spectrometry and bacterial taxonomy. *Trends In Analytical Chemistry* **19**, 507–516.

Lay, J. O. (2001). MALDI-TOF mass spectrometry of bacteria. *Mass Spectrometry Reviews* **20**, 172–194.

Leenders, F., Stein, T. H., Kablitz, B., Franke, P. & Vater, J. (1999). Rapid typing of *Bacillus subtilis* strains by their secondary metabolites using matrix-assisted laser desorption/ionization mass spectrometry of intact cells. *Rapid Communications in Mass Spectrometry* **13**, 943–949.

Leifert, C., Li, H., Chidburee, S., Hampson, S., Workman, S., Sigee, D., Epton, H. A. S. & Harbour, A. (1995). Antibiotic production and biocontrol activity by *Bacillus subtilis* CL27 and *Bacillus pumilus* CL45. *Journal of Applied Bacteriology* **78**, 97–108.

Li, W., Raoult, D. & Fournier, P.-E. (2009). Bacterial strain typing in the genomic era. *FEMS Microbiology Reviews* **33**, 892–916.

Li, Y.-M., Haddad, N. I. A., Yang, S.-Z. & Mu, B.-Z. (2008). Variants of lipopeptides produced by *Bacillus licheniformis* HSN221 in different medium components evaluated by a rapid method ESI-MS. *International Journal of Peptide Research and Therapeutics* **14**, 229–235.

Lin, G.-H., Chen, L.-C., Tschen, J. S.-M., Tsay, S.-S., Chang, Y.-S. & Liu, S.-T. (1998a). Molecular cloning and characterization of fengycin synthetase gene *fenB* from *Bacillus subtilis*. *Journal of Bacteriology* **180**, 1338–1341.

Lin, S.-C., Chen, Y.-C. & Lin, Y.-M. (1998b). General approach for the development of high-performance liquid chromatography methods for biosurfactant analysis and purification. *Journal of Chromatography A* **825**, 149–159.

Lin, T.-P., Chen, C.-L., Fu, H.-C., Wu, C.-Y., Lin, G.-H., Huang, S.-H., Chang, L.-K. & Liu, S.-T. (2005). Functional analysis of fengycin synthetase FenD. *Biochimica et Biophysica Acta* **1730**, 159–164.

Lindow, S. (2006). Phyllosphere microbiology: A perspective. In *Microbial Ecology of Aerial Plant Surfaces*, pp. 1–20. Edited by M. J. Bailey, A. K. Lilley, T. M. Timms-Wilson and P. T. N. Spencer-Phillips: CAB International.

Lindow, S. E. & Brandl, M. T. (2003). Microbiology of the phyllosphere. *Applied and Environmental Microbiology* **69**, 1875–1883.

Lindow, S. E. & Leveau, J. H. J. (2002). Phyllosphere microbiology. *Current Opinion in Biotechnology* **18**, 238–243.

Logan, N. A., Berge, O., Bishop, A. H. & [Enter number of additional authors] other authors (2009). Proposed minimal standards for describing new taxa of aerobic, endospore-forming bacteria. *International Journal of Systematic and Evolutionary Microbiology* **59**, 2114–2121.

Madonna, A. J., Voorhees, K. J., Taranenko, N. I., Lalko, V. V. & Doroshenko, V. M. (2003). Detection of cyclic lipopeptide biomarkers from *Bacillus* species using atmospheric pressure matrix-assisted laser desorption/ionization mass spectrophotometry. *Analytical Chemistry* **75**, 1628–1637.

Malfanova, N., Franzil, L., Lugtenberg, B., Chebotar, V. & Ongena, M. (2012). Cyclic lipopeptide profile of the plant-beneficial endophytic bacterium *Bacillus subtilis* HC8. *Archives of Microbiology* **194**, 893–899.

Mari, M., Guizzardi, M. & Pratella, G. C. (1996). Biological control of gray mold in pears by antagonistic bacteria. *Biological Control* **7**, 30–37.

Marroni, M. V., Viljanen-Rollinson, S. L. H., Butler, R. C. & Deng, Y. (2006). Fungicide timing for the control of *Septoria tritici* of wheat. *New Zealand Plant Protection* **59**, 160–165.

Martínez, M. A. & Siñeriz, F. (2004). PCR fingerprinting of rRNA intergenic spacer regions for molecular characterization of environmental bacteria isolates. In *Environmental Microbiology: Methods and Protocols*, pp. 159–166. Edited by J. F. T. Spencer and A. L. Ragout de Spencer: Humana Press.

Mathre, D. E., Cook, R. J. & Callan, N. W. (1999). From discovery to use: Traversing the world of commercializing biocontrol agents for plant disease control. *Plant Disease* **83**, 972–983.

Maughan, H. & Van der Auwera, G. (2011). *Bacillus* taxonomy in the genomic era finds phenotypes to be essential though often misleading. *Infection, Genetics and Evolution* **11**, 789–797.

May, R., Volksch, B. & Kampmann, G. (1997). Antagonistic activities of epiphytic bacteria from soybean leaves against *Pseudomonas syringae* pv. *glycinea* *in vitro* and *in planta*. *Microbial Ecology* **34**, 118–124.

McGrath, M. T. (2001). Fungicide resistance in cucurbit powdery mildew: Experiences and challenges. *Plant Disease* **85**, 236–245.

McKeen, C. D., Reilly, C. C. & Pusey, P. L. (1986). Production and partial characterization of antifungal substances antagonistic to *Monilinia fructicola* from *Bacillus subtilis*. *Phytopathology* **76**, 136–139.

McSpadden Gardener, B. B. (2004). Ecology of *Bacillus* and *Paenibacillus* spp. in agricultural systems. *Phytopathology* **94**, 1252–1258.

McSpadden Gardener, B. B. & Diks, A. (2004). Overview of the nature and application of biocontrol microbes: *Bacillus* spp. *Phytopathology*, 1244.

Mercier, J. & Lindow, S. E. (2000). Role of leaf surface sugars in colonization of plants by epiphytes. *Applied and Environmental Microbiology* **66**, 369–374.

Merriman, P. & Russell, K. (1990). Screening strategies for biological control. In *Biological Control of Soil-borne Plant Pathogens*, pp. 427–435. Edited by D. Hornby. Wallingford: CAB International.

Mileham, A. J. (1997). Identification of microorganisms using random primed PCR. *Molecular Biotechnology* **8**, 139–145.

Mizuki, E., Ichimatsu, T., Hwang, S.-H., Park, Y. S., Saitoh, H., Higuchi, K. & Ohba, M. (1999). Ubiquity of *Bacillus thuringiensis* on phylloplanes of arboreous and herbaceous plants in Japan. *Journal of Applied Microbiology* **88**.

Mora, I., Cabrefiga, J. & Montesinos, E. (2011). Antimicrobial peptide genes in *Bacillus* strains from plant environments. *International Microbiology: The Official Journal of the Spanish Society for Microbiology* **14**, 213–223.

Moré, M. I., Herrick, J. B., Silva, M. C., Ghiorse, W. C. & Madsen, E. L. (1994). Quantitative cell lysis of indigenous microorganisms and rapid extraction of microbial DNA from sediment. *Applied and Environmental Microbiology* **60**, 1572–1580.

Moyne, A. L., Cleveland, T. E. & Tuzun, S. (2004). Molecular characterization and analysis of the operon encoding the antifungal lipopeptide bacillomycin D. *FEMS Microbiology Letters* **234**, 43–49.

Mukherjee, S., Das, P. & Sen, R. (2009). Rapid quantification of a microbial surfactant by a simple turbidometric method. *Journal of Microbiological Methods* **76**, 38–42.

Nagórksa, K., Bikowski, M. & Obuchowski, M. (2007). Multicellular behaviour and production of a wide variety of toxic substances support usage of *Bacillus subtilis* as a powerful biocontrol agent. *Acta Biochimica Polonica* **54**, 495–508.

Nagpal, M. L., Fox, K. F. & Fox, A. (1998). Utility of 16S–23S rRNA spacer region methodology: How similar are interspace regions within a genome and between strains for closely related organisms? *Journal of Microbiological Methods* **33**, 211–219.

Nair, J. R., Singh, G. & Sekar, V. (2002). Isolation and characterization of a novel *Bacillus* strain from coffee phyllosphere showing antifungal activity. *Journal of Applied Microbiology* **93**, 772–780.

Niedermeyer, T. H. J. & Strohal, M. (2012). mMass as a software tool for the annotation of cyclic peptide tandem mass spectra. *PLoS ONE* **7**.

Nilsson, J., Svensson, B., Ekelund, K. & Christiansson, A. (1998). A RAPD-PCR method for large-scale typing of *Bacillus cereus*. *Letters in Applied Microbiology* **27**, 168–172.

Olive, M. D. & Bean, P. (1999). Principles and applications of methods for DNA-based typing of microbial organisms. *Journal of Clinical Microbiology* **37**, 1661–1669

Olsen, G. J. & Woese, C. R. (1993). Ribosomal RNA: a key to phylogeny. *The FASEB Journal* **7**, 113–123.

Ongena, M., Duby, F., Jourdan, E., Beaudry, T., Jadin, V., Dommès, J. & Thonart, P. (2005a). *Bacillus subtilis* M4 decreases plant susceptibility towards fungal pathogens by increasing host resistance associated with differential gene expression. *Applied Microbiology and Biotechnology* **67**, 692–698.

Ongena, M., Henry, G., Adam, A., Jourdan, E. & Thonart, P. (2009). Insights into the plant defense mechanisms induced by *Bacillus* lipopeptides. In XIV International Congress on Molecular Plant–Microbe Interactions. Quebec, Canada.

Ongena, M., Henry, G. & Thonart, P. (2010). The roles of cyclic lipopeptides in the biocontrol activity of *Bacillus subtilis*. In Recent Developments in Management of Plant Diseases, pp. 59–69. Edited by U. Gisi, I. Chet and M. L. Gullino: Springer Science and Business Media.

Ongena, M. & Jacques, P. (2008). *Bacillus* lipopeptides: Versatile weapons for plant disease biocontrol. *Trends in Microbiology* **16**, 115–125.

Ongena, M., Jacques, P., Touré, Y., Destain, J., Jabrane, A. & Thonart, P. (2005b). Involvement of fengycin-type lipopeptides in the multifaceted biocontrol potential of *Bacillus subtilis*. *Applied Microbiology and Biotechnology* **69**, 29–38.

Ongena, M., Jourdan, E., Adam, A., Paquot, M., Brans, A., Joris, B., Arpigny, J.-L. & Thonart, P. (2007). Surfactin and fengycin lipopeptides of *Bacillus subtilis* as elicitors of induced systemic resistance in plants. *Environmental Microbiology* **9**, 1084–1090.

Pal, K. K. & McSpadden Gardener, B. (2006). Biological control of plant pathogens. *The Plant Health Instructor*, 1–25.

Pavankumar, A. R., Ayyappasamy, S. P. & Sankaran, K. (2011). Small RNA fragments in complex culture media cause alterations in protein profiles of three species of bacteria. *Biotechniques* **50**, 167–172.

Pérez-García, A., Mingorance, E., Rivera, M. E., Del Pino, D., Romero, D., Torés, J. A. & De Vincente, A. (2006). Long-term preservation of *Podosphaera fusca* using silica gel. *Journal of Phytopathology* **154**.

Pérez-García, A., Ollalla, L., Rivera, E., Del Pino, D., Cánovas, I., De Vincente, A. & Torés, J. A. (2001). Development of *Sphaerotheca fusca* on susceptible, resistant and temperature-sensitive resistant melon cultivars. *Mycological research* **105**, 1216–1222.

Pérez-García, A., Romero, D. & De Vincente, A. (2011). Plant protection and growth stimulation by microorganisms: Biotechnological applications of Bacilli in agriculture. *Current Opinion in Biotechnology* **22**, 187–193.

Pérez-García, A., Romero, D., Fernández-Ortuño, D., López-Ruiz, F., De Vincente, A. & Torés, J. A. (2009). The powdery mildew fungus *Podosphaera fusca* (synonym *Podosphaera xanthii*), a constant threat to cucurbits. *Molecular Plant Pathology* **10**, 153–160.

Pliego, C., Ramos, C., de Vincente, A. & Cazorla, F. M. (2011). Screening for candidate bacterial biocontrol agents against soilborne fungal plant pathogens. *Plant and Soil* **340**, 505–520.

Poole, C. F. (2003). Thin-layer chromatography: Challenges and opportunities. *Journal of Chromatography A* **1000**, 963–984.

Prabhakar, A. & Bishop, A. H. (2014). Comparative studies to assess bacterial communities on the clover phylloplane using MLST, DGGE and T-RFLP. *World Journal of Microbiology and Biotechnology* **30**, 153–161.

Price, N. P. J., Rooney, A. P., Swezey, J. L., Perry, E. P. & Cohan, F. M. (2007). Mass spectrometric analysis of lipopeptides from *Bacillus* strains isolated from diverse geographical locations. *FEMS Microbiology Letters* **271**, 83–89.

Pryor, S. W., Siebert, K. J., Gibson, D. M., Gossett, J. M. & Walker, L. P. (2007). Modeling production of antifungal compounds and their role in biocontrol product inhibitory activity. *Journal of Agricultural and Food Chemistry* **55**, 9530–9536.

Quan, C. S., Wang, X. & S.D., F. (2010). Antifungal compounds of plant growth promoting rhizobacteria and its action mode. In *Plant Growth and Health Promoting Bacteria*, pp. 117–156. Edited by D. K. Maheshwari: Springer.

Quinn, J. A. & Powell, C. C. (1982). Effects of temperature, light, and relative humidity on powdery mildew of begonia. *Phytopathology* **72**.

Raaijmakers, J. M., de Bruijn, I. & de Kock, M. J. D. (2006). Cyclic lipopeptide production by plant-associated *Pseudomonas* spp.: Diversity, activity, biosynthesis, and regulation. *Molecular Plant–Microbe Interactions* **19**, 699–710.

Raaijmakers, J. M., de Bruijn, I., Nybroe, O. & Ongena, M. (2010). Natural functions of lipopeptides from *Bacillus* and *Pseudomonas*: more than surfactants and antibiotics. *FEMS Microbiology Reviews* **34**, 1037–1062.

Raaijmakers, J. M., Vlami, M. & de Souza, J. T. (2002). Antibiotic production by bacterial biocontrol agents. *Antonie van Leeuwenhoek* **81**, 537–547.

Rademaker, J. L. W., Aarts, H. J. M. & Vinuesa, P. (2005). Molecular typing of environmental isolates. In *Molecular Microbial Ecology*, pp. 97–135. Edited by A. M. Osborn and C. J. Smith: Taylor and Francis Group.

Ramarathnam, R. (2007). Mechanisms of phyllosphere biological control of *Leptosphaeria maculans*, the blackleg pathogen of canola, using antagonistic bacteria. Department of Plant Science, pp. 1–219: University of Manitoba.

Ramarathnam, R., Bo, S., Chen, Y., Fernando, W. G. D., Xuewen, G. & de Kievit, T. (2007). Molecular and biochemical detection of fengycin- and bacillomycin D producing *Bacillus* spp. antagonistic to fungal pathogens of canola and wheat. *Canadian Journal of Microbiology* **53**, 901–911.

Ranjard, L., Poly, F. & Nazaret, S. (2000). Monitoring complex bacterial communities using culture-independent molecular techniques: Application to soil environment. *Research in Microbiology* **151**, 167–177.

Razafindralambo, H., Paquot, M., Hbid, C., Jacques, P., Destain, J. & Thonart, P. (1993). Purification of antifungal lipopeptides by reversed-phase high-performance liquid chromatography. *Journal of Chromatography* **639**, 81–85.

Razdan, V. K. & Gupta, S. (2009). Integrated disease management: Concepts and practices. In Integrated Pest Management: Innovation-Development Process, pp. 369–389. Edited by R. Peshin and A. K. Dhawan: Springer.

Reuvani, M., Agapov, V. & Reuvani, R. (1995). Suppression of cucumber powdery mildew (*Sphaerotheca fuliginea*) by foliar sprays of phosphate and potassium salts. *Plant Pathology* **44**, 31–39.

Reva, O. N., Dixelius, C., Meijer, J. & Priest, F. G. (2004). Taxonomic characterization and plant colonizing abilities of some bacteria related to *Bacillus amyloliquefaciens* and *Bacillus subtilis*. *FEMS Microbiology Ecology* **48**, 249–259.

Roberts, M. S., Nakamura, L. K. & Cohan, F. M. (1994). *Bacillus mojaviensis* sp. nov., distinguishable from *Bacillus subtilis* by sexual isolation, divergence in DNA sequence, and differences in fatty acid composition. *International Journal of Systematic Bacteriology* **44**, 256–264.

Robinson, R. W. & Decker-Walters, D. S. (1997). *Cucurbits*: CAB International.

Romero, D., de Vicente, A., Rakotoaly, R. H., Dufour, S. E., Veening, J.-M., Arrebola, E., Cazorla, F. M., Kuipers, O. P., Paquot, M. & Pérez-García, A. (2007a). The iturin and fengycin families of lipopeptides are key factors in antagonism of *Bacillus subtilis* toward *Podosphaera fusca*. *Molecular Plant–Microbe Interactions* **20**, 430–440.

Romero, D., de Vincente, A., Olmos, J. L., Dávila, J. C. & Pérez-Garcia, A. (2007b). Effect of lipopeptides of antagonistic strains of *Bacillus subtilis* on the morphology and ultrastructure of the cucurbit pathogen *Podosphaera fusca*. *Journal of Applied Microbiology* **103**, 969–976.

Romero, D., de Vincente, A., Zeriouh, H., Cazorla, F. M., Fernandez-Ortuño, D., Torés, J. A. & Pérez-García, A. (2007c). Evaluation of biological control agents for managing cucurbit powdery mildew on greenhouse-grown melon. *Plant Pathology* **56**, 976–986.

Romero, D., Pérez-García, A., Rivera, M. E., Cazorla, F. M. & de Vicente, A. (2004). Isolation and evaluation of antagonistic bacteria towards the cucurbit powdery mildew fungus *Podosphaera fusca*. *Applied Microbiology and Biotechnology* **64**, 263–269.

Romero, D., Rivera, M. E., Carzola, F. M., de Vincente, A. & Pérez-García, A. (2003). Effect of mycoparasitic fungi on the development of *Sphaerotheca fusca* in melon leaves. *Mycological Research* **107**, 64–71.

Ron, E. Z. & Rosenberg, E. (2001). Natural roles of biosurfactants. *Environmental Microbiology* **3**, 229–236.

Rooney, A. P., Price, N. P. J., Ehrhardt, C., Swezey, J. L. & Bannan, J. D. (2009). Phylogeny and molecular taxonomy of the *Bacillus subtilis* species complex and description of *Bacillus subtilis* subsp. *inaquosorum* subsp. nov. *International Journal of Systematic and Evolutionary Microbiology* **59**, 2429–2436.

Saenz, A. J., Petersen, C. E., Valentine, N. B., Gantt, S. L., Jarman, K. H., Kingsley, M. T. & Wahl, K. L. (1999). Reproducibility of matrix-assisted laser desorption/ionization time-of-flight mass spectrometry for replicate bacterial culture analysis. *Rapid Communications in Mass Spectrometry* **13**, 1580–1585.

Saitou, N. & Nei, M. (1987). The neighbor-joining method: A new method for reconstructing phylogenetic trees. *Molecular Biology and Evolution* **4**, 406–425.

Sauer, S., Freiwald, A., Maier, T., Kube, M., Reinhardt, R., Kostrzewa, M. & Geider, K. (2008). Classification and identification of bacteria by mass spectrometry and computational analysis. *PLoS One* **3**, 1–10.

Savadogo, A., Tapi, A., Chollet, M., Wathelet, B., Traoré, A. S. & Jacques, P. (2011). Identification of surfactin producing strains in *Soumbala* and *Bikalga* fermented condiments using polymerase chain reaction and matrix assisted laser desorption/ionization-mass spectrometry methods. *International Journal of Food Microbiology* **151**, 299–306.

Schisler, D. A. & Slininger, P. J. (1997). Microbial selection strategies that enhance the likelihood of developing commercial biological control products. *Journal of Industrial Microbiology and Biotechnology* **19**, 172–179.

Schleifer, K.-H. (2009). The Firmicutes. In *Bergey's Manual of Systematic Bacteriology*, pp. 19–128. Edited by A. C. Parte, W. B. Whitman, P. De Vos, G. M. Garrity, D. Jones, N. R. Krieg, W. Ludwig, F. A. Rainey and K.-H. Schleifer. New York, NY: Springer.

Schütte, U. M., Abdo, Z., Bent, S. J., Shyu, C., Williams, C. J., Pierson, J. D. & Forney, L. J. (2008). Advances in the use of terminal restriction fragment length polymorphism (T-RFLP) analysis of 16S rRNA genes to characterize microbial communities. *Applied Microbiology and Biotechnology* **80**, 365–380.

Šedo, O., Sedláček, I. & Zdráhal, Z. (2011). Sample preparation methods for MALDI-MS profiling of bacteria. *Mass Spectrometry Reviews* **30**, 417 – 434.

Shaner, G. & Finney, R. E. (1977). The effect of nitrogen fertilization on the expression of slow mildewing resistance in Knox wheat. *Phytopathology* **67**, 1051–1056.

Shaver, Y. J., Nagpal, M. L., Fox, K. F., Rudner, R. & Fox, A. (2001). Variation in 16S–23S rRNA intergenic spacer regions among *Bacillus subtilis* 168 isolates. *Molecular Microbiology* **42**, 101–109.

Shishkoff, N. & McGrath, M. T. (2002). A Q10 biofungicide combined with chemical fungicides or AddQ spray adjuvant for control of cucurbit powdery mildew in detached leaf culture. *Plant Disease* **86**, 915–918.

Shoda, M. (2000). Bacterial control of plant diseases. *Journal of Bioscience and Bioengineering* **89**, 515–521.

Singh, J. & Faull, J. L. (1988). Antagonism and biocontrol. In *Biocontrol of Plant Diseases*, pp. 167–175. Edited by K. G. Mukerji and K. L. Garg. Florida: CRC Press, Inc.

Slepecky, R. A. & Hemphill, H. E. (2006). The genus *Bacillus*—Nonmedical. In *The Prokaryotes*, pp. 530–562. Edited by M. Dworkin, S. Falkow, E. Rosenberg, K.-H. Schleifer and E. Stackebrandt: Springer.

Song, J. Y., Kim, H. A., Kim, J.-S. & [Enter number of additional authors] other authors (2012). Genome sequence of the plant growth-promoting rhizobacterium *Bacillus* sp. strain JS. *Journal of Bacteriology* **194**, 3760–3761.

South African Department of Agriculture, Forestry and Fisheries (2013). South African cucurbit production 2013.

Souto, G. I., Correa, O. S., Montecchia, M. S., Kerber, N. L., Pucheu, N. L. & Bachur, M. (2004). Genetic and functional characterization of a *Bacillus* sp. strain excreting surfactin and antifungal metabolites partially identified as iturin-like compounds. *Journal of Applied Microbiology* **97**, 1247–1256.

Spurr, H. W. (1985). Bioassays: Critical to biocontrol of plant disease. *Journal of Agricultural Entomology* **2**, 117–122.

Stein, T. (2005). *Bacillus subtilis* antibiotics: Structures, syntheses and specific functions. *Molecular Microbiology* **56**, 845–857.

Strohalm, M., Hassman, M., Kořata, B. & Kodíček, M. (2008). mMass data miner: An open source alternative for mass spectrometric data analysis. *Rapid Communications in Mass Spectrometry* **22**, 905–908.

Strohalm, M., Kavan, D., Novák, P., Volný, M. & Havlíček, V. (2010). mMass 3: A cross-platform software environment for precise analysis of mass spectrometric data. *Analytical Chemistry* **82**, 4648–4651.

Tamura, K., Nei, M. & Kumar, S. (2004). Prospects for inferring very large phylogenies by using the neighbor-joining method. *Proceedings of the National Academy of Sciences (USA)* **101**, 11030–11035.

Tamura, K., Stecher, G., Peterson, D., Filipski, A. & Kumar, S. (2013). MEGA6: molecular evolutionary genetics analysis version 6.0. *Molecular Biology and Evolution* **30**, 2725–2729.

Tapi, A., Chollet-Imbert, M., Scherens, B. & Jacques, P. (2010). New approach for the detection of non-ribosomal peptide synthetase genes in *Bacillus* strains by polymerase chain reaction. *Applied Microbiology and Biotechnology* **85**, 1521–1531.

Tendulkar, S. R., Saikumari, Y. K., Patel, V., Raghotama, S., Munshi, T. K., Balaram, P. & Chattoo, B. B. (2007). Isolation, purification and characterization of an antifungal molecule produced by *Bacillus licheniformis* BC98, and its effect on phytopathogen *Magnaporthe grisea*. *Journal of Applied Microbiology* **103**, 2331–2339.

Teperi, E., Keskinen, M., Ketoja, E. & Tahvonen, R. (1998). Screening for fungal antagonists of seed-borne *Fusarium culmorum* on wheat using *in vivo* tests. *European Journal of Plant Pathology* **104**, 243–251.

Tesfagiorgis, H. B. (2009). Studies on the use of biocontrol agents and soluble silicon against powdery mildew of zucchini and zinnia. Discipline of Plant Pathology, School of Agricultural

Sciences and Agribusiness, Faculty of Science and Agriculture, pp. 1–182: University of KwaZulu-Natal.

Tewelde, T. W. (2004). Characterization of selected *Bacillus* isolates exhibiting broad spectrum antifungal activity. Discipline of Microbiology, School of Applied and Environmental Sciences, Faculty of Science and Agriculture, pp. 1–150: University of KwaZulu-Natal

Thakore, Y. (2006). The biopesticide market for global agricultural use. *Biocontrol* **2**, 193–208.

Touré, Y., Ongena, M., Jacques, P., Guirio, A. & Thonart, P. (2004). Role of lipopeptides produced by *Bacillus subtilis* GA1 in the reduction of grey mould disease caused by *Botrytis cinerea* on apple. *Journal of Applied Microbiology* **95**, 1151–1160.

Tsuge, K., Akiyama, T. & Shoda, M. (2001). Cloning, sequencing and characterization of the iturin A operon. *Journal of Bacteriology* **183**, 6265–6273.

Tyler, K. D., Wang, G., Tyler, S. D. & Johnson, W. M. (1997). Factors affecting reliability and reproducibility of amplification-based DNA fingerprinting of representative bacterial pathogens. *Journal of Clinical Microbiology* **35**, 339–346.

Valentine, N., Wunschel, S., Wunschel, D., Petersen, C. & Wahl, K. L. (2005). Effect of culture conditions on microorganism identification by matrix-assisted laser desorption ionization mass spectrometry. *Applied and Environmental Microbiology* **71**, 58–64.

van Belkum, A. (1994). DNA fingerprinting of medically important microorganisms by use of PCR. *Clinical Microbiology Reviews* **7**, 174–184.

Vater, J., Kablitz, B., Wilde, C., Franke, P., Mehta, N. & Singh Cameotra, S. (2002). Matrix-assisted laser desorption ionization-time of flight mass spectrometry of lipopeptide biosurfactants in whole cells and culture filtrates of *Bacillus subtilis* C-1 isolated from petroleum sludge. *Applied and Environmental Microbiology* **68**, 6210–6219.

Velho, R. V., Medina, L. F. C., Segalin, J. & Brandelli, A. (2011). Production of lipopeptides among *Bacillus* strains showing growth inhibition of phytopathogenic fungi. *Folia Microbiologica* **56**, 297–303.

Vorholt, J. A. (2012). Microbial life in the phyllosphere. *Nature Reviews Microbiology* **10**, 828–840.

Wang, J., Liu, J., Wang, X., Yao, J. & Yu, Z. (2004). Application of electrospray ionization mass spectrometry in rapid typing of fengycin homologues produced by *Bacillus subtilis*. *Letters in Applied Microbiology* **39**, 98–102.

Wang, Z., Russon, L., Li, L., Roser, D. C. & Long, S. R. (1998). Investigation of spectral reproducibility in direct analysis of bacteria proteins by matrix-assisted laser desorption/ionization time-of-flight mass spectrometry. *Rapid Communications in Mass Spectrometry* **12**, 456–464.

Welker, M. & Moore, E. R. B. (2011). Applications of whole-cell matrix-assisted laser-desorption/ionization time-of-flight mass spectrometry in systematic microbiology. *Systematic and Applied Microbiology* **34**, 2–11.

Williams, B. H., Hathout, Y. & Fenselau, C. (2002). Structural characterization of lipopeptide biomarkers isolated from *Bacillus globigii*. *Journal of Mass Spectrometry* **37**, 259–264.

Woo, P. C. Y., Lau, S. K. P., Teng, J. L. L. & Yuen, K.-Y. (2008). Then and now: use of 16S rDNA gene sequencing for bacterial identification and discovery of novel bacteria in clinical microbiology laboratories. *Clinical Microbiology and Infection* **14**, 908–934.

Wunschel, S. C., Jarman, K. H., Petersen, C. E., Valentine, N. B., Wahl, K. L., Schauki, D., Jackman, J., Nelson, C. P. & White, E. (2005). Bacterial analysis by MALDI-TOF mass spectrometry: an inter-laboratory comparison. *Journal of the American Society for Mass Spectrometry* **16**, 456–462.

Xu, D. & Cote, J. C. (2003). Phylogenetic relationships between *Bacillus* species and related genera inferred from comparison of 3' end 16S rDNA and 5' end 16S–23S ITS nucleotide sequences. *International Journal of Systematic and Evolutionary Microbiology* **53**, 695–704.

Xun-Chao, C., Hui, L., Ya-Rong, X. & Chang-Hong, L. (2013). Study of endophytic *Bacillus amyloliquefaciens* CC09 and its antifungal cyclic lipopeptides. *Journal of Applied Biology and Biotechnology* **1**, 1–5.

Yoshida, S., Hiradate, S., Tsukamoto, T., Hatakeda, K. & Shirata, A. (2001). Antimicrobial activity of culture filtrate of *Bacillus amyloliquefaciens* RC-2 isolated from mulberry leaves. *Phytopathology* **91**, 181–187.

Yu, G. Y., Sinclair, J. B., Hartman, G. L. & Bertagnolli, B. L. (2002). Production of iturin A by *Bacillus amyloliquefaciens* suppressing *Rhizoctonia solani*. *Soil Biology and Biochemistry* **34**, 955–963.

Zerriouh, H., Romero, D., Garcia-Gutierrez, L., Cazorla, F. M., de Vicente, A. & Perez-Garcia, A. (2011). The iturin-like lipopeptides are essential components in the biological control arsenal of *Bacillus subtilis* against bacterial diseases of cucurbits. *Molecular Plant–Microbe Interactions* **24**, 1540–1552.

Zhang, B., Bai, Z., Hoefel, D., Tang, L., Zhuang, G., Yang, J. & Zhang, H. (2008). Assessing the impact of the biological control agent *Bacillus thuringiensis* on the indigenous microbial community within the pepperplant phyllosphere. *FEMS Microbiology Letters* **284**, 102–108.

Zhang, Z., Schwartz, S., Wagner, L. & Miller, W. (2000). A greedy algorithm for aligning DNA sequences. *Journal of Computational Biology* **7**, 203–214.

Zitter, T. A., Hopkins, D. L. & Thomas, C. E. (1996). *Compendium of Cucurbit Diseases*. USA: APS Press.